NASA TECHNICAL MEMORANDUM

NASA TM 78,432

NASA TM 78,432

AERODYNAMIC CHARACTERISTICS OF AN F-8 AIRCRAFT CONFIGURATION WITH A VARIABLE CAMBER WING AT MACH NUMBERS FROM 0.70 TO 1.15

Frederick W. Boltz and Douglas F. Pena

Ames Research Center
Moffett Field, California 94035

December 1977

1. Report No.	2. Government Accession No.	3. Recipient's Catalog No.
TM 78,432		

4. Title and Subtitle	5. Report Date
AERODYNAMIC CHARACTERISTICS OF AN F-8 AIRCRAFT CONFIGURATION WITH A VARIABLE CAMBER WING AT MACH NUMBERS FROM 0.70 TO 1.15	December 1977
	6. Performing Organization Code
7. Author(s)	8. Performing Organization Report No.
Frederick W. Boltz and Douglas F. Pena	
9 Performing Organization Name and Address	10. Work Unit No.
NASA Ames Research Center, Moffett Field, Calif. 94035 and ARO, Inc., Moffett Field, Calif. 94035	505-11-41
	11. Contract or Grant No.
12. Sponsoring Agency Name and Address	13. Type of Report and Period Covered
National Aeronautics and Space Administration Washington, D. C. 20546	Technical Memorandum
	14. Sponsoring Agency Code

15. Supplementary Notes

16. Abstract

A 0.1-scale model of an F-8 aircraft was tested in the Ames 14-Foot Transonic Wind Tunnel at Mach numbers from 0.7 to 1.15. Angle of attack was varied from -2° to 22° at sideslip angles of 0° and -5°. Reynolds number, dictated by the atmospheric stagnation pressure, varied with Mach number from 3.4 to 4.0 million based on mean aerodynamic chord.

The model was configured with a wing designed to simulate the downward deflection of the leading and trailing edges of an advanced-technology-conformal-variable camber wing (ATCVCW). This wing was also equipped with conventional (simple hinge) flaps. In addition, the model was tested with the basic F-8 wing to provide a reference for extrapolating to flight data.

In general, at all Mach numbers the use of conformal flap deflections at both the leading edge and trailing edge resulted in slightly higher maximum lift coefficients and lower drag coefficients than with the use of simple hinge flaps. There were also found to be small improvements in the pitching-moment characteristics with the use of conformal flaps.

17. Key Words (Suggested by Author(s))	18. Distribution Statement
F-8 Aircraft model test Variable camber wing Simple hinge flaps	Unlimited STAR Category 08

19. Security Classif. (of this report)	20. Security Classif. (of this page)	21. No of Pages	22. Price*
Unclassified	Unclassified	125	

*For sale by the National Technical Information Service, Springfield, Virginia 22161

CONTENTS

NOMENCLATURE

The axis system and sign convention are presented in figure 1. Data are presented in the body and stability axis coordinate systems. Because the data were computer plotted, the corresponding plot symbol, where used, is given together with the conventional symbol.

Symbol	Plot Symbol	Definition
a		speed of sound
A_b		base area
b		wing span
$\bar{c}$		wing mean aerodynamic chord
C_A		axial-force coefficient, axial force/$q_\infty S$
C_{A_b}		base-force coefficient, base force/$q_\infty S$
C_D	C_D	stability axis drag coefficient, drag/$q_\infty S$
C_{D_b}		stability axis base drag coefficient, base drag/$q_\infty S$
C_L	C_L	lift coefficient, lift/$q_\infty S$
C_ℓ		body axis rolling-moment coefficient, rolling-moment $q_\infty Sb$
C_{ℓ_s}	C_ℓ(STAB)	stability axis rolling-moment coefficient, rolling-moment $q_\infty Sb$
c_m	C_m	stability and body axis pitching-moment coefficient, pitching moment/q $S\bar{c}$
C_N		normal-force coefficient, normal force/$q_\infty S$
C_n	C_n(STAB)	stability and wind axis yawing-moment coefficient, yawing moment/$q_\infty Sb$

Symbol	Plot Symbol	Definition
C_{n_b}	Cn	body axis yawing-moment coefficient, yawing moment/$q_\infty Sb$
C_{p_x}		static pressure coefficient, $(p_x-p_\infty)/q_\infty$ where x designates pressure orifices 1-29, 31-35, 37-64
C_y	CY	stability and body axis side force coefficients, side force/$q_\infty S$
M_∞	MACH	free-stream Mach number
p_x		model surface static pressure, where x designates pressure orifices 1-29, 31-35, 37-64
p_{t_∞}		free-stream total pressure
p_∞		free-stream static pressure
q_∞	Q	free-stream dynamic pressure
RN,RN/L	RN, RN/L	Reynolds number based on mean-aerodynamic chord
S		wing area
T_{t_∞}		free-stream total temperature
V_∞		free-stream velocity
α	α	angle of attack, deg
β	BETA	angle of sideslip, deg

Configuration Notation

B	B	basic F-8 body
H	H	basic F-8 horizontal tail
P	P	inlet duct plugged
V	V	basic F-8 vertical tail
W_1	W1	basic F-8 wing

Configuration Notation

Symbol	Plot Symbol	Definition
W_2	W2	variable camber wing with simple hinge flaps
W_3	W3	variable camber wing with conformal flaps
W_4	W4	variable camber wing with conformal flaps for the leading edge and outboard trailing edge and simple hinge flaps for the inboard trailing edge
W_5	W5	variable camber wing with conformal flaps for the leading edge and simple hinge flaps for the trailing edge

Surface Definitions

δ_H	DH	horizontal tail incidence angle, positive trailing edge down, deg
δ_{LE}	DLE	wing leading edge deflection angle, positive leading edge down, deg
δ_{LTEI}	DTEI-L	wing left inboard trailing edge deflection angle, positive trailing edge down, deg
δ_{RTEI}	DTEI-R	wing right inboard trailing edge deflection angle, positive trailing edge down, deg
δ_{TEO}	DTEO	wing outboard trailing edge deflection angle, positive trailing edge down, deg
δ_{TEI}	DTEI	wing inboard trailing edge deflection angle, positive trailing edge down, deg

AERODYNAMIC CHARACTERISTICS OF AN F-8 AIRCRAFT CONFIGURATION WITH A VARIABLE CAMBER WING AT MACH NUMBERS FROM 0.70 TO 1.15

Frederick W. Boltz and Douglas F. Pena*

Ames Research Center

SUMMARY

A 0.1-scale model of an F-8 aircraft was tested in the Ames 14-Foot Transonic Wind Tunnel at Mach numbers from 0.7 to 1.15. Angle of attack was varied from -2° to 22° at sideslip angles of 0° and -5°. Reynolds number, dictated by the atmospheric stagnation pressure, varied with Mach number from 3.4 to 4.0 million based on mean aerodynamic chord.

The model was configured with a wing designed to simulate the downward deflection of the leading and trailing edges of an advanced-technology-conformal-variable camber wing (ATCVCW). This wing was also equipped with conventional (simple hinge) flaps. In addition, the model was tested with the basic F-8 wing to provide a reference for extrapolating to flight data.

In general, at all Mach numbers the use of conformal flap deflections at both the leading edge and trailing edge resulted in slightly higher maximum lift coefficients and lower drag coefficients than with the use of simple hinge flaps. There were also found to be small improvements in the pitching-moment characteristics with the use of conformal flaps.

INTRODUCTION

The camber of an airfoil has a fundamental effect on its aerodynamic performance and provides the maximum efficiency only at the design flight condition. To offset the reduction in efficiency at other flight conditions, various devices such as leading-edge slots and leading- and trailing-edge flaps have been employed. However, the resulting discontinuities in the airfoil contours produce disturbances in the flow which limit the aerodynamic gains from such devices. It would, therefore, be desirable to alter the camber in a manner so as to avoid such disturbances and maintain smooth flow across the airfoil. An example of such an approach is the variable camber Krueger flap.

In order to investigate the effectiveness of the variable camber concept for the improvement of performance and handling qualities of supersonic

*Project Engineer, ARO, Inc., Moffett Field, Calif. 94035

attack/fighter aircraft, a wind-tunnel test was conducted in the Ames 14-by 14-Foot Transonic Wind Tunnel. The results of the investigation in which an F-8 aircraft configuration was used are presented herein with a minimum of analysis.

TEST FACILITY

The investigation was performed in the Ames 14- by 14-Foot Transonic Wind Tunnel, which is an atmospheric pressure, closed-circuit facility. The air exchanger, located in the compressor discharge section of the circuit, is used to maintain the air temperature within suitable limits. The tunnel has a flexible-wall nozzle, and the test section is slotted on all four sides. The Mach number range is from 0.4 to 1.2, and the Reynolds number is approximately 3.75×10^6/ft for a stagnation temperature of 640° R at a Mach number of 1.2.

MODEL DESCRIPTION

The model tested was a 0.1-scale F-8 aircraft configuration. The geometry of the model is given in table 1. Drawings of the model are presented in figure 2, and photographs of the model installation in the wind tunnel are presented in figure 3.

The model was tested with a wing designed to simulate the advanced-technology-conformal-variable camber wing (ATCVCW) as well as with the basic F-8 wing. The variable camber wing had a leading-edge sweep angle of 47.13°, a trailing-edge sweep angle of 20.28°, and a modified TR42A (Boeing Co.) airfoil section. The basic F-8 wing had a leading-edge sweep of 47.17°, a trailing-edge sweep of 20.35°, an NACA 65A006 airfoil section at the root, and an NACA 65A005 airfoil section at the tip. The horizontal and vertical tails had NACA 65A006 and modified NACA 65A005.3 airfoil sections, respectively.

The variable camber wing had the capability of simulating leading- and trailing-edge deflections and aileron deflections. In addition, the incidence angle of the horizontal tail could be varied.

The aft end of the model was modified to accept the model-support sting.

TESTING AND PROCEDURE

The investigation was conducted at Mach numbers from 0.7 to 1.15 at

Reynolds numbers from 3.4 to 4.0 million based on the wing mean-aerodynamic chord. Data were obtained at model angles of attack from -2° to 22° at sideslip angles of 0° and -5°.

Wing leading-edge deflection angles of 0°, 7.5°, 10°, 15°, 20°, 22.5° and 30° and wing trailing-edge deflection angles of -2°, 0°, 5°, 10°, and 18° were tested. Trailing-edge inboard deflection angles were set differentially (left/right) at 25°/-15°, 10°/-5°, 5°/-5°, and 0°/-15°. The horizontal tail incidence was set at 0°, -5°, and -10°.

Aerodynamic forces and moments on the model were measured using a six-component internal strain-gage balance. A pressure transducer mounted in the model-support system was used to measure base pressure. The angle of attack was sensed with an angle-of-attack transducer mounted on the model-support system.

The model was provided with boundary-layer transition strips of glass beads having a nominal size of 0.0178 cm (0.0070 in.). A strip 0.3175 cm (0.125 in.) wide was placed on the wing upper surface and on the tail surfaces at 5 percent chord from the leading edge and on the wing lower surface at 30 percent chord. Transition strips were also located 1.27 cm (0.5 in.) aft on both the nose and the nose inlet. Effectiveness of the transition trip was not verified. However, based on experience, the configuration selected was deemed more than adequate.

DATA REDUCTION

The six-component force and moment data were reduced about the model moment-reference center in the body-axis system. The axis systems are defined in figure 1, and the moment center was assumed to be at fuselage station 114.79 cm, waterline 25.40 cm and buttock line 0. The angles of attack and angles of sideslip were corrected for deflection of the sting and balance under aerodynamic load. Angles of attack and appropriate aerodynamic coefficients were corrected for model weight tares. Body- and stability-axis coefficients were corrected for base force, but no stream-angle corrections were applied to the data.

Data repeatability for the test was estimated by reviewing repeat points and is as follows:

$C_L = \pm 0.0106$	$C_\ell = \pm 0.0016$	$\alpha = \pm 0.0500°$
$C_D = \pm 0.0022$	$C_m = \pm 0.0029$	$\beta = \pm 0.0170°$
$C_y = \pm 0.0054$	$C_n = \pm 0.0008$	$RN/L = \pm 0.1337 \times 10^6/ft$
		$M_\infty = \pm 0.0033$

RESULTS AND DISCUSSION

Lift, drag, and pitching-moment characteristics for the model at Mach numbers of 0.7, 0.9, and 1.15 are presented in figures 4 through 14 for various configurations and control-surface deflections. In figure 14 the side-force, yawing-moment, and rolling-moment characteristics are also presented.

The effects of leading-edge flap deflections for simple hinge and conformal flaps are shown in figure 4 for the model with the horizontal tail off. It is seen that at subsonic speeds there are small improvements in the lift, drag, and pitching-moment characteristics at the higher lift coefficients associated with the use of conformal flaps rather than simple hinge flaps. No such improvements are evident in the data obtained at a Mach number of 1.15.

The effects of symmetrical trailing-edge deflections of conformal flaps are shown in figure 5 with the leading edge deflected and the horizontal tail off. The effects of symmetrical trailing-edge deflections of combined simple hinge and conformal flaps are shown in figure 6 for the model with the horizontal tail off. In figure 8 are shown the effects of symmetrical trailing-edge deflections of outboard simple hinge flaps with the horizontal tail off. The subsonic results of figures 5 and 6 illustrate the effectiveness of conformal trailing-edge flaps in providing increased lift with a minimum increase in drag and loss of static longitudinal stability.

Aerodynamic characteristics of the model with the horizontal tail on are presented in figures 7 and 9 through 14. In figure 7 are shown the effects of asymmetric trailing-edge deflections for combined simple hinge and conformal flaps. Data are also presented for the model with the variable-camber wing having conformal flap deflection at the leading edge. These results again illustrate the effectiveness of conformal flaps at subsonic speeds in providing improvements in the lift, drag, and pitching-moment characteristics.

The effect of the horizontal tail for both the basic F-8 wing and the conformal-variable-camber wing with all control surfaces undeflected is shown in figure 9. The most notable difference in effect of the tail is a larger change in the value of pitching moment at zero lift for the model with the basic F-8 wing.

The effect of horizontal tail deflection for the conformal-variable camber wing in its undeflected configuration is shown in figure 10. Data are also presented for the model with the horizontal tail off. It is evident that the effectiveness of the horizontal tail is satisfactory at all Mach numbers tested.

The effects of symmetrical simple-hinge-flap deflections on the variable-camber wing with the leading edge deflected and the horizontal tail off are shown in figure 11.

The effects of symmetrical-conformal-flap deflections with the wing leading edge deflected and the horizontal tail on are shown in figure 12. Here again, these results illustrate the effectiveness of conformal flaps in providing improvements in the lift, drag, and pitching-moment characteristics.

The effects of symmetrical, simple-hinge-flap deflections on the variable-camber wing with the leading edge deflected and the horizontal tail both off and on are shown in figure 13.

In figure 14, the effects of sideslip are shown for the tail-on model with both the basic F-8 wing and the variable-camber wing.

CONCLUDING REMARKS

The aerodynamic characteristics of a 0.1-scale model of an F-8 aircraft equipped with an advanced-technology-variable-camber wing at Mach numbers of 0.7, 0.9, and 1.15 have been presented. Corresponding data are presented for the F-8 model equipped with the same wing having simple conventional flaps and with the basic F-8 wing.

In general, the use of conformal flap deflections at both the leading edge and trailing edge resulted in slightly higher maximum lift coefficients and lower drag coefficients than with the use of simple hinge flaps at all Mach numbers. There were also found to be small improvements in the pitching-moment characteristics with the use of conformal flaps.

TABLE 1. - MODEL GEOMETRY

Wing assembly (Advanced Technology Wing)	
Total area (reference)	0.3484 m^2 (3.750 ft^2)
Total exposed area	0.6580 m^2 (7.083 ft^2)
Span (reference)	1.0872 m (3.567 ft)
Mean aerodynamic chord (reference)	0.3591 m (1.178 ft)
Aspect ratio	3.4
Taper ratio	0.25
Dihedral	-5.00°
Incidence	5.00°
Twist	-7.22°
Sweepback angle	
Leading edge	47.13°
0.25 element line	42.00°
Trailing edge	20.28°
Root chord	0.5130 m (1.683 ft)
Tip chord	0.1283 m (0.4209 ft)
Airfoil section	
Root	Modified TR 42A
Tip	Modified TR 42A
Wing assembly (Basic F-8 wing)	
Total area (reference)	0.3484 m^2 (3.750 ft^2)
Total exposed area	0.5907 m^2 (6.358 ft^2)
Span (reference)	1.0872 m (3.567 ft)
Mean aerodynamic chord (reference)	0.3591 m (1.178 ft)
Aspect ratio	3.4
Taper ratio	0.247
Dihedral	-5.00°
Incidence	-1.00°
Twist	0.0
Sweepback angle	
Leading edge	47.17°
0.25 element line	42.00°
Trailing edge	20.35°
Root chord	0.4663 m (1.530 ft)
Tip chord	0.1268 m (0.416 ft)
Airfoil section	
Root	NACA 65A006
Tip	NACA 65A005

TABLE 1. - Concluded.

Fuselage	
Length	1.6093 m (5.280 ft)
Maximum width	14.99 cm (5.90 in)
Maximum depth	19.28 cm (7.59 in)
Fineness ratio	10.88
Maximum cross-section area[a]	0.0242 m^2 (0.260 ft^2)
Planform area	0.2103 m^2 (2.264 ft^2)
Wetted area	0.7442 m^2 (8.010 ft^2)
Horizontal tail	
Planform area	0.0868 m^2 (0.9343 ft^2)
Exposed wetted area	0.1054 m^2 (1.135 ft^2)
Span	0.5538 m (1.817 ft)
Dihedral	5.42°
Mean aerodynamic chord	0.1864 m (0.612 ft)
Root chord length	0.2744 m (0.900 ft)
Tip chord length	0.0405 m (0.133 ft)
Sweepback angle	
Leading edge	50.46°
Hinge line	0.0
Trailing edge	20.12°
Vertical tail	
Planform area	0.0922 m^2 (0.9924 ft^2)
Exposed wetted area	0.1319 m^2 (1.420 ft^2)
Span	0.3683 m (1.208 ft)
Mean aerodynamic chord	0.2789 m (0.915 ft)
Root chord length	0.3967 m (1.302 ft)
Tip chord length	0.1041 m (0.342 ft)
Sweepback angle	
Leading edge	50.15°
Hinge line	22.00°
Trailing edge	22.00°

[a]Includes flow through duct area

INDEX OF DATA FIGURES

FIGURE	TITLE	CONDITIONS VARYING	PLOTTED COEFFICIENTS SCHEDULE	PAGE
4	EFFECT OF L.E. FLAP DEFL. FOR SIMPLE HINGE AND CONFORMAL FLAPS, TAIL OFF.	CONFIG. DLE, MACH	A	1-9
5	EFFECT OF SYMM. T.E. DEFL. FOR CONFORMAL FLAPS. TAIL OFF.	DTEO,DTEI, DLE, MACH	A	10-15
6	EFFECT OF SYMM. T.E. DEFL. FOR SIMPLE HINGE AND CONFORMAL FLAPS. TAIL OFF	CONFIG., DTEO DTEI, MACH	A	16-21
7	EFFECT OF ASYM. T.E. DEFL. FOR SIMPLE HINGE AND CONFORMAL FLAPS. TAIL ON	CONFIG.,DTEI-L, DTEI-R,DTEO,DLE, MACH	A	22-27
8	EFFECT OF OUTBD. SYMM. T.E. DEFL., SIMPLE HINGE FLAPS. TAIL OFF	DTEO, MACH	A	28-36
9	EFFECT OF HORIZONTAL TAIL FOR BOTH WINGS. ALL CONTROL SURFACE DEFL. ZERO.	CONFIG., MACH	A	37-51
10	EFFECT OF HORIZ. TAIL DEFL. ON AT WING. ALL WING CONT. SURF. DEFL. ZERO.	CONFIG., DH, MACH	A	52-60
11	EFFECT OF HORIZ. TAIL WITH SYMM. CONFORMAL FLAP DEFLECTIONS. DLE = 10.	DTEO, MACH	A	61-69
12	EFFECT OF HORIZ. TAIL WITH SYMM. CONFORMAL FLAP DEFLECTIONS. DLE = 0 OR 30	CONFIG.,MACH,DH, DTEO, DTEI, DLE	A	70-78
13	EFFECT OF HORIZ. TAIL WITH SYMM. SIMPLE HINGE FLAP DEFLECTIONS, DLE = 20.	CONFIG., MACH, DH DTEO, DTEI	A	79-84
14	EFFECT OF SIDESLIP ANGLE FOR BOTH WINGS. ALL CONT. SURF. ZERO. TAIL ON.	CONFIG., MACH BETA	B	85-102

COEFFICIENTS SCHEDULE:

C_L vs. α; C_D versus C_L; C_L versus C_m

C_Y, C_n(STAB), C_ℓ(STAB), C_L versus α; C_D versus C_L; C_L versus C_m

Note: Positive directions of force coefficients, moment coefficients, and angles are indicated by arrows.

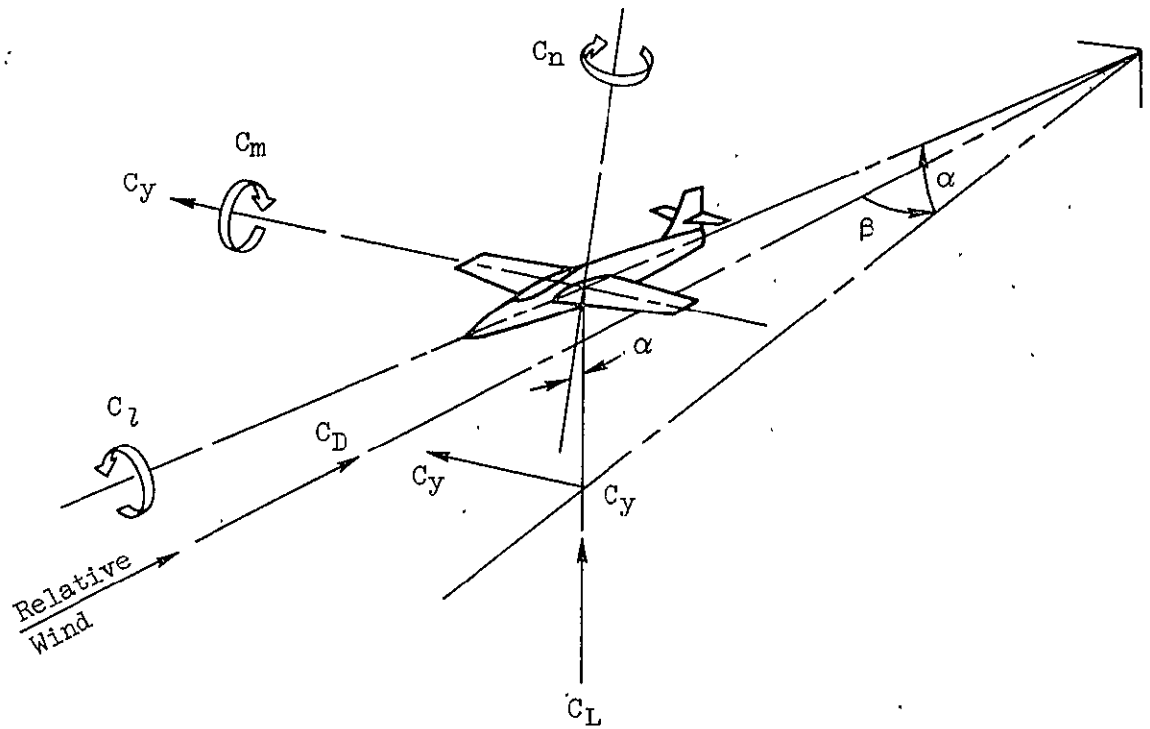

Figure 1. - Axis system

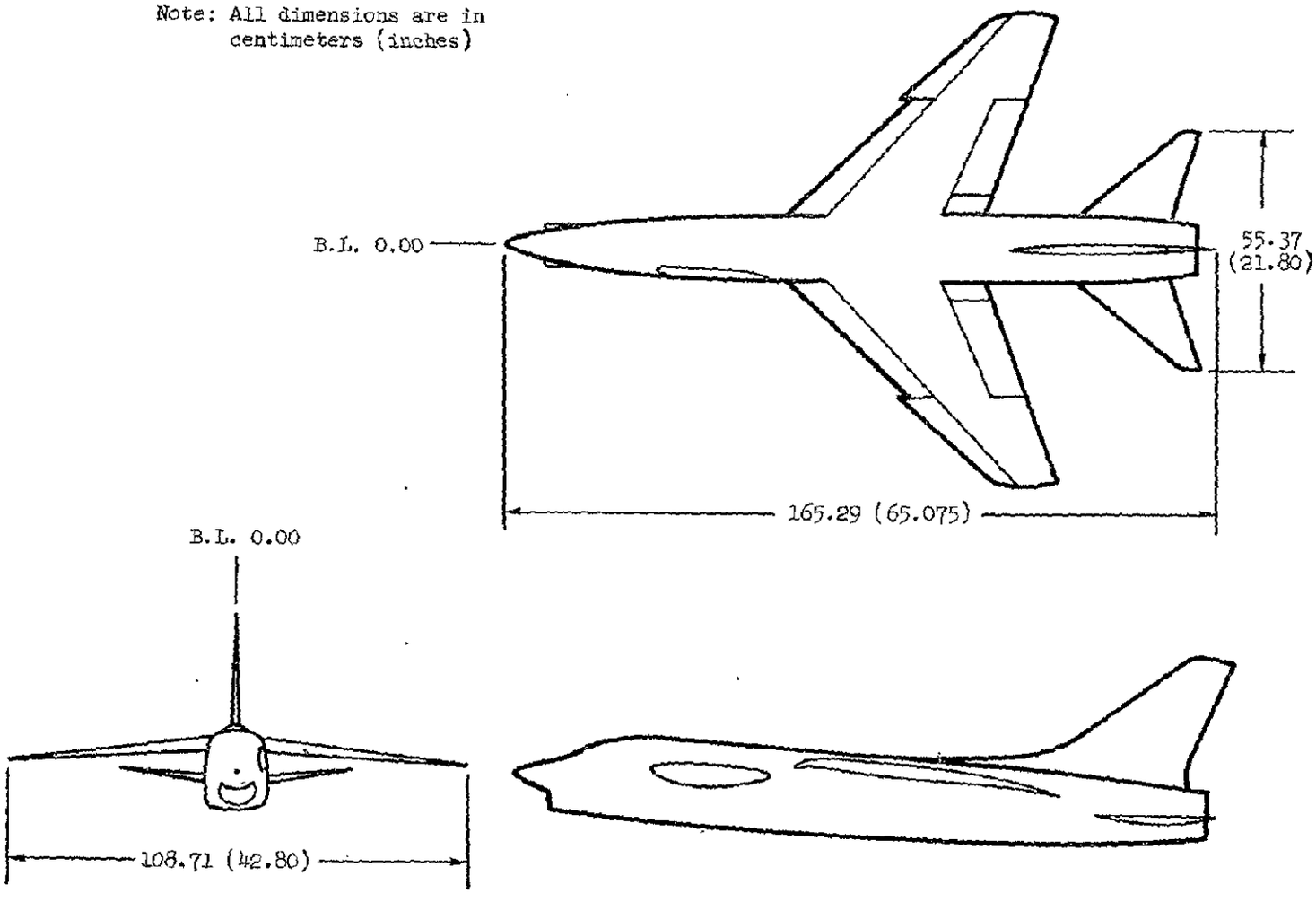

(a) Three view

Figure 2. - Model drawings.

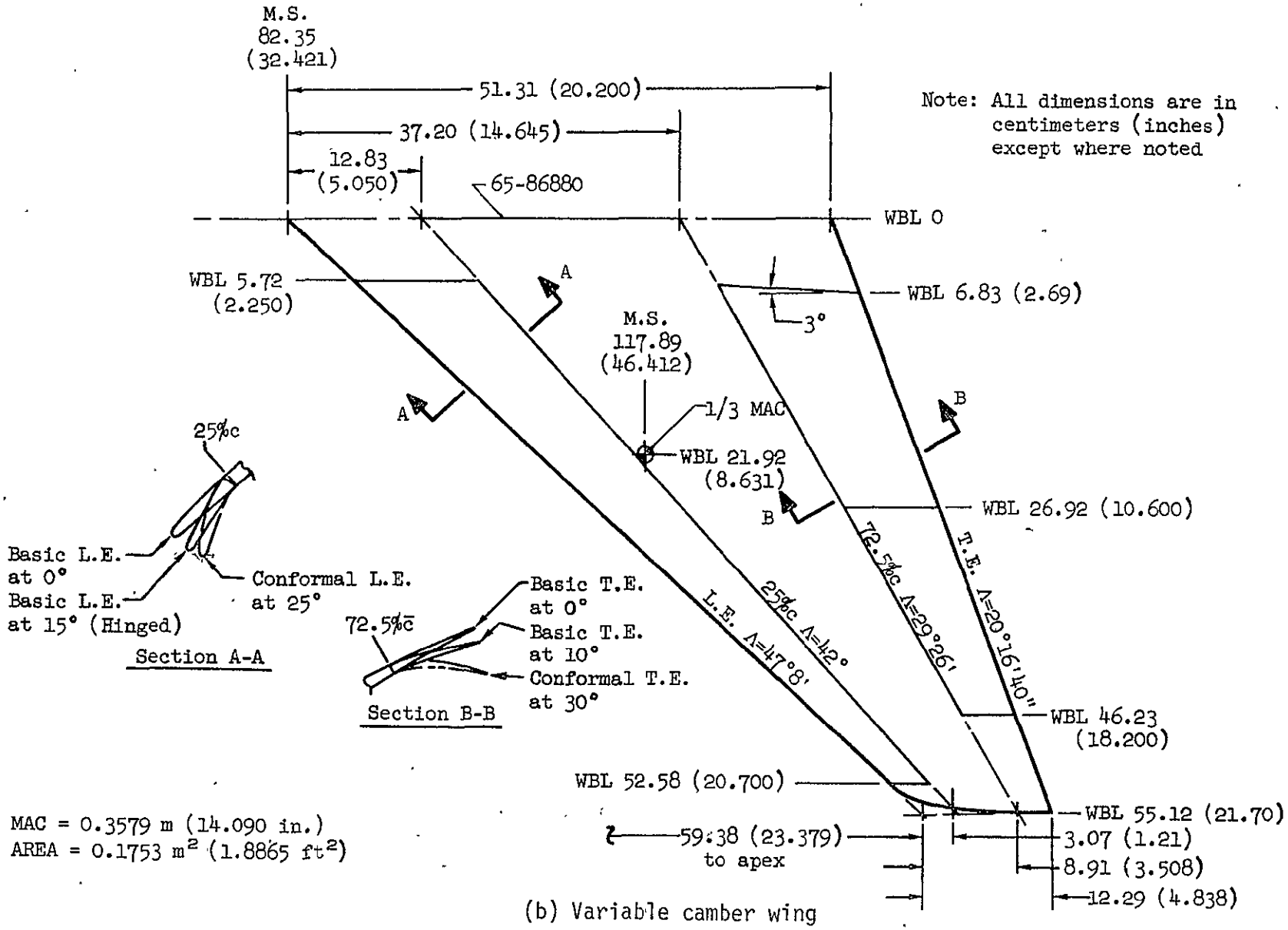

(b) Variable camber wing

Figure 2. - Continued.

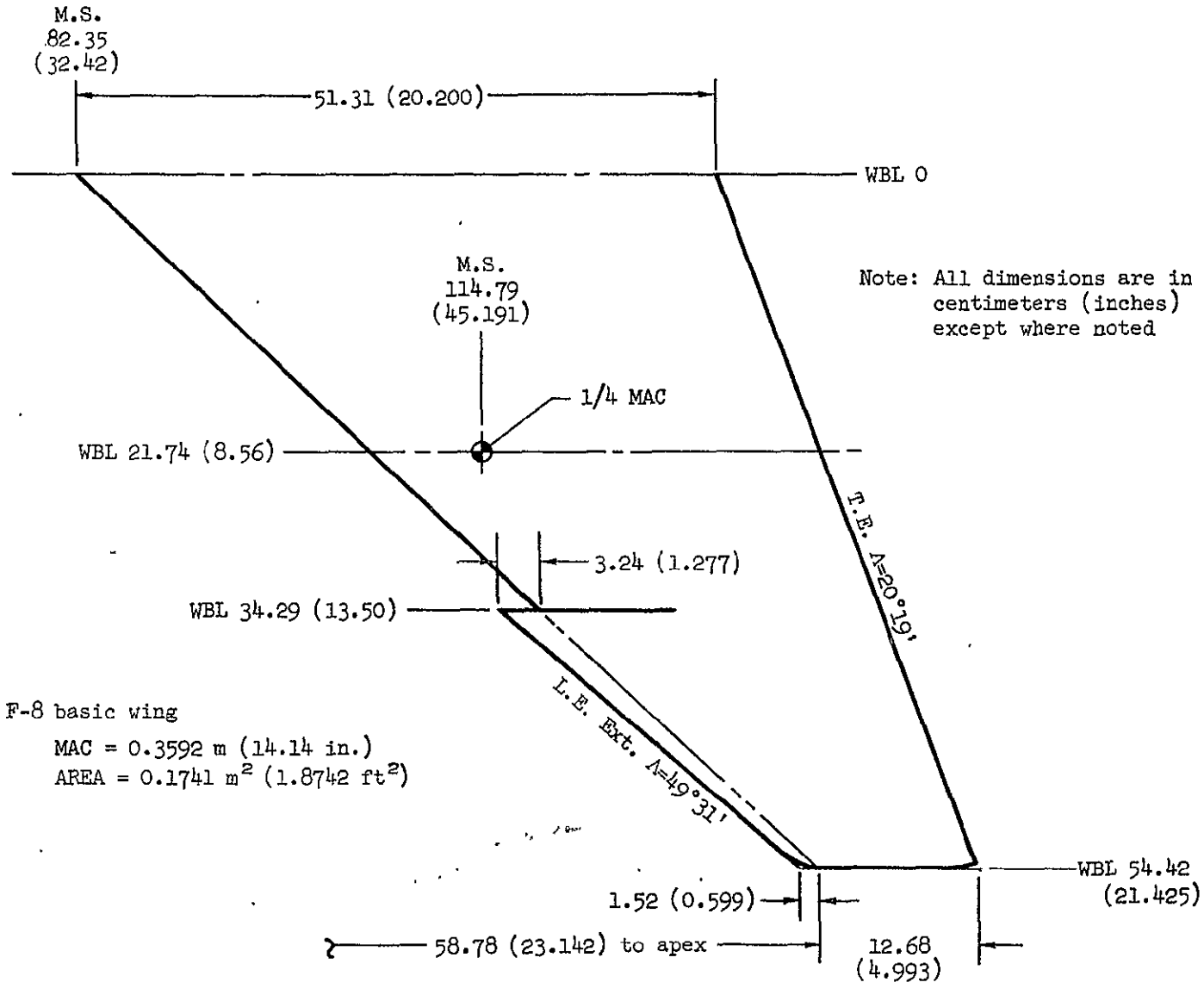

(c) F-8 basic wing

Figure 2. - Continued.

Note: All dimensions are in centimeters
(inches) except where noted

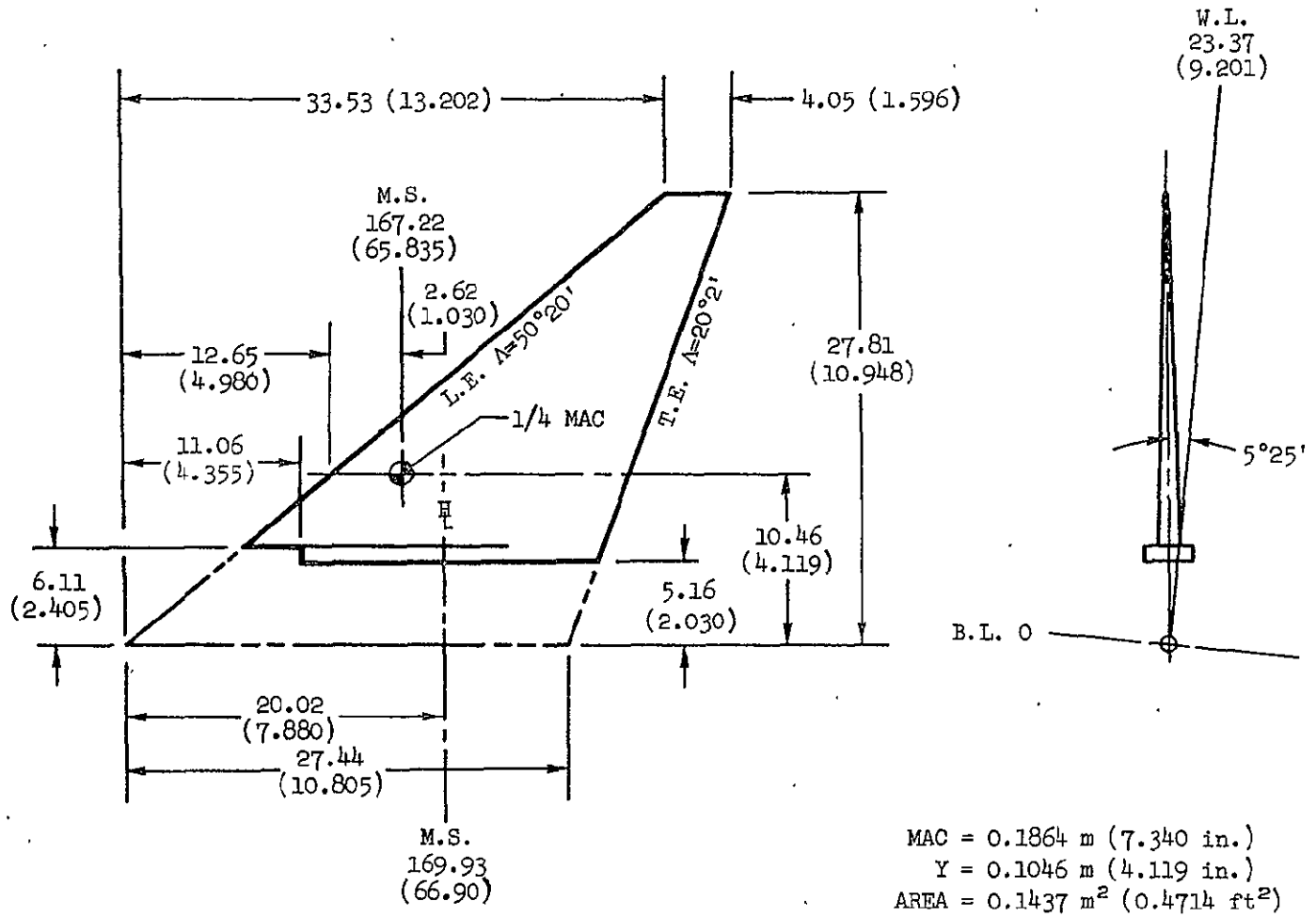

MAC = 0.1864 m (7.340 in.)
Y = 0.1046 m (4.119 in.)
AREA = 0.1437 m^2 (0.4714 ft^2)

(d) Horizontal tail

Figure 2. - Continued.

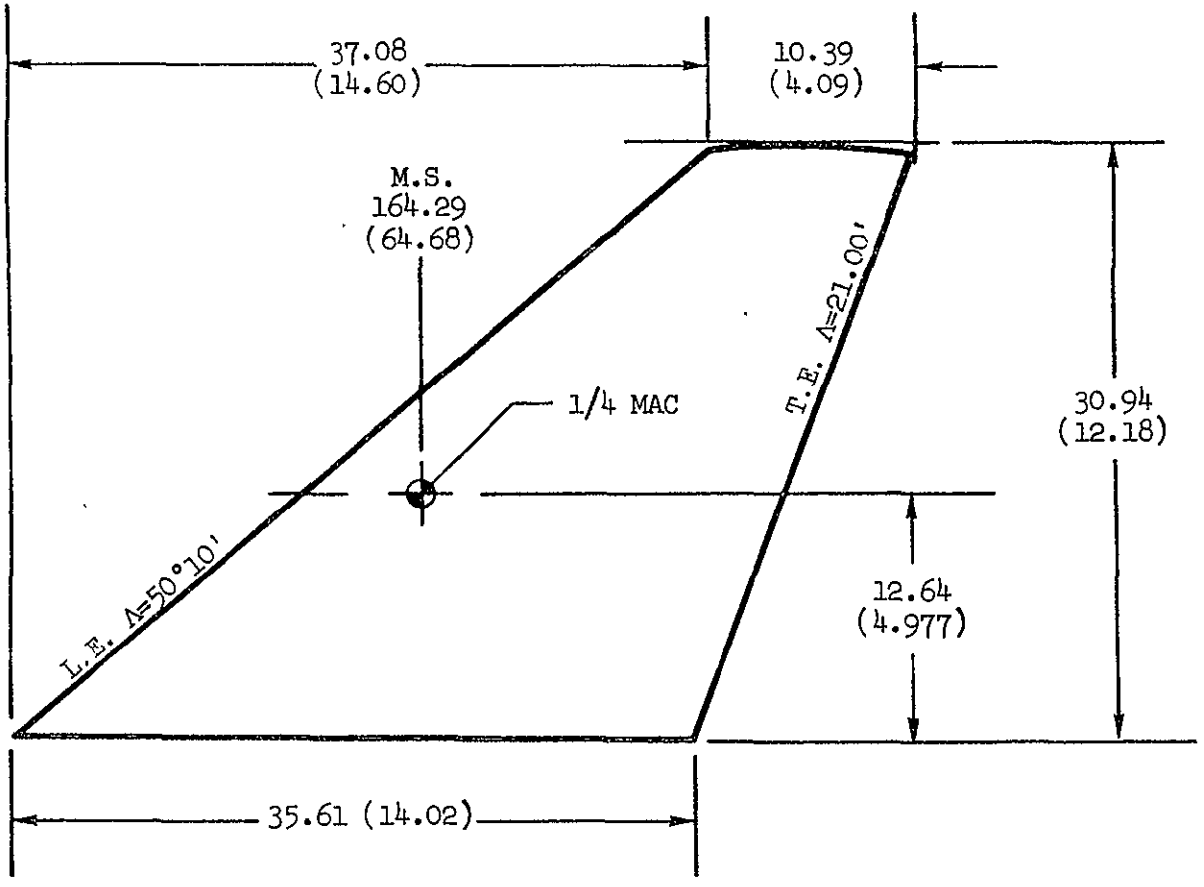

MAC = 0.2530 ft (9.962 in.)
AREA = 0.07115 m^2 (0.7659 ft^2)

Note: All dimensions are in centimeters (inches) except where noted

(e) Vertical tail

Figure 2. - Continued.

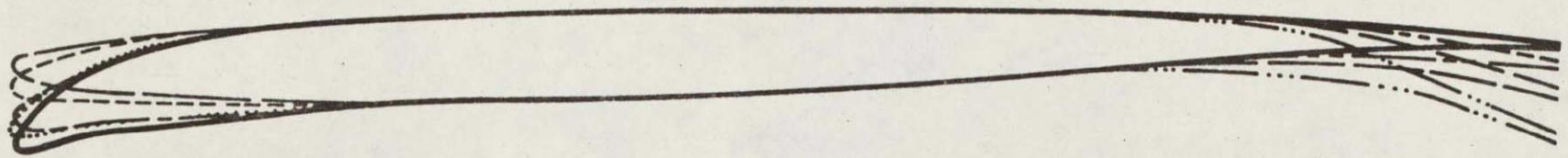

30° L.E.
22.5° L.E.
15° L.E.
7.5° L.E.
10° T.E.
5° T.E.
18° T.E.

(f) Some typical leading- and trailing-edge angles for variable camber wing

Figure 2. - Concluded.

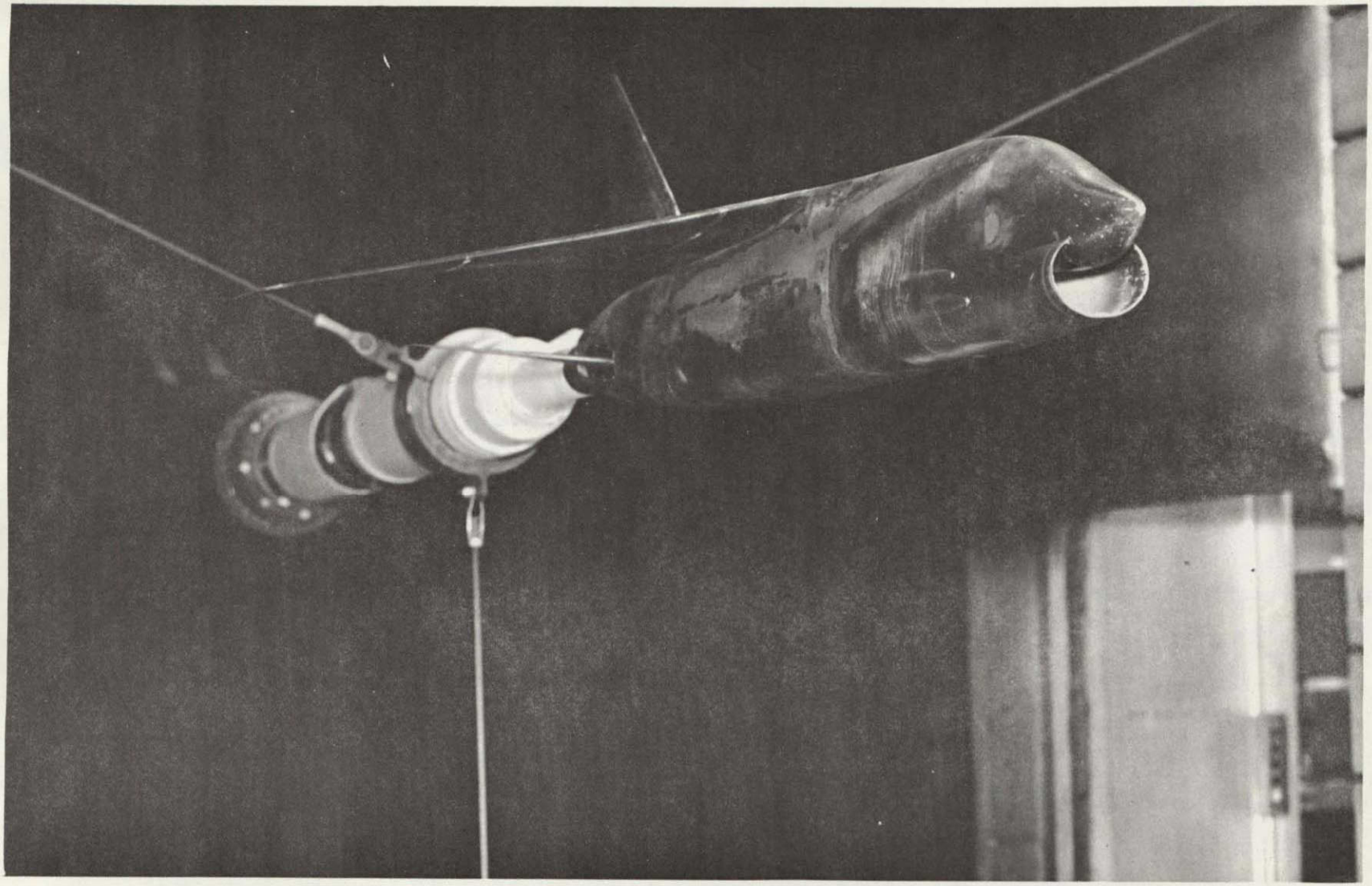

(a) Three-quarter front view

Figure 3. - Model installation photographs.

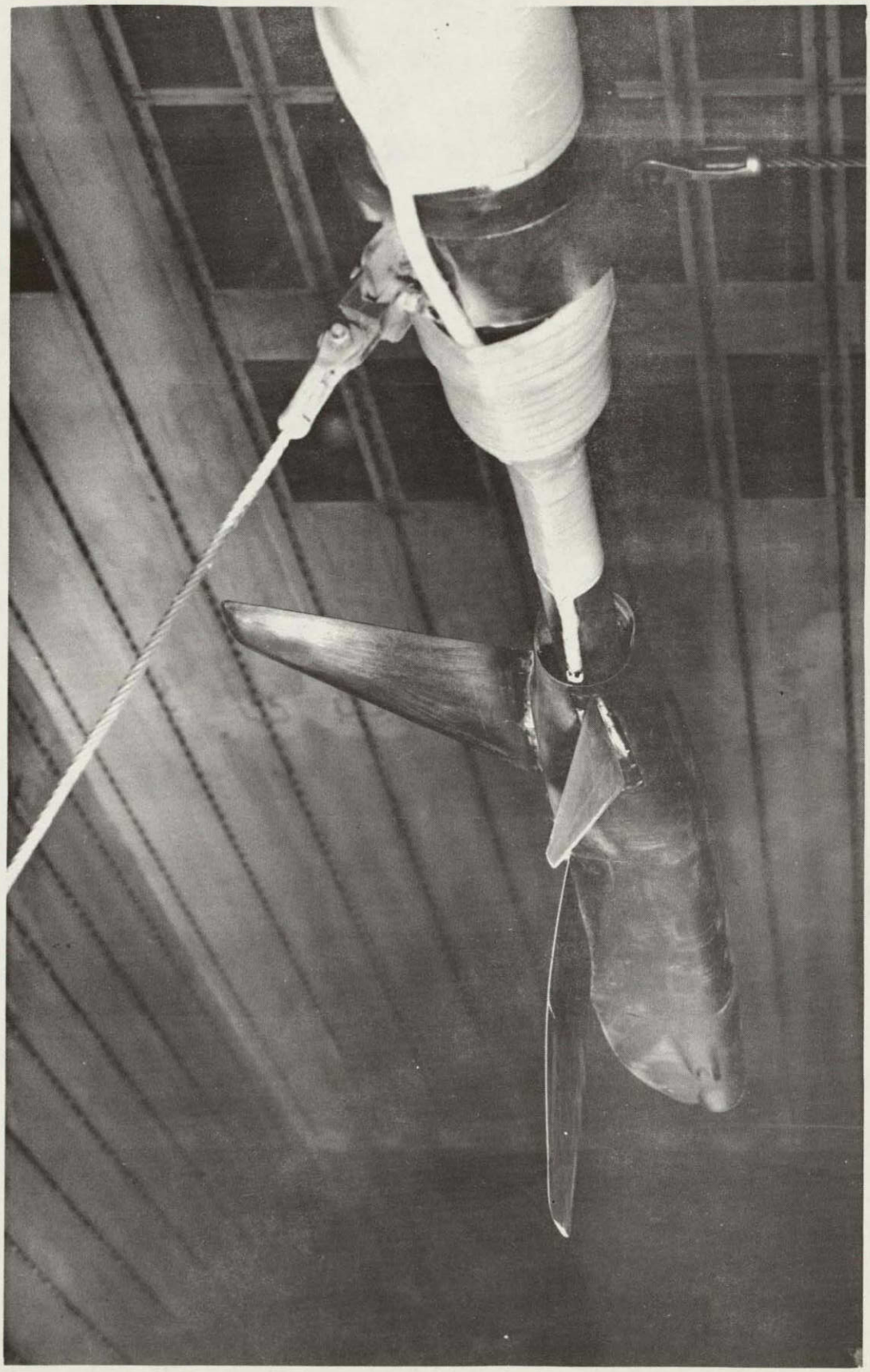

(b) Three-quarter rear view
Figure 3. - Concluded.

(Reverse of this page is blank.)

DATA SET	SYMBOL	CONFIGURATION DESCRIPTION	DLE	DTEO	DTEI	BETA
(BFK007)	○	B V W2	.000	.000	.000	.000
(JFK016)	□	B V W2	20.000	.000	.000	.000
(JFK018)	◇	B V W3	7.500	.000	.000	.000
(JFK031)	△	B V W3	15.000	.000	.000	.000
(JFK017)	▷	B V W3	22.500	.000	.000	.000
(JFK019)	▱	B V W3	30.000	.000	.000	.000

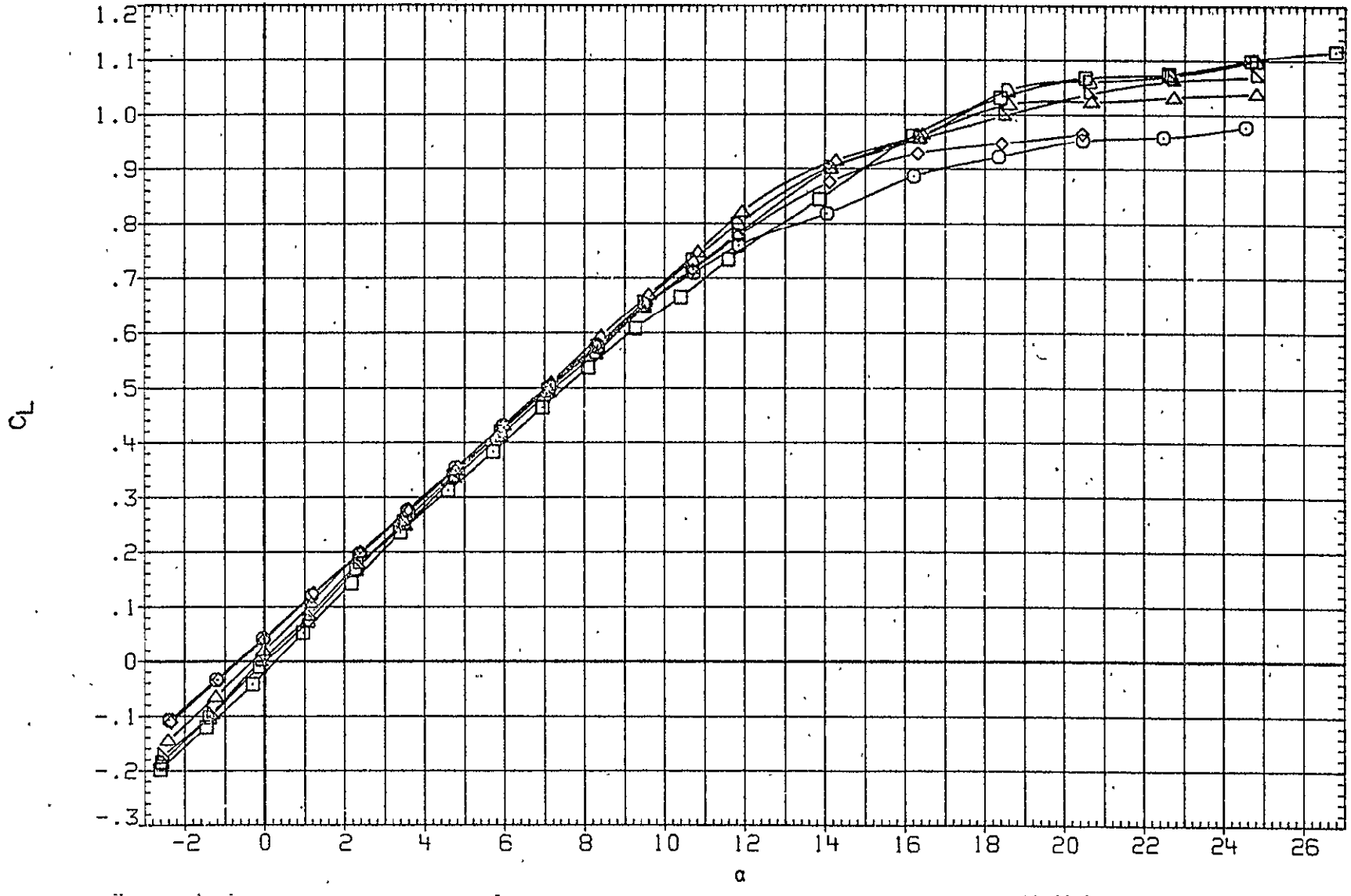

FIG. 4 EFFECT OF L.E. FLAP DEFL. FOR SIMPLE HINGE AND CONFORMAL FLAPS. TAIL OFF.

(A)MACH = .70

DATA SET	SYMBOL	CONFIGURATION DESCRIPTION	DLE	DTEO	DTEI	BETA
(BFK007)	○	B V W2	.000	.000	.000	.000
(JFK016)	□	B V W2	20.000	.000	.000	.000
(JFK018)	◇	B V W3	7.500	.000	.000	.000
(JFK031)	△	B V W3	15.000	.000	.000	.000
(JFK017)	▷	B V W3	22.500	.000	.000	.000
(JFK019)	D	B V W3	30.000	.000	.000	.000

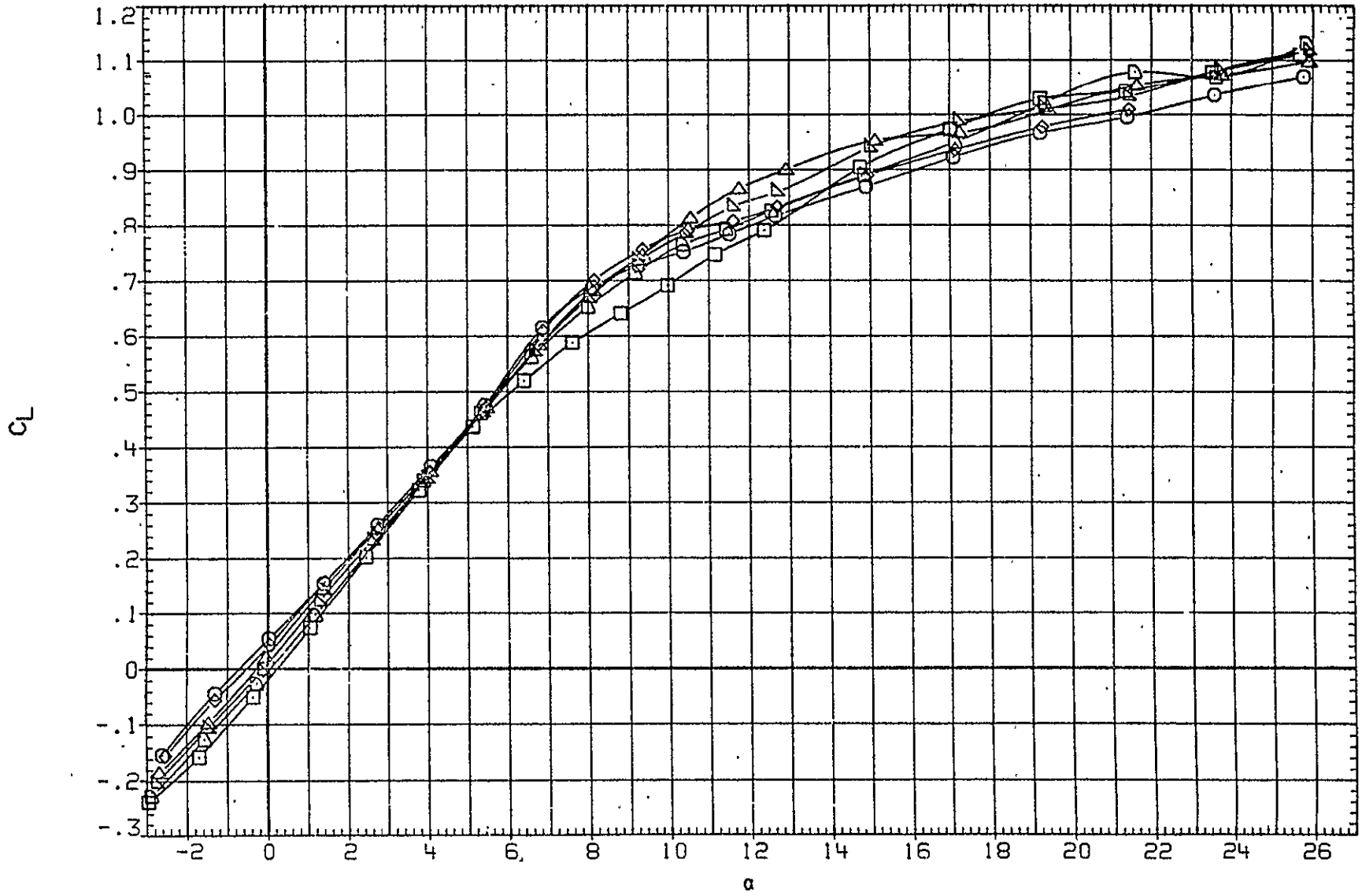

FIG. 4 EFFECT OF L.E. FLAP DEFL. FOR SIMPLE HINGE AND CONFORMAL FLAPS. TAIL OFF.

(B) MACH = .90

DATA SET	SYMBOL	CONFIGURATION DESCRIPTION	DLE	DTEO	DTEI	BETA
(BFK007)	○	B V W2	.000	.000	.000	.000
(JFK016)	□	DATA NOT AVAILABLE	20.000	.000	.000	.000
(JFK018)	◇	DATA NOT AVAILABLE	7.500	.000	.000	.000
(JFK031)	△	B V W3.	15.000	.000	.000	.000
(JFK017)	◁	B V W3	22.500	.000	.000	.000
(JFK019)	D	DATA NOT AVAILABLE	30.000	.000	.000	.000

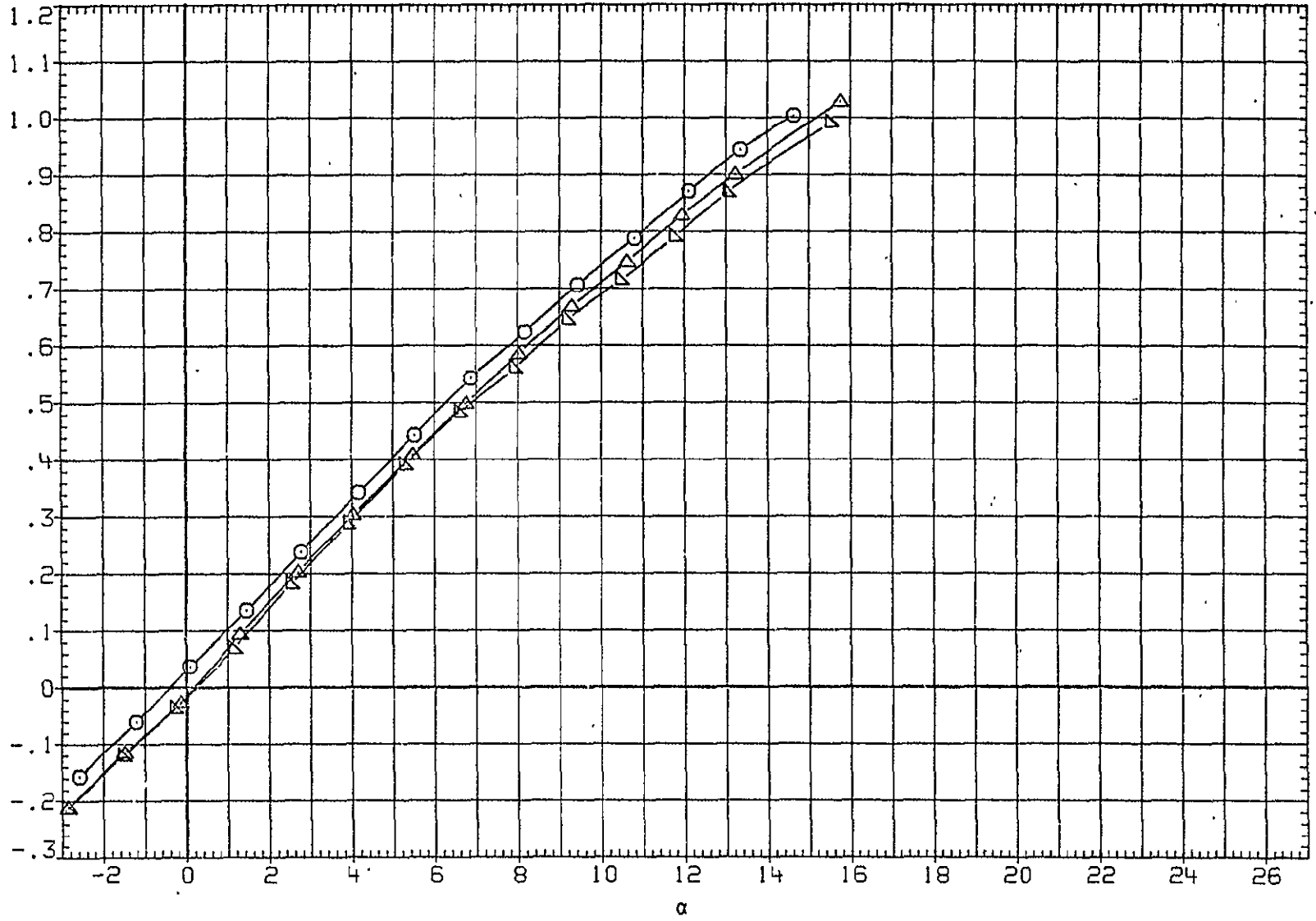

FIG. 4 EFFECT OF L.E. FLAP DEFL. FOR SIMPLE HINGE AND CONFORMAL FLAPS. TAIL OFF.

(C)MACH = 1.15

DATA SET	SYMBOL	CONFIGURATION DESCRIPTION	DLE	DTEO	DTEI	BETA
(BFK007)	○	B V W2	.000	.000	.000	.000
(JFK016)	□	B V W2	20.000	.000	.000	.000
(JFK018)	◇	B V W3	7.500	.000	.000	.000
(JFK031)	△	B V W3	15.000	.000	.000	.000
(JFK017)	◁	B V W3	22.500	.000	.000	.000
(JFK019)	▷	B V W3	30.000	.000	.000	.000

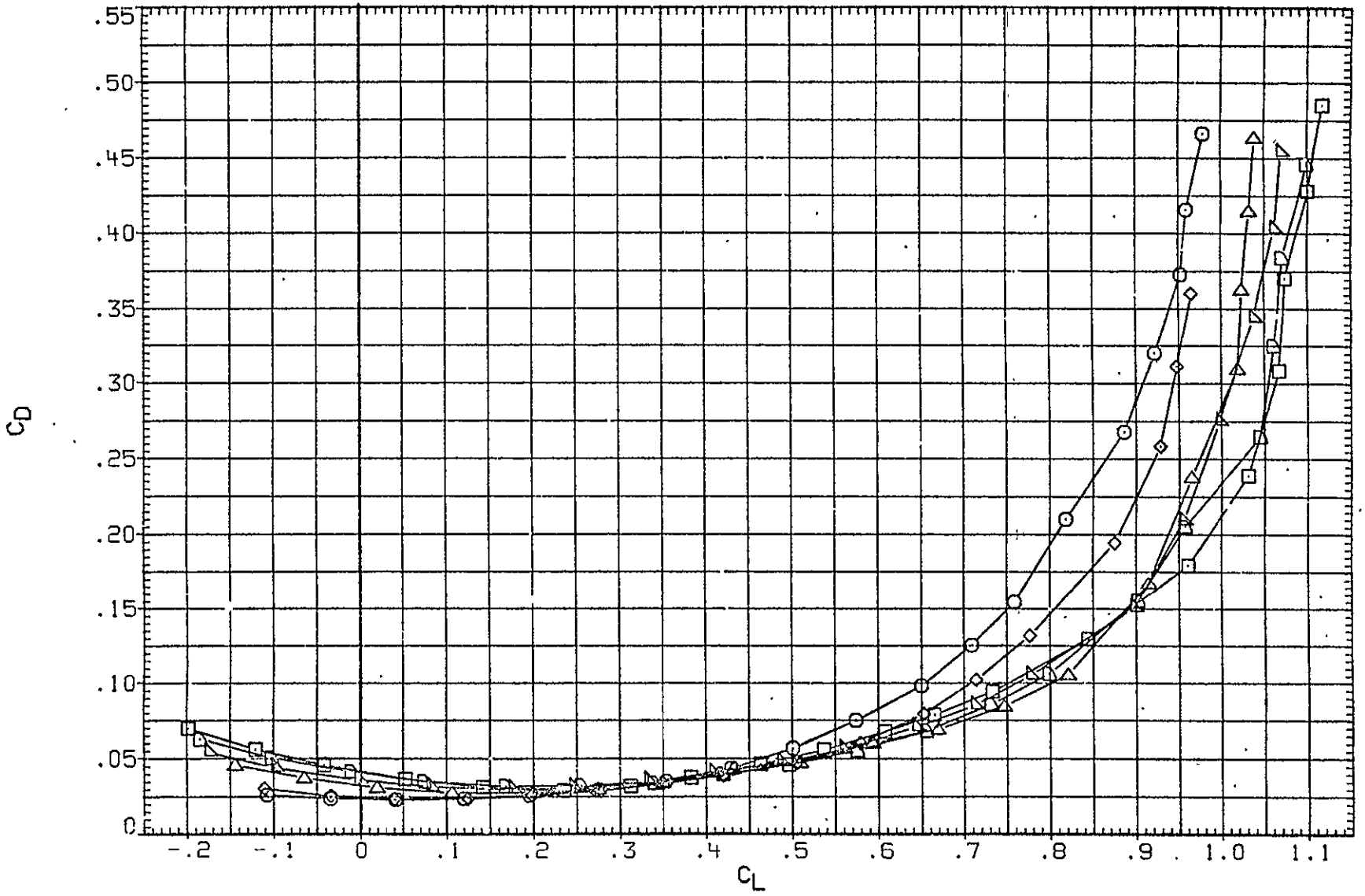

FIG. 4 EFFECT OF L.E. FLAP DEFL. FOR SIMPLE HINGE AND CONFORMAL FLAPS. TAIL OFF.

(A) MACH = .70

DATA SET	SYMBOL	CONFIGURATION DESCRIPTION	DLE	DTEO	DTEI	BETA
(BFK007)	○	B V W2	.000	.000	.000	.000
(JFK016)	□	B V W2	20.000	.000	.000	.000
(JFK018)	◇	B V W3	7.500	.000	.000	.000
(JFK031)	△	B V W3	15.000	.000	.000	.000
(JFK017)	◸	B V W3	22.500	.000	.000	.000
(JFK019)	D	B V W3	30.000	.000	.000	.000

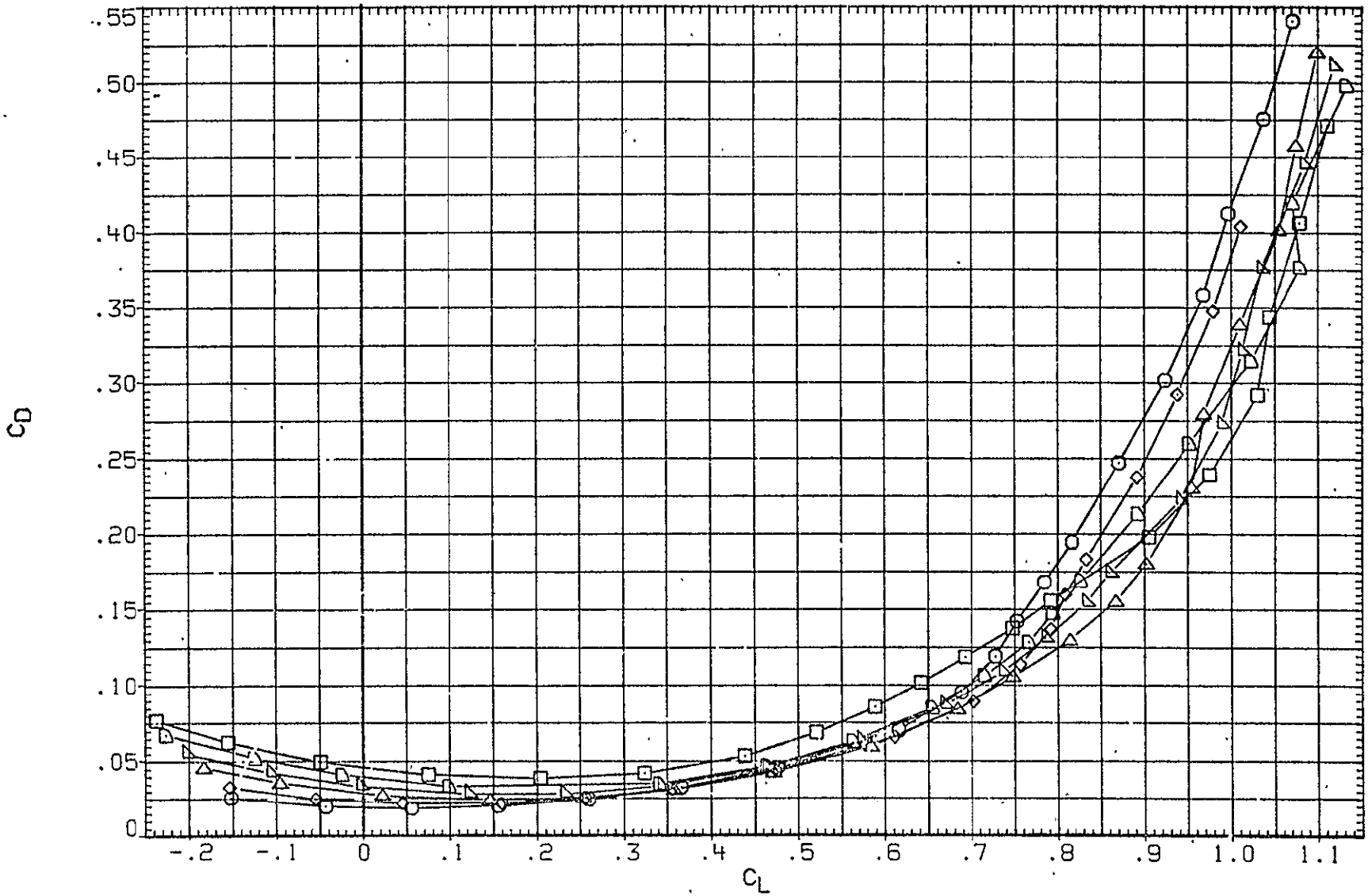

FIG. 4 EFFECT OF L.E. FLAP DEFL. FOR SIMPLE HINGE AND CONFORMAL FLAPS. TAIL OFF.

(B)MACH = .90

DATA SET	SYMBOL	CONFIGURATION DESCRIPTION	DLE	DTEO	DTEI	BETA
(BFK007)	○	B V W2	.000	.000	.000	.000
(JFK016)	□	DATA NOT AVAILABLE	20.000	.000	.000	.000
(JFK018)	◇	DATA NOT AVAILABLE	7.500	.000	.000	.000
(JFK031)	△	B V W3	15.000	.000	.000	.000
(JFK017)	◸	B V W3	22.500	.000	.000	.000
(JFK019)	▱	DATA NOT AVAILABLE	30.000	.000	.000	.000

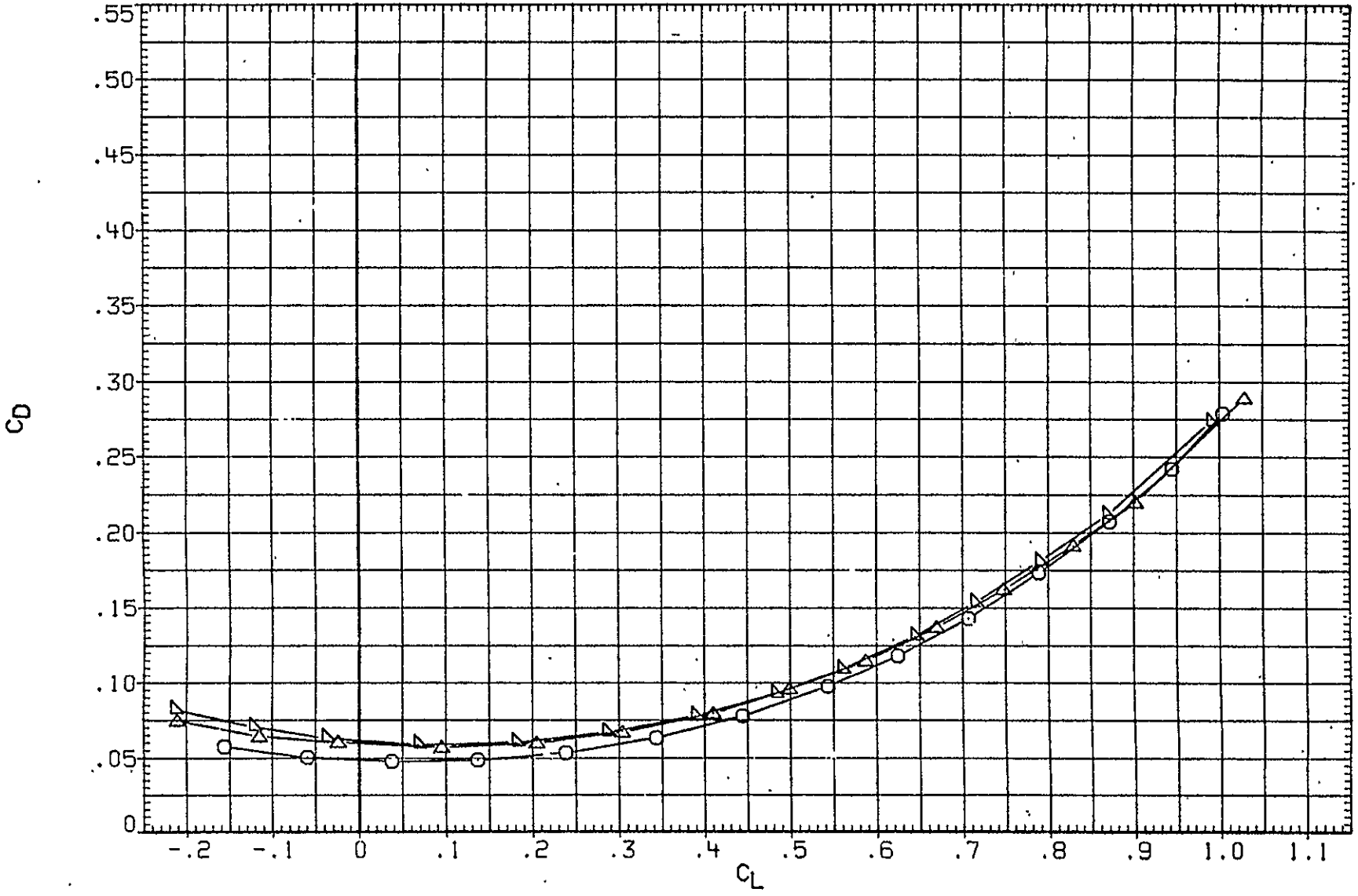

FIG. 4 EFFECT OF L.E. FLAP DEFL. FOR SIMPLE HINGE AND CONFORMAL FLAPS. TAIL OFF.

(C)MACH = 1.15

ORIGINAL PAGE IS
OF POOR QUALITY

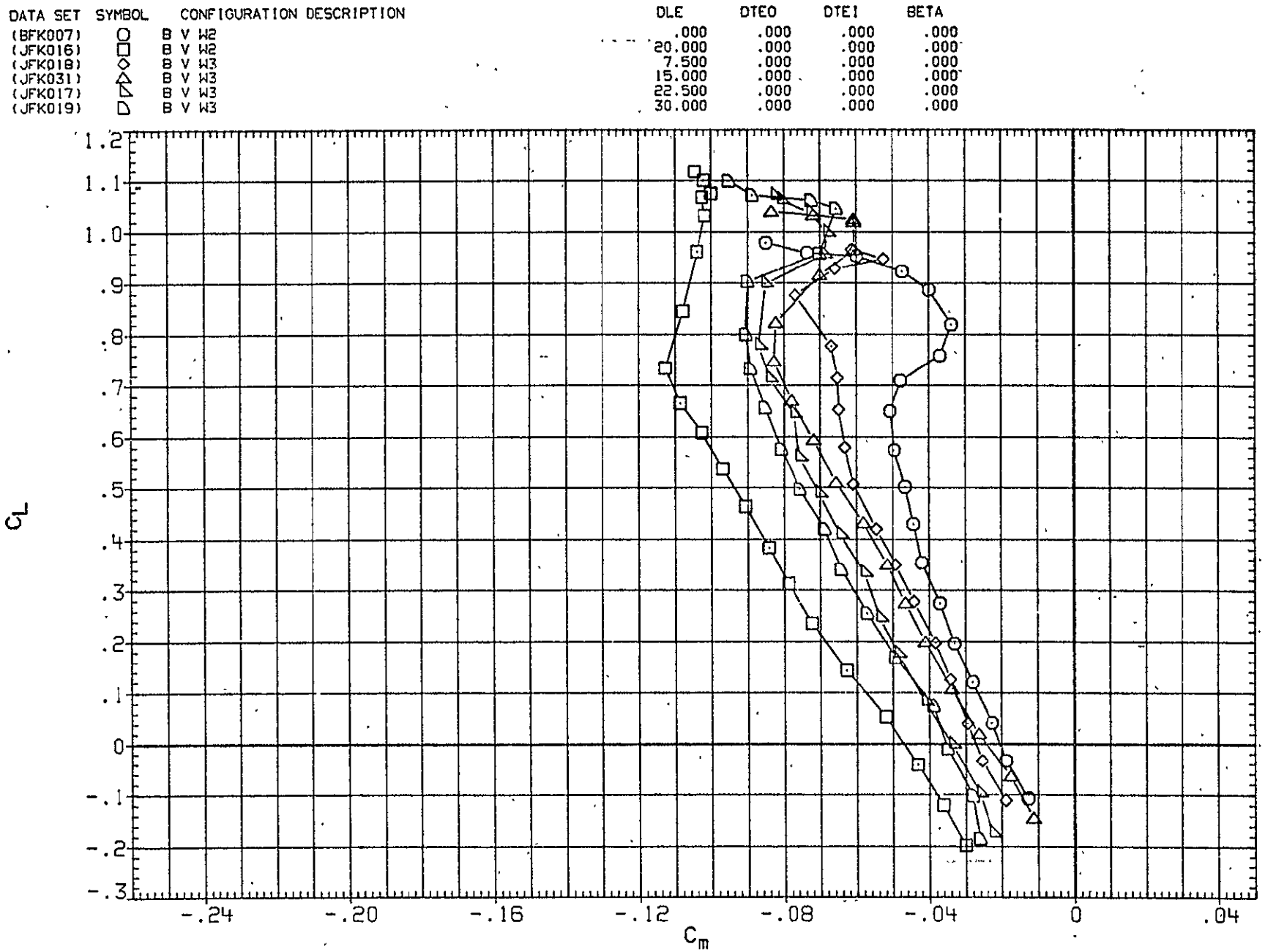

FIG. 4 EFFECT OF L.E. FLAP DEFL. FOR SIMPLE HINGE AND CONFORMAL FLAPS. TAIL OFF.

(A) MACH = .70

DATA SET	SYMBOL	CONFIGURATION DESCRIPTION	DLE	DTEO	DTEI	BETA
(BFK007)	○	B V W2	.000	.000	.000	.000
(JFK016)	□	B V W2	20.000	.000	.000	.000
(JFK018)	◇	B V W3	7.500	.000	.000	.000
(JFK031)	△	B V W3	15.000	.000	.000	.000
(JFK017)	▷	B V W3	22.500	.000	.000	.000
(JFK019)	▯	B V W3	30.000	.000	.000	.000

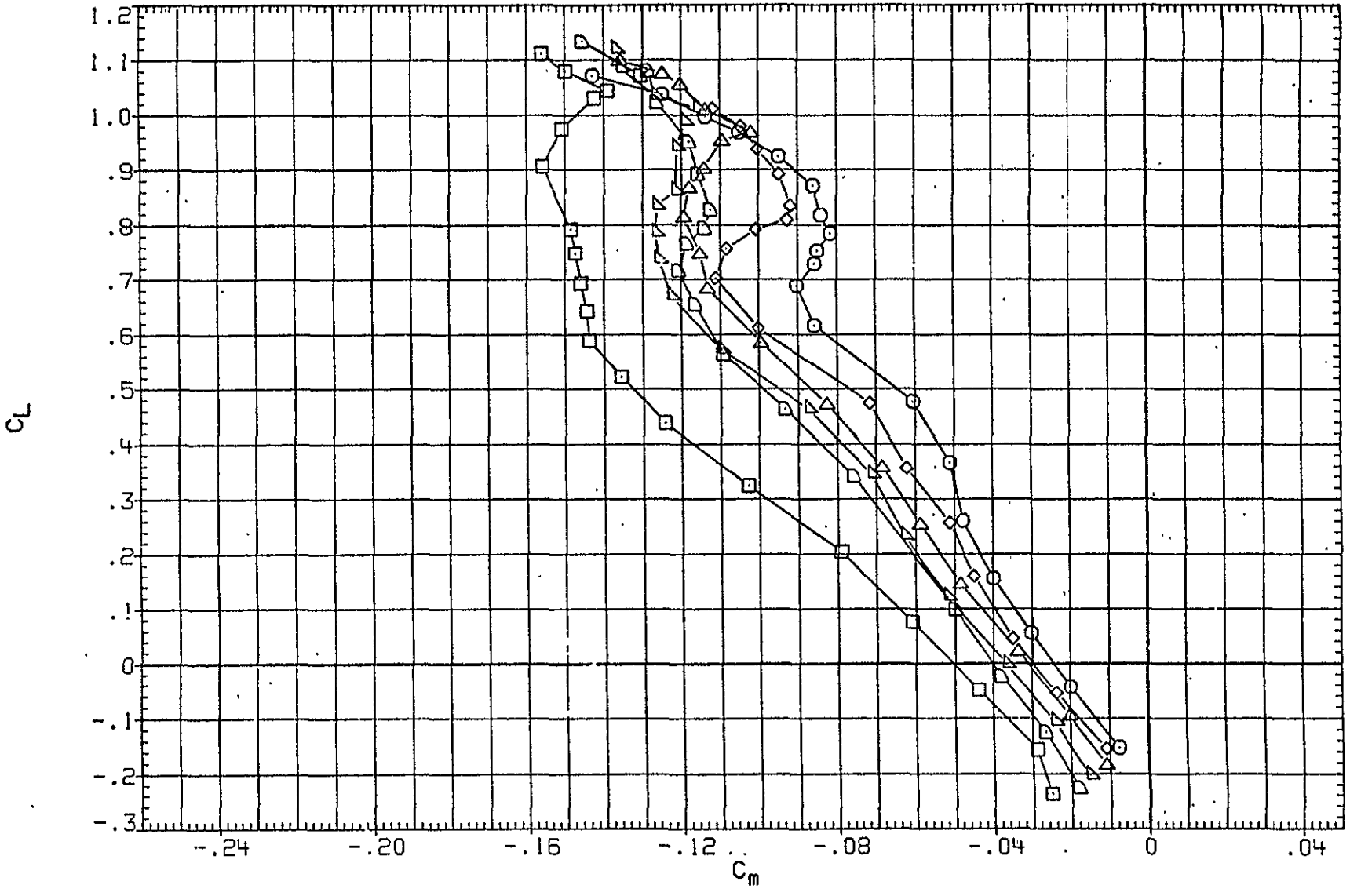

FIG. 4 EFFECT OF L.E. FLAP DEFL. FOR SIMPLE HINGE AND CONFORMAL FLAPS. TAIL OFF.

(B)MACH = .90

DATA SET	SYMBOL	CONFIGURATION DESCRIPTION	DLE	DTEO	DTEI	BETA
(BFK007)	○	B V W2	.000	.000	.000	.000
(JFK016)	□	DATA NOT AVAILABLE	20.000	.000	.000	.000
(JFK018)	◇	DATA NOT AVAILABLE	7.500	.000	.000	.000
(JFK031)	◁	B V W3	15.000	.000	.000	.000
(JFK017)	△	B V W3	22.500	.000	.000	.000
(JFK019)	D	DATA NOT AVAILABLE	30.000	.000	.000	.000

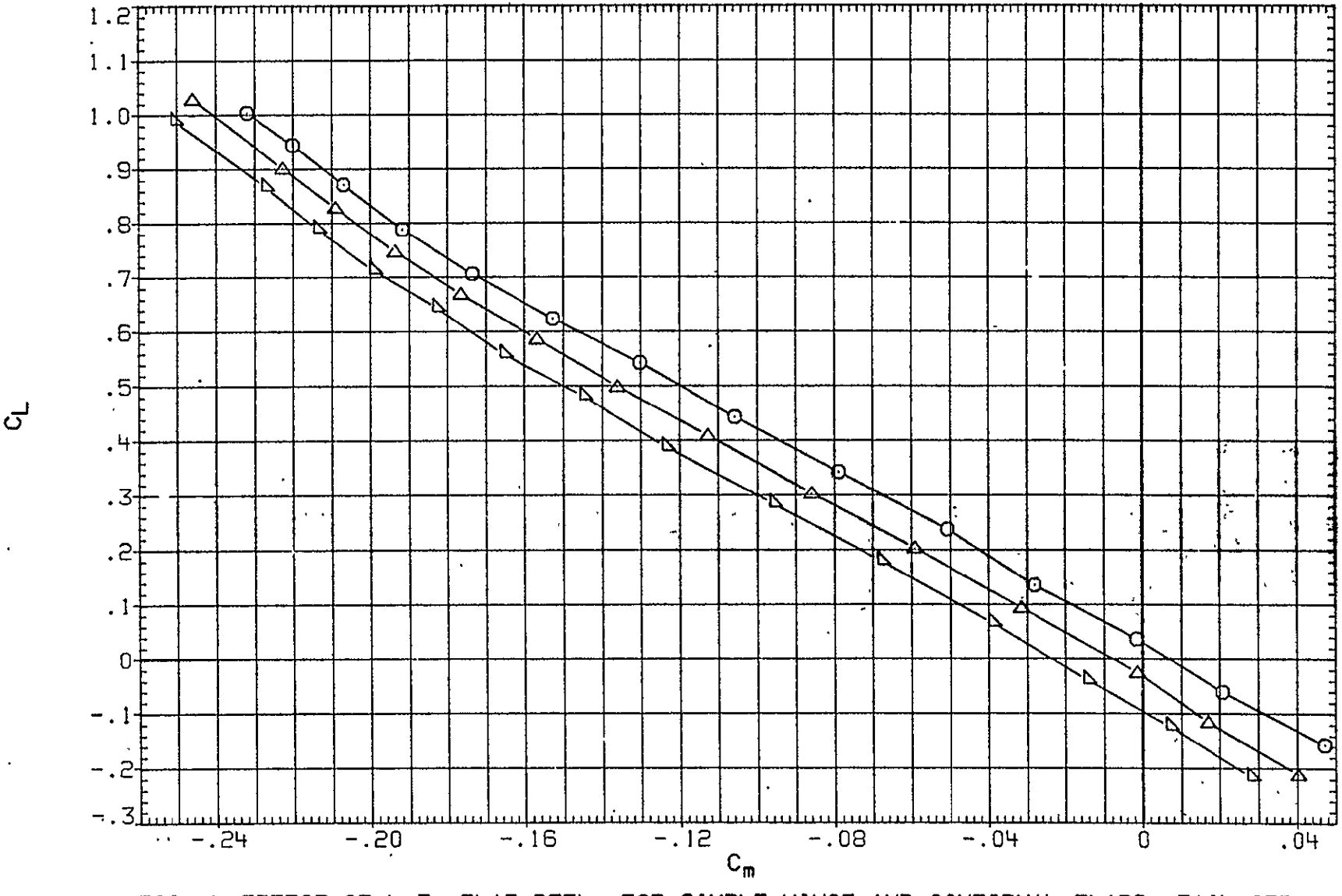

FIG. 4 EFFECT OF L.E. FLAP DEFL. FOR SIMPLE HINGE AND CONFORMAL FLAPS. TAIL OFF.

(C)MACH = 1.15.

DATA SET	SYMBOL	CONFIGURATION DESCRIPTION	DTEO	DTEI	DLE	BETA
(BFK031)	○	B V W3	.000	.000	15.000	.000
(JFK033)	□	B V W3	10.000	10.000	15.000	.000
(JFK019)	◇	B V W3	.000	.000	30.000	.000
(JFK020)	△	B V W3	5.000	5.000	30.000	.000
(JFK024)	◁	B V W3	10.000	10.000	30.000	.000
(JFK025)	D	B V W3	18.000	18.000	30.000	.000

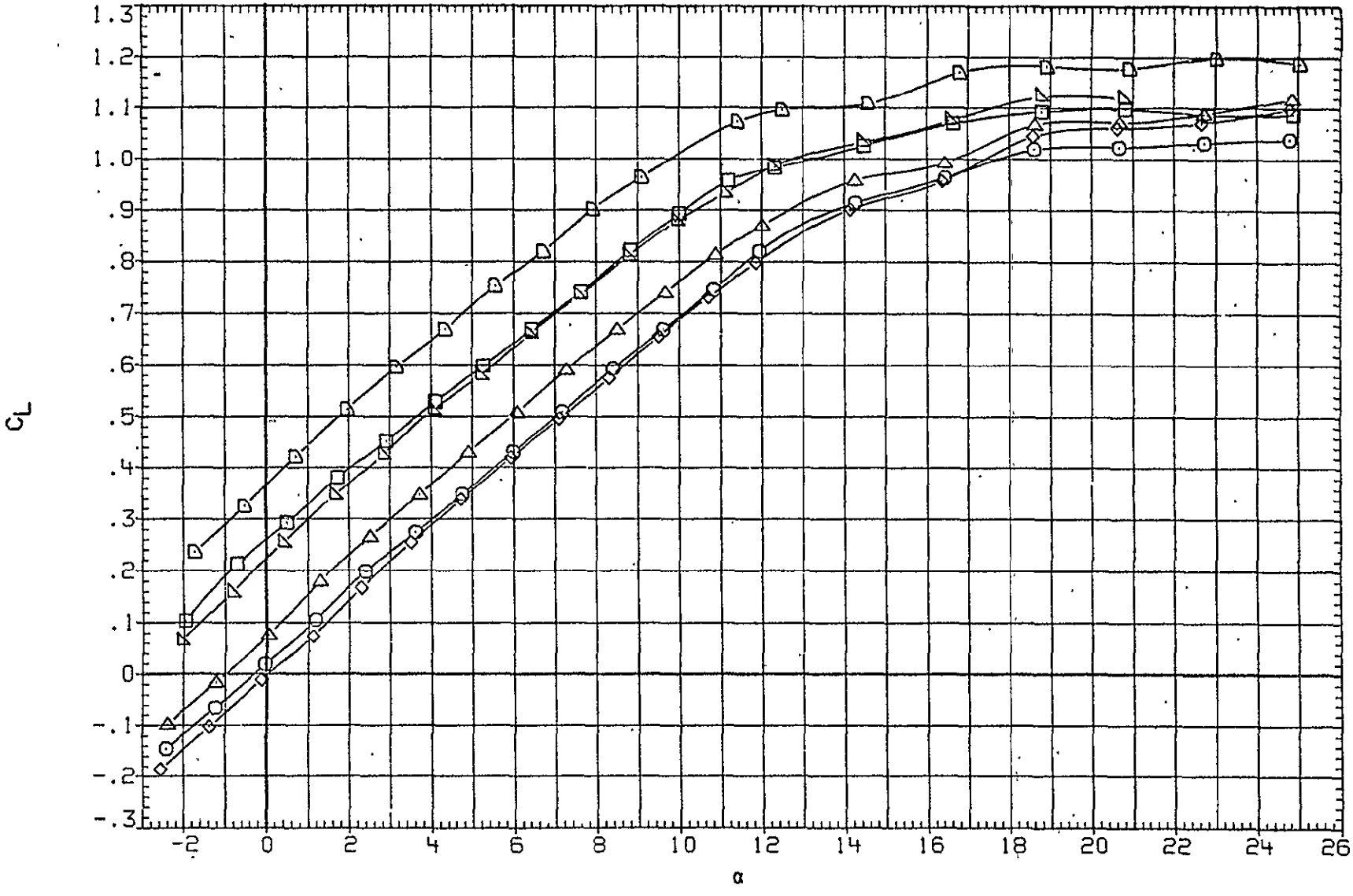

FIG. 5 EFFECT OF SYMM. T.E. DEFL. FOR CONFORMAL FLAPS. TAIL OFF.

(A)MACH = .70

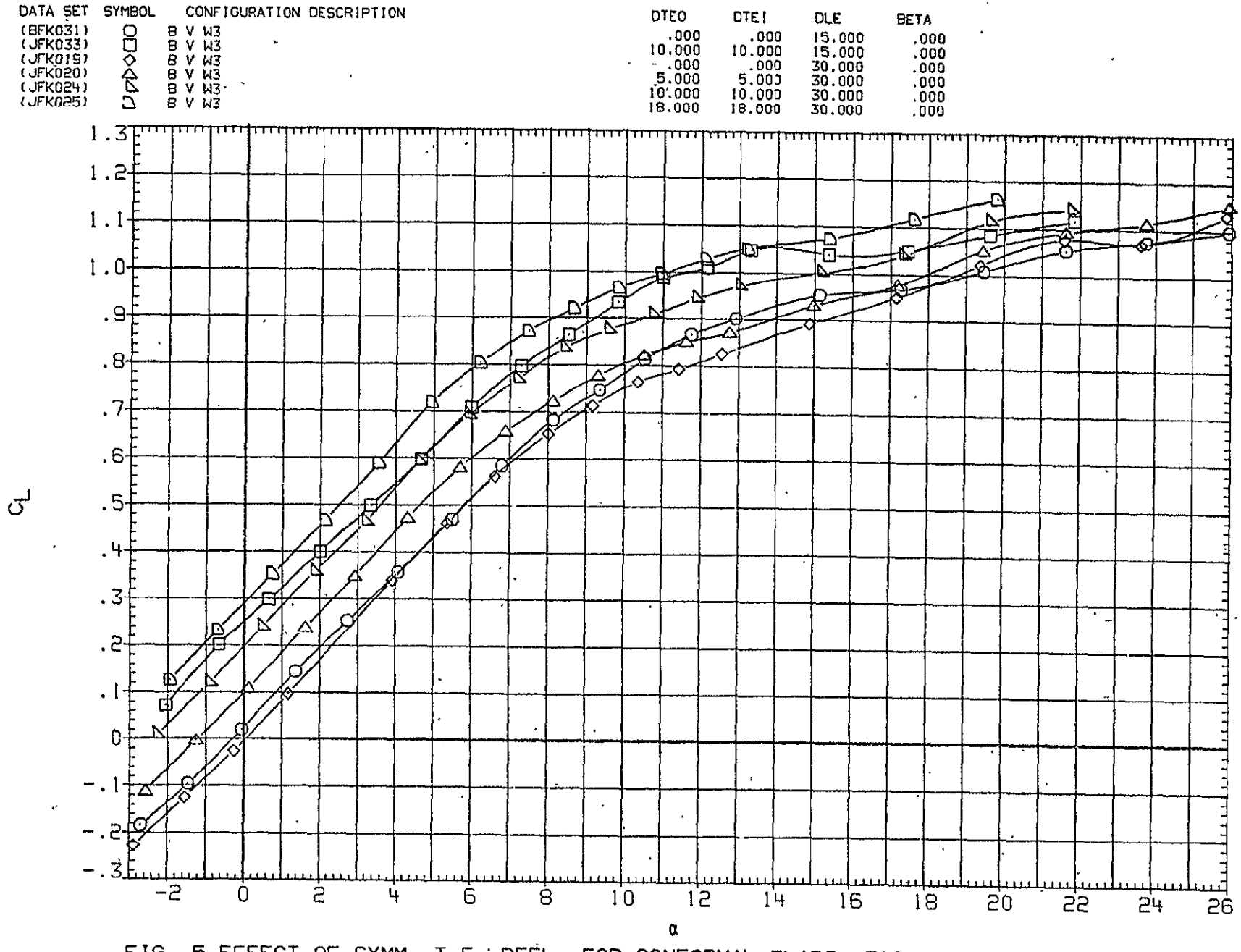

FIG. 5 EFFECT OF SYMM. T.E. DEFL. FOR CONFORMAL FLAPS, TAIL OFF.

(B)MACH = .90

DATA SET	SYMBOL	CONFIGURATION DESCRIPTION	DTEO	DTEI	DLE	BETA
(BFK031)	○	B V W3	.000	.000	15.000	.000
(JFK033)	□	B V W3	10.000	10.000	15.000	.000
(JFK019)	◇	B V W3	.000	.000	30.000	.000
(JFK020)	△	B V W3	5.000	5.000	30.000	.000
(JFK024)	◺	B V W3	10.000	10.000	30.000	.000
(JFK025)	▱	B V W3	18.000	18.000	30.000	.000

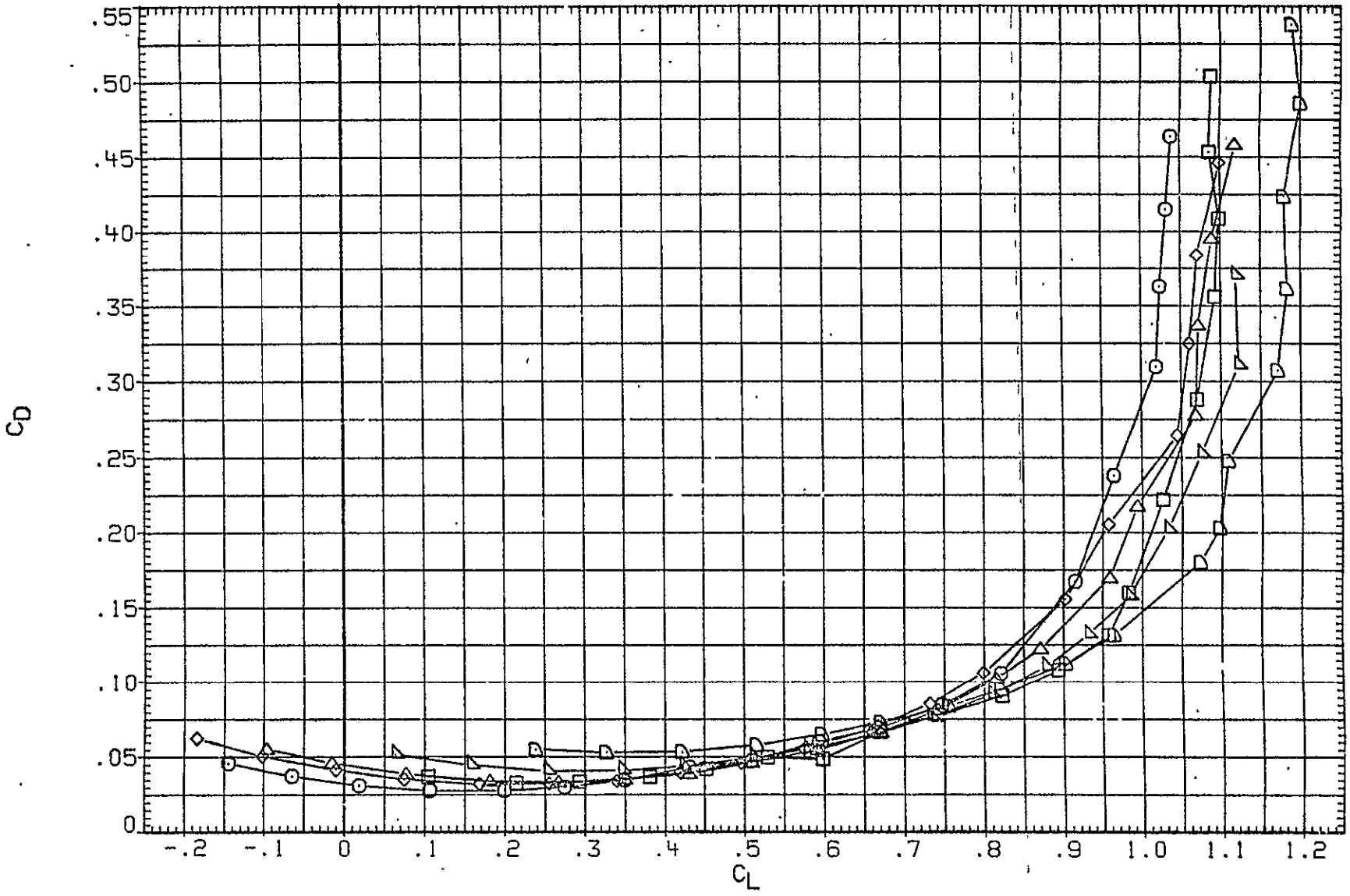

FIG. 5 EFFECT OF SYMM. T.E. DEFL. FOR CONFORMAL FLAPS. TAIL OFF.

(A) MACH = .70

DATA SET	SYMBOL	CONFIGURATION DESCRIPTION	DTEO	DTEI	DLE	BETA
(BFK031)	○	B V W3	.000	.000	15.000	.000
(JFK033)	□	B V W3	10.000	10.000	-15.000	.000
(JFK019)	◇	B V W3	.000	.000	30.000	.000
(JFK020)	△	B V W3	5.000	5.000	30.000	.000
(JFK024)	△	B V W3	10.000	10.000	30.000	.000
(JFK025)	▱	B V W3	18.000	18.000	30.000	.000

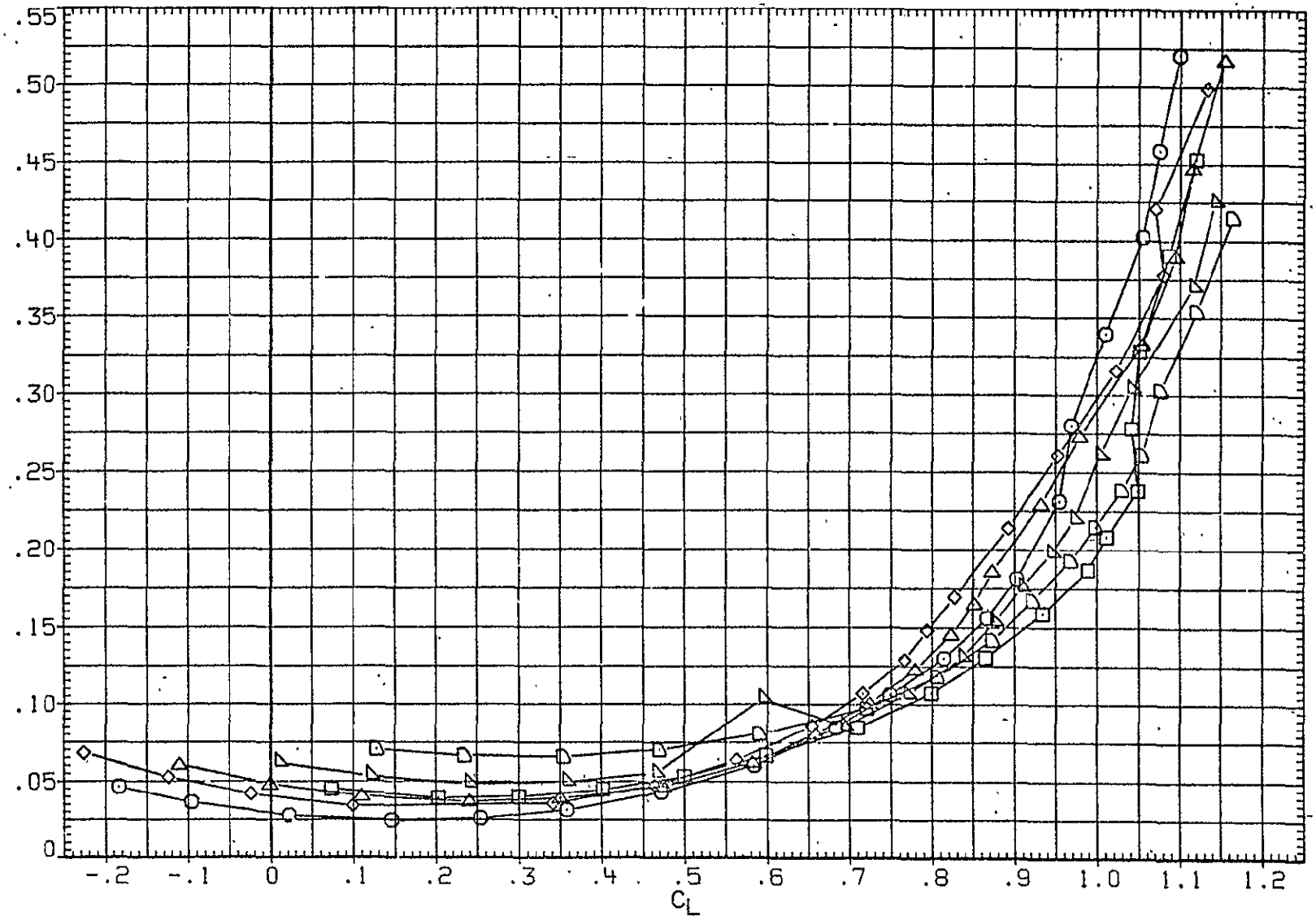

FIG. 5 EFFECT OF SYMM. T.E. DEFL. FOR CONFORMAL FLAPS. TAIL OFF.

(B) MACH = .90

DATA SET	SYMBOL	CONFIGURATION DESCRIPTION	DTEO	DTEI	DLE	BETA
(BFK031)	○	B V W3	.000	.000	15.000	.000
(JFK033)	□	B V W3	10.000	10.000	15.000	.000
(JFK019)	◇	B V W3	.000	.000	30.000	.000
(JFK020)	△	B V W3	5.000	5.000	30.000	.000
(JFK024)	◁	B V W3	10.000	10.000	30.000	.000
(JFK025)	⬠	B V W3	18.000	18.000	30.000	.000

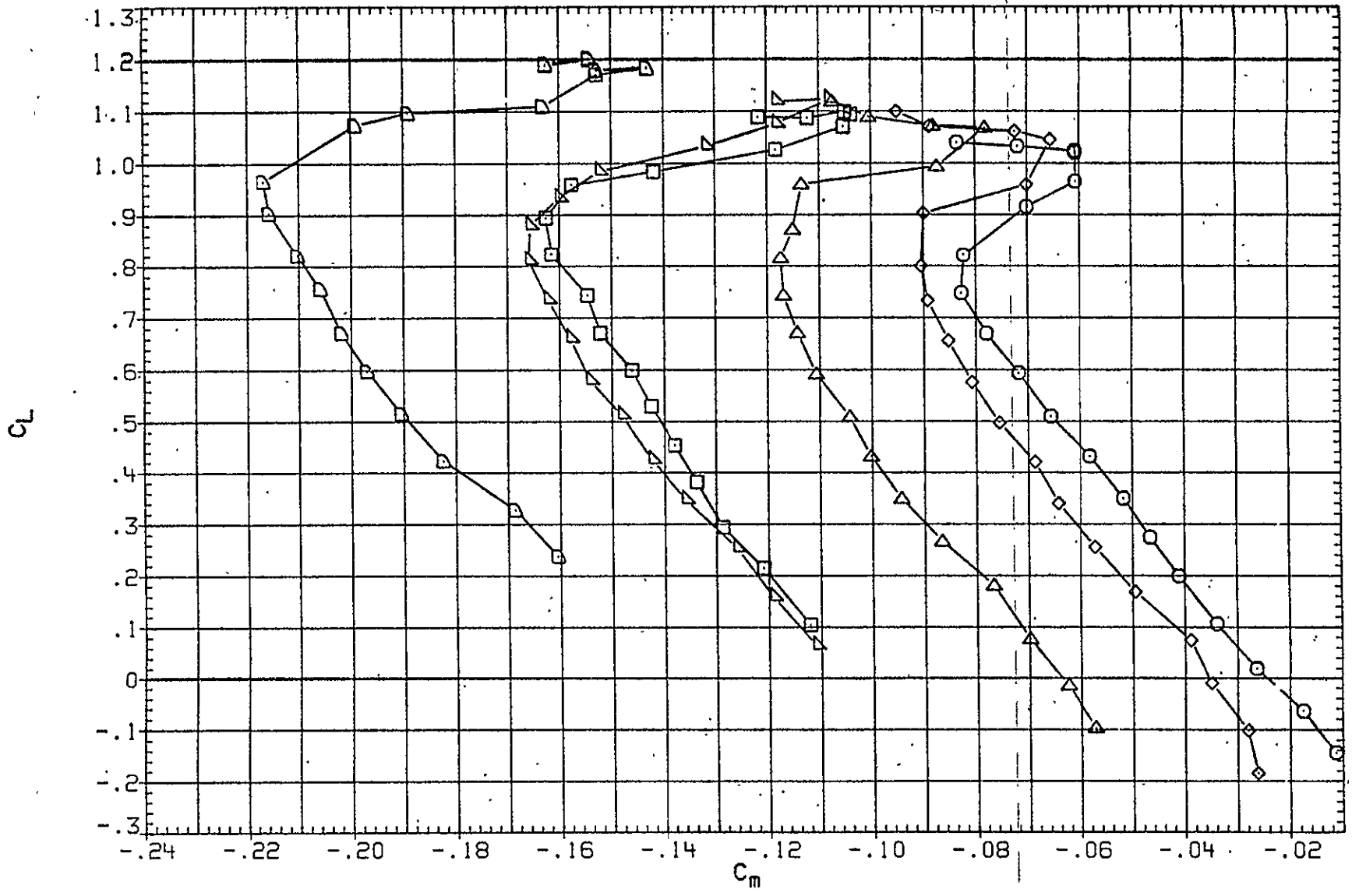

FIG. 5 EFFECT OF SYMM. T.E. DEFL. FOR CONFORMAL FLAPS. TAIL OFF.

(A)MACH = .70

DATA SET	SYMBOL	CONFIGURATION DESCRIPTION	DTEO	DTEI	DLE	BETA
(BFK031)	○	B V W3	.000	.000	15.000	.000
(JFK033)	□	B V W3	10.000	10.000	15.000	.000
(JFK019)	◇	B V W3	.000	.000	30.000	.000
(JFK020)	△	B V W3	5.000	5.000	30.000	.000
(JFK024)	⊿	B V W3	10.000	10.000	30.000	.000
(JFK025)	▱	B V W3	18.000	18.000	30.000	.000

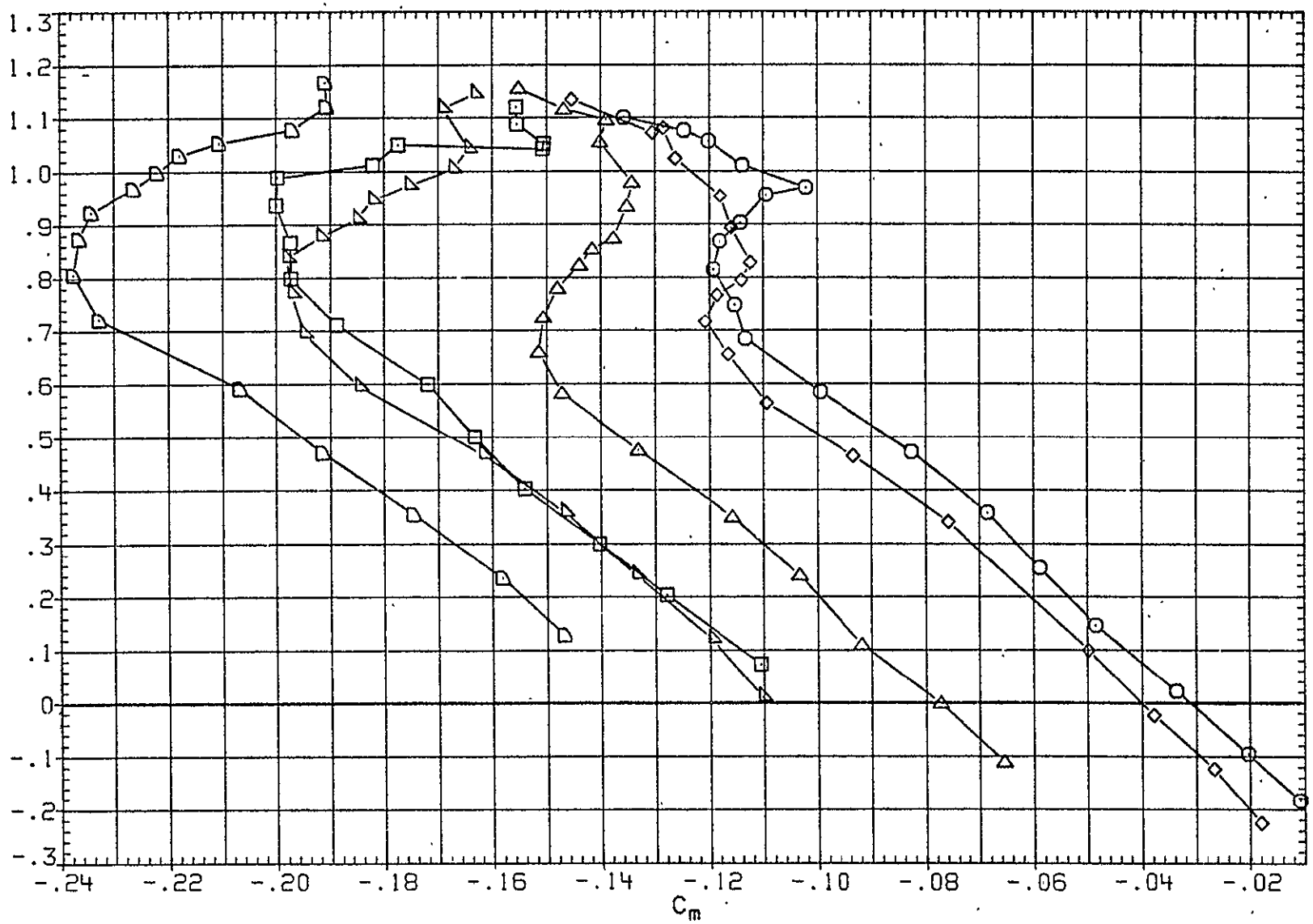

FIG. 5 EFFECT OF SYMM. T.E. DEFL. FOR CONFORMAL FLAPS. TAIL OFF.

(B)MACH = .90

DATA SET	SYMBOL	CONFIGURATION DESCRIPTION	DTEO	DTEI	DLE	BETA'
(JFK028)	○	B V W5	10.000	10.000	30.000	.000
(JFK027)	□	B V W4	18.000	18.000	30.000	.000

FIG. 6 EFFECT OF SYMM. T.E. DEFL. FOR SIMPLE HINGE AND CONFORMAL FLAPS. TAIL OFF

(A) MACH = .70

DATA SET	SYMBOL	CONFIGURATION DESCRIPTION	DTEO	DTEI	DLE	BETA
(JFK028)	○	B V W5	10.000	10.000	30.000	.000
(JFK027)	□	B V W4	18.000	18.000	30.000	.000

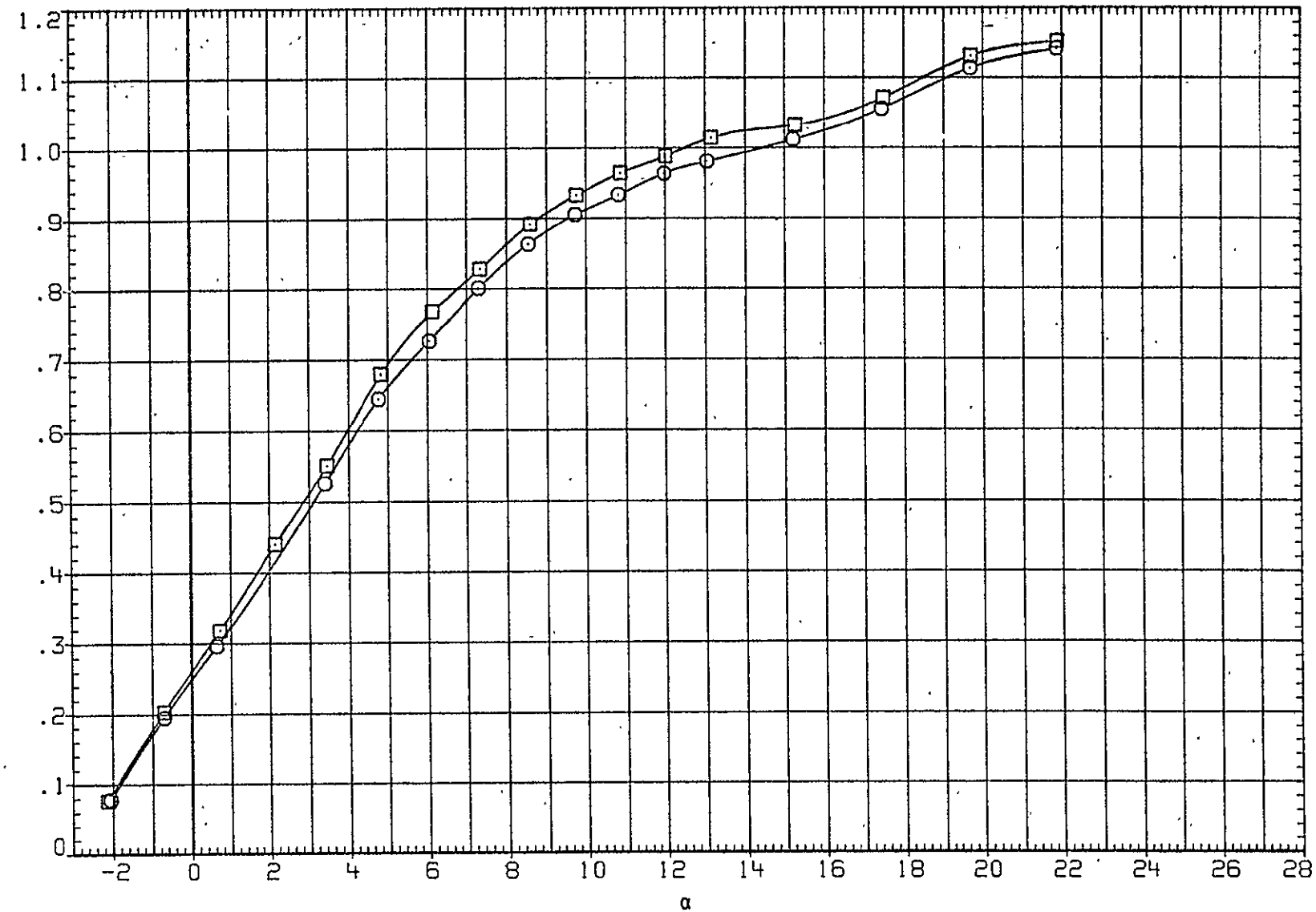

FIG. 6 EFFECT OF SYMM. T.E. DEFL. FOR SIMPLE HINGE AND CONFORMAL FLAPS. TAIL OFF

(B) MACH = .90

DATA SET	SYMBOL	CONFIGURATION DESCRIPTION	DTEO	DTEI	DLE	BETA
(JFK028)	○	B V W5	10.000	10.000	30.000	.000
(JFK027)	□	B V W4	18.000	18.000	30.000	.000

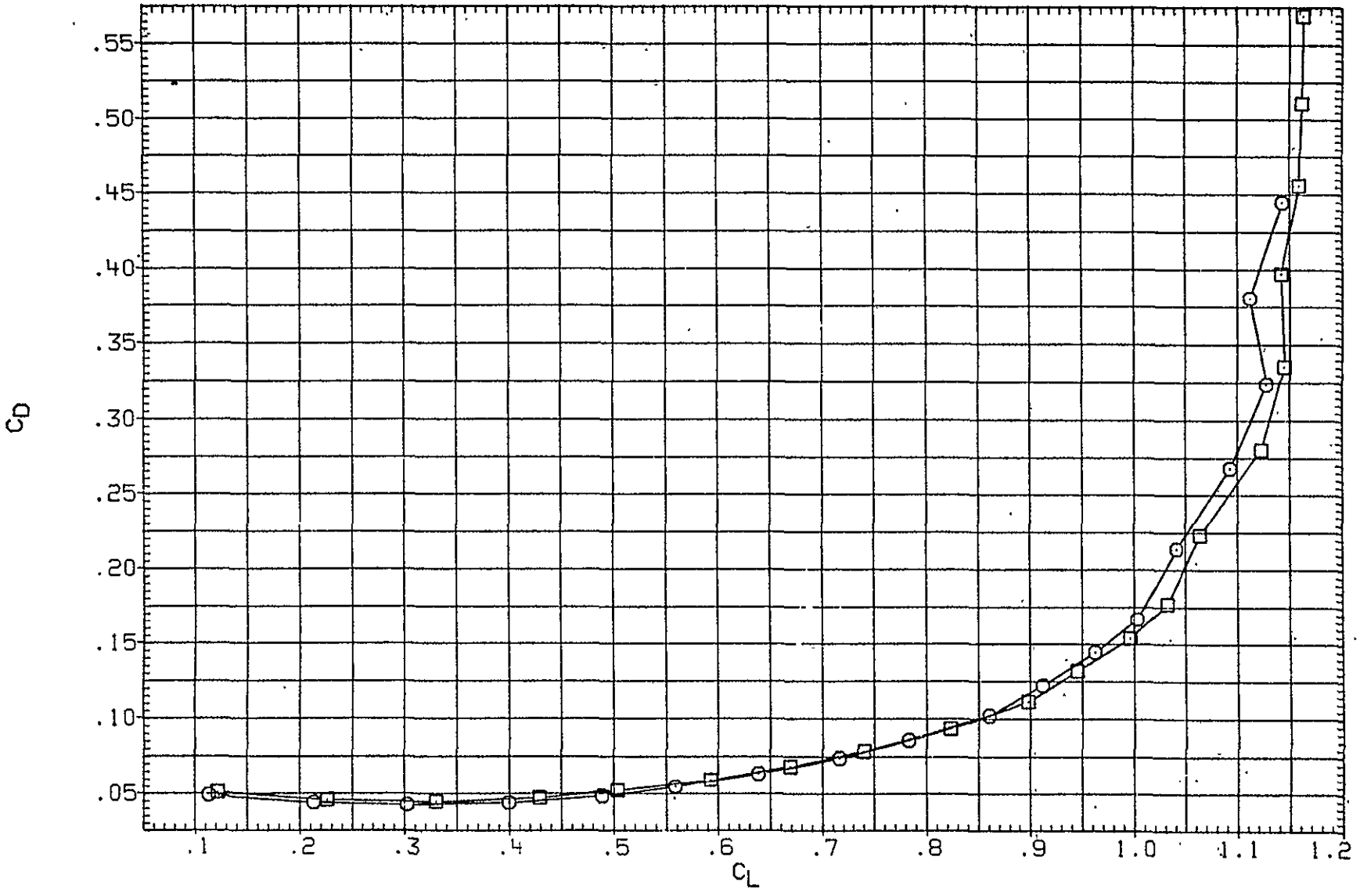

FIG. 6 EFFECT OF SYMM. T.E. DEFL. FOR SIMPLE HINGE AND CONFORMAL FLAPS. TAIL OFF

(A) MACH = .70

DATA SET	SYMBOL	CONFIGURATION DESCRIPTION	DTEO	DTEI	DLE	BETA
(JFK028)	○	B V W5	10.000	10.000	30.000	.000
(JFK027)	□	B V W4	18.000	18.000	30.000	.000

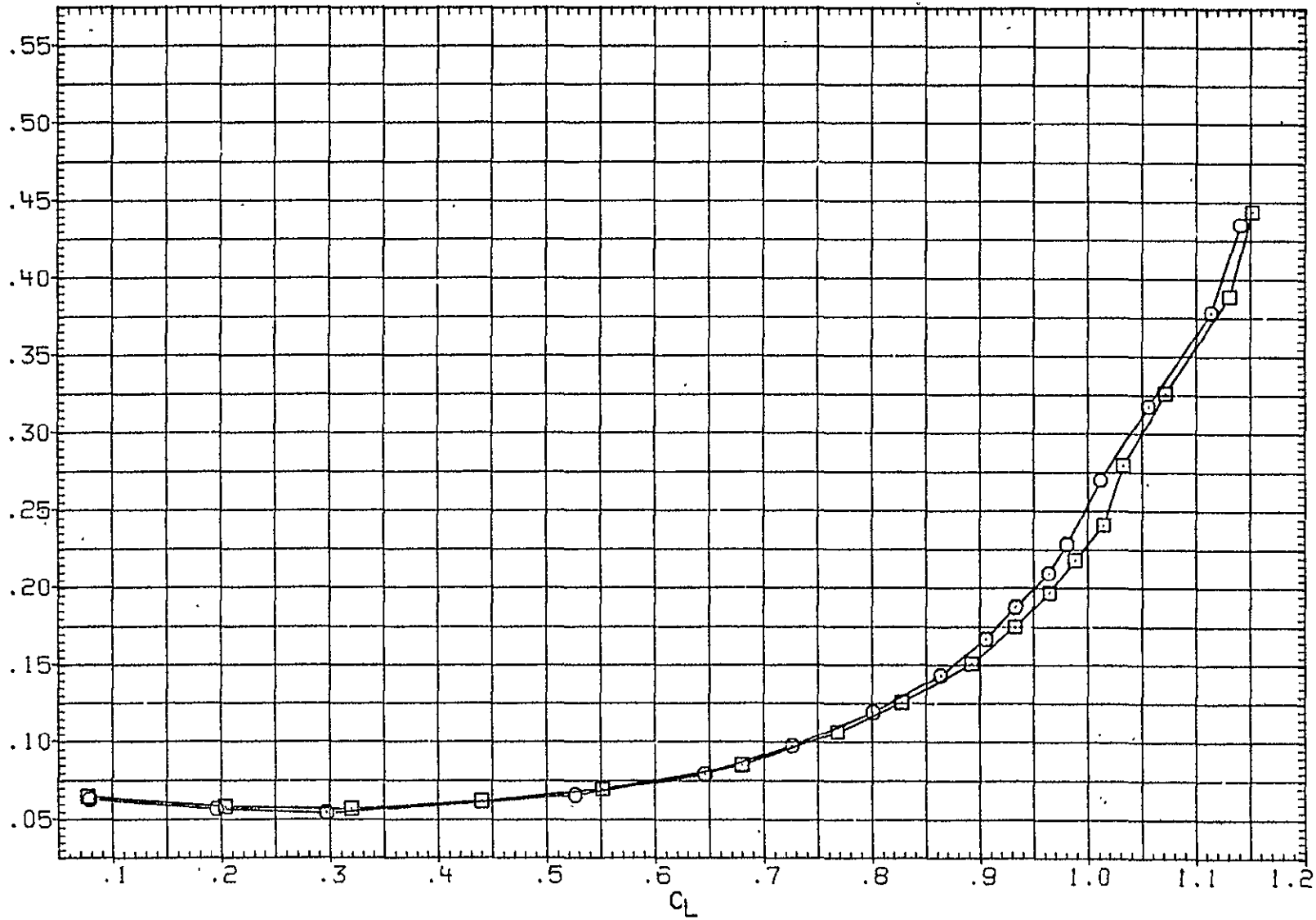

FIG. 6 EFFECT OF SYMM. T.E. DEFL. FOR SIMPLE HINGE AND CONFORMAL FLAPS. TAIL OFF

(B) MACH = .90

DATA SET	SYMBOL	CONFIGURATION DESCRIPTION	DTEO	DTEI	DLE	BETA
(JFK028)	○	B V W5	10.000	10.000	30.000	.000
(JFK027)	□	B V W4	18.000	18.000	30.000	.000

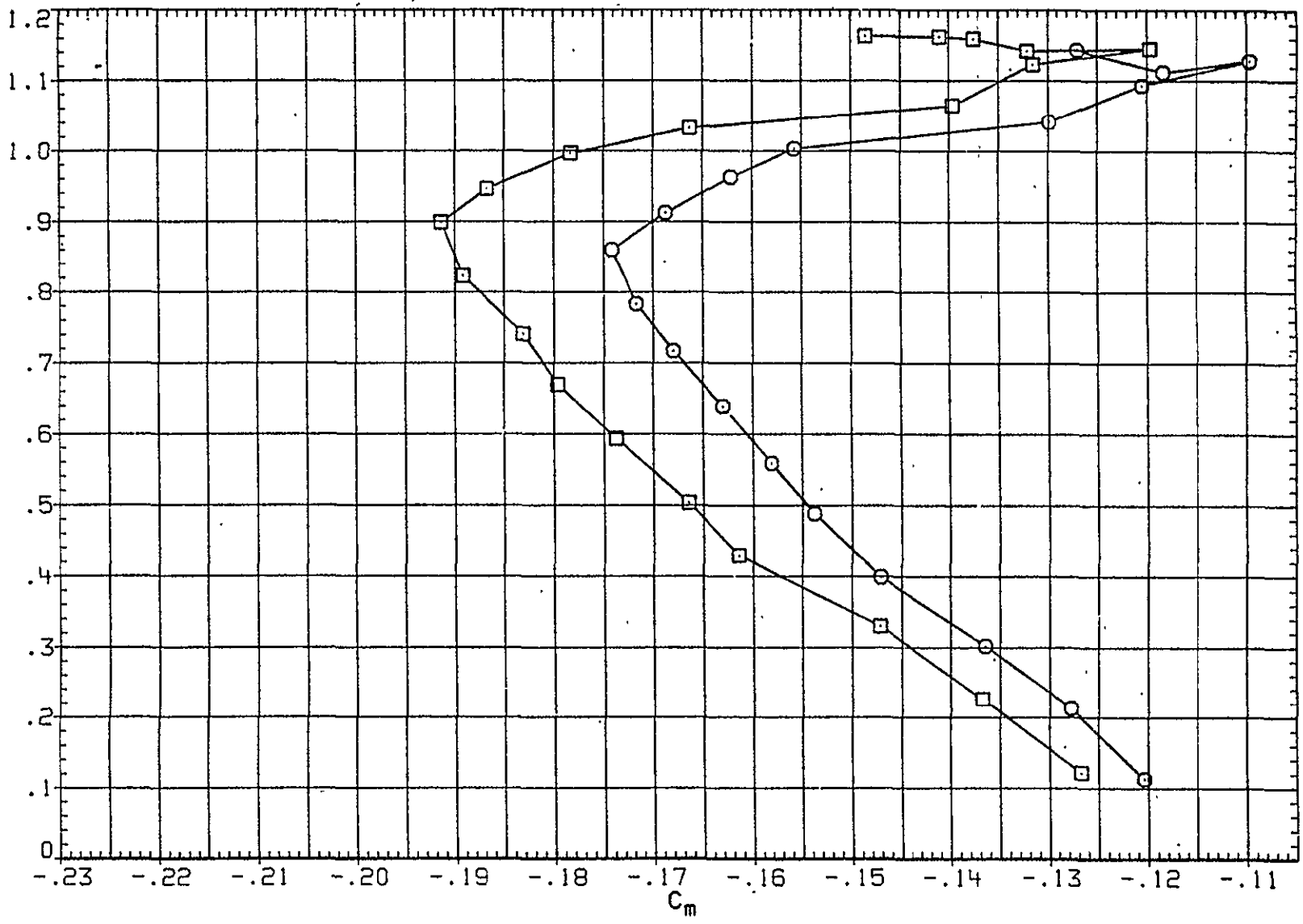

FIG. 6 EFFECT OF SYMM. T.E. DEFL. FOR SIMPLE HINGE AND CONFORMAL FLAPS. TAIL OFF

(A)MACH = .70

DATA SET	SYMBOL	CONFIGURATION DESCRIPTION	DTEO	DTEI	DLE	BETA
(JFK028)	○	B V W5	10.000	10.000	30.000	.000
(JFK027)	□	B V W4	18.000	18.000	30.000	.000

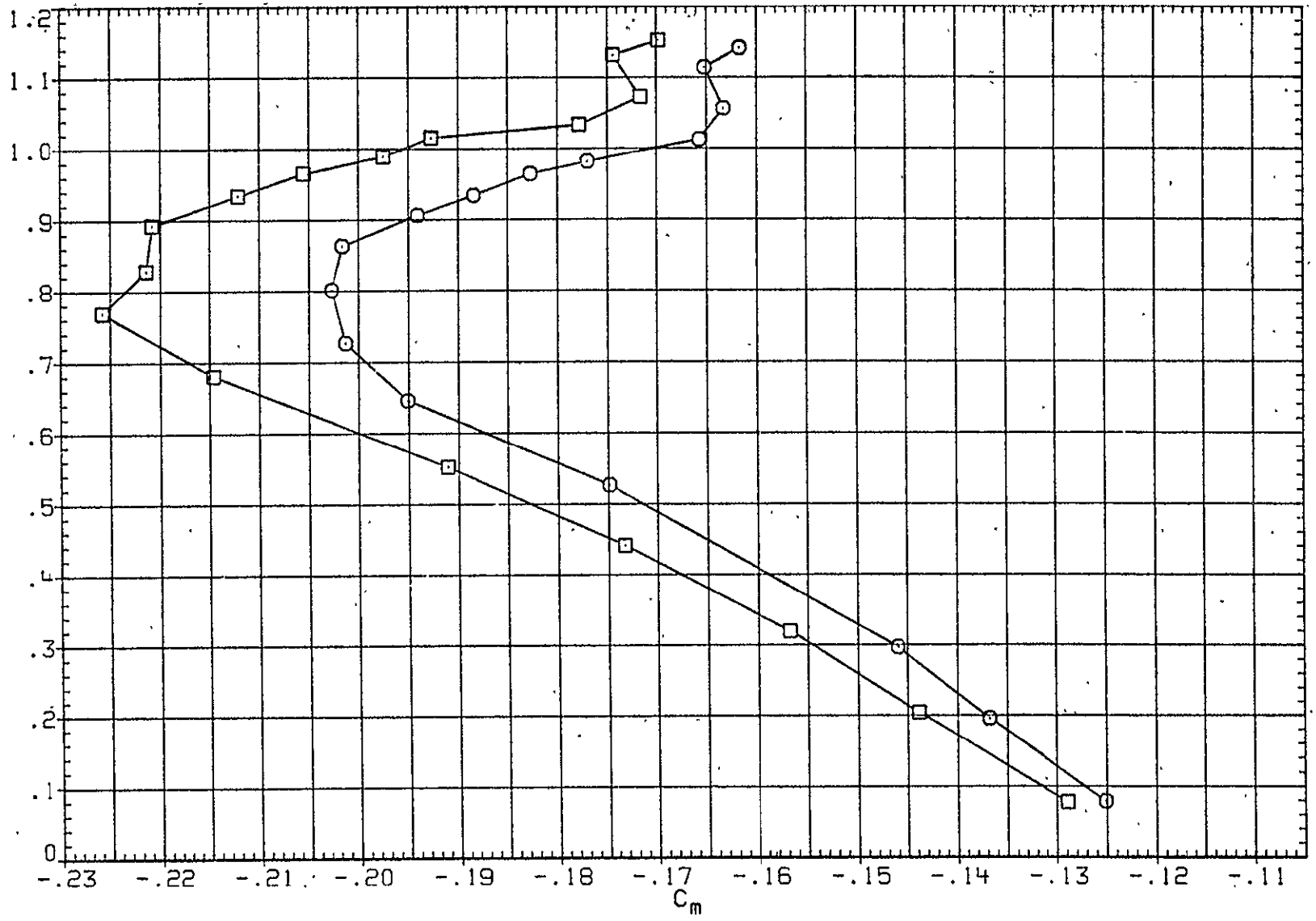

FIG. 6 EFFECT OF SYMM. T.E. DEFL. FOR SIMPLE HINGE AND CONFORMAL FLAPS. TAIL OFF

(B)MACH = .90

DATA SET	SYMBOL	CONFIGURATION DESCRIPTION	DTEI-L	DTEI-R	DTEO	DLE
(JFK038)	○	B V W2H	.000	-15.000	.000	.000
(BFK036)	□	B V W2H	5.000	-5.000	.000	.000
(JFK037)	◇	B V W2H	25.000	-15.000	.000	.000
(JFK030)	◁	B V W4H	10.000	-5.000	10.000	30.000
(JFK029)	△	B V W4H	25.000	-15.000	10.000	30.000

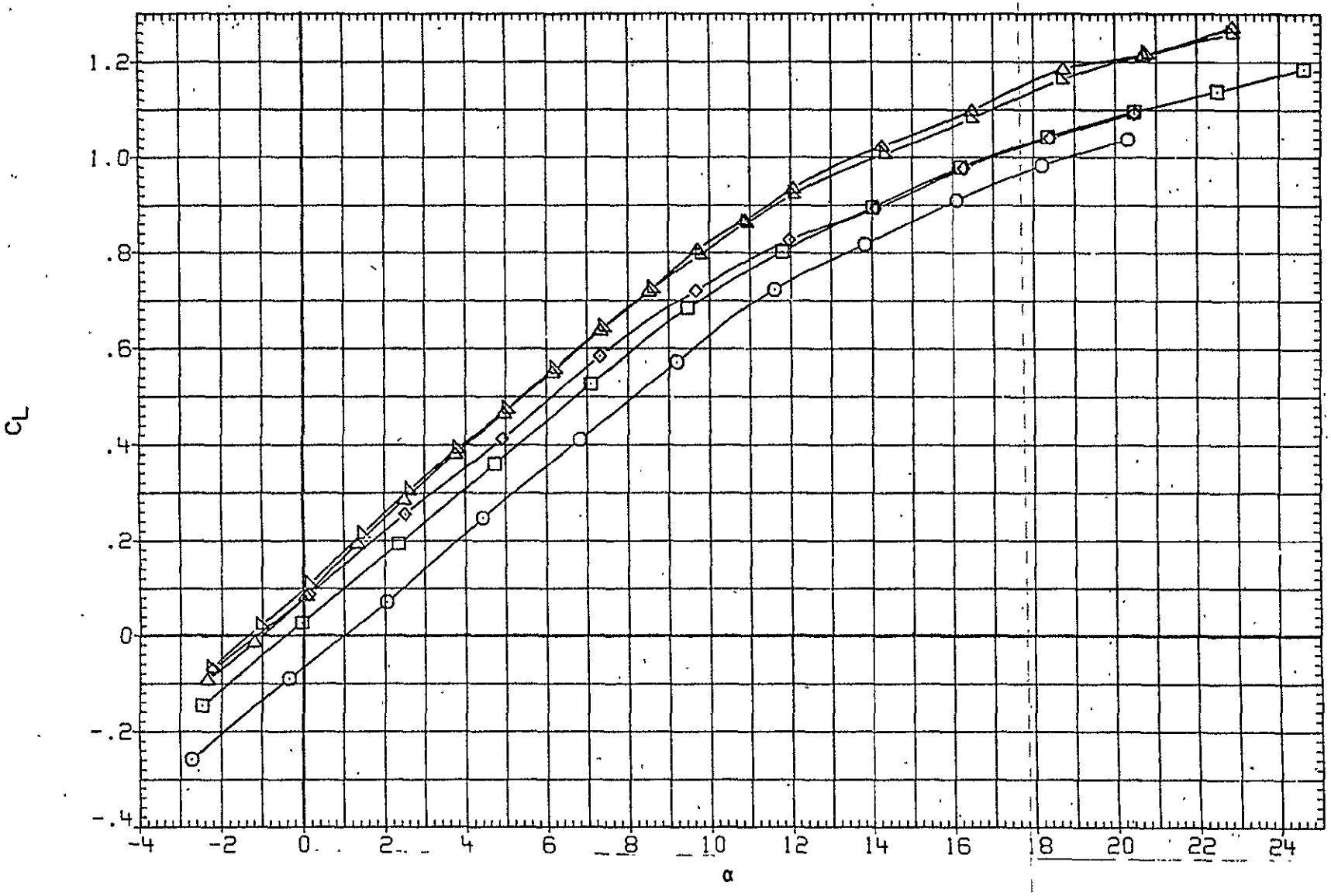

FIG. 7 EFFECT OF ASYM. T.E. DEFL. FOR SIMPLE HINGE AND CONFORMAL FLAPS. TAIL ON

(A) MACH = .70

DATA SET	SYMBOL	CONFIGURATION DESCRIPTION	DTEI-L	DTEI-R	DTEO	DLE
(JFK038)	○	B V W2H	.000	-15.000	.000	.000
(BFK036)	□	B V W2H	5.000	-5.000	.000	.000
(JFK037)	◇	B V W2H	25.000	-15.000	.000	.000
(JFK030)	△	B V W4H	10.000	-5.000	10.000	30.000
(JFK029)	◁	B V W4H	25.000	-15.000	10.000	30.000

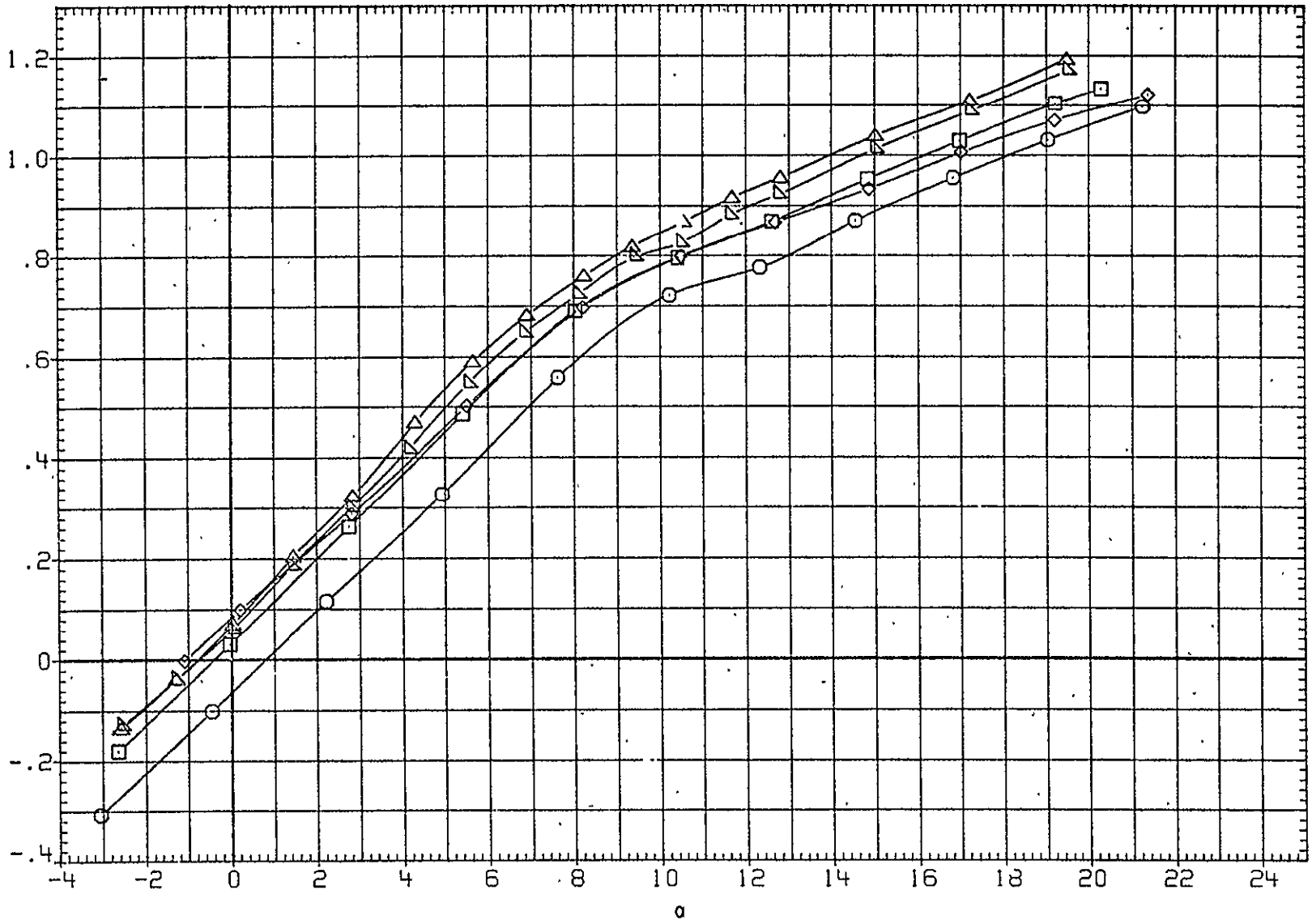

FIG. 7 EFFECT OF ASYM. T.E. DEFL. FOR SIMPLE HINGE AND CONFORMAL FLAPS. TAIL ON

(B) MACH = .90

DATA SET	SYMBOL	CONFIGURATION DESCRIPTION	DTEI-L	DTEI-R	DTEO	DLE
(JFK038)	○	B V W2H	.000	-15.000	.000	.000
(BFK036,	□	B V W2H	5.000	-5.000	.000	.000
(JFK037)	◇	B V W2H	25.000	-15.000	.000	.000
(JFK030)	△	B V W4H	10.000	-5.000	10.000	30.000
(JFK029)	◺	B V W4H	25.000	-15.000	10.000	30.000

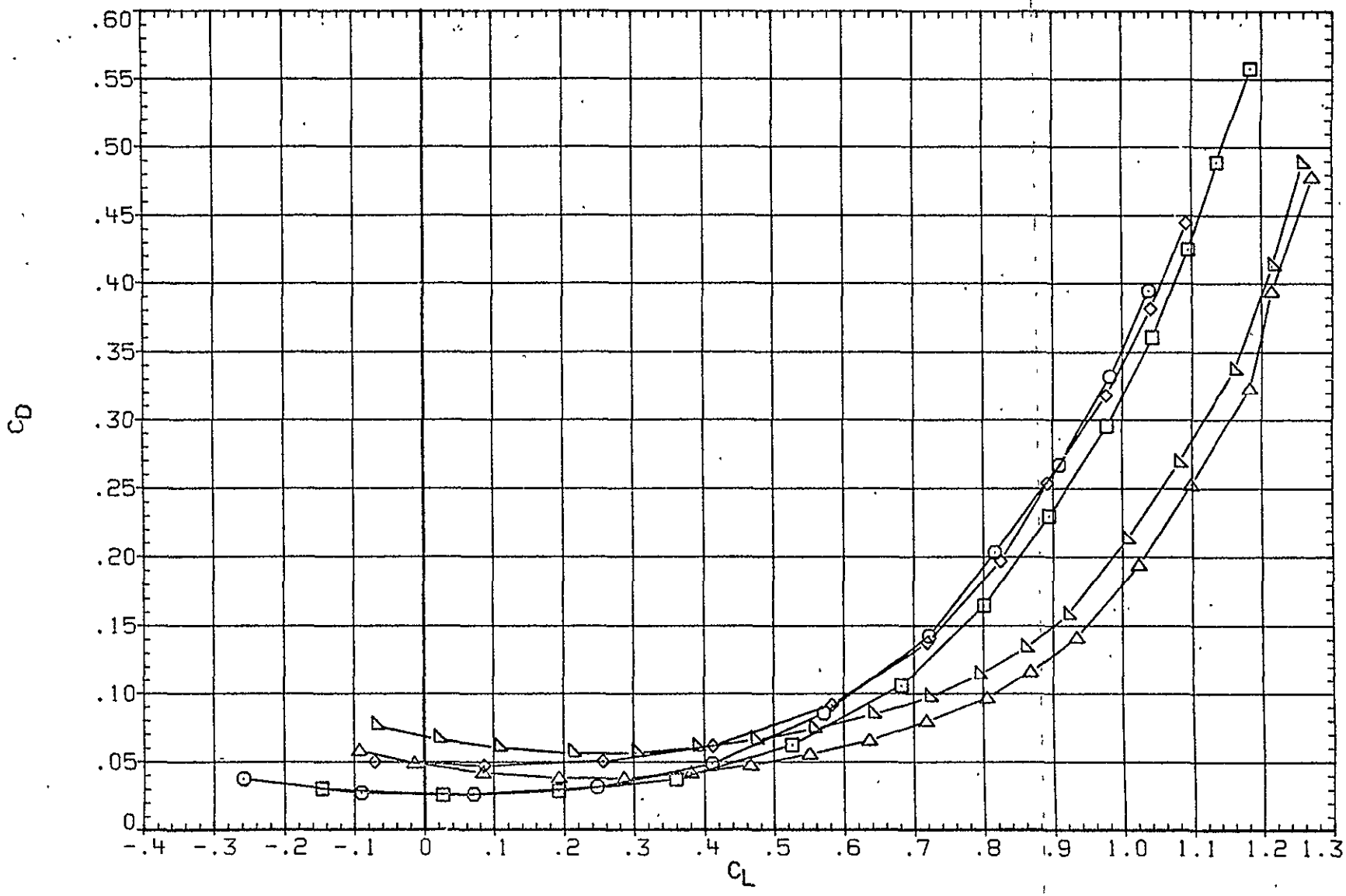

FIG. 7 EFFECT OF ASYM. T.E. DEFL. FOR SIMPLE HINGE AND CONFORMAL FLAPS. TAIL ON

(A) MACH = .70

DATA SET	SYMBOL	CONFIGURATION DESCRIPTION	DTEI-L	DTEI-R	DTEO	DLE
(JFK038)	○	B V W2H	.000	-15.000	.000	.000
(BFK036)	□	B V W2H	5.000	-5.000	.000	.000
(JFK037)	◇	B V W2H	25.000	-15.000	.000	.000
(JFK030)	◁	B V W4H	10.000	-5.000	10.000	30.000
(JFK029)	△	B V W4H	25.000	-15.000	10.000	30.000

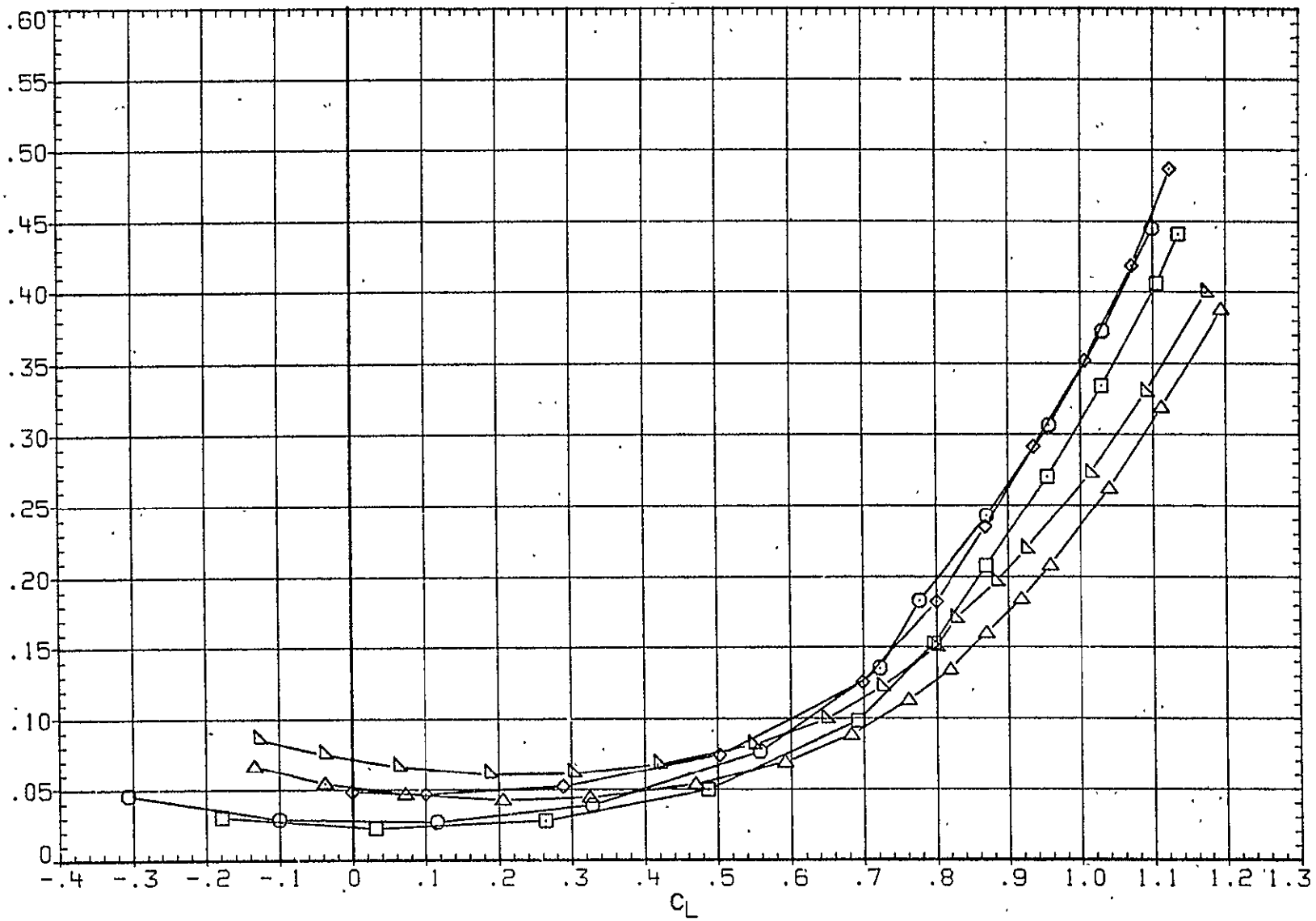

FIG. 7 EFFECT OF ASYM. T.E. DEFL. FOR SIMPLE HINGE AND CONFORMAL FLAPS. TAIL ON

(B) MACH = .90

DATA SET	SYMBOL	CONFIGURATION DESCRIPTION	DTEI-L	DTEI-R	DTEO	DLE
(JFK038)	○	B V W2H	.000	-15.000	.000	.000
(BFK036)	□	B V W2H	5.000	-5.000	.000	.000
(JFK037)	◇	B V W2H	25.000	-15.000	.000	.000
(JFK030)	△	B V W4H	10.000	-5.000	10.000	30.000
(JFK029)	◺	B V W4H	25.000	-15.000	10.000	30.000

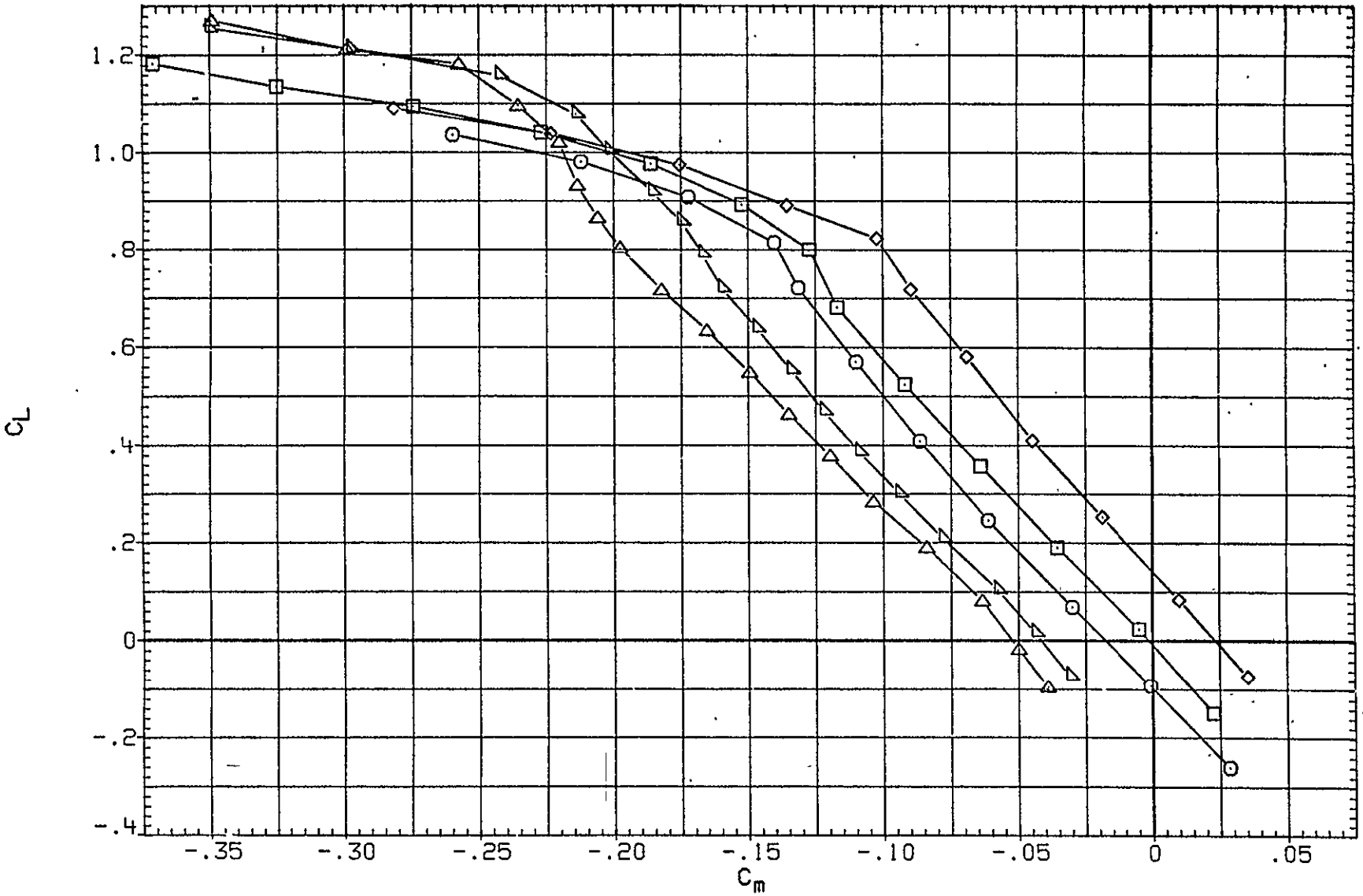

FIG. 7 EFFECT OF ASYM. T.E. DEFL. FOR SIMPLE HINGE AND CONFORMAL FLAPS. TAIL ON

(A)MACH = .70

DATA SET	SYMBOL	CONFIGURATION DESCRIPTION
(JFK038)	○	B V W2H
(BFK036)	□	B V W2H
(JFK037)	◇	B V W2H
(JFK030)	△	B V W4H
(JFK029)	◁	B V W4H

DTEI-L	DTEI-R	DTEO	DLE
.000	-15.000	.000	.000
5.000	-5.000	.000	.000
25.000	-15.000	.000	.000
10.000	-5.000	10.000	30.000
25.000	-15.000	10.000	30.000

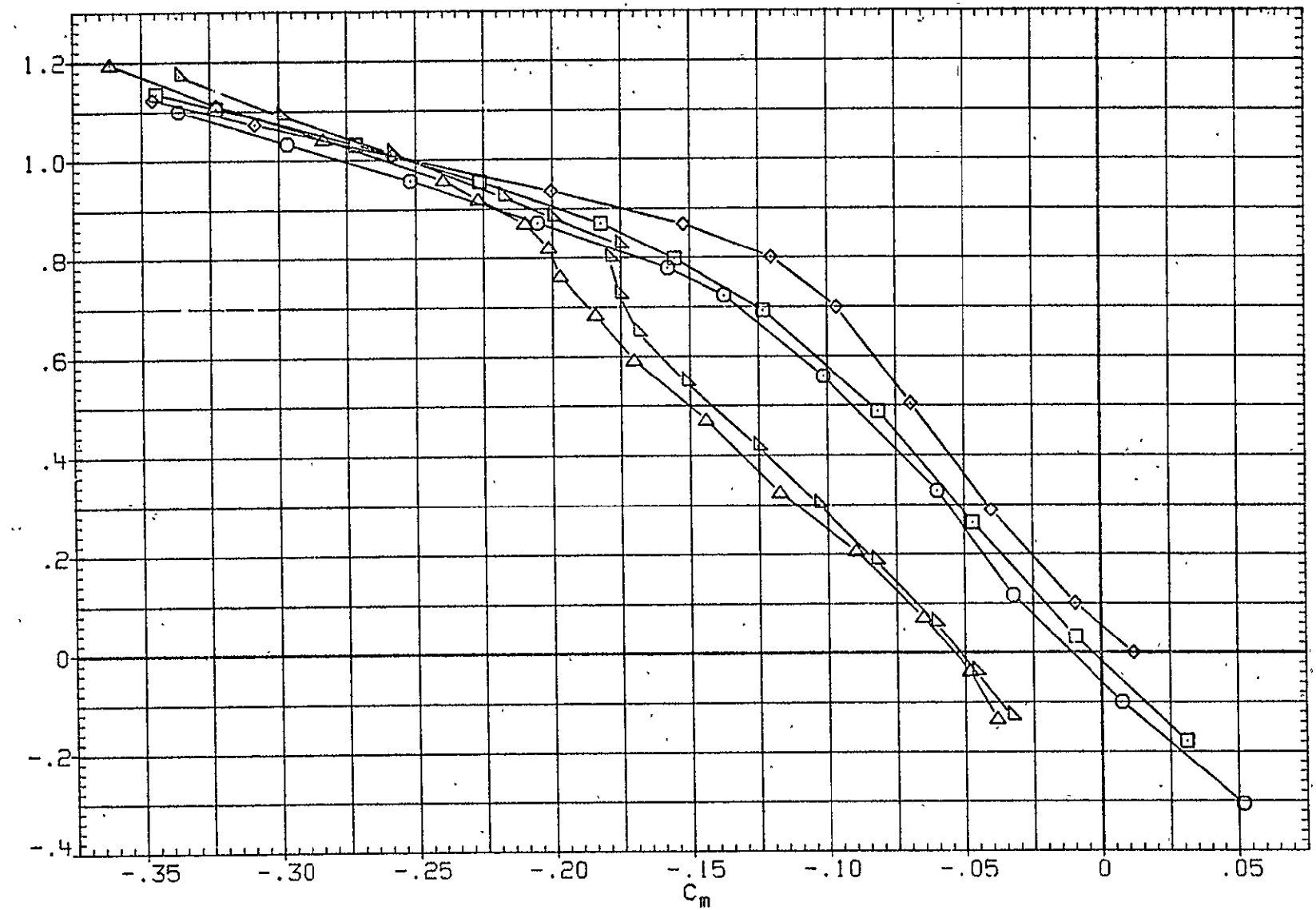

FIG. 7 EFFECT OF ASYM. T.E. DEFL. FOR SIMPLE HINGE AND CONFORMAL FLAPS. TAIL ON

(B)MACH = .90

DATA SET	SYMBOL	CONFIGURATION DESCRIPTION	DTEO	DTEI	DLE	BETA
(JFK010)	○	B V W2	.000	5.000	10.000	.000
(JFK011)	□	B V W2	-5.000	5.000	10.000	.000

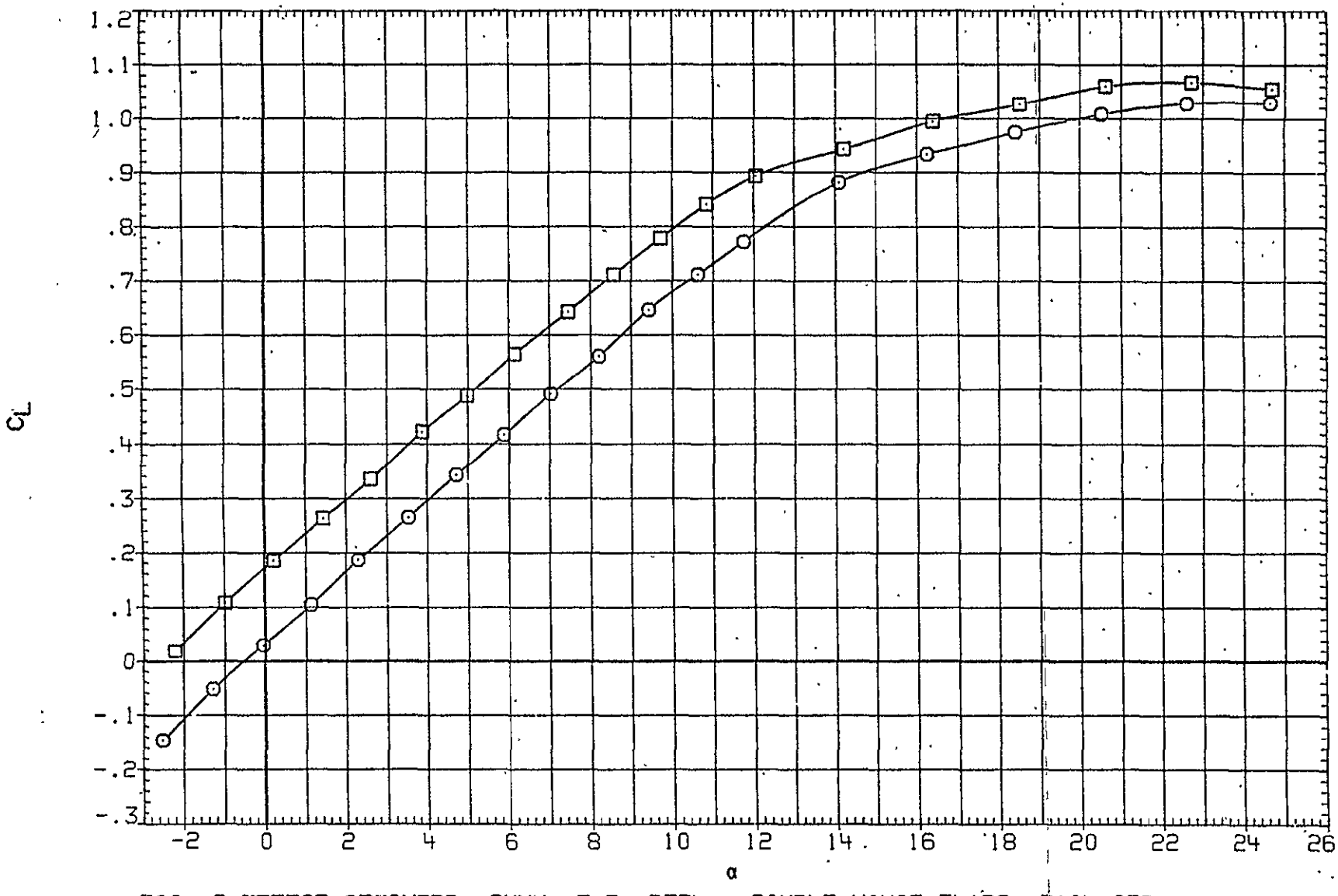

FIG. 8 EFFECT OF OUTBD. SYMM. T.E. DEFL., SIMPLE HINGE FLAPS. TAIL OFF

(A)MACH = .70

DATA SET	SYMBOL	CONFIGURATION DESCRIPTION	DTEO	DTEI	DLE	BETA
(JFK010)	○	B V W2	.000	5.000	10.000	.000
(JFK011)	□	B V W2	5.000	5.000	10.000	.000

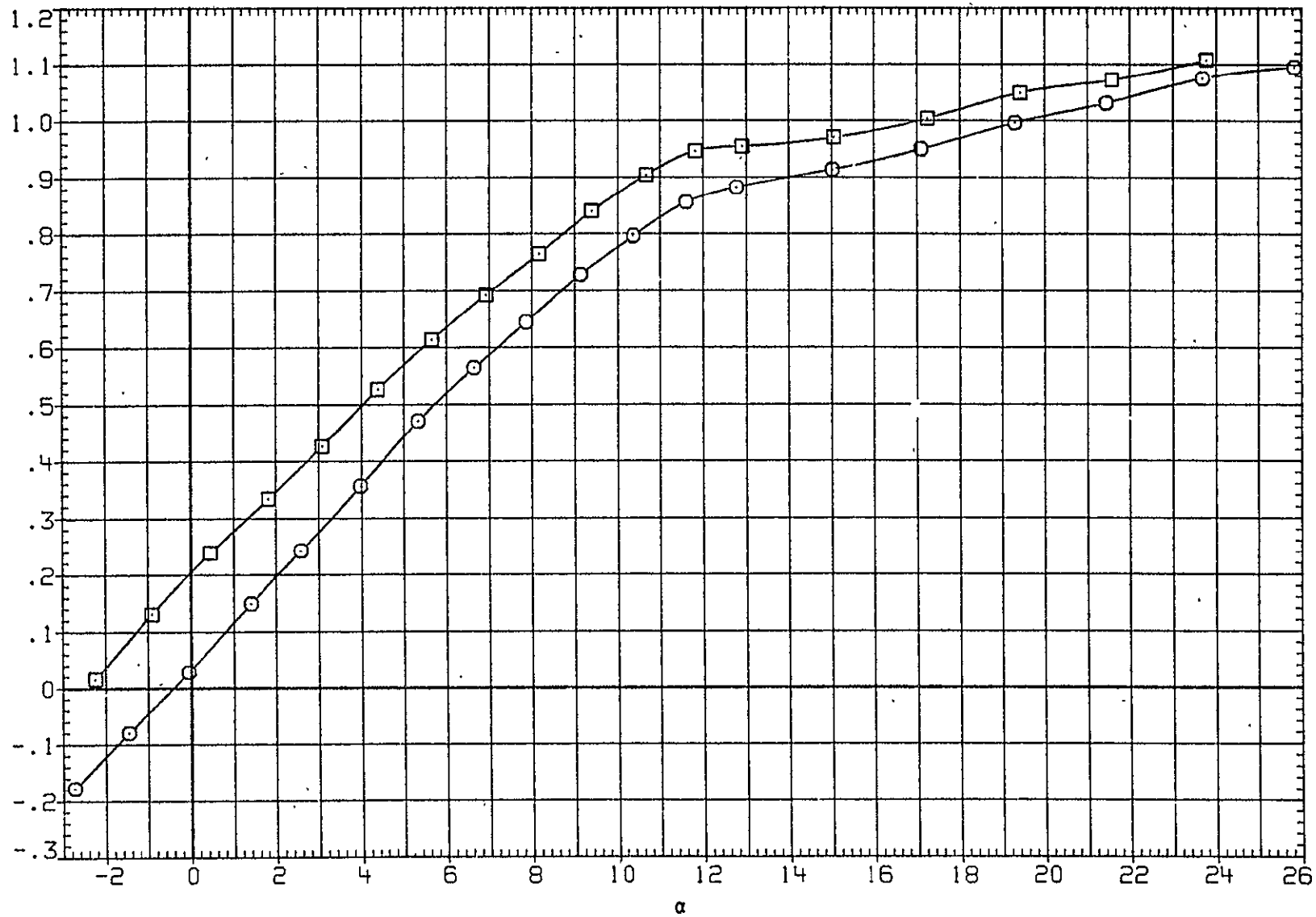

FIG. 8 EFFECT OF OUTBD. SYMM. T.E. DEFL., SIMPLE HINGE FLAPS. TAIL OFF

(B)MACH = .90

DATA SET	SYMBOL	CONFIGURATION DESCRIPTION	DTEO	DTEI	DLE	BETA
(JFK010)	⊙	B V W2	.000	5.000	10.000	.000
(JFK011)	□	DATA NOT AVAILABLE	5.000	-5.000	10.000	.000

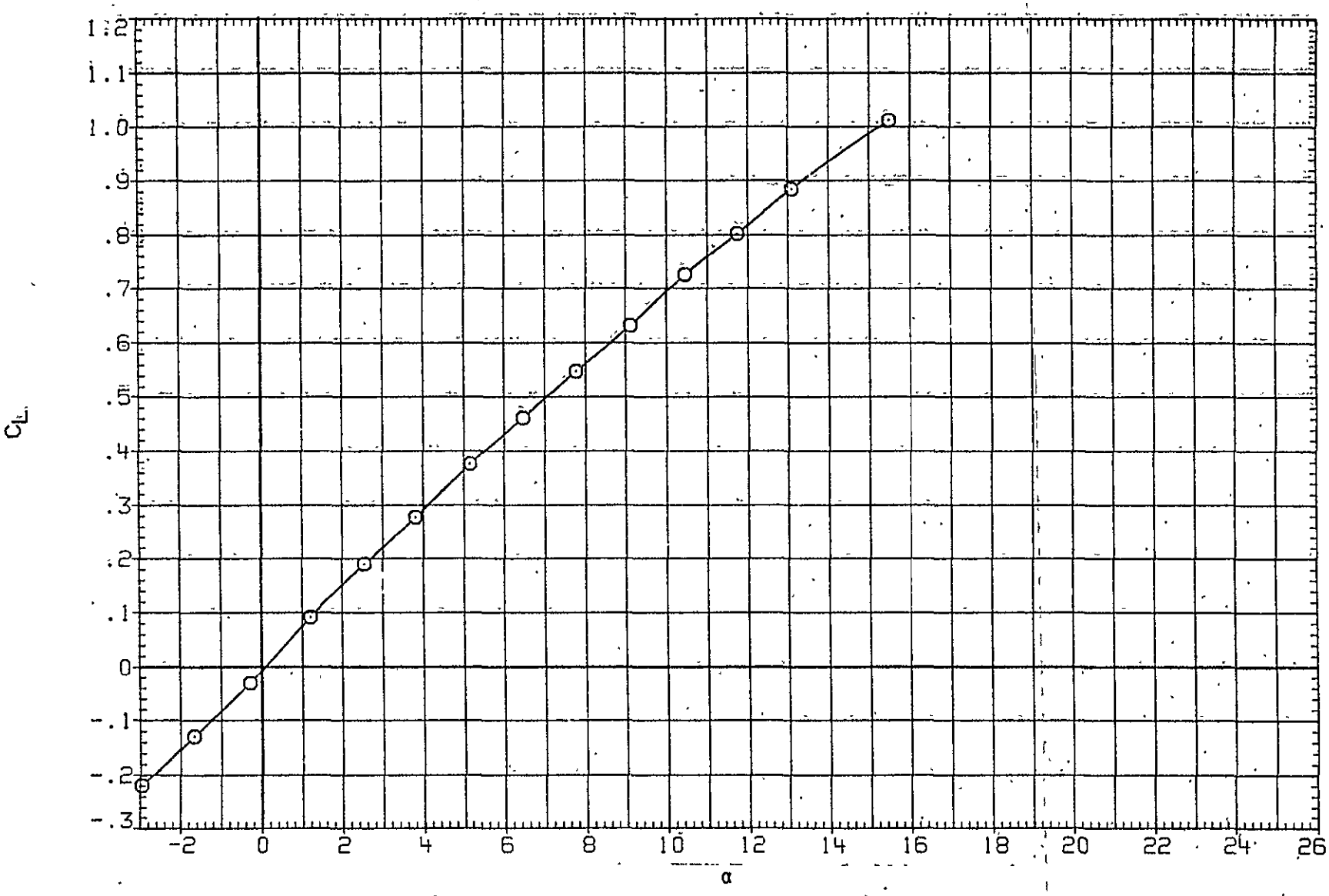

FIG. 8 EFFECT OF OUTBD. SYMM. T.E. DEFL., SIMPLE HINGE FLAPS. -TAIL OFF

(C)MACH = 1.15

DATA SET	SYMBOL	CONFIGURATION DESCRIPTION	DTEO	DTEI	DLE	BETA
(JFK010)	○	B V W2	.000	5.000	10.000	.000
(JFK011)	□	B V W2	5.000	5.000	10.000	.000

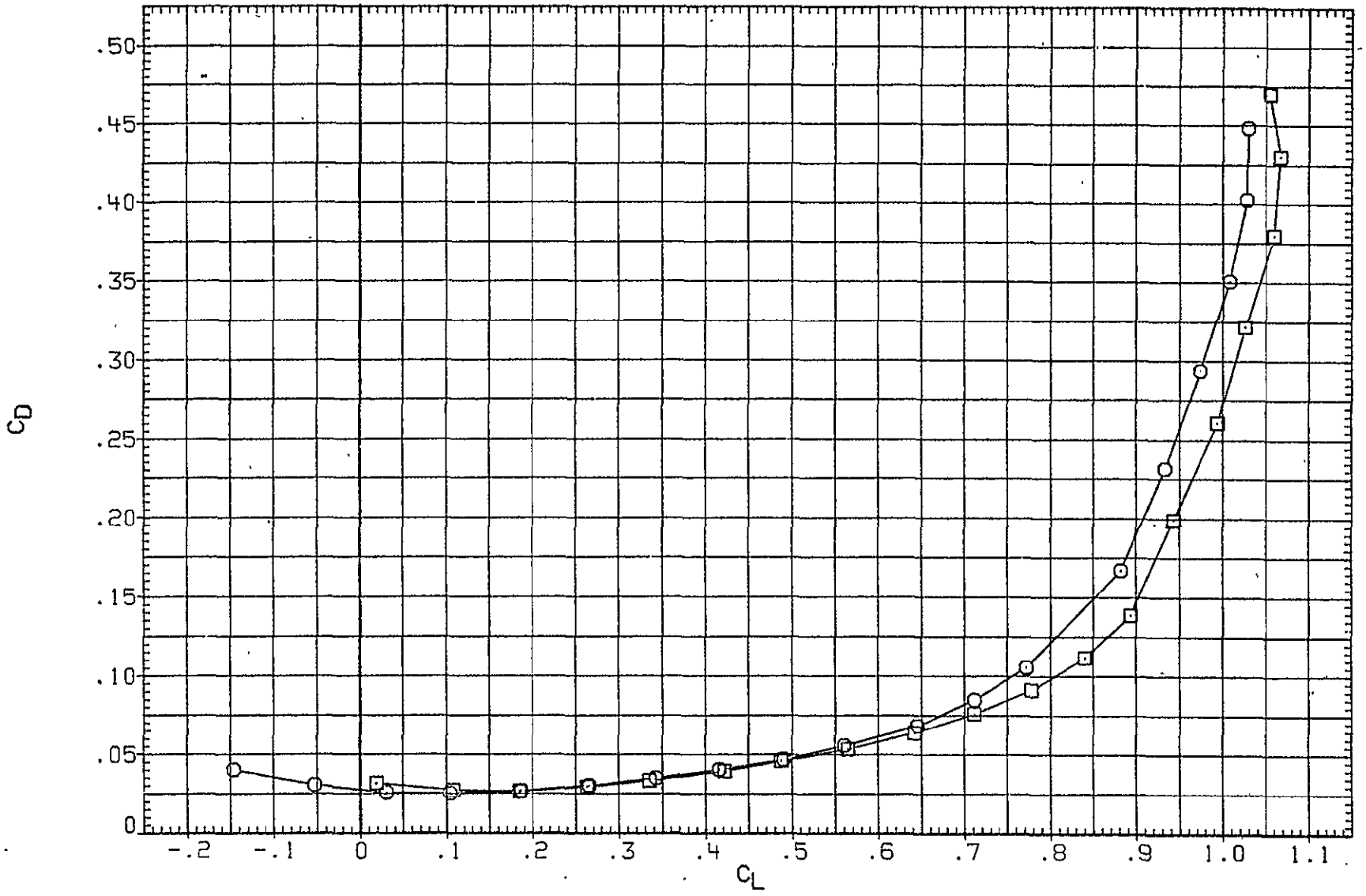

FIG. 8 EFFECT OF OUTBD. SYMM. T.E. DEFL., SIMPLE HINGE FLAPS. TAIL OFF

(A)MACH = .70

DATA SET	SYMBOL	CONFIGURATION DESCRIPTION	DTEO	DTEI	DLE	BETA
(JFK010)	○	B V W2	.000	5.000	10.000	.000
(JFK011)	□	B V W2	5.000	5.000	10.000	.000

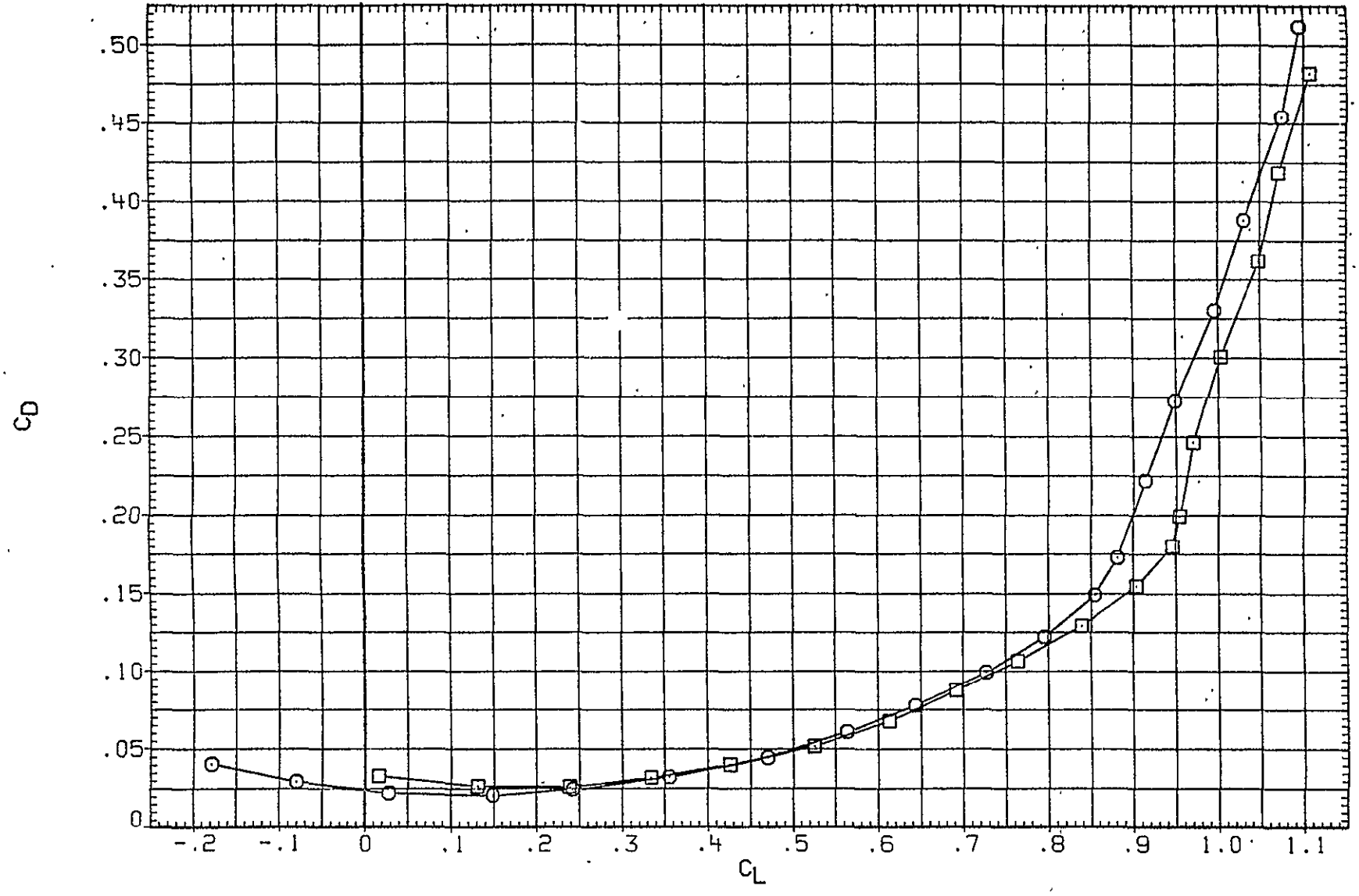

FIG. 8 EFFECT OF OUTBD. SYMM. T.E. DEFL., SIMPLE HINGE FLAPS. TAIL OFF

(B)MACH = .90

DATA SET	SYMBOL	CONFIGURATION DESCRIPTION	DTEO	DTEI	DLE	BETA
(JFK010)	○	B V W2	.000	5.000	10.000	.000
(JFK011)	□	DATA NOT AVAILABLE	5.000	5.000	10.000	.000

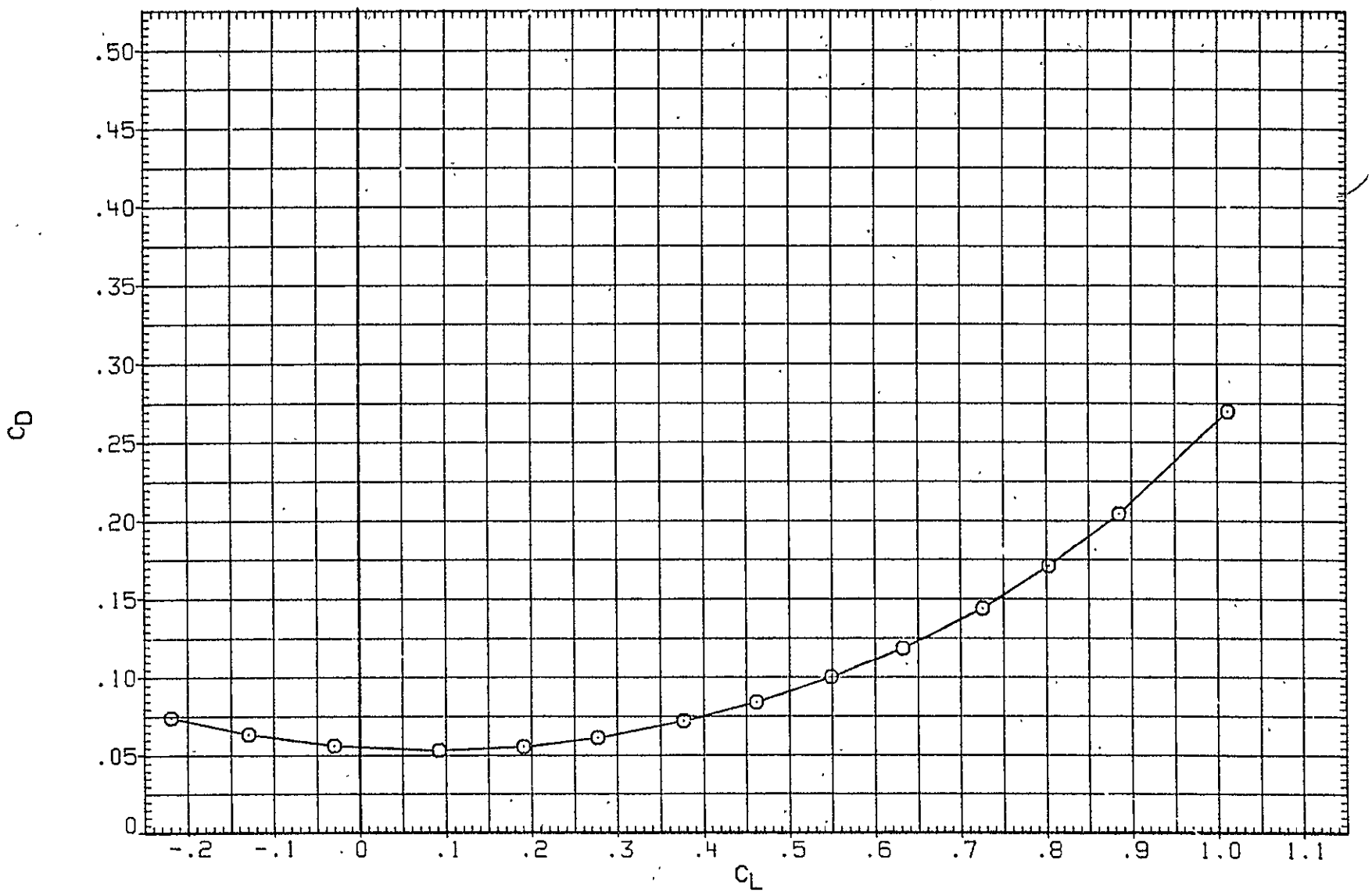

FIG. 8 EFFECT OF OUTBD. SYMM. T.E. DEFL., SIMPLE HINGE FLAPS. TAIL OFF

(C)MACH = 1.15

DATA SET	SYMBOL	CONFIGURATION DESCRIPTION	DTEO	DTEI	DLE	BETA
(JFK010)	○	B V W2	.000	5.000	10.000	.000
(JFK011)	□	B V W2	5.000	5.000	10.000	.000

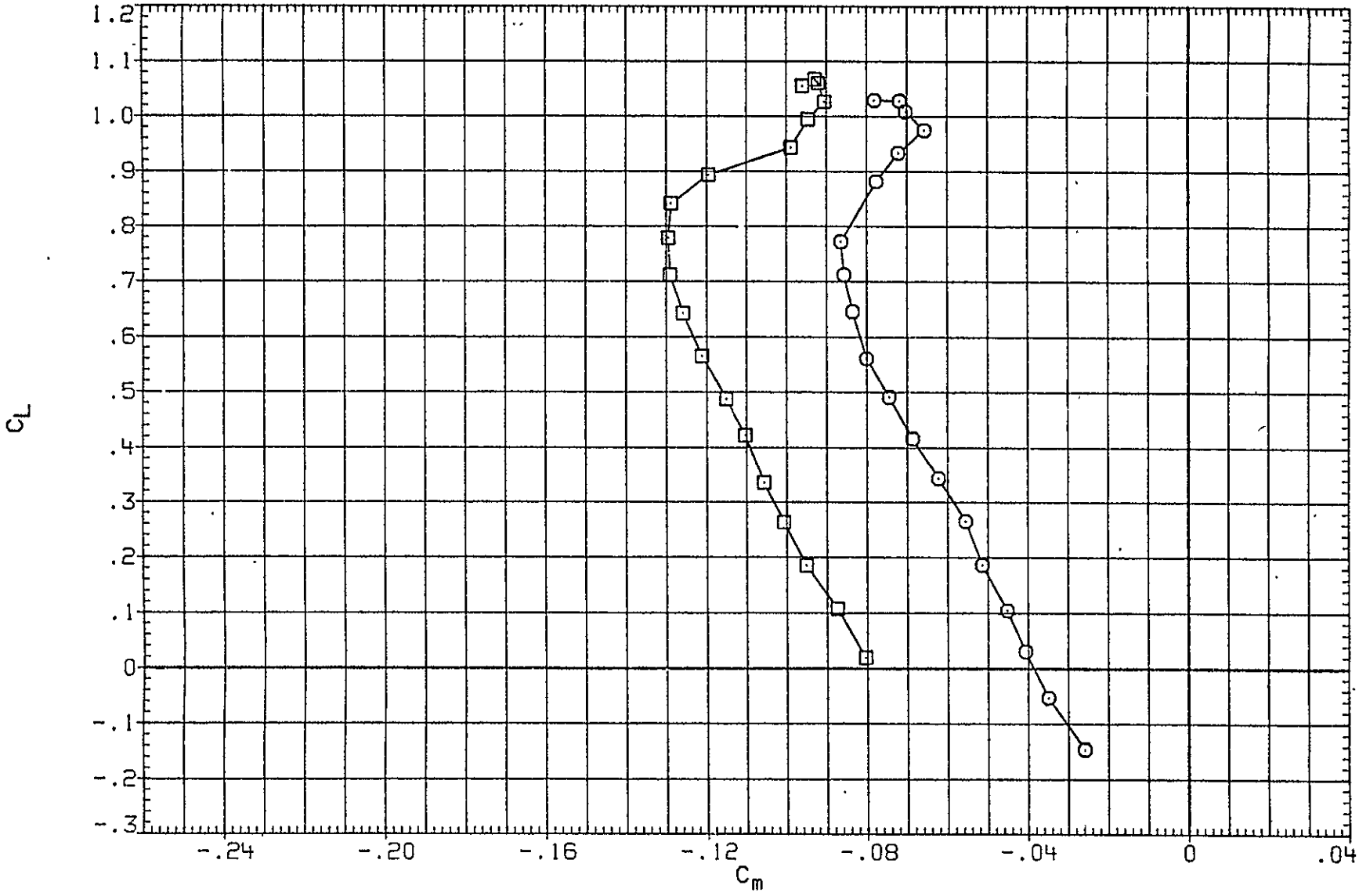

FIG. 8 EFFECT OF OUTBD. SYMM. T.E. DEFL., SIMPLE HINGE FLAPS. TAIL OFF

(A)MACH = .70

DATA SET	SYMBOL	CONFIGURATION DESCRIPTION	DTEO	DTEI	DLE	BETA
(JFK010)	○	B V W2	.000	5.000	10.000	.000
(JFK011)	□	B V W2	5.000	5.000	10.000	.000

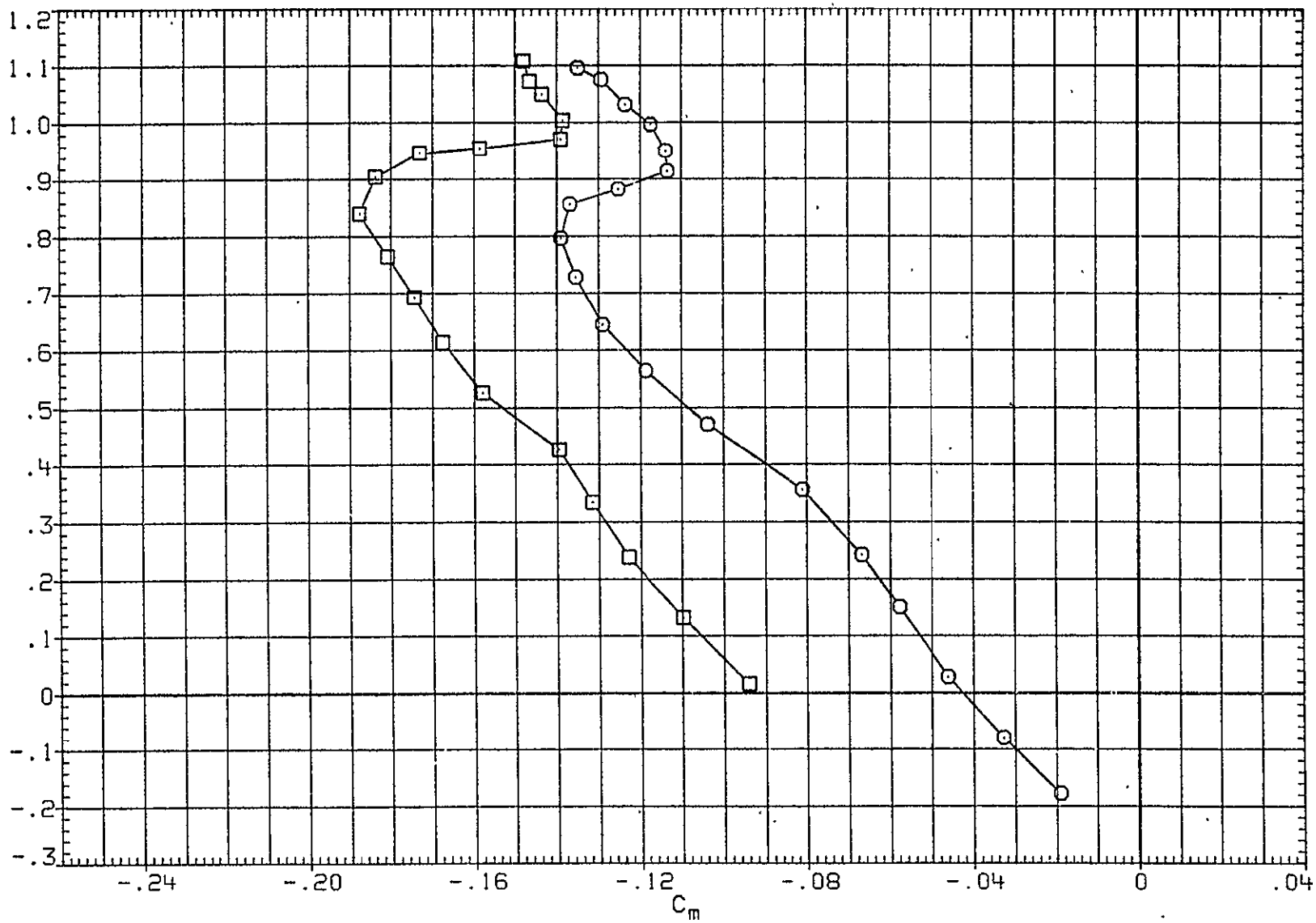

FIG. 8 EFFECT OF OUTBD. SYMM. T.E. DEFL., SIMPLE HINGE FLAPS. TAIL OFF

(B)MACH = .90

DATA SET	SYMBOL	CONFIGURATION DESCRIPTION	DTEO	DTEI	DLE	BETA
(JFK010)	○	B V W2	.000	5.000	10.000	.000
(JFK011)	□	DATA NOT AVAILABLE	5.000	5.000	10.000	.000

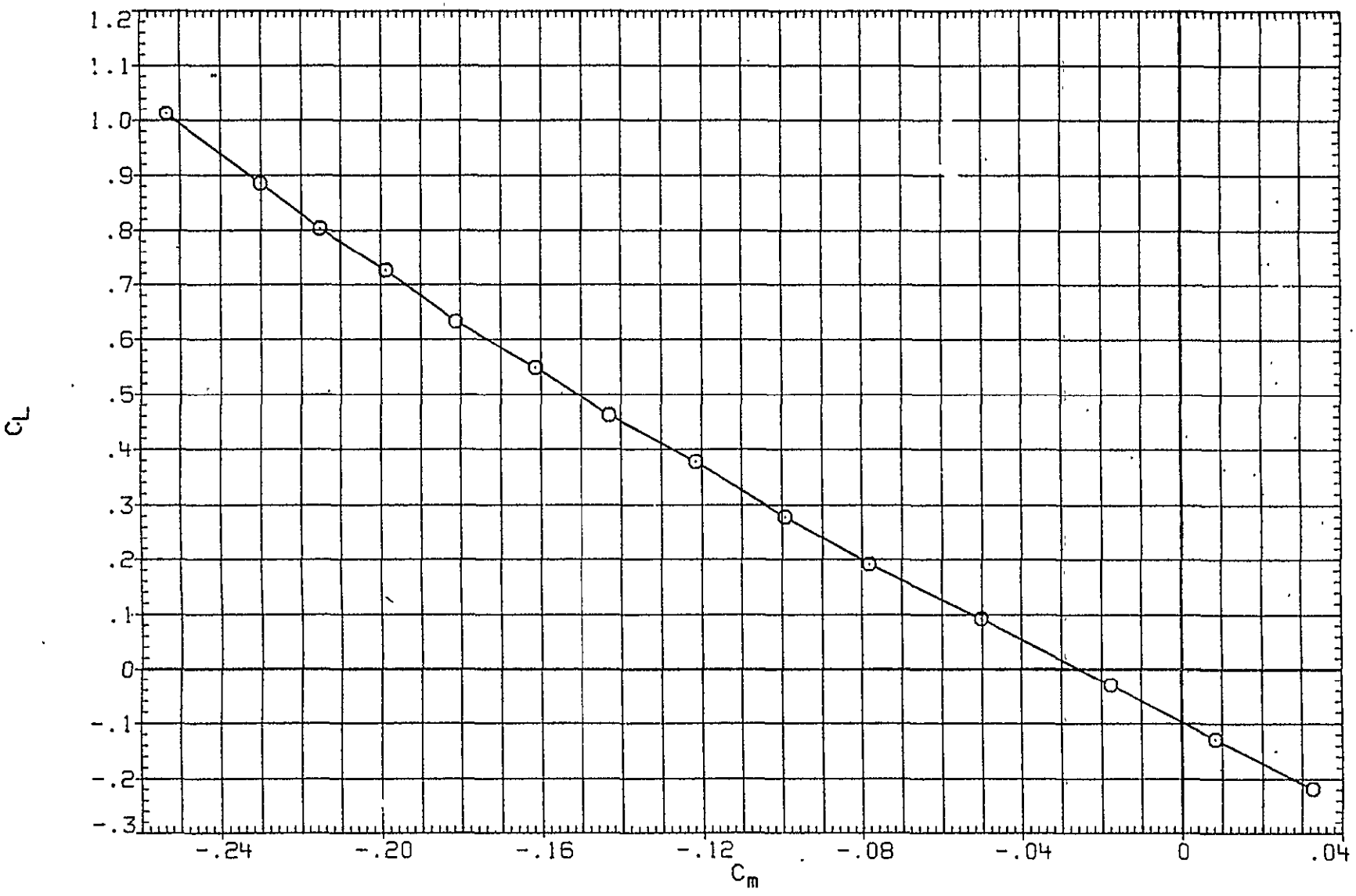

FIG. 8 EFFECT OF OUTBD. SYMM. T.E. DEFL., SIMPLE HINGE FLAPS. TAIL OFF

(C) MACH = 1.15

DATA SET	SYMBOL	CONFIGURATION DESCRIPTION	DH	BETA
(JFK001)	○	B V W1		.000
(ZFK007)	□	B V W2		.000
(JFK002)	◇	B V W1H	.000	.000
(JFK006)	△	B V W2H	.000	.000

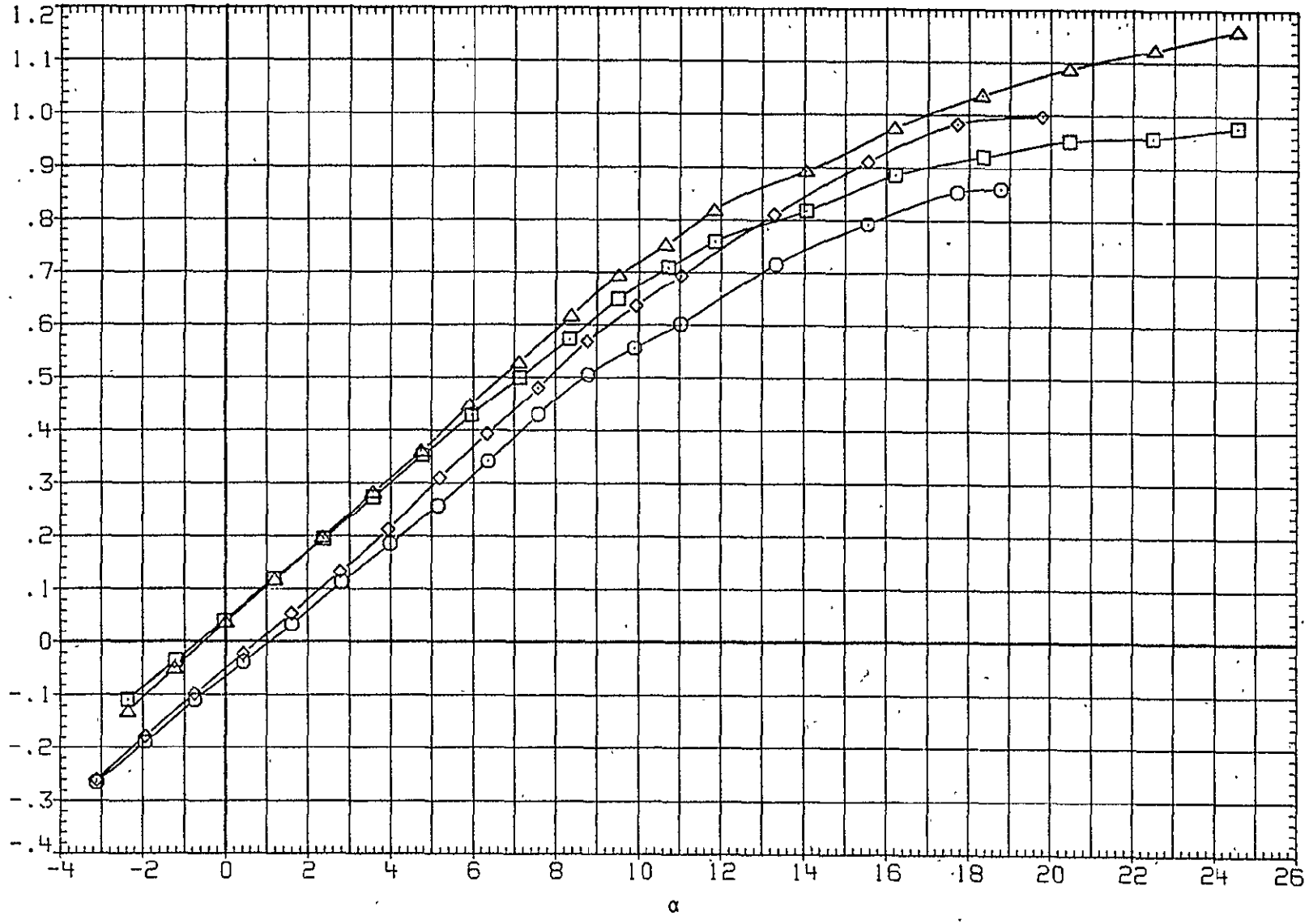

FIG. 9 EFFECT OF HORIZONTAL TAIL FOR BOTH WINGS. ALL CONTROL SURFACE DEFL. ZERO.

(A) MACH = .70

DATA SET	SYMBOL	CONFIGURATION DESCRIPTION	DH	BETA
(JFK001)	○	B V W1		.000
(ZFK007)	□	B V W2		.000
(JFK002)	◇	B V W1H	.000	.000
(JFK006)	△	B V W2H	.000	.000

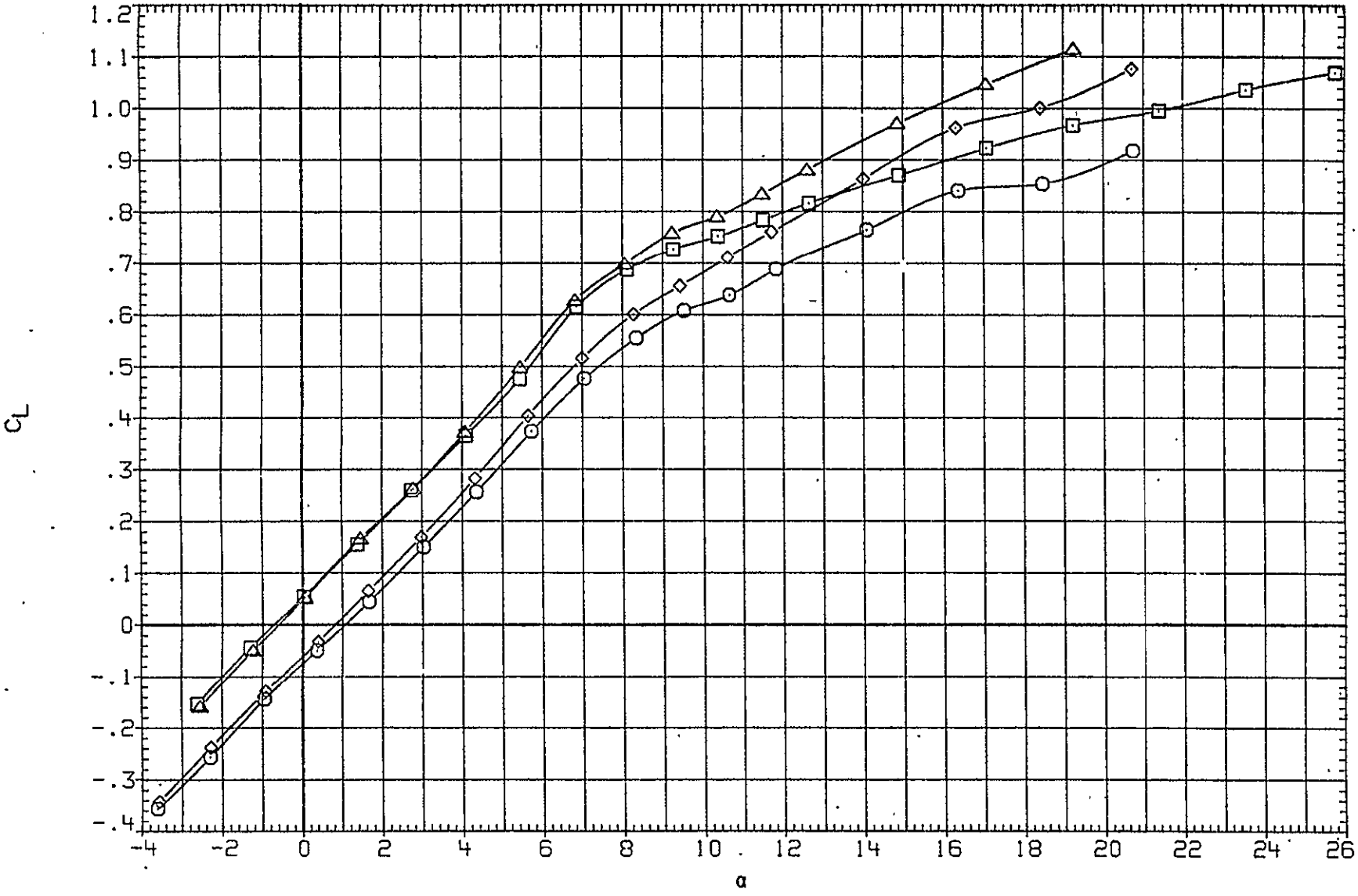

FIG. 9 EFFECT OF HORIZONTAL TAIL FOR BOTH WINGS. ALL CONTROL SURFACE DEFL. ZERO.

(B) MACH = .90

DATA SET	SYMBOL	CONFIGURATION DESCRIPTION	DH	BETA
(JFK001)	○	B V W1		.000
(ZFK007)	□	B V W2		.000
(JFK002)	◇	DATA NOT AVAILABLE	.000	.000
(JFK006)	△	DATA NOT AVAILABLE	.000	.000

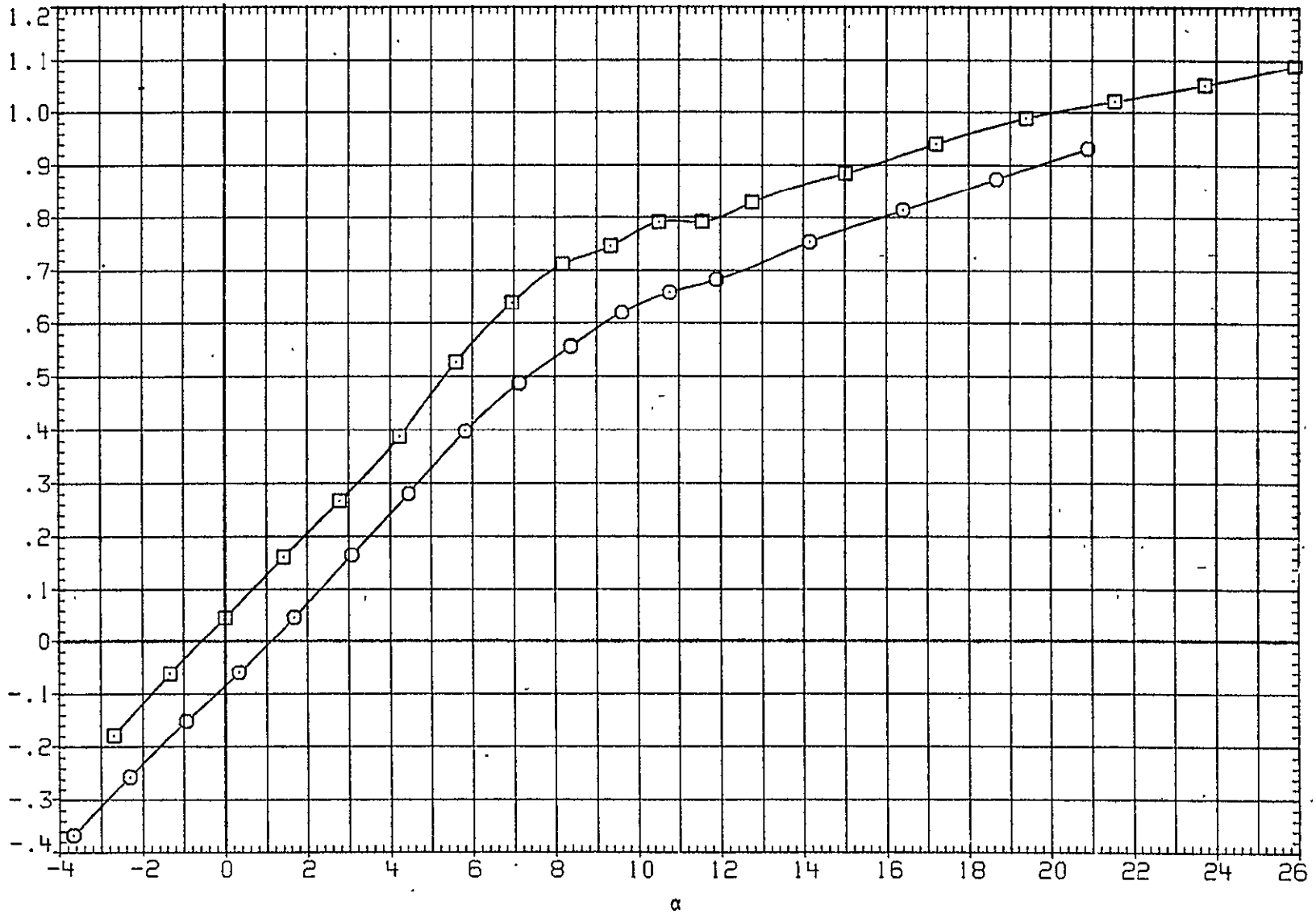

FIG. 9 EFFECT OF HORIZONTAL TAIL FOR BOTH WINGS. ALL CONTROL SURFACE DEFL. ZERO.

(C)MACH = .92

DATA SET	SYMBOL	CONFIGURATION DESCRIPTION	DH	BETA
(JFK001)	○	B V W1		.000
(ZFK007)	□	B V W2		.000
(JFK002)	◇	DATA NOT AVAILABLE	.000	.000
(JFK006)	△	DATA NOT AVAILABLE	.000	.000

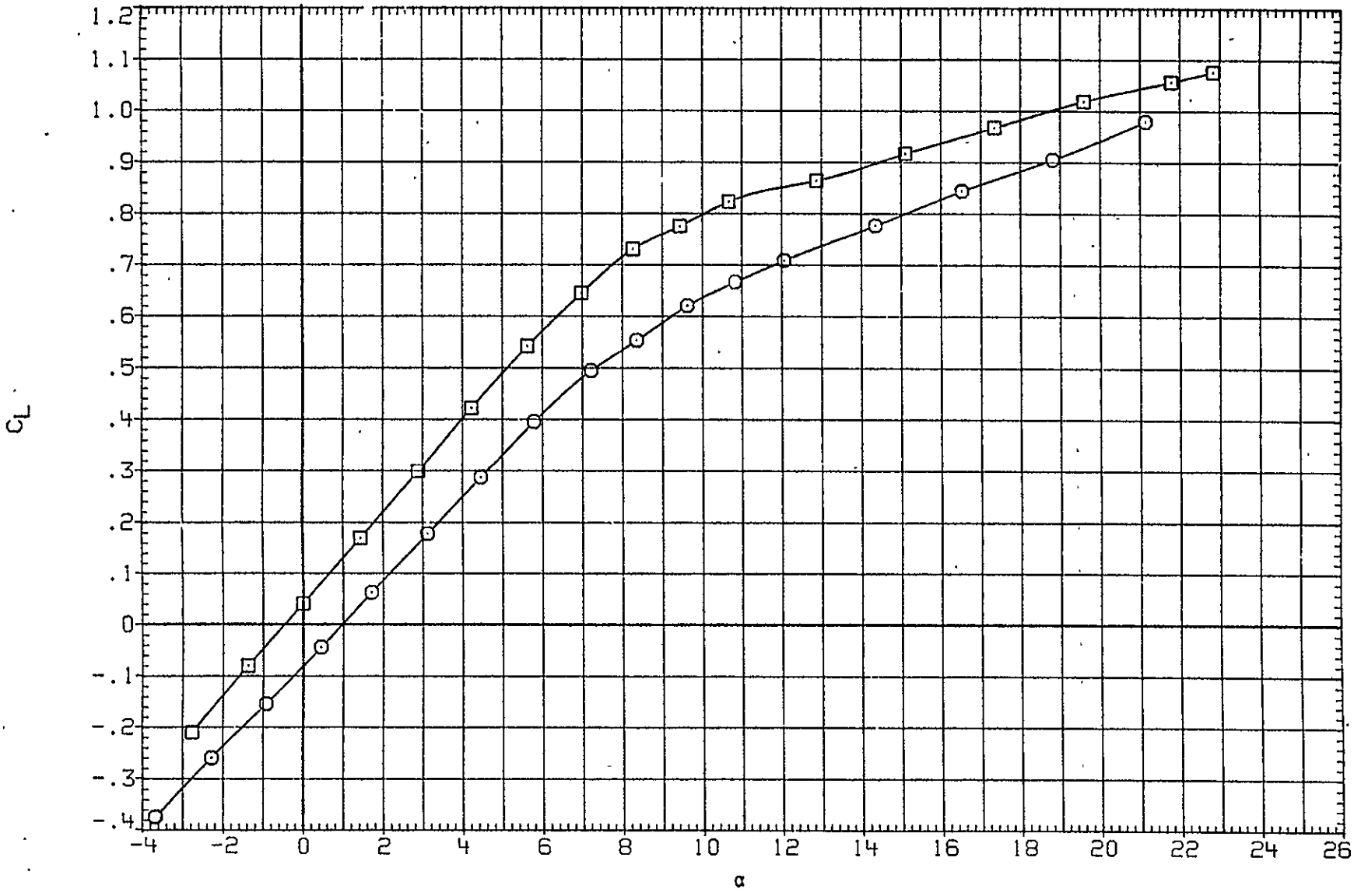

FIG. 9 EFFECT OF HORIZONTAL TAIL FOR BOTH WINGS. ALL CONTROL SURFACE DEFL. ZERO.

(D)MACH = .95

DATA SET	SYMBOL	CONFIGURATION DESCRIPTION	DH	BETA
(JFK001)	○	B V W1		.000
(ZFK007)	□	B V W2		.000
(JFK002)	◇	B V W1H	.000	.000
(JFK006)	△	B V W2H	.000	.000

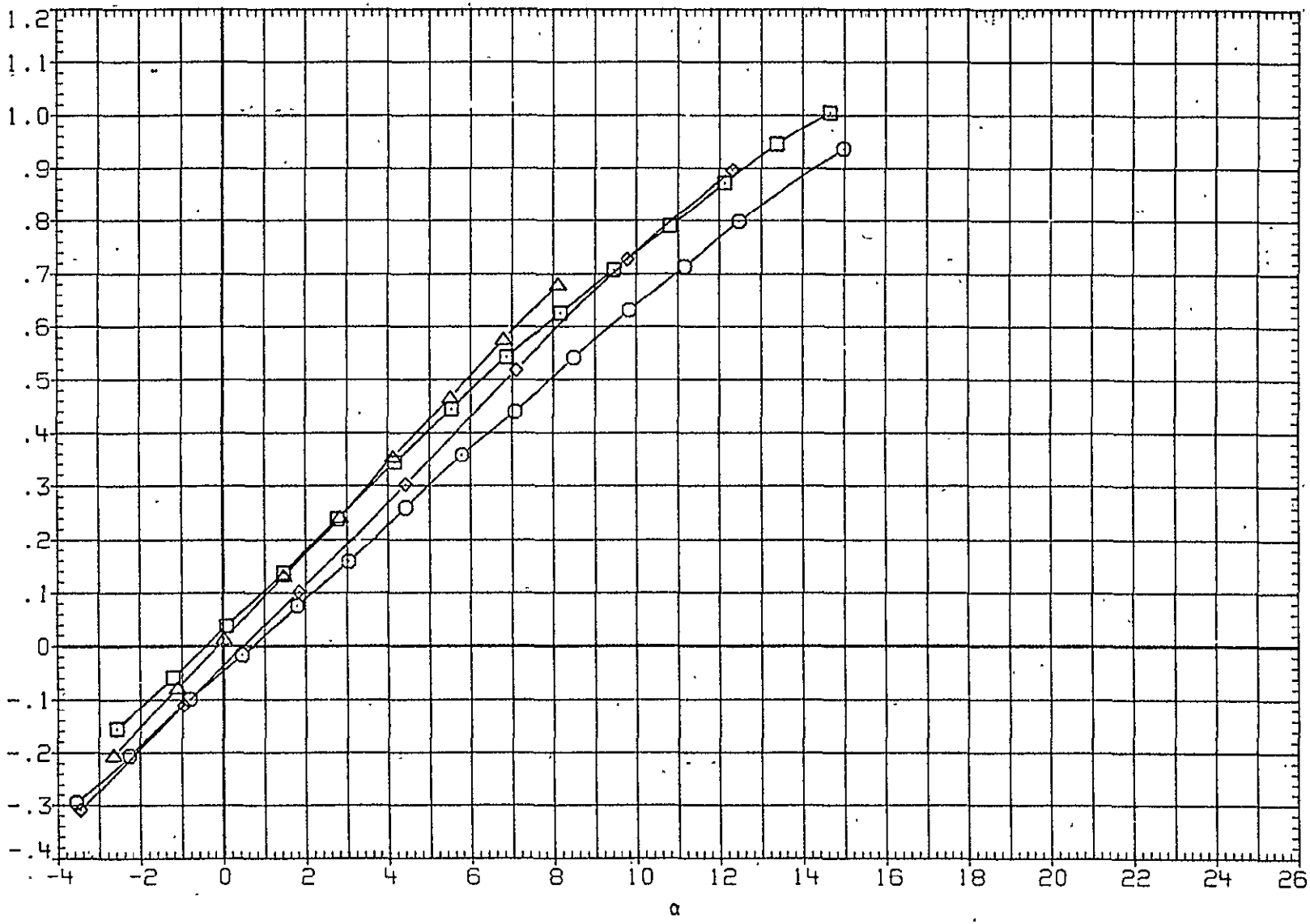

FIG. 9 EFFECT OF HORIZONTAL TAIL FOR BOTH WINGS. ALL CONTROL SURFACE DEFL. ZERO.

(E)MACH = 1.15

DATA SET	SYMBOL	CONFIGURATION DESCRIPTION	DH	BETA
(JFK001)	○	B V W1		.000
(ZFK007)	□	B V W2		.000
(JFK002)	◇	B V W1H	.000	.000
(JFK006)	△	B V W2H	.000	.000

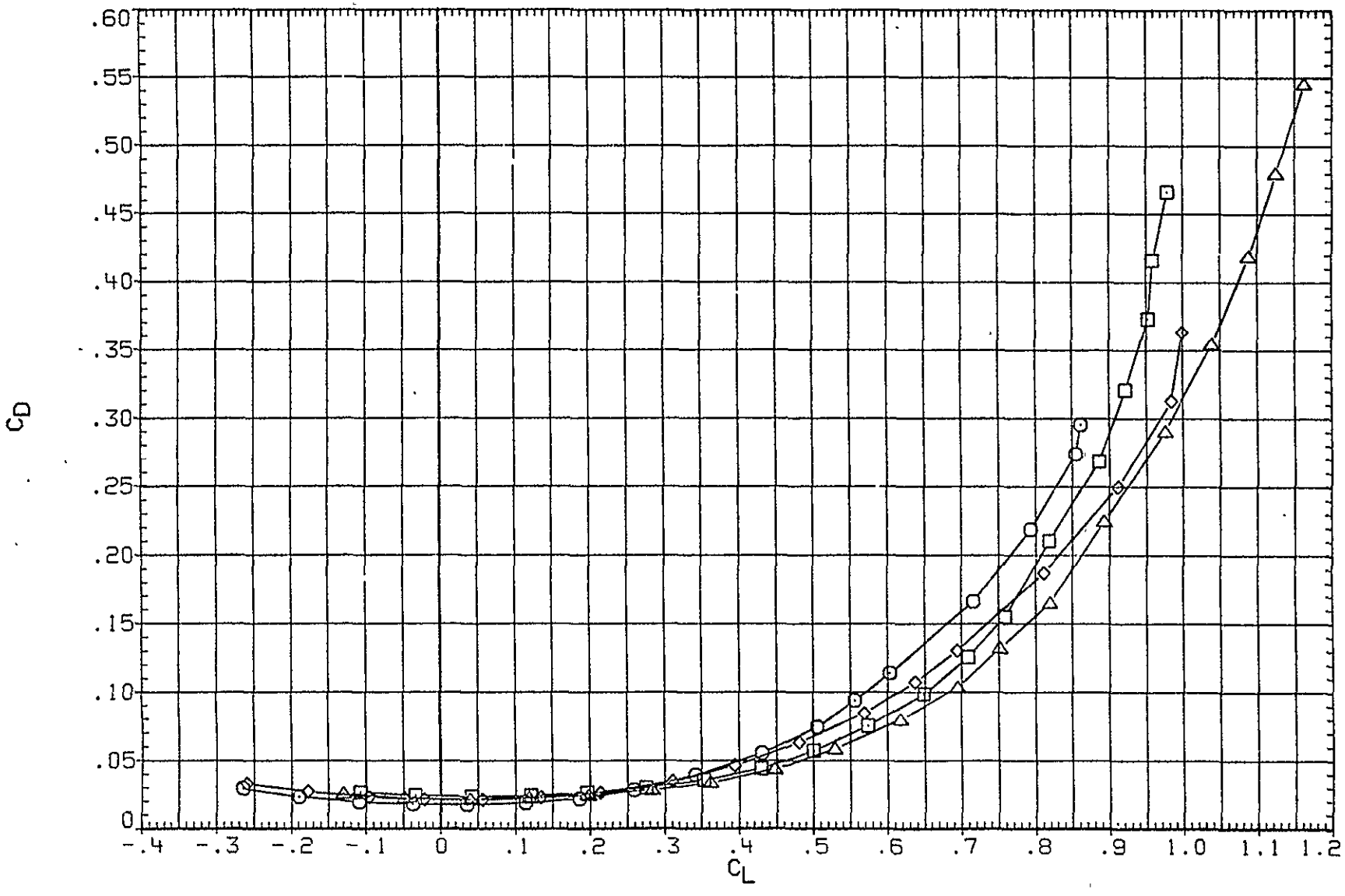

FIG. 9 EFFECT OF HORIZONTAL TAIL FOR BOTH WINGS. ALL CONTROL SURFACE DEFL. ZERO.

(A) MACH = .70

DATA SET	SYMBOL	CONFIGURATION DESCRIPTION	DH	BETA
(JFK001)	○	B V W1		.000
(ZFK007)	□	B V W2		.000
(JFK002)	◇	B V W1H	.000	.000
(JFK006)	△	B V W2H	.000	.000

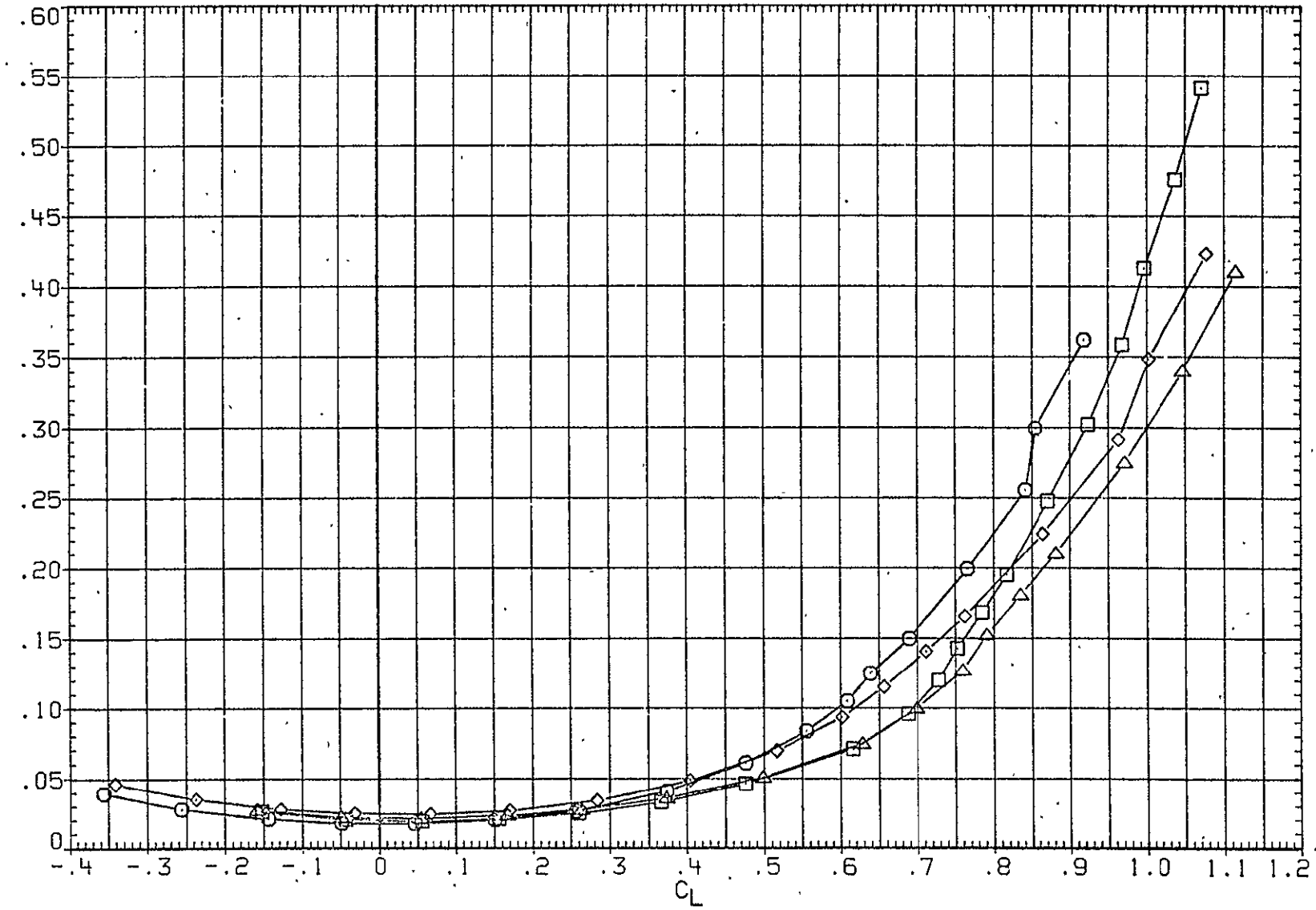

FIG. 9 EFFECT OF HORIZONTAL TAIL FOR BOTH WINGS. ALL CONTROL SURFACE DEFL. ZERO.

(B)MACH = .90

DATA SET	SYMBOL	CONFIGURATION DESCRIPTION	DH	BETA
(JFK001)	○	B V W1		.000
(ZFK007)	□	B V W2		.000
(JFK002)	◇	DATA NOT AVAILABLE	.000	.000
(JFK006)	△	DATA NOT AVAILABLE	.000	.000

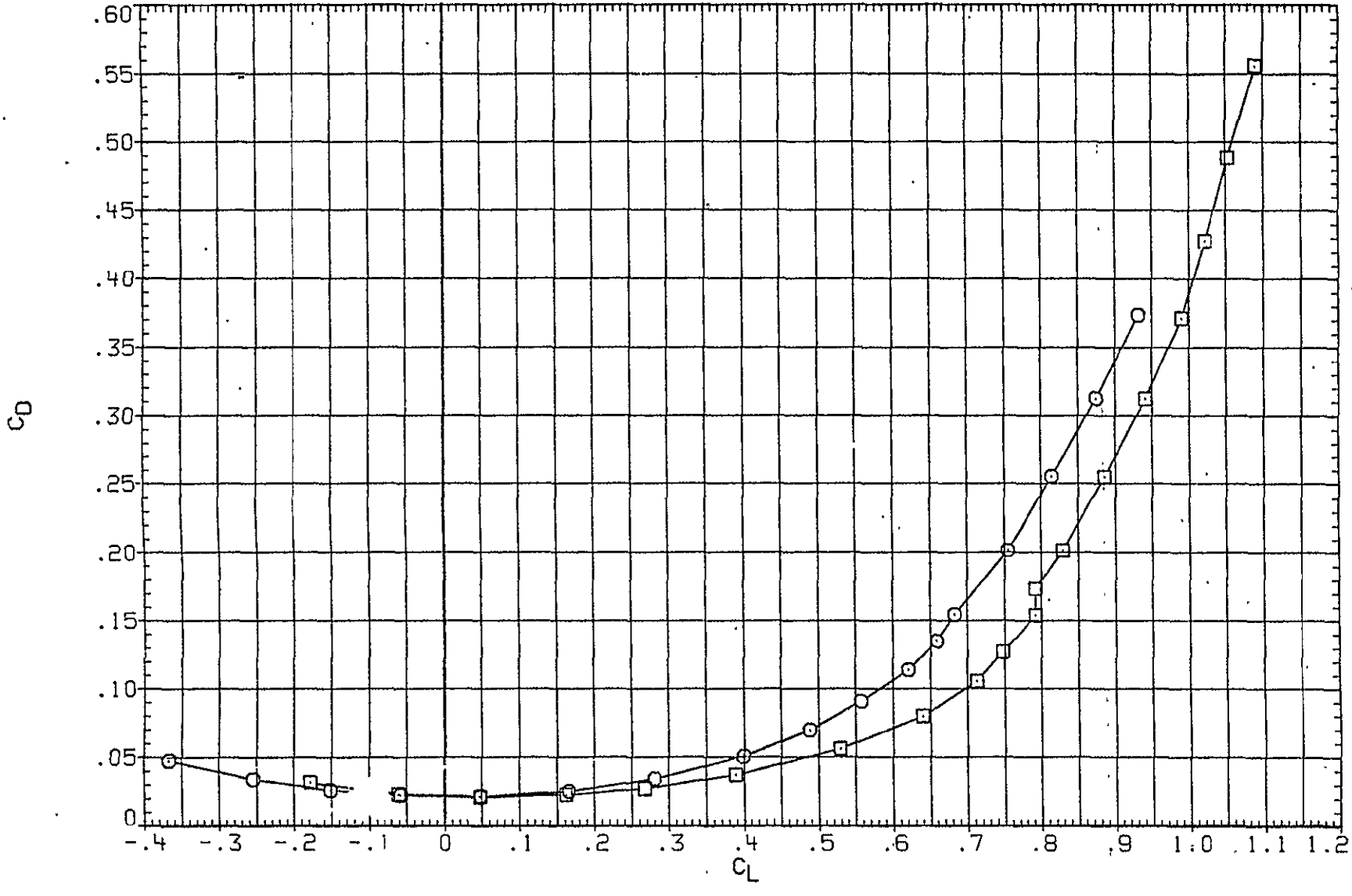

FIG. 9 EFFECT OF HORIZONTAL TAIL FOR BOTH WINGS. ALL CONTROL SURFACE DEFL. ZERO.

(C)MACH = .92

DATA SET	SYMBOL	CONFIGURATION DESCRIPTION	DH	BETA
(JFK001)	○	B V W1		.000
(ZFK007)	□	B V W2		.000
(JFK002)	◇	DATA NOT AVAILABLE	.000	.000
(JFK006)	△	DATA NOT AVAILABLE	.000	.000

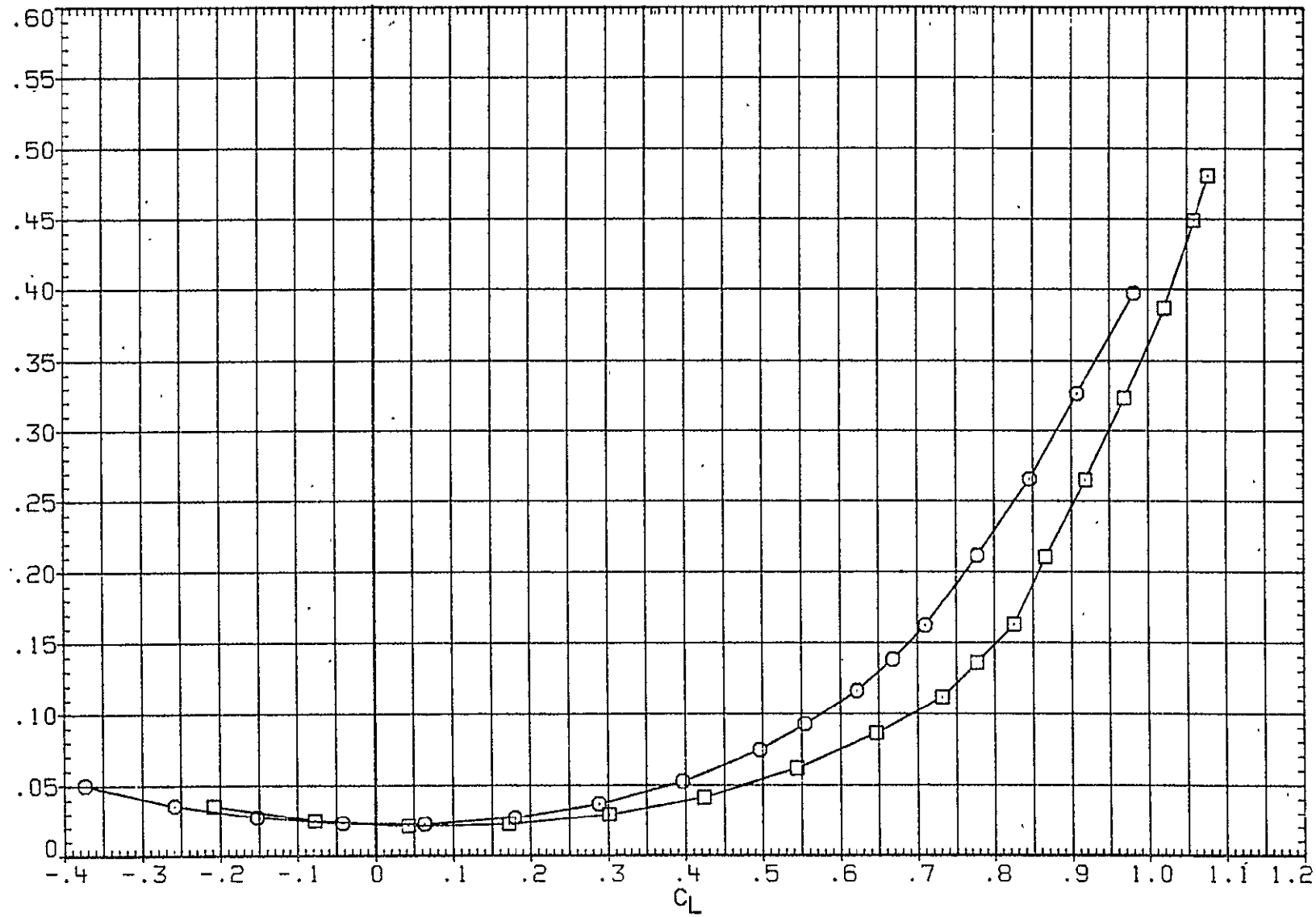

FIG. 9 EFFECT OF HORIZONTAL TAIL FOR BOTH WINGS. ALL CONTROL SURFACE DEFL. ZERO.

(D) MACH = .95

DATA SET	SYMBOL	CONFIGURATION DESCRIPTION	DH	BETA
(JFK001)	○	B V W1		.000
(ZFK007)	□	B V W2		.000
(JFK002)	◇	B V W1H	.000	.000
(JFK006)	△	B V W2H	.000	.000

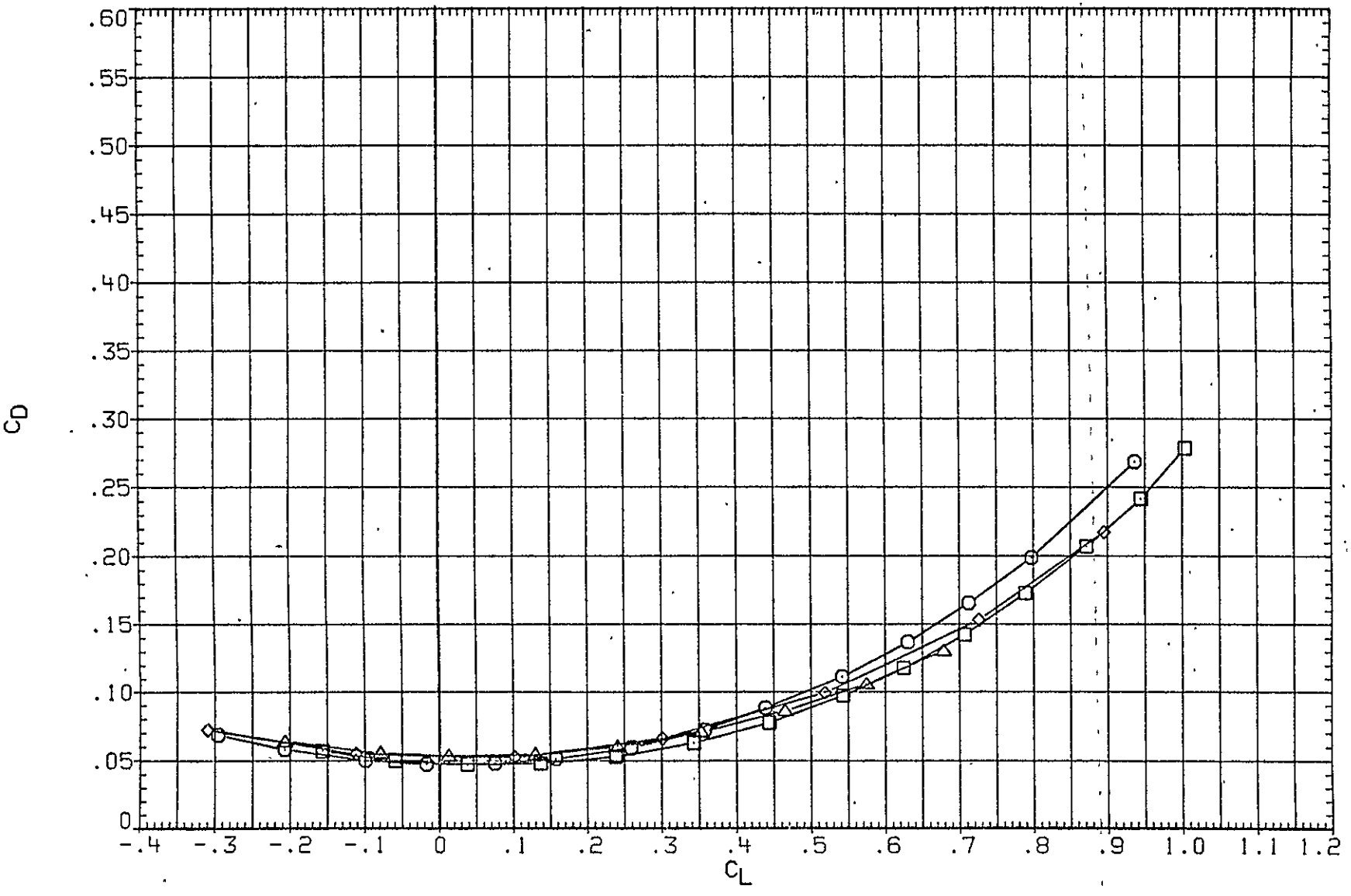

FIG. 9 EFFECT OF HORIZONTAL TAIL FOR BOTH WINGS. ALL CONTROL SURFACE DEFL. ZERO.

(E) MACH = 1.15

DATA SET	SYMBOL	CONFIGURATION DESCRIPTION	DH	BETA
(JFK001)	○	B V W1		.000
(ZFK007)	□	B V W2		.000
(JFK002)	◇	B V W1H	.000	.000
(JFK006)	△	B V W2H	.000	.000

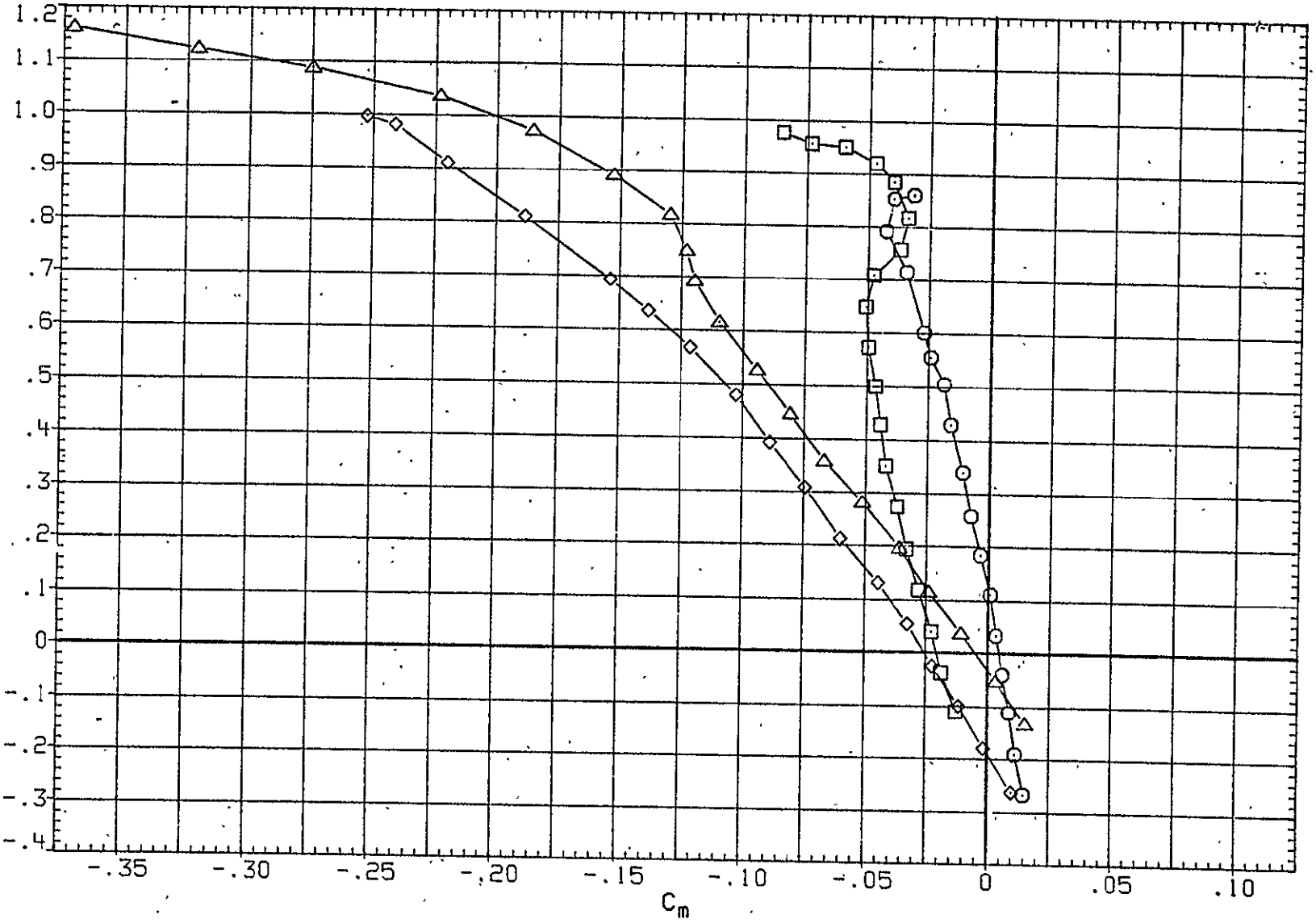

FIG. 9 EFFECT OF HORIZONTAL TAIL FOR BOTH WINGS. ALL CONTROL SURFACE DEFL. ZERO.

(A)MACH = .70

DATA SET	SYMBOL	CONFIGURATION DESCRIPTION	DH	BETA
(JFK001)	○	B V W1		.000
(ZFK007)	□	B V W2		.000
(JFK002)	◇	B V W1H	.000	.000
(JFK006)	△	B V W2H	.000	.000

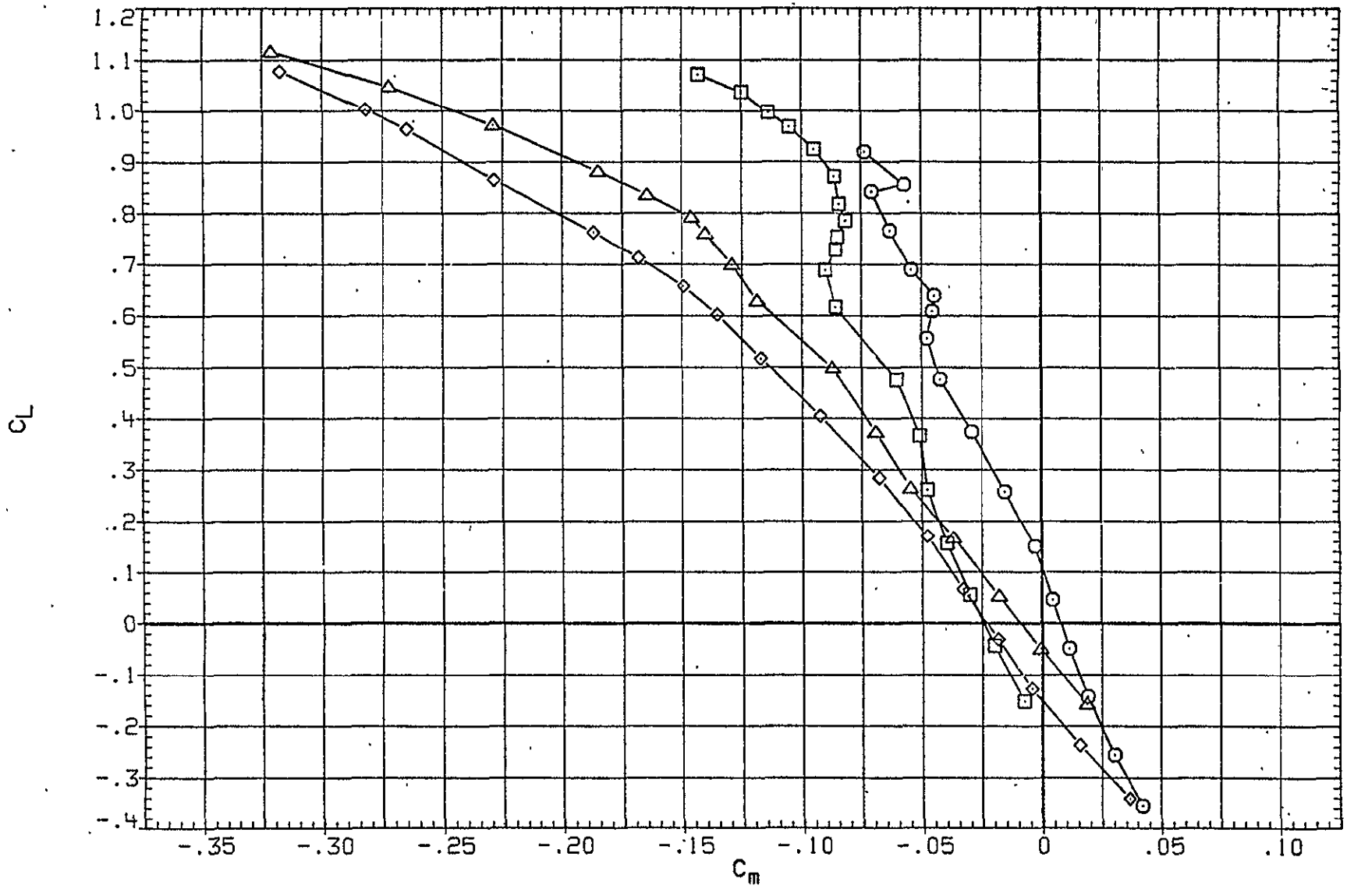

FIG. 9 EFFECT OF HORIZONTAL TAIL FOR BOTH WINGS. ALL CONTROL SURFACE DEFL. ZERO.

(B)MACH = .90

DATA SET	SYMBOL	CONFIGURATION DESCRIPTION	DH	BETA
(JFK001)	○	B V W1		.000
(ZFK007)	□	B V W2		.000
(JFK002)	◇	DATA NOT AVAILABLE	.000	.000
(JFK006)	△	DATA NOT AVAILABLE	.000	.000

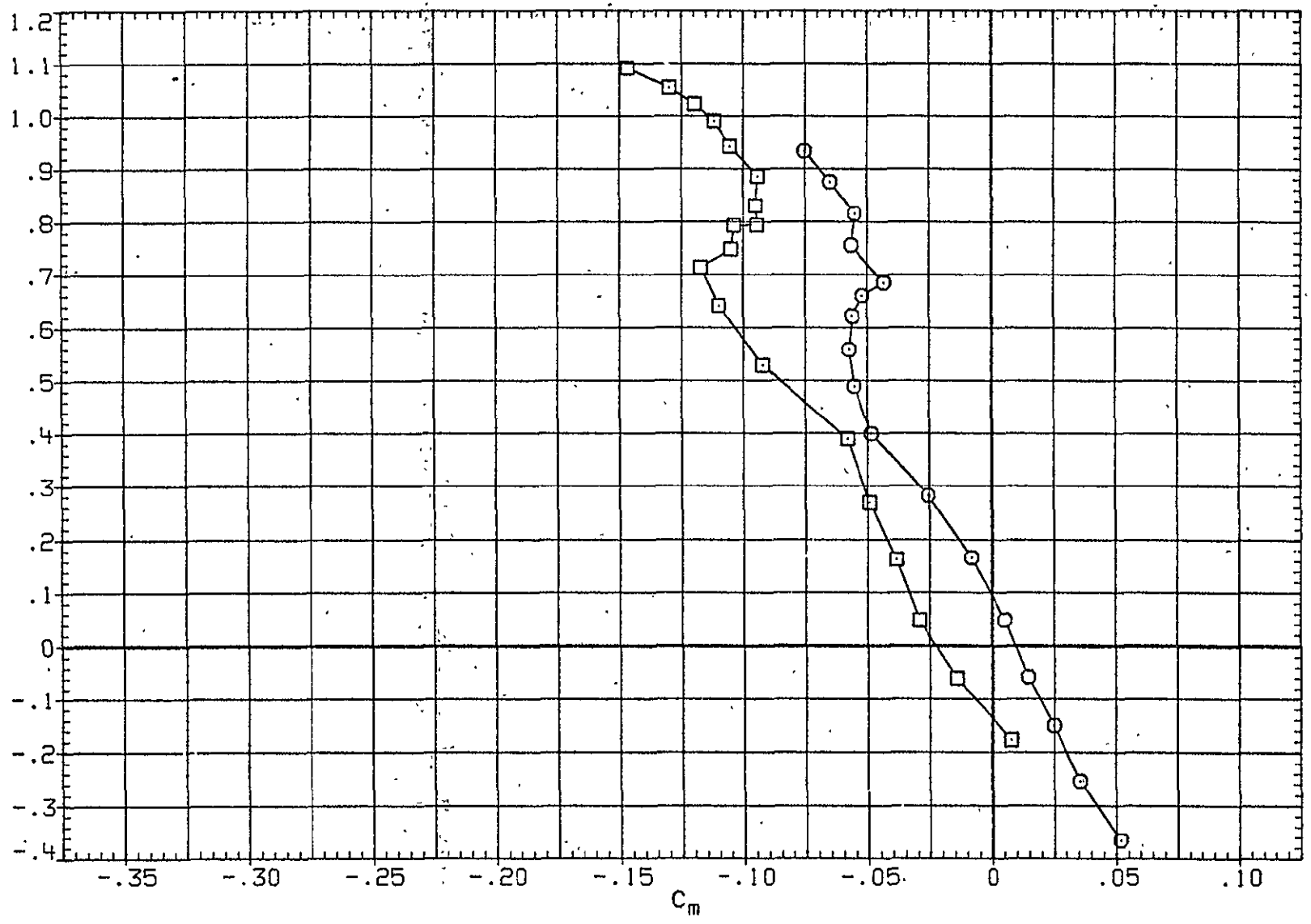

FIG. 9 EFFECT OF HORIZONTAL TAIL FOR BOTH WINGS. ALL CONTROL SURFACE DEFL. ZERO.

(C)MACH = .92

DATA SET	SYMBOL	CONFIGURATION DESCRIPTION	DH	BETA
(JFK001)	○	B V W1		.000
(ZFK007)	□	B V W2		.000
(JFK002)	◇	DATA NOT AVAILABLE	.000	.000
(JFK006)	△	DATA NOT AVAILABLE	.000	.000

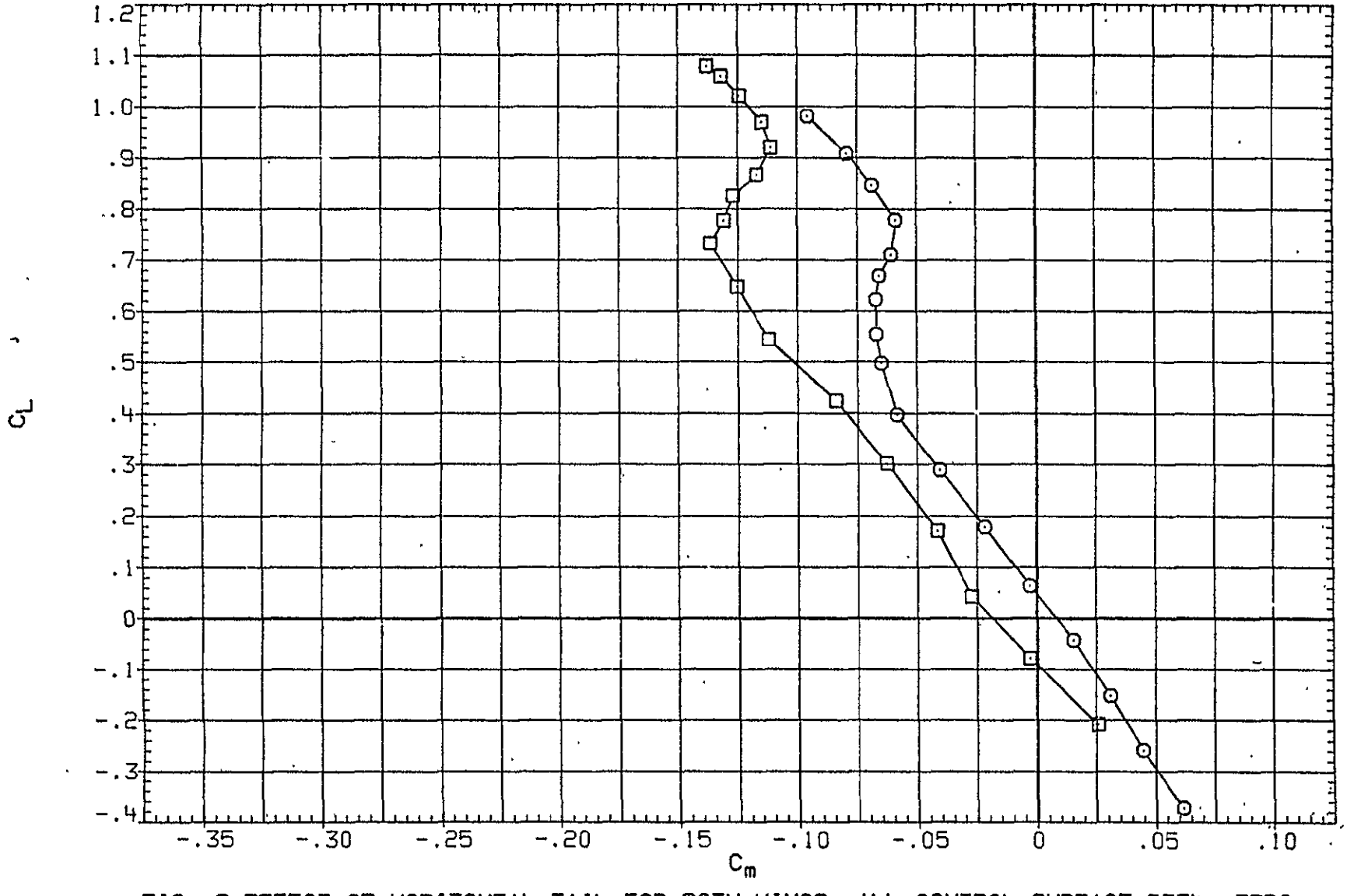

FIG. 9 EFFECT OF HORIZONTAL TAIL FOR BOTH WINGS. ALL CONTROL SURFACE DEFL. ZERO.

(D) MACH = .95

DATA SET	SYMBOL	CONFIGURATION DESCRIPTION	DH	BETA
(JFK001)	○	B V W1		.000
(ZFK007)	□	B V W2		.000
(JFK002)	◇	B V W1H	.000	.000
(JFK006)	△	B V W2H	.000	.000

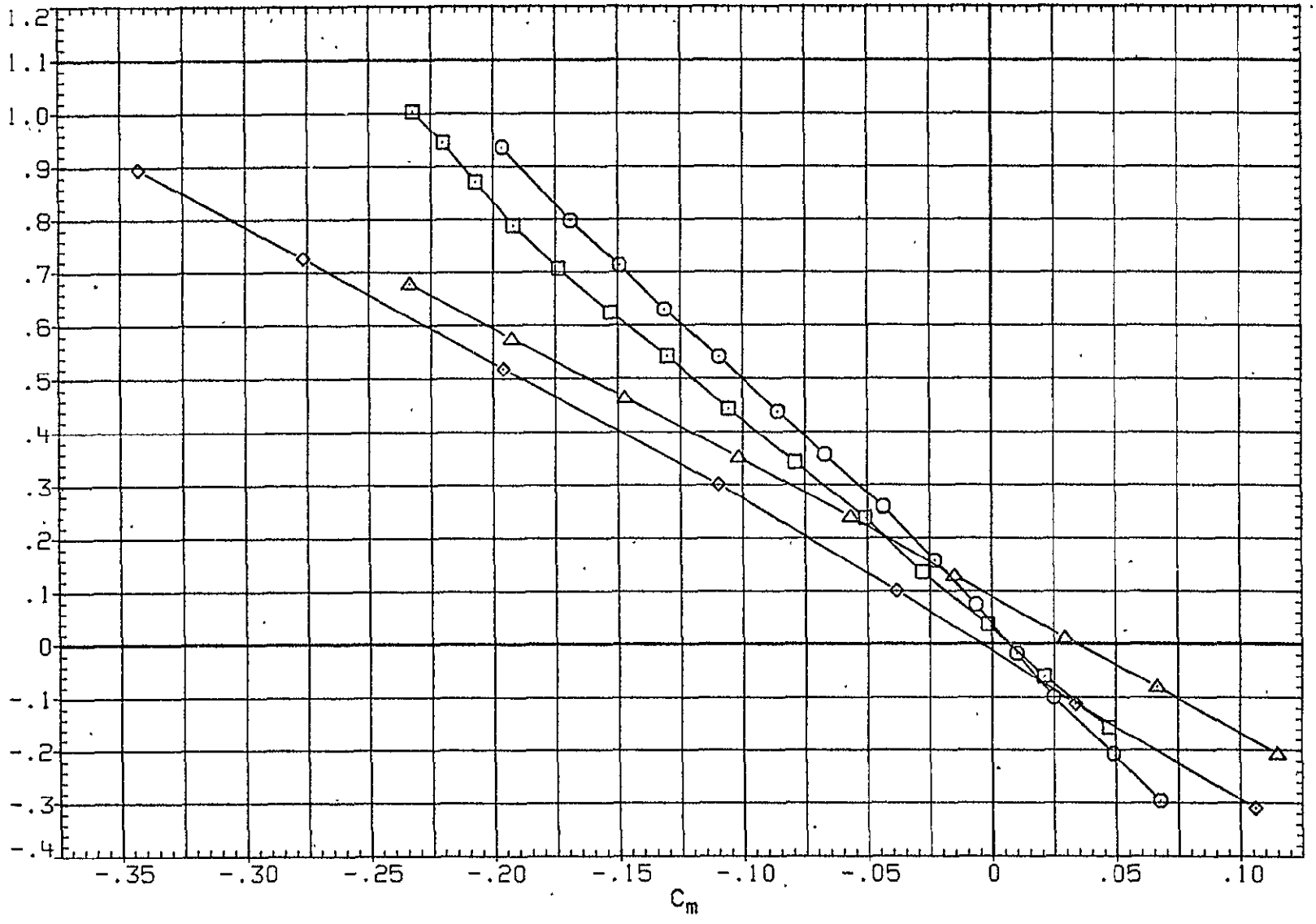

FIG. 9 EFFECT OF HORIZONTAL TAIL FOR BOTH WINGS. ALL CONTROL SURFACE DEFL. ZERO.

(E)MACH = 1.15

DATA SET	SYMBOL	CONFIGURATION DESCRIPTION	DH	BETA
(BFK007)	○	B V W2		.000
(JFK006)	□	B V W2H	.000	.000
(JFK009)	◇	B V W2H	-5.000	.000
(JFK008)	△	B V W2H	-10.000	.000

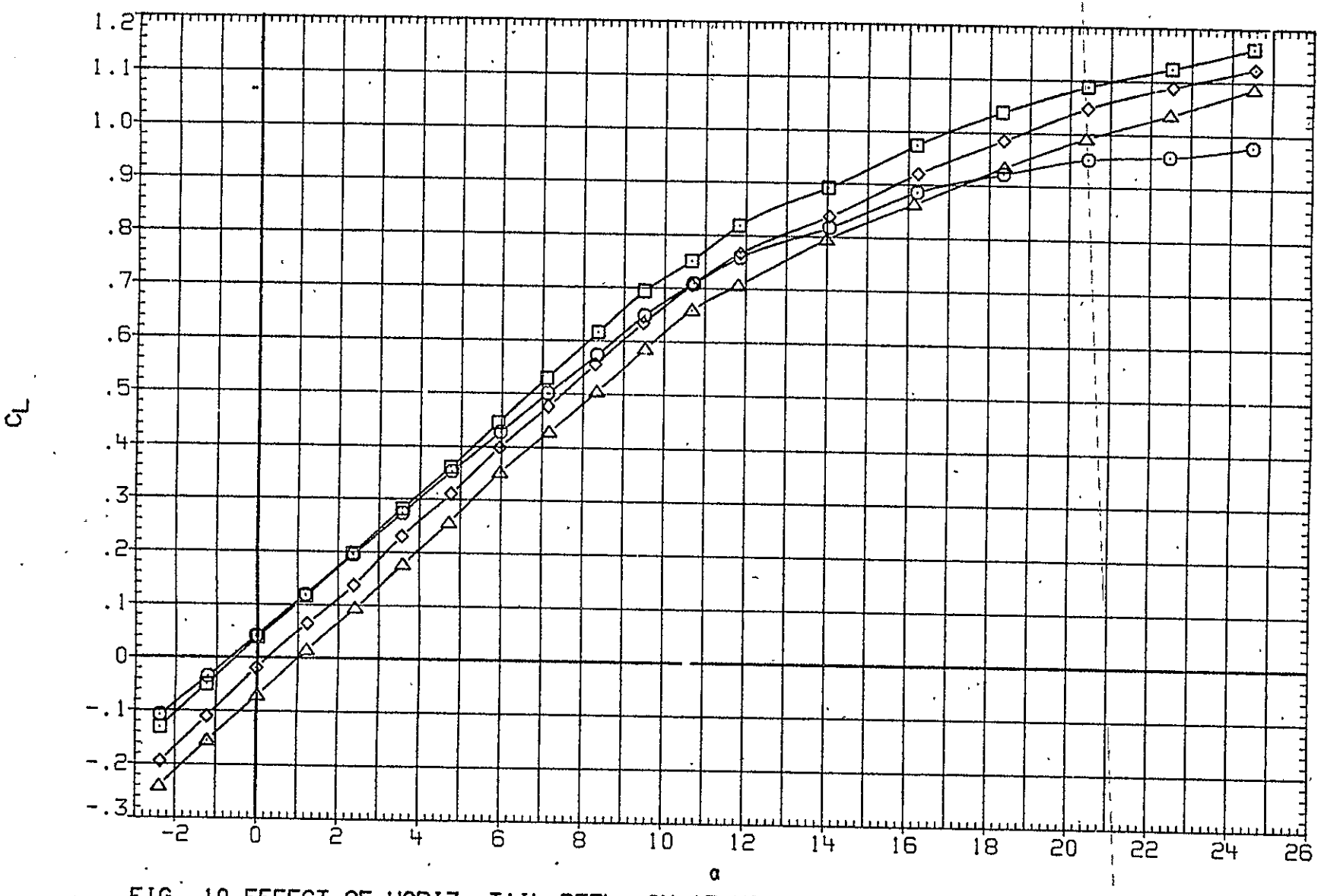

FIG. 10 EFFECT OF HORIZ. TAIL DEFL. ON AT WING. ALL WING CONT. SURF. DEFL. ZERO.

(A) MACH = .70

DATA SET	SYMBOL	CONFIGURATION DESCRIPTION	DH	BETA
(BFK007)	○	B V W2		.000
(JFK006)	□	B V W2H	.000	.000
(JFK009)	◇	B V W2H	-5.000	.000
(JFK008)	△	B V W2H	-10.000	.000

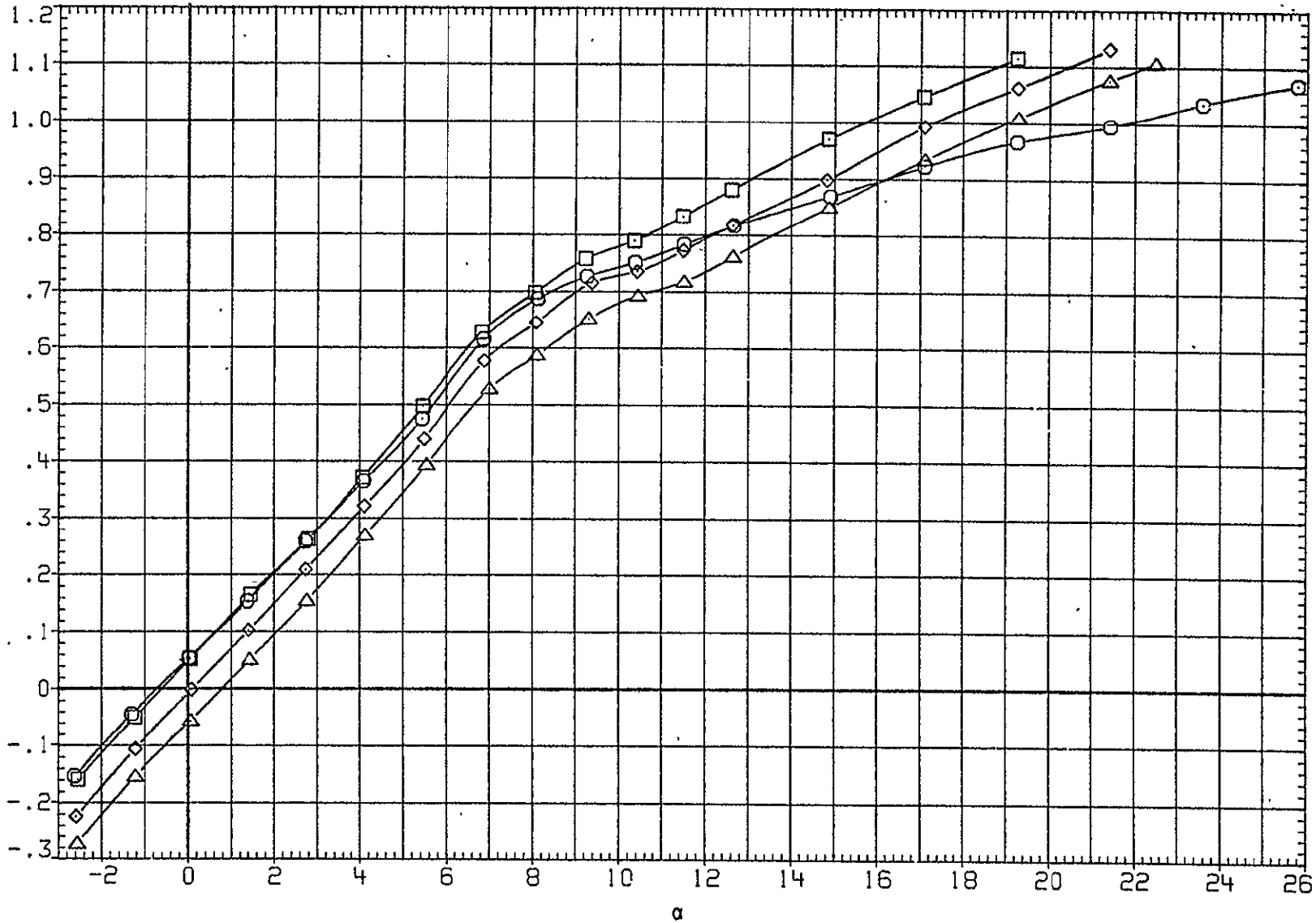

FIG. 10 EFFECT OF HORIZ. TAIL DEFL. ON AT WING. ALL WING CONT. SURF. DEFL. ZERO.

(B) MACH = .90

DATA SET	SYMBOL	CONFIGURATION DESCRIPTION	DH	BETA
(BFK007)	○	B V W2		.000
(JFK006)	□	B V W2H	.000	.000
(JFK009)	◇	B V W2H	-5.000	.000
(JFK008)	△	B V W2H	-10.000	.000

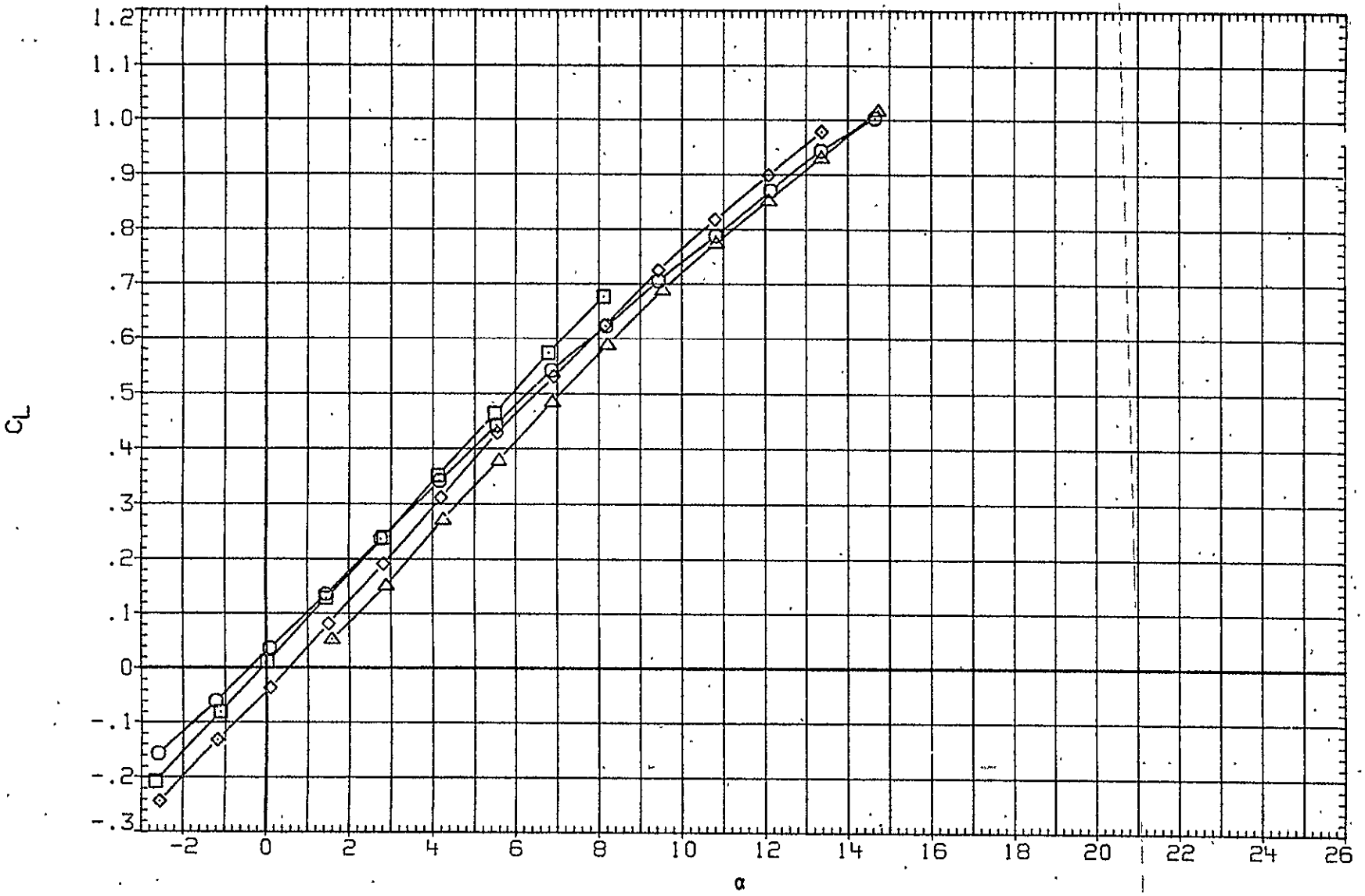

FIG. 10 EFFECT OF HORIZ. TAIL DEFL. ON AT WING. ALL WING CONT. SURF. DEFL. ZERO.

(C) MACH = 1.15

DATA SET	SYMBOL	CONFIGURATION DESCRIPTION	DH	BETA
(BFK007)	○	B V W2		.000
(JFK006)	□	B V W2H	.000	.000
(JFK009)	◇	B V W2H	-5.000	.000
(JFK008)	△	B V W2H	-10.000	.000

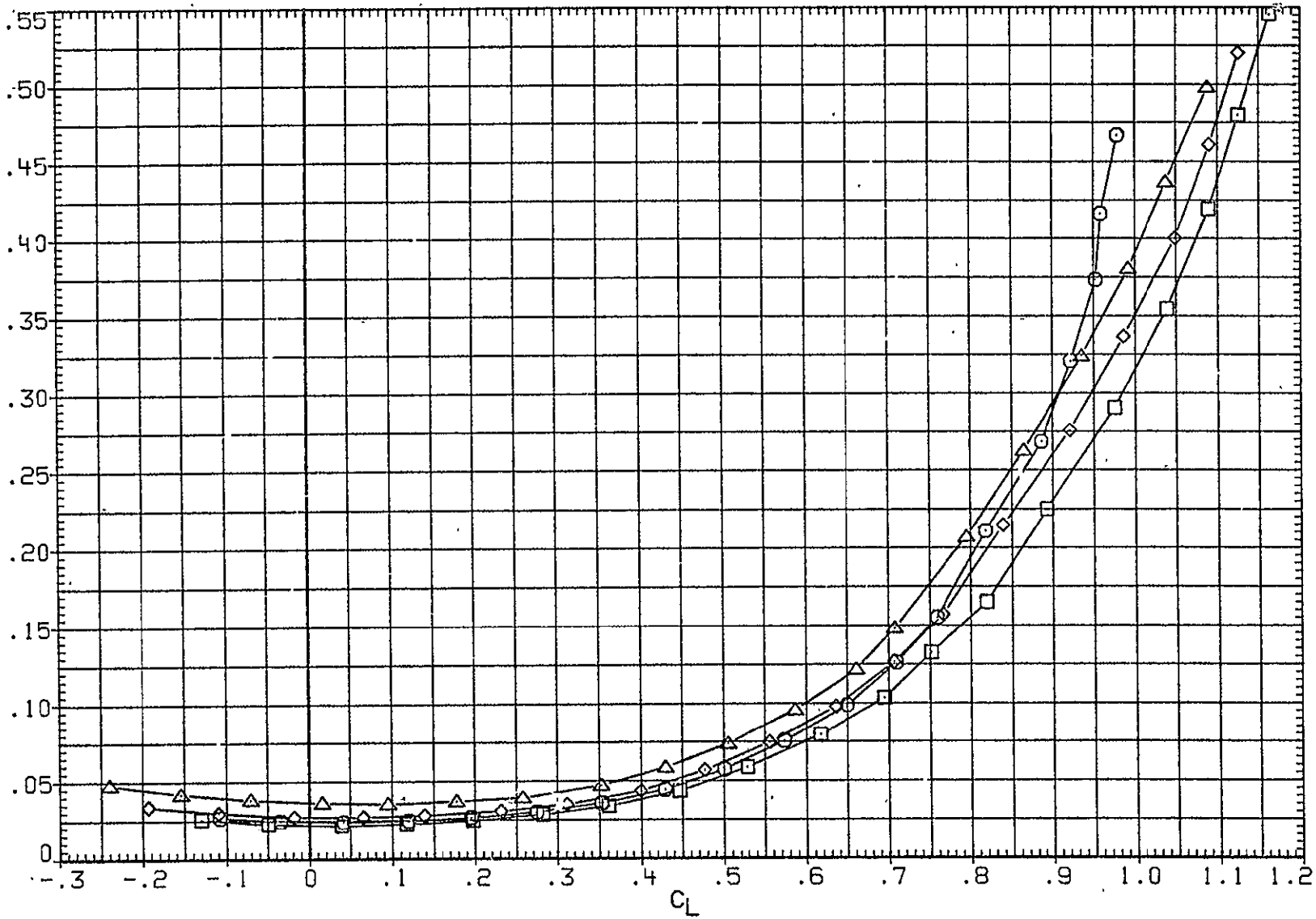

FIG. 10 EFFECT OF HORIZ. TAIL DEFL. ON AT WING. ALL WING CONT. SURF. DEFL. ZERO.

(A)MACH = .70

DATA SET	SYMBOL	CONFIGURATION DESCRIPTION	DH	BETA
(BFK007)	○	B V W2		.000
(JFK006)	□	B V W2H	.000	.000
(JFK009)	◇	B V W2H	-5.000	.000
(JFK008)	△	B V W2H	-10.000	.000

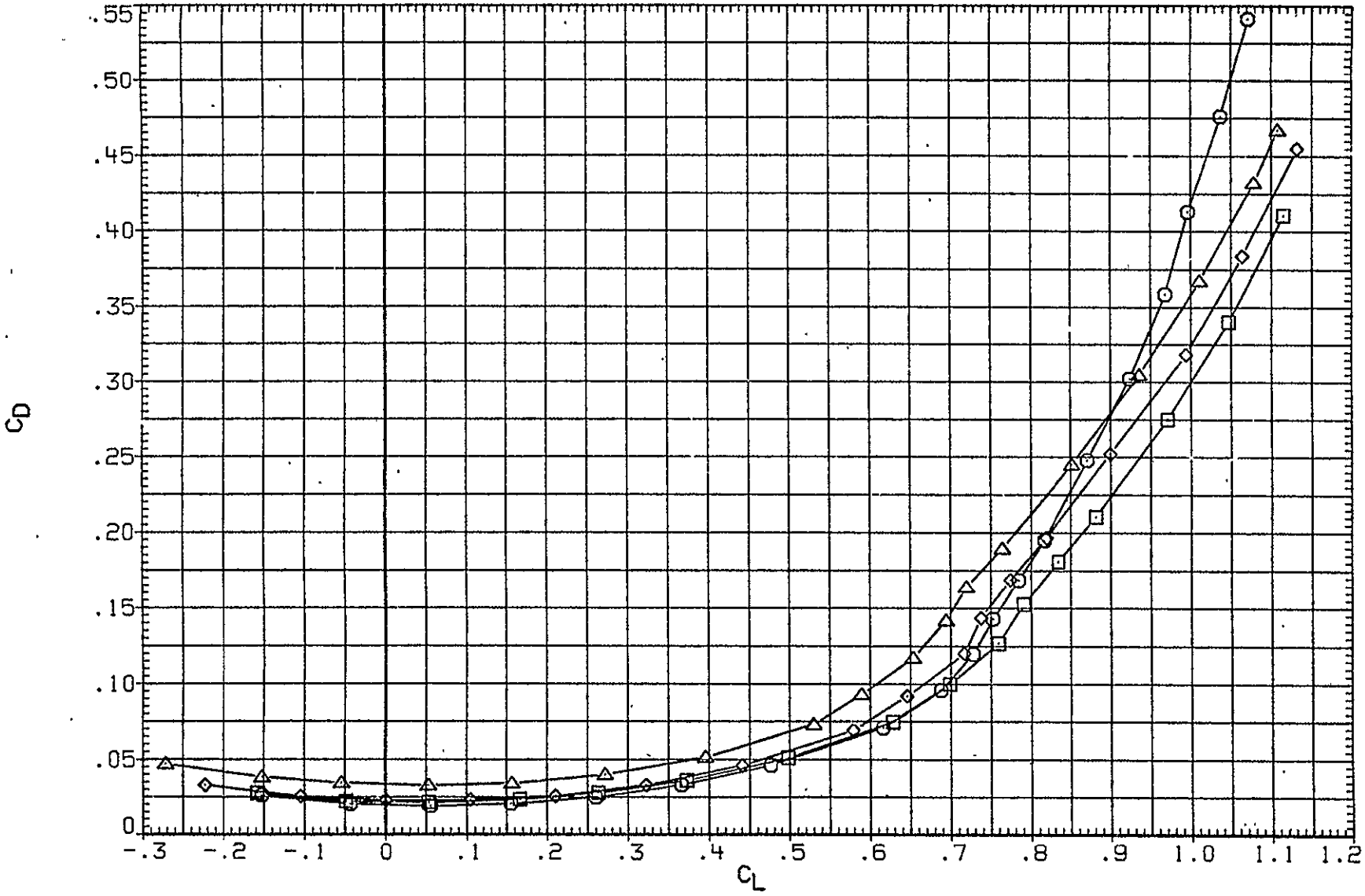

FIG. 10 EFFECT OF HORIZ. TAIL DEFL. ON AT WING, ALL WING CONT. SURF. DEFL. ZERO.

(B) MACH = .90

DATA SET	SYMBOL	CONFIGURATION DESCRIPTION	DH	BETA
(BFK007)	○	B V W2		.000
(JFK006)	□	B V W2H	.000	.000
(JFK009)	◇	B V W2H	-5.000	.000
(JFK008)	△	B V W2H	-10.000	.000

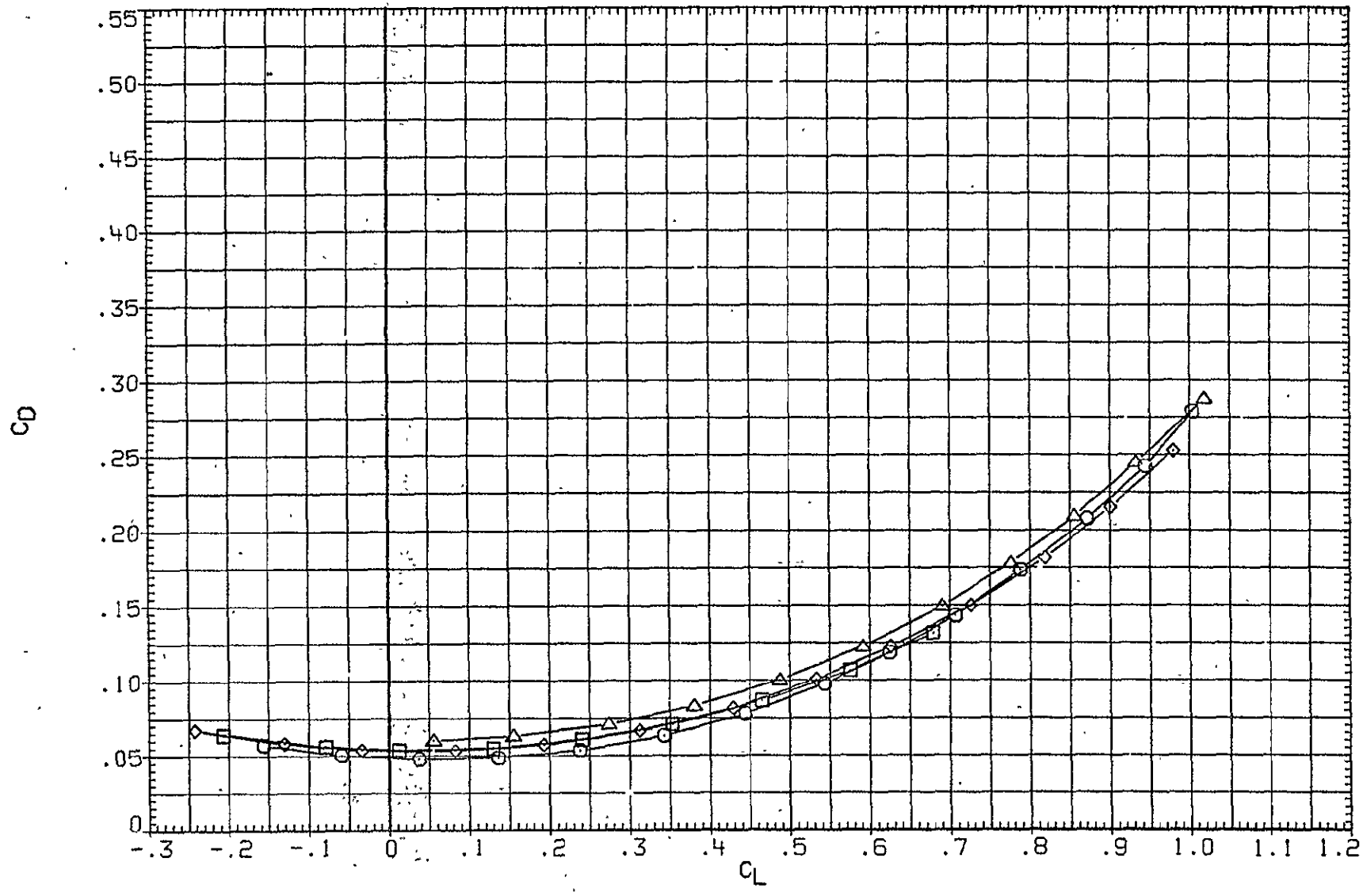

FIG. 10 EFFECT OF HORIZ. TAIL DEFL. ON AT WING, ALL WING CONT. SURF. DEFL. ZERO.

(C) MACH = 1.15

DATA SET	SYMBOL	CONFIGURATION DESCRIPTION	DH	BETA
(BFK007)	○	B V W2		.000
(JFK006)	□	B V W2H	.000	.000
(JFK009)	◇	B V W2H	-5.000	.000
(JFK008)	△	B V W2H	-10.000	.000

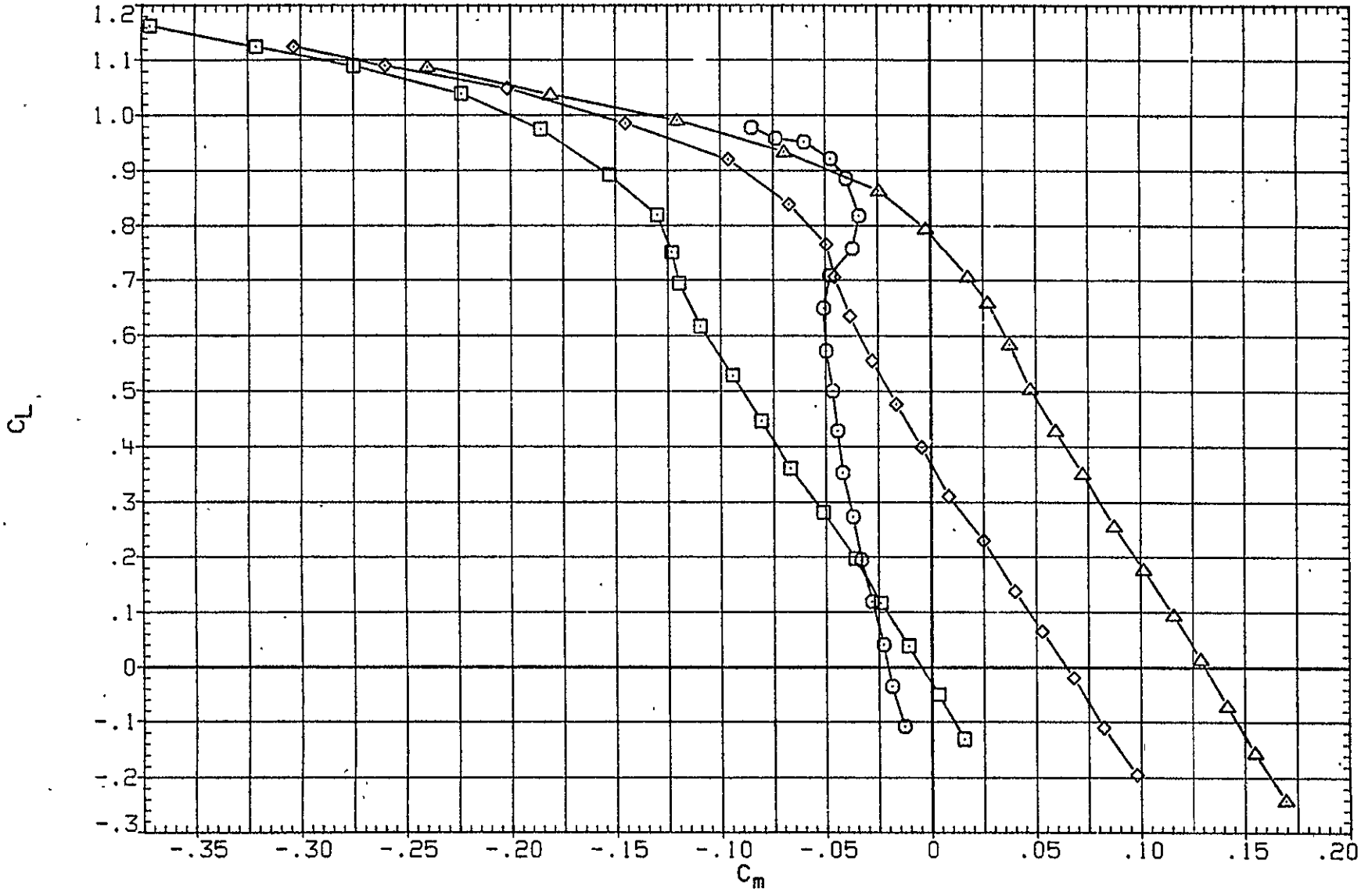

FIG. 10 EFFECT OF HORIZ. TAIL DEFL. ON AT WING. ALL WING CONT. SURF. DEFL. ZERO.

(A) MACH = .70

DATA SET	SYMBOL	CONFIGURATION DESCRIPTION	DH	BETA
(BFK007)	○	B V W2		.000
(JFK006)	□	B V W2H	.000	.000
(JFK009)	◇	B V W2H	-5.000	.000
(JFK008)	△	B V W2H	-10.000	.000

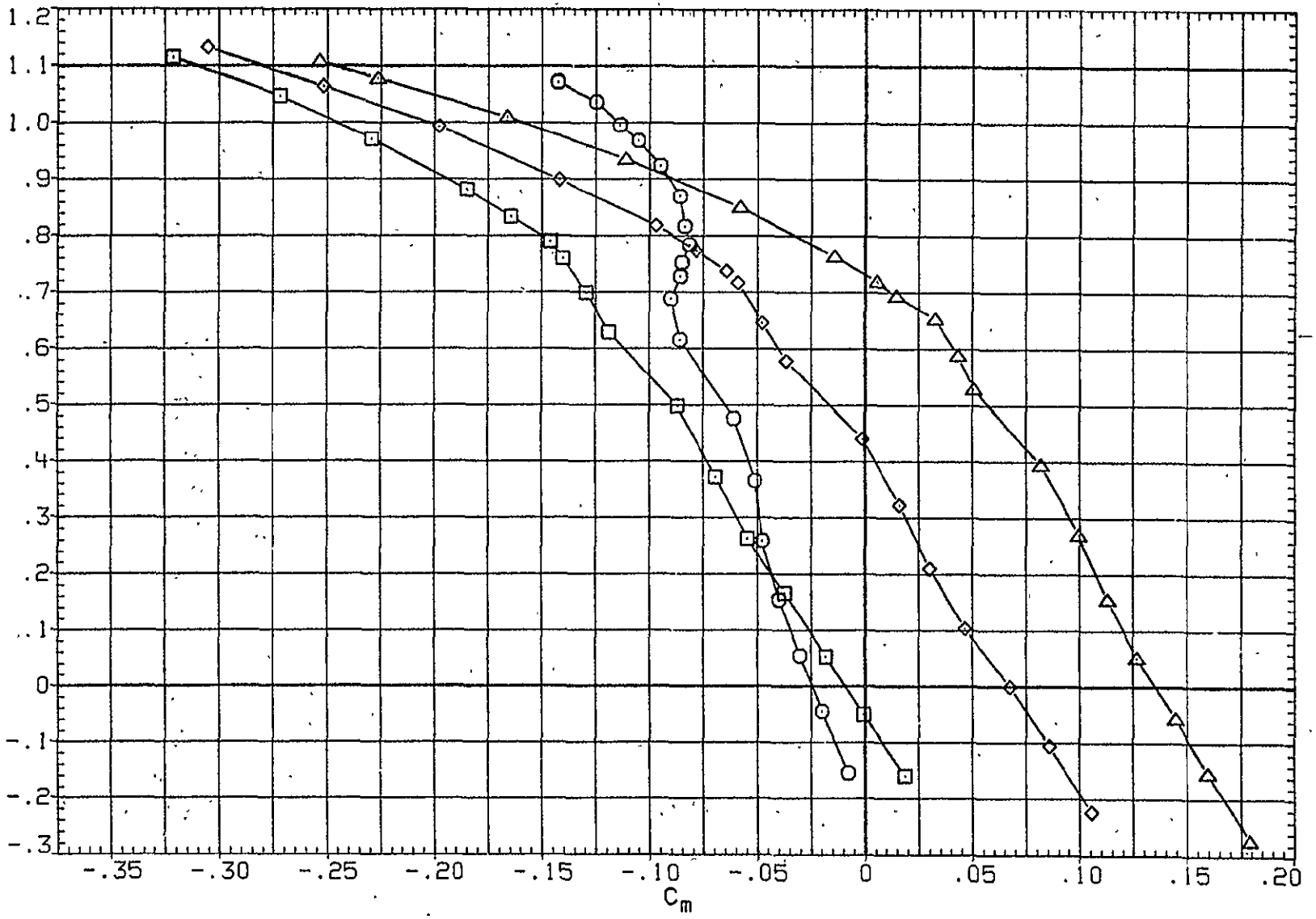

FIG. 10 EFFECT OF HORIZ. TAIL DEFL. ON AT WING. ALL WING CONT. SURF. DEFL. ZERO.

(B)MACH = .90

DATA SET	SYMBOL	CONFIGURATION DESCRIPTION	DH	BETA
(BFK007)	○	B V W2		.000
(JFK006)	□	B V W2H	.000	.000
(JFK009)	◇	B V W2H	-5.000	.000
(JFK008)	△	B V W2H	-10.000	.000

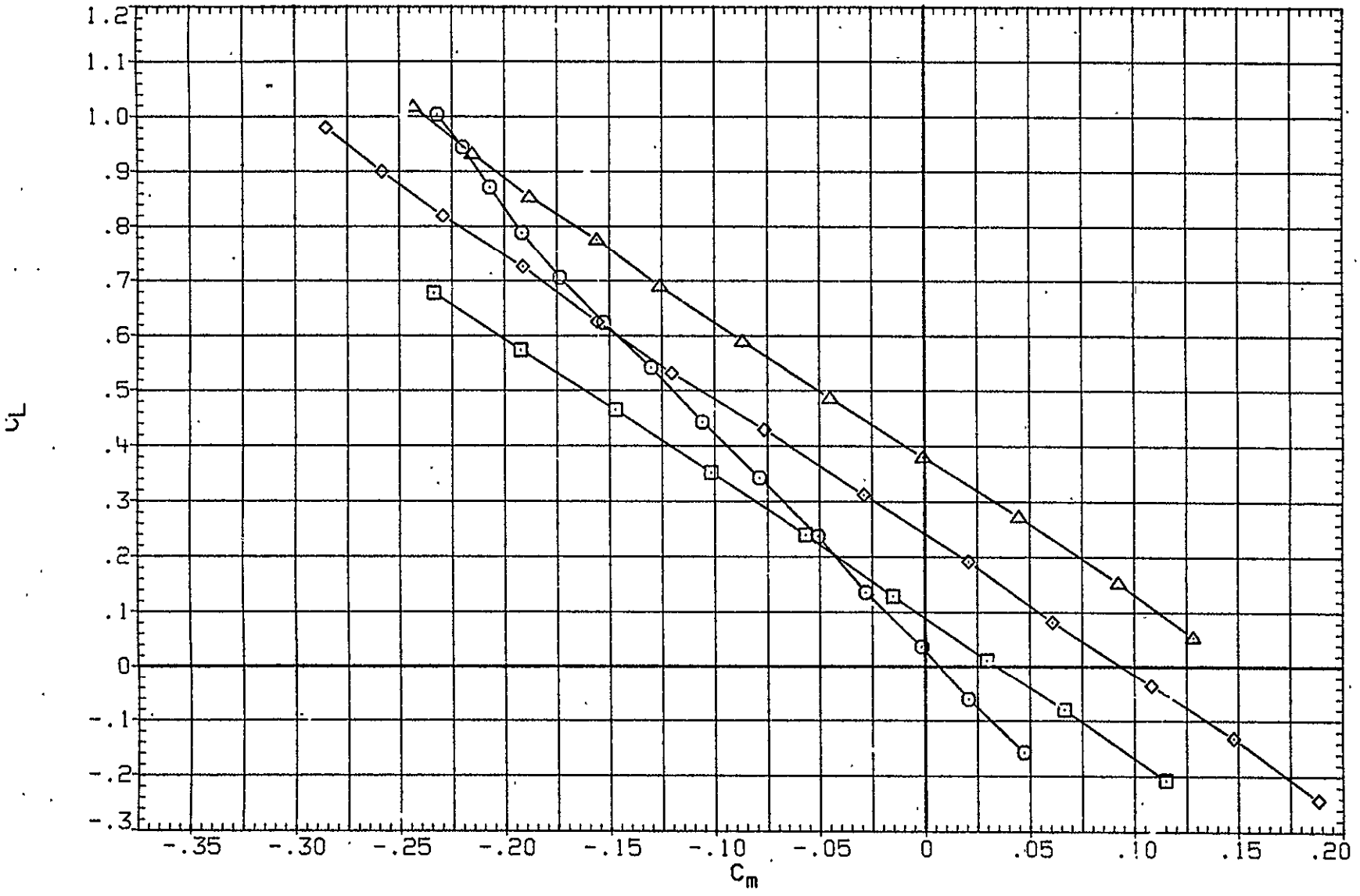

FIG. 10 EFFECT OF HORIZ. TAIL DEFL. ON AT WING. ALL WING CONT. SURF. DEFL. ZERO.

(C)MACH = 1.15

DATA SET	SYMBOL	CONFIGURATION DESCRIPTION	DH	DTEO	DTEI	DLE
(JFK010)	○	B V W2		.000	5.000	10.000
(JFK011)	□	B V W2		5.000	5.000	10.000

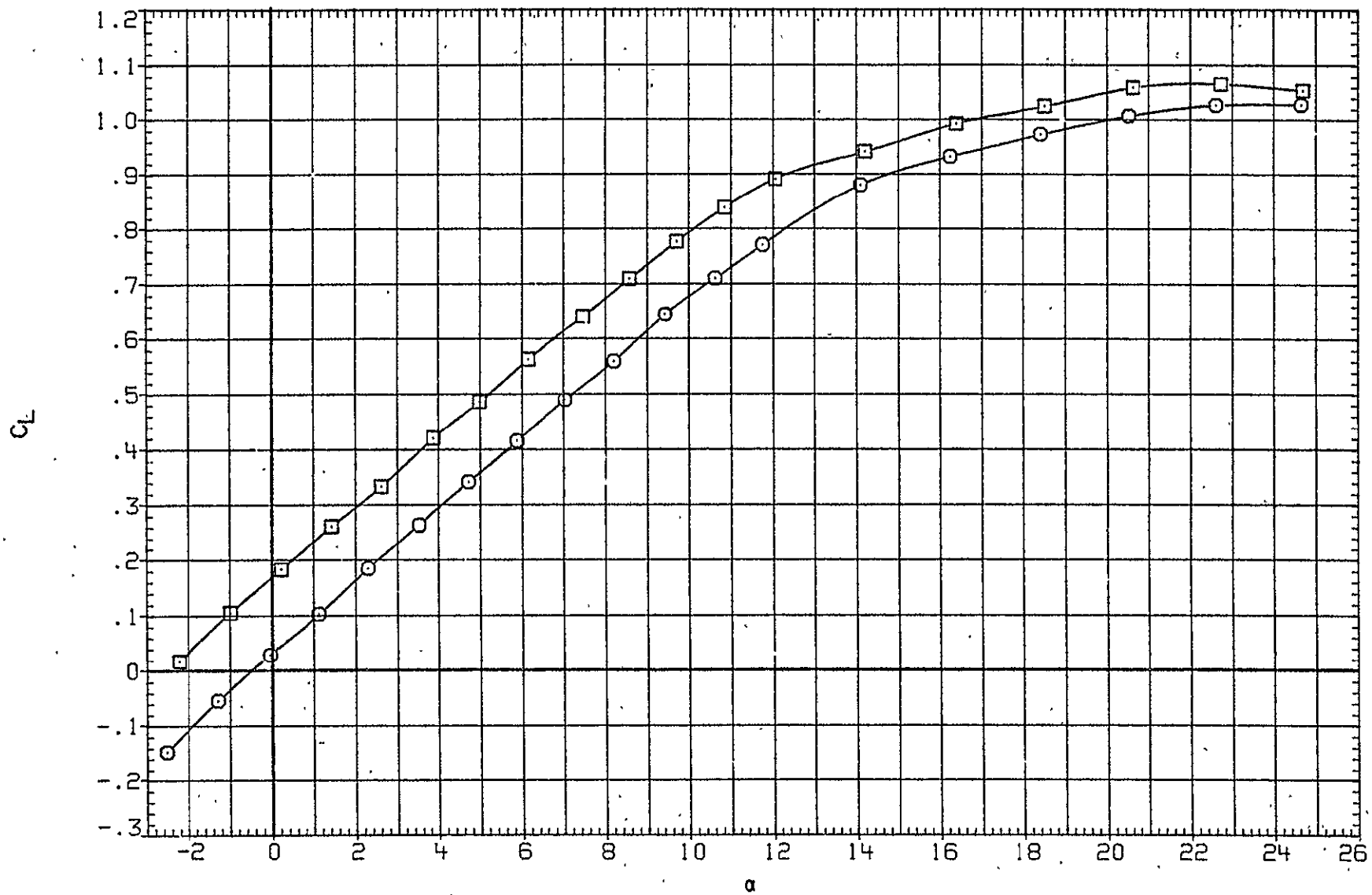

FIG. 11 EFFECT OF HORIZ. TAIL WITH SYMM. CONFORMAL FLAP DEFLECTIONS. DLE=30.

(A)MACH = .70

DATA SET	SYMBOL	CONFIGURATION DESCRIPTION	DH	DTEO	DTEI	DLE
(JFK010)	○	B V W2		.000	5.000	10.000
(JFK011)	□	B V W2		5.000	5.000	10.000

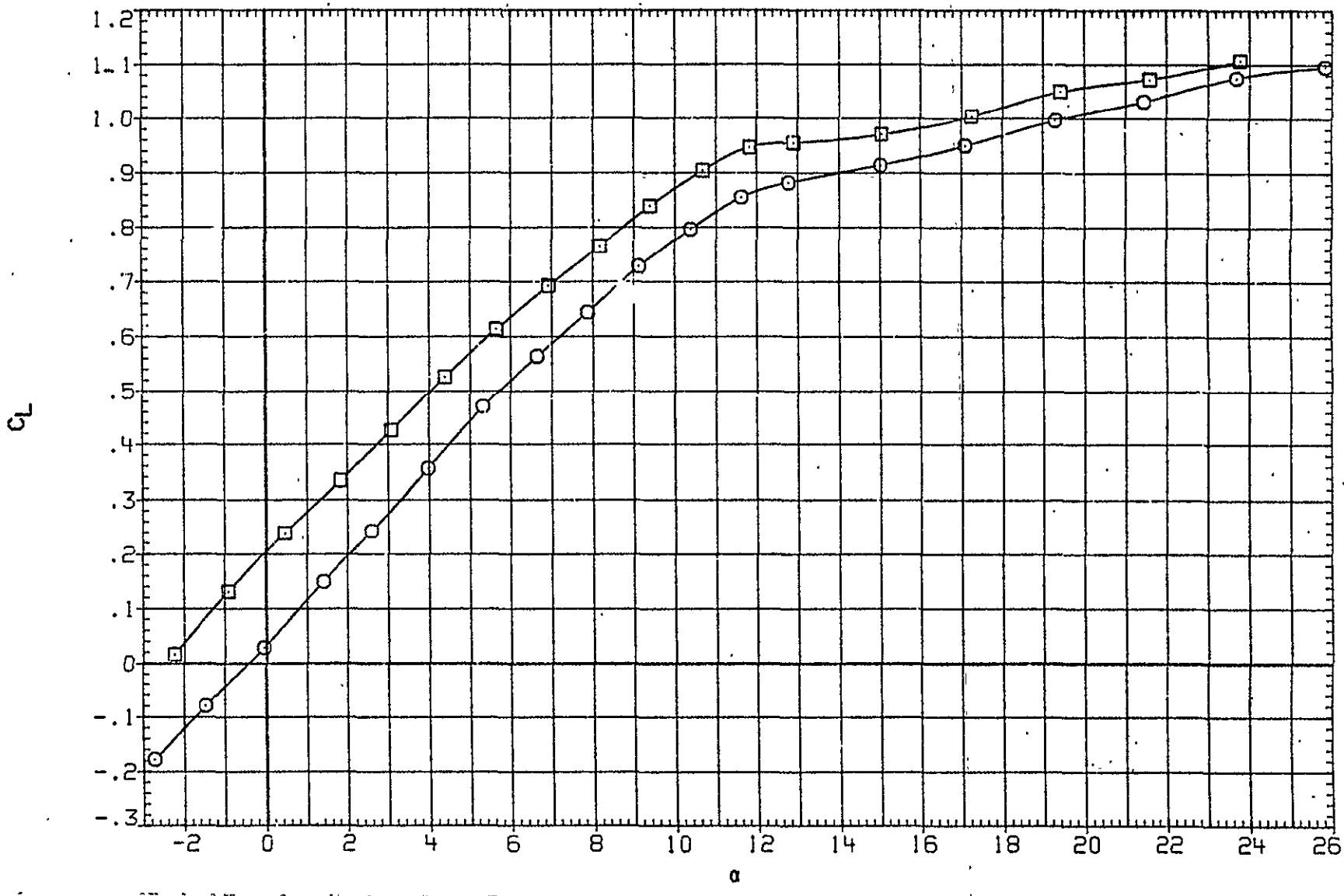

FIG. 11 EFFECT OF HORIZ. TAIL WITH SYMM. CONFORMAL FLAP DEFLECTIONS. DLE=30.

(B)MACH = .90

DATA SET	SYMBOL	CONFIGURATION DESCRIPTION	DH	DTEO	DTEI	DLE
(JFK010)	○	B V W2		.000	5.000	10.000
(JFK011)	□	DATA NOT AVAILABLE		5.000	5.000	10.000

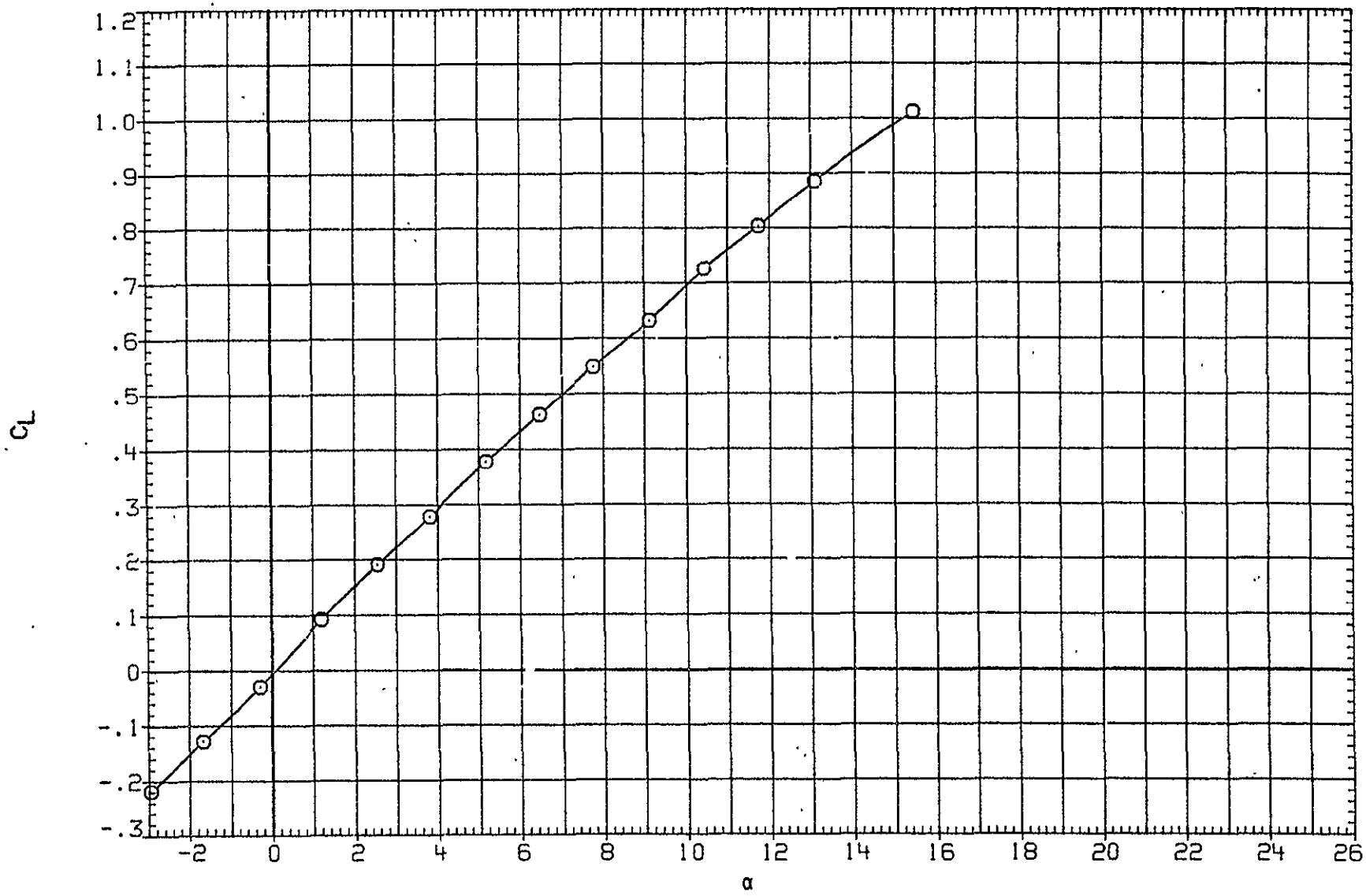

FIG. 11 EFFECT OF HORIZ. TAIL WITH SYMM. CONFORMAL FLAP DEFLECTIONS. DLE=30.

(C)MACH = 1.15

DATA SET	SYMBOL	CONFIGURATION DESCRIPTION	DH	DTEO	DTEI	DLE
(JFK010)	○	B V W2		.000	5.000	10.000
(JFK011)	□	B V W2		5.000	5.000	10.000

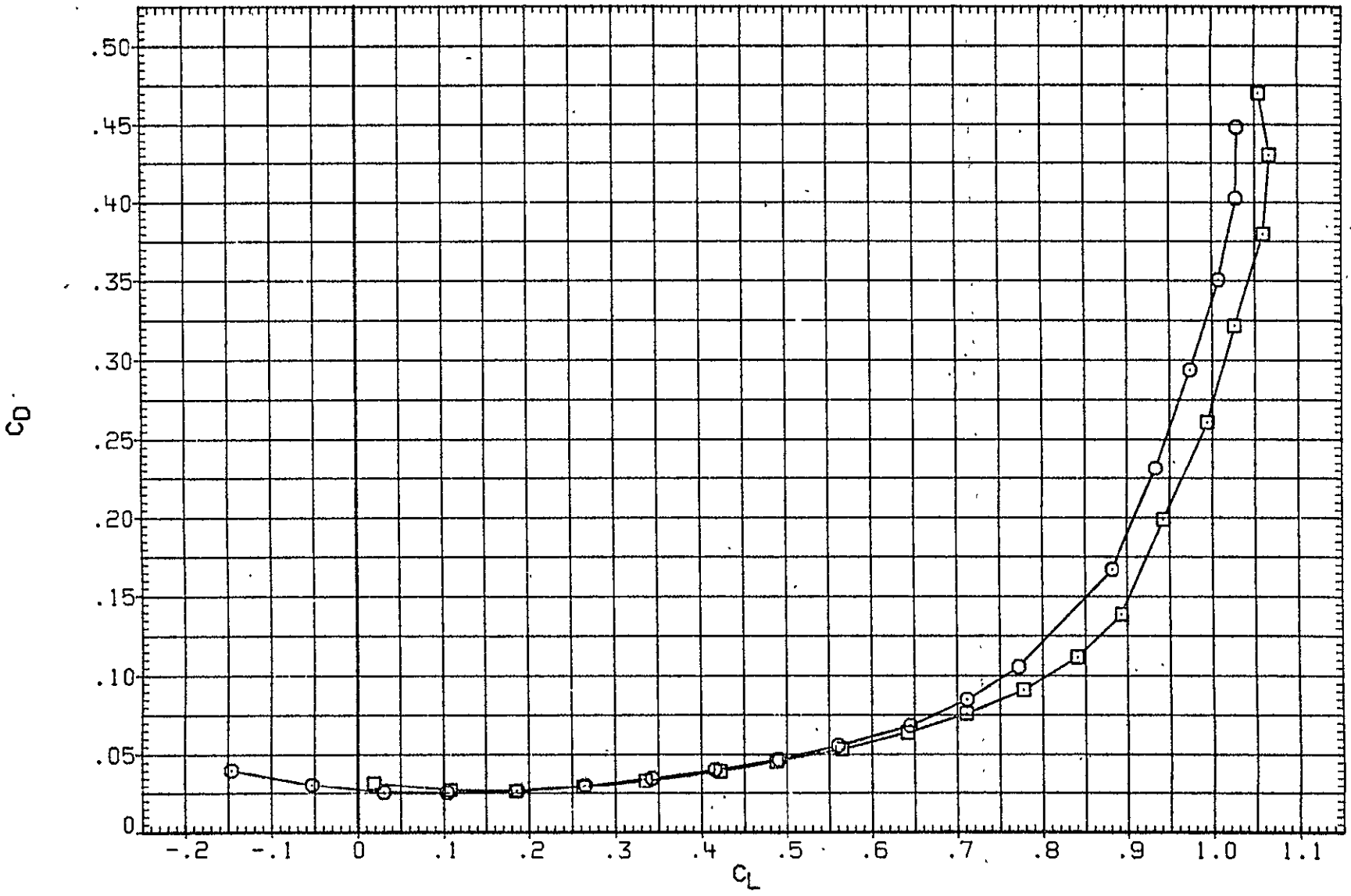

FIG. 11 EFFECT OF HORIZ. TAIL WITH SYMM. CONFORMAL FLAP DEFLECTIONS. DLE=30.

(A) MACH = .70

DATA SET	SYMBOL	CONFIGURATION DESCRIPTION	DH	DTEO	DTEI	DLE
(JFK010)	○	B V W2		.000	5.000	10.000
(JFK011)	□	B V W2		5.000	5.000	10.000

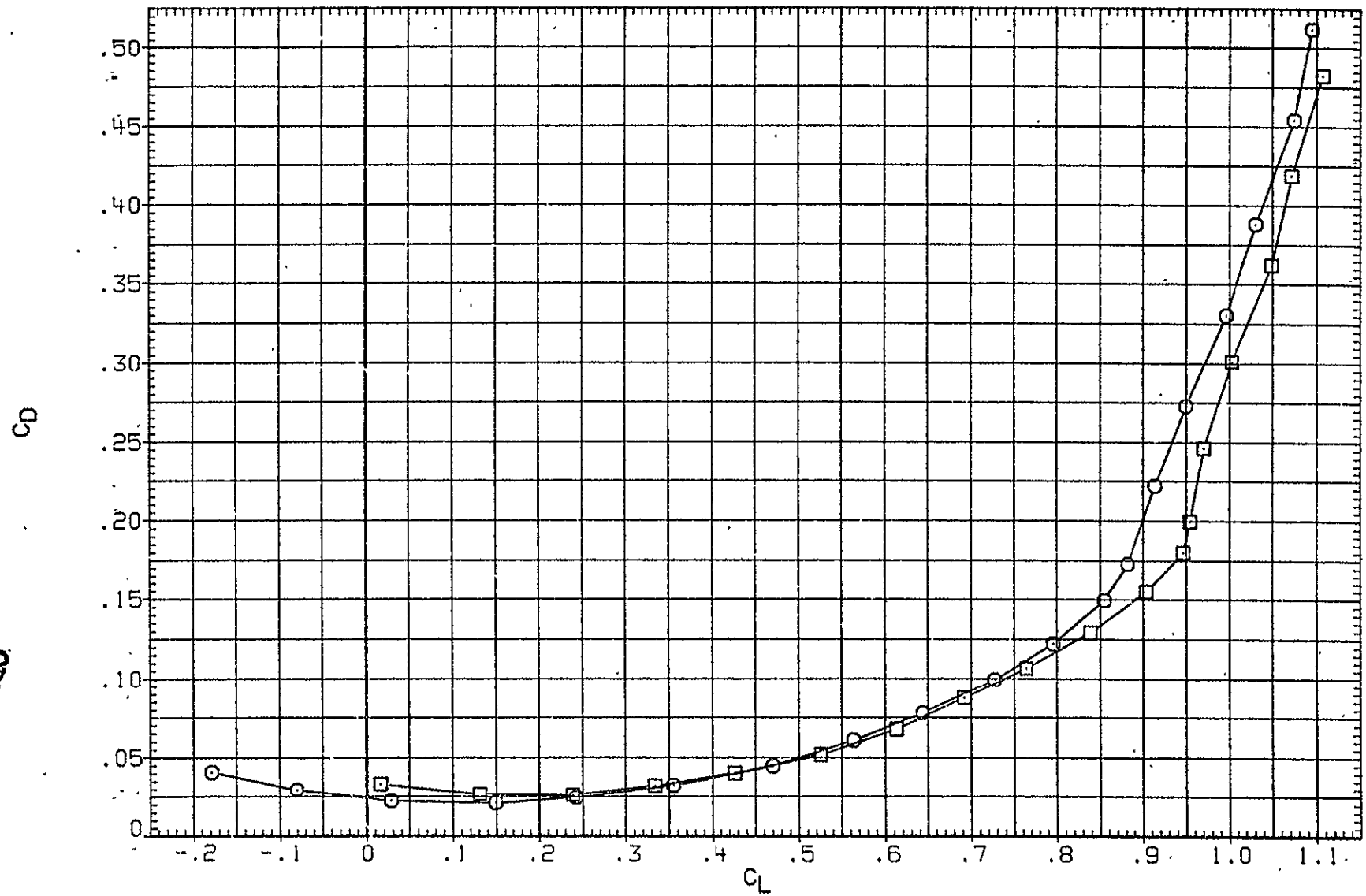

FIG. 11 EFFECT OF HORIZ. TAIL WITH SYMM. CONFORMAL FLAP DEFLECTIONS. DLE=30.

(B) MACH = .90

DATA SET	SYMBOL	CONFIGURATION DESCRIPTION	DH	DTEO	DTEI	DLE
(JFK010)	○	B V W2		.000	5.000	10.000
(JFK011)	□	DATA NOT AVAILABLE		5.000	5.000	10.000

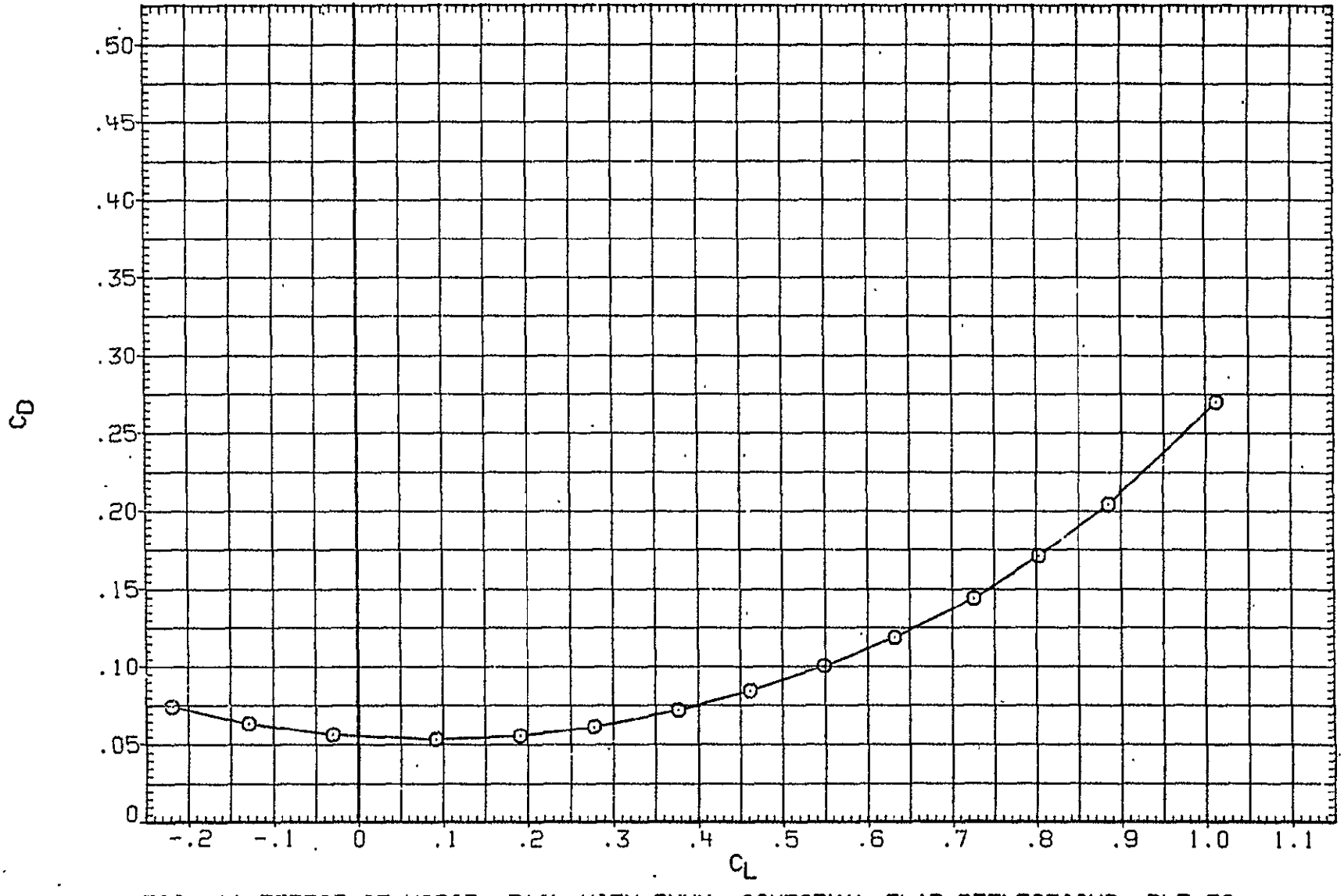

FIG. 11 EFFECT OF HORIZ. TAIL WITH SYMM. CONFORMAL FLAP DEFLECTIONS. DLE=30.

(C) MACH = 1.15

DATA SET	SYMBOL	CONFIGURATION DESCRIPTION	DH	DTEO	DTEI	DLE
(JFK010)	○	B V W2		.000	5.000	10.000
(JFK011)	□	B V W2		5.000	5.000	10.000

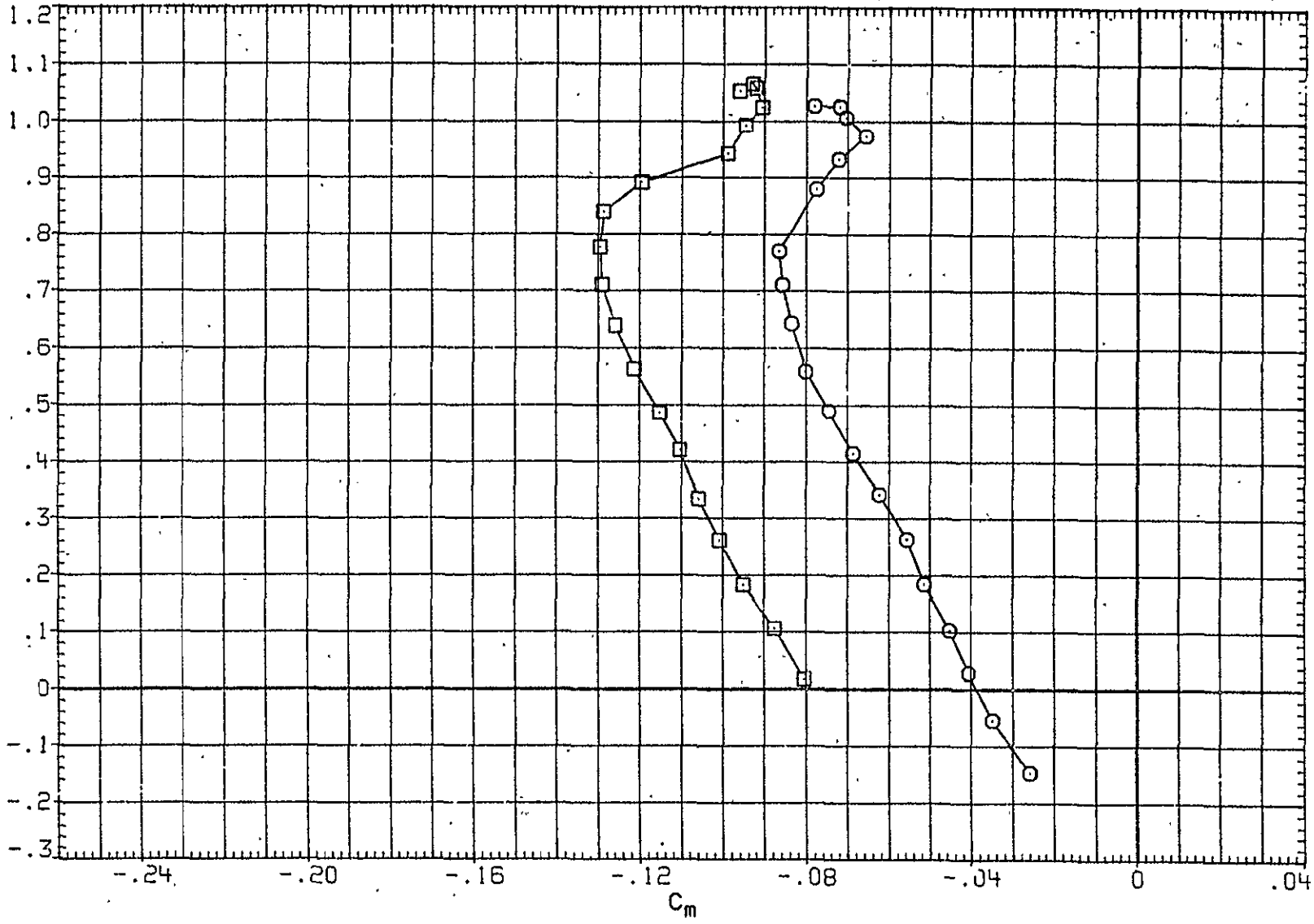

FIG. 11 EFFECT OF HORIZ. TAIL WITH SYMM. CONFORMAL FLAP DEFLECTIONS. DLE=30.

(A)MACH = .70

DATA SET	SYMBOL	CONFIGURATION DESCRIPTION	DH	DTEO	DTEI	DLE
(JFK010)	○	B V W2		.000	5.000	10.000
(JFK011)	□	B V W2		5.000	5.000	10.000

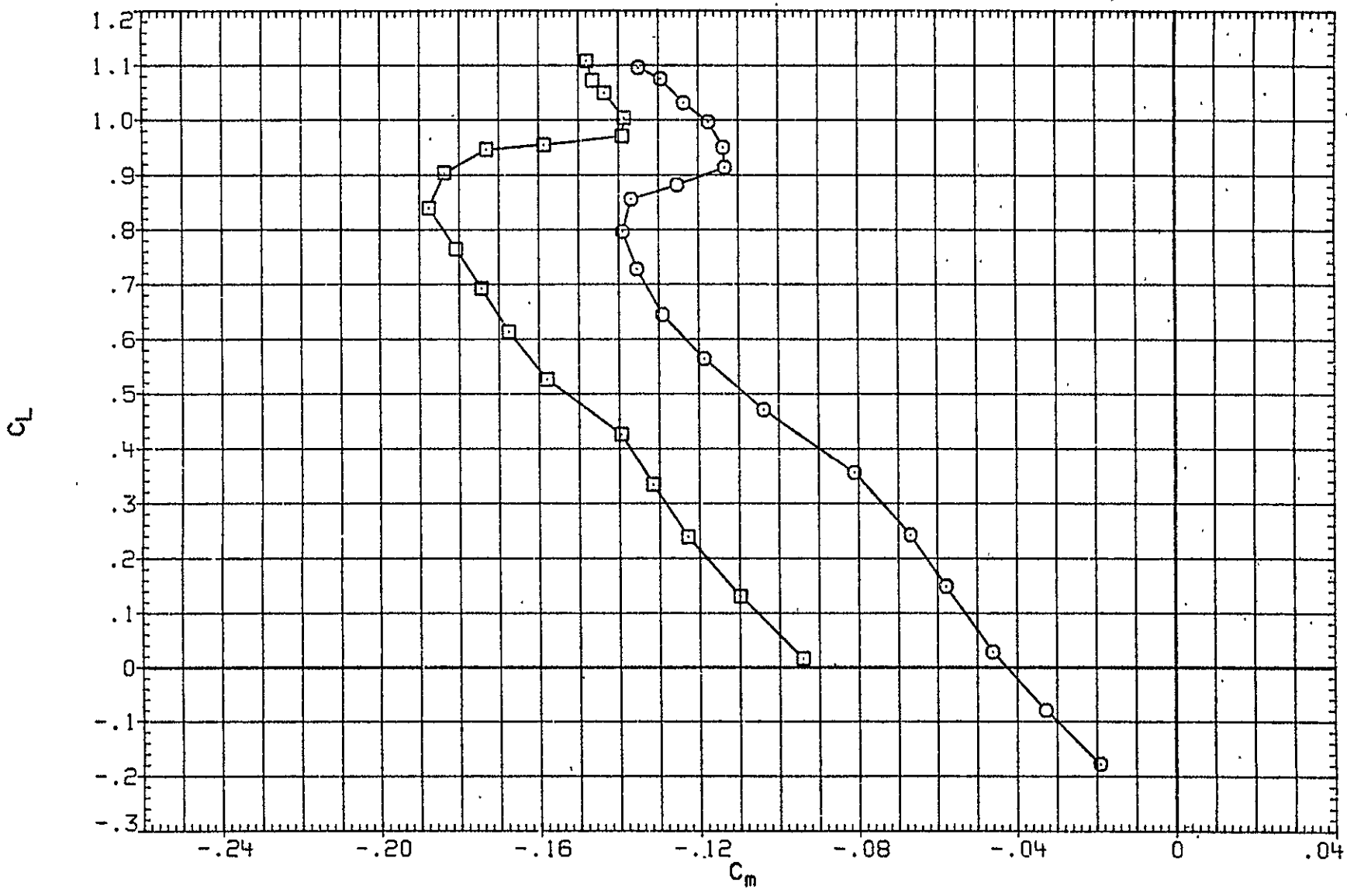

FIG. 11 EFFECT OF HORIZ. TAIL WITH SYMM. CONFORMAL FLAP DEFLECTIONS. DLE=30.

(B) MACH = .90

DATA SET	SYMBOL	CONFIGURATION DESCRIPTION	DH	DTEO	DTEI	DLE
(JFK010)	○	B V W2		.000	5.000	10.000
(JFK011)	□	DATA NOT AVAILABLE		5.000	5.000	10.000

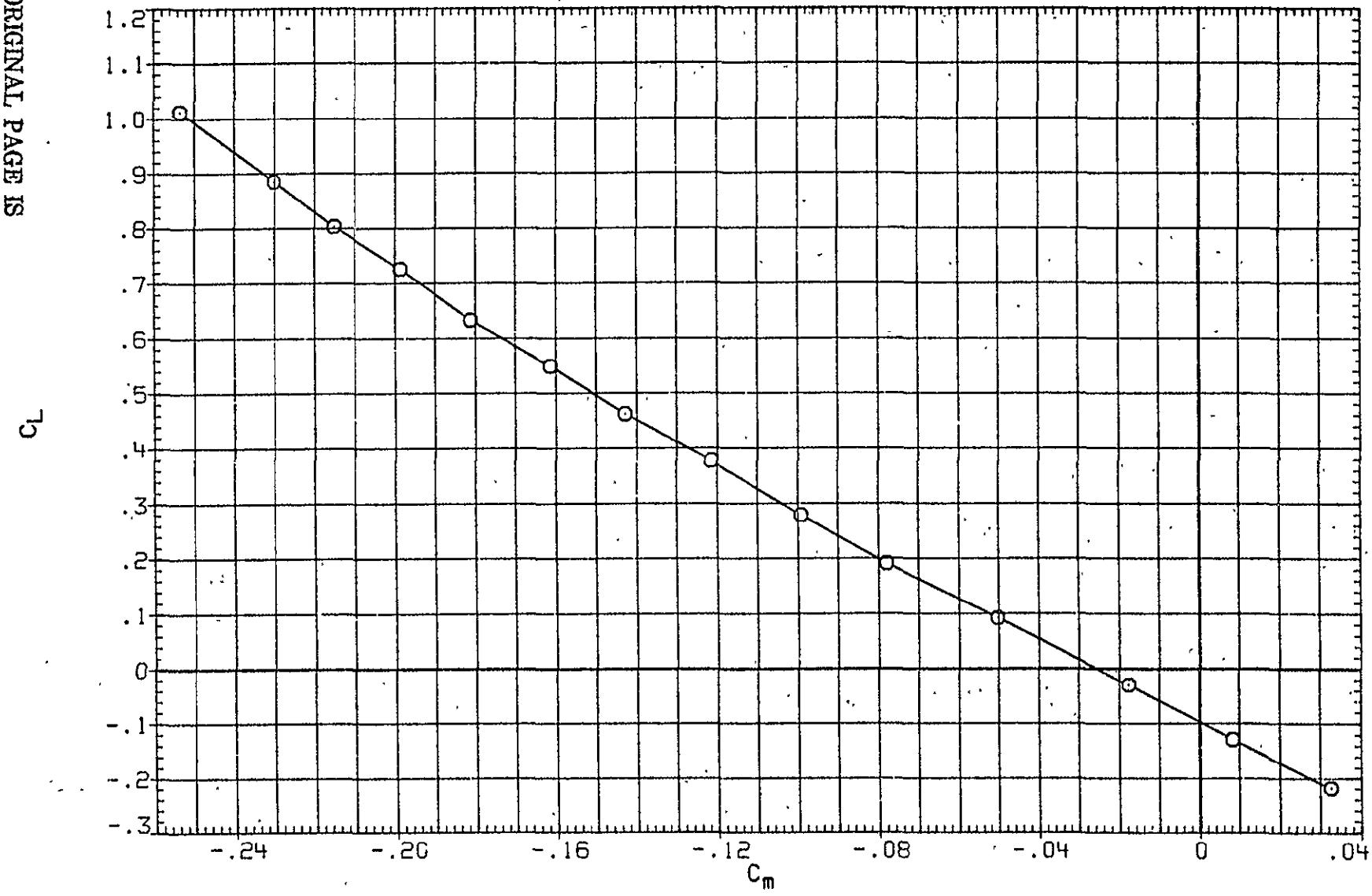

FIG. 11 EFFECT OF HORIZ. TAIL WITH SYMM. CONFORMAL FLAP DEFLECTIONS. DLE=30.

(C)MACH = 1.15

DATA SET	SYMBOL	CONFIGURATION DESCRIPTION	DH	DTEO	DTEI	DLE
(JFK024)	○	B V W3		10.000	10.000	30.000
(JFK022)	□	B V W3H	.000	10.000	10.000	30.000
(JFK023)	◇	B V W3H	-5.000	10.000	10.000	30.000
(JFK034)	△	B V W2		-2.000	-2.000	.000
(JFK035)	◁	B V W2H	.000	-2.000	-2.000	.000

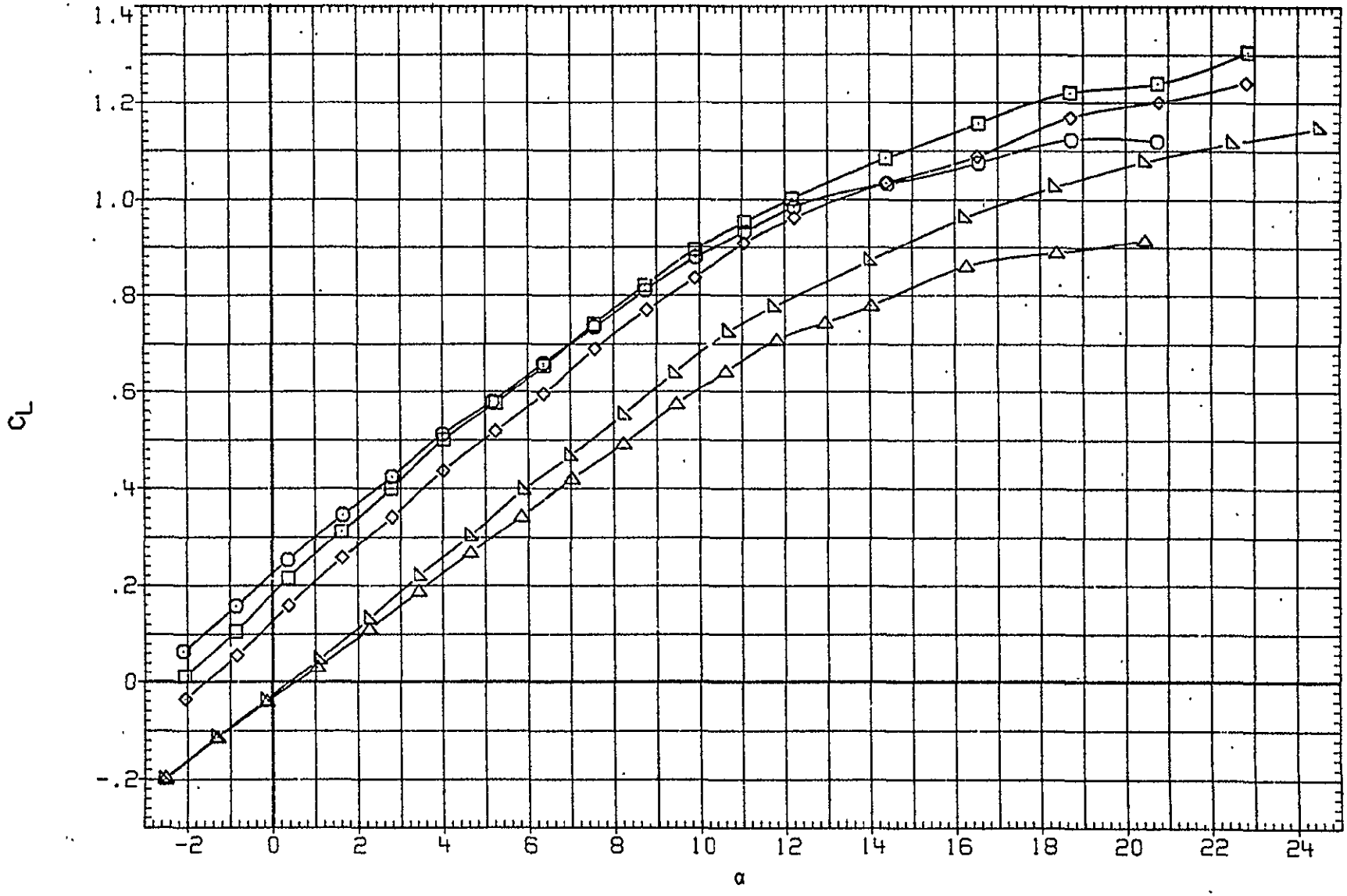

FIG. 12 EFFECT OF HORIZ. TAIL WITH SYMM. CONFORMAL FLAP DEFLECTIONS. DLE=0 OR 30

(A)MACH = .70

DATA SET	SYMBOL	CONFIGURATION DESCRIPTION	DH	DTEO	DTEI	DLE
(JFK024)	○	B V W3		10.000	10.000	30.000
(JFK022)	□	B V W3H	.000	10.000	10.000	30.000
(JFK023)	◇	B V W3H	-5.000	10.000	10.000	30.000
(JFK034)	◁	B V W2		-2.000	-2.000	.000
(JFK035)	◁	B V W2H	.000	-2.000	-2.000	.000

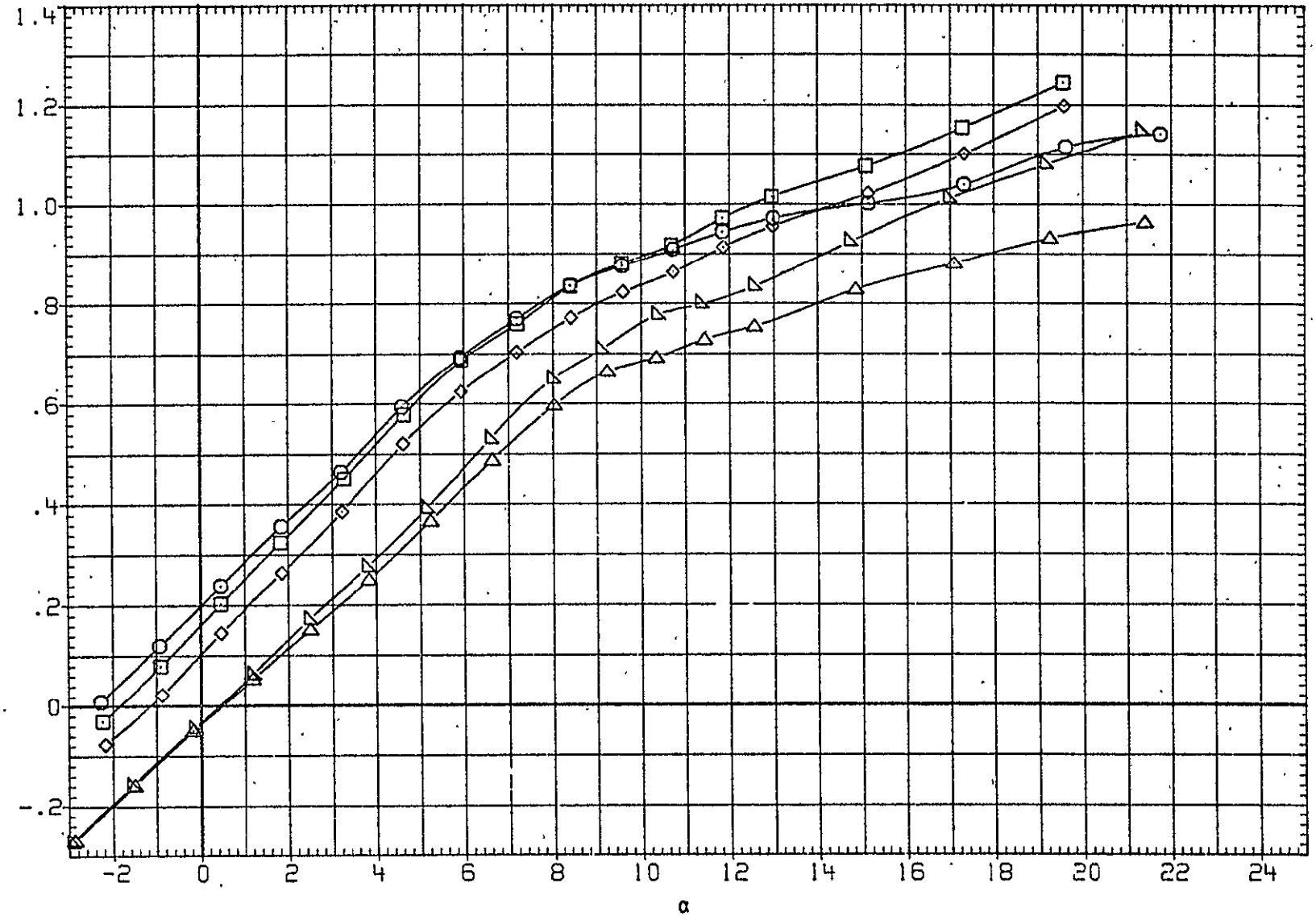

FIG. 12 EFFECT OF HORIZ. TAIL WITH SYMM. CONFORMAL FLAP DEFLECTIONS. DLE=0 OR 30

(B) MACH = .90

DATA SET	SYMBOL	CONFIGURATION DESCRIPTION	DH	DTEO	DTEI	DLE
(JFK024)	○	DATA NOT AVAILABLE		10.000	10.000	30.000
(JFK022)	□	DATA NOT AVAILABLE	.000	10.000	10.000	30.000
(JFK023)	◇	DATA NOT AVAILABLE	-5.000	10.000	10.000	30.000
(JFK034)	△	B V W2		-2.000	-2.000	.000
(JFK035)	◺	B V W2H	.000	-2.000	-2.000	.000

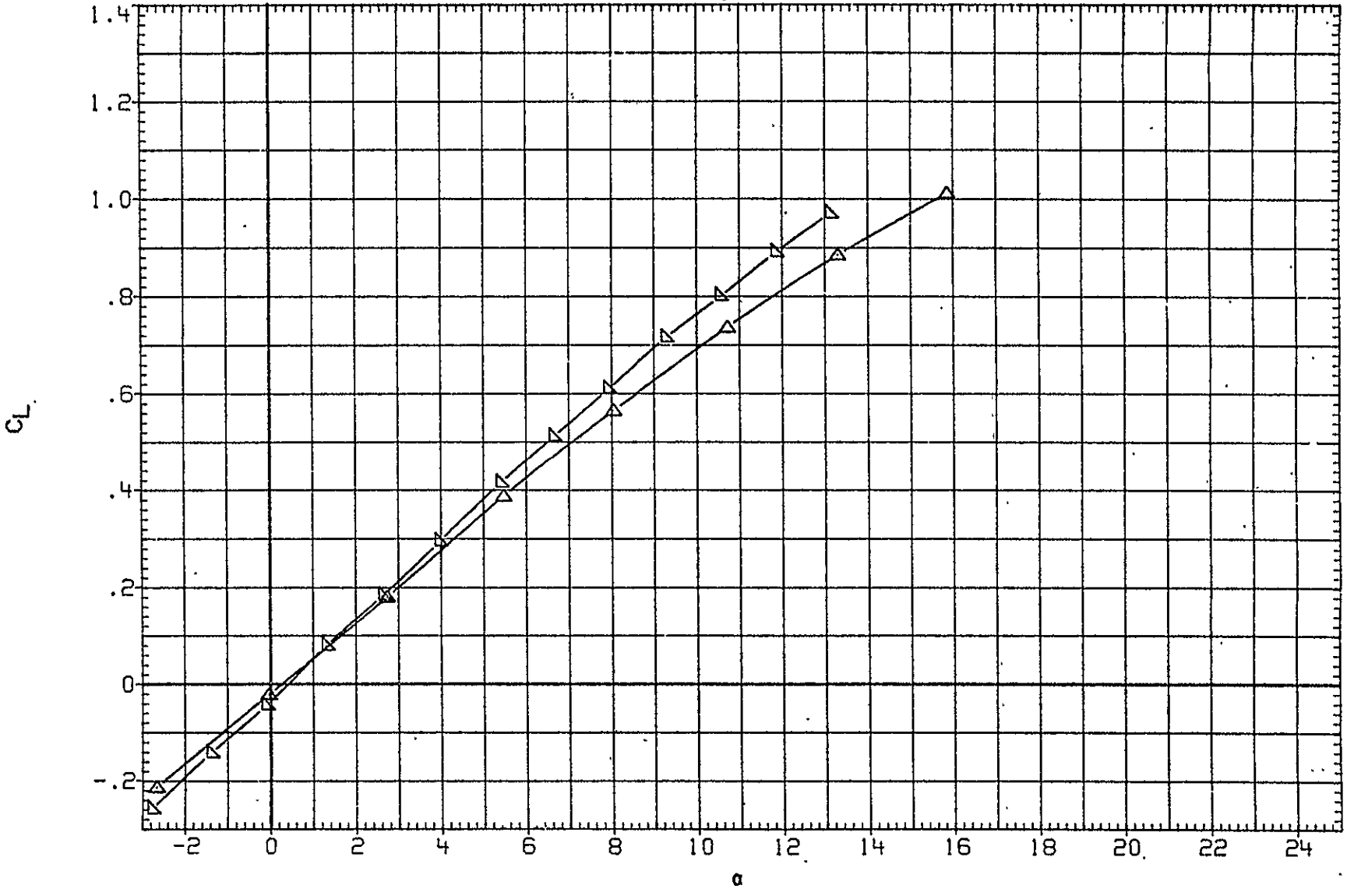

FIG. 12 EFFECT OF HORIZ. TAIL WITH SYMM. CONFORMAL FLAP DEFLECTIONS. DLE=0 OR 30

(C) MACH = 1.15

ORIGINAL PAGE IS
OF POOR QUALITY

DATA SET	SYMBOL	CONFIGURATION DESCRIPTION	DH	DTEO	DTEI	DLE
(JFK024)	○	B V W3		10.000	10.000	30.000
(JFK022)	□	B V W3H	.000	10.000	10.000	30.000
(JFK023)	◇	B V W3H	-5.000	10.000	10.000	30.000
(JFK034)	◁	B V W2		-2.000	-2.000	.000
(JFK035)	△	B V W2H	.000	-2.000	-2.000	.000

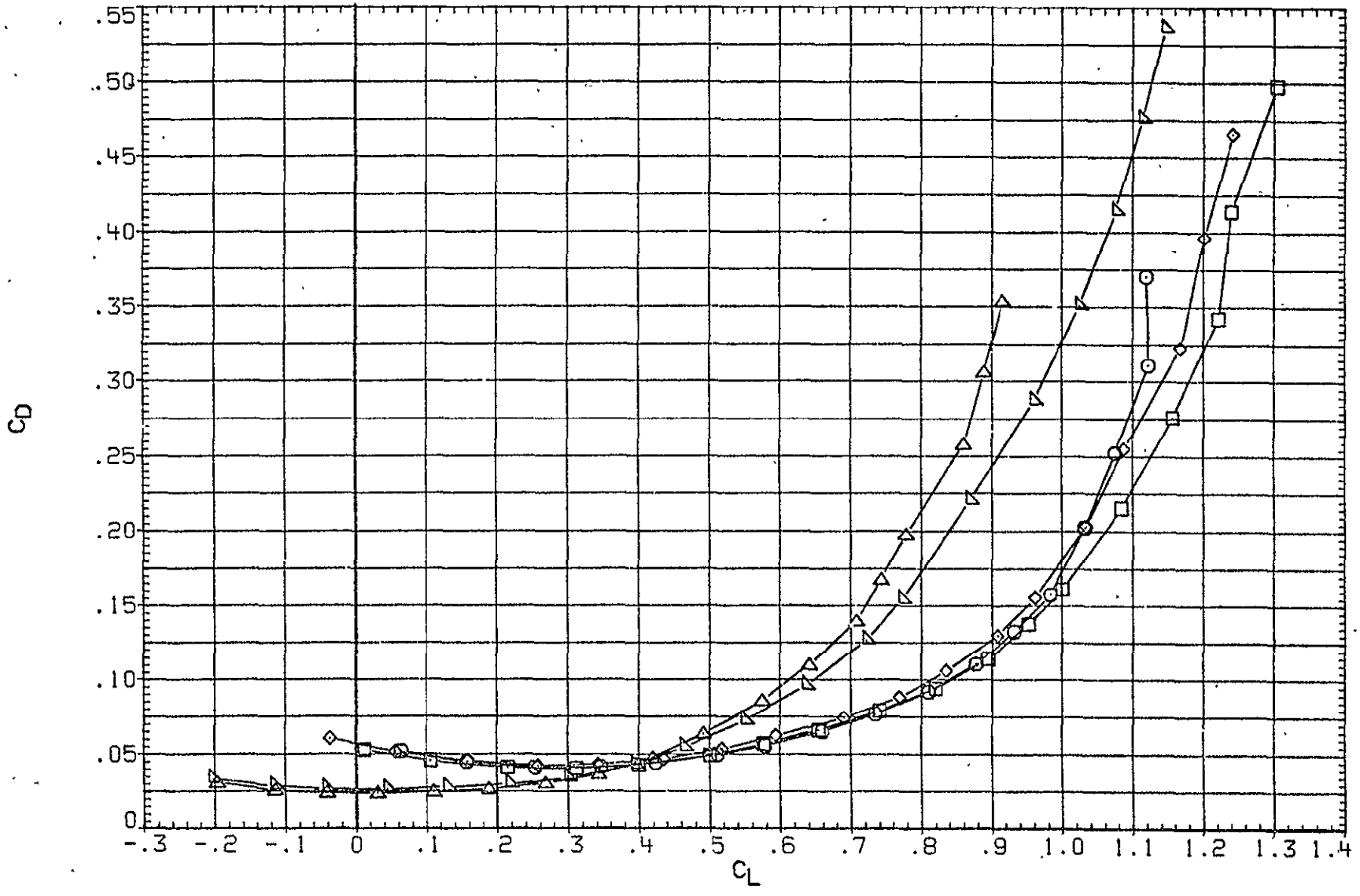

FIG. 12 EFFECT OF HORIZ. TAIL WITH SYMM. CONFORMAL FLAP DEFLECTIONS. DLE=0 OR 30

(A) MACH = .70

DATA SET	SYMBOL	CONFIGURATION DESCRIPTION	DH	DTEO	DTEI	DLE
(JFK024)	○	B V W3		10.000	10.000	30.000
(JFK022)	□	B V W3H	.000	10.000	10.000	30.000
(JFK023)	◇	B V W3H	-5.000	10.000	10.000	30.000
(JFK034)	△	B V W2		-2.000	-2.000	.000
(JFK035)	◺	B V W2H	.000	-2.000	-2.000	.000

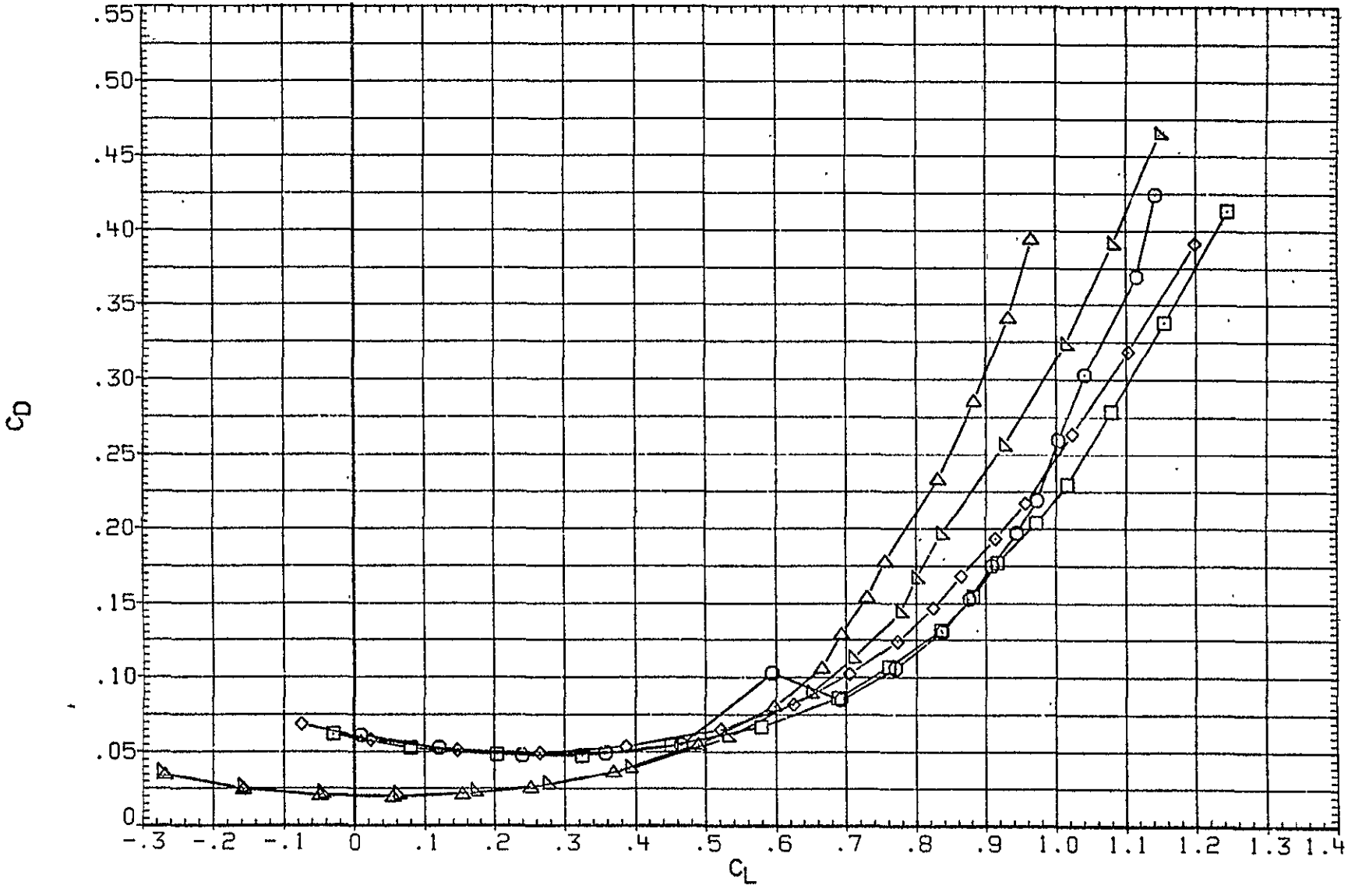

FIG. 12 EFFECT OF HORIZ. TAIL WITH SYMM. CONFORMAL FLAP DEFLECTIONS. DLE=0 OR 30

(B) MACH = .90

C-2

DATA SET	SYMBOL	CONFIGURATION DESCRIPTION	DH	DTEO	DTEI	DLE
(JFK024)	○	DATA NOT AVAILABLE		10.000	10.000	30.000
(JFK022)	□	DATA NOT AVAILABLE	.000	10.000	10.000	30.000
(JFK023)	◇	DATA NOT AVAILABLE	-5.000	10.000	10.000	30.000
(JFK034)	△	B V W2		-2.000	-2.000	.000
(JFK035)	◺	B V W2H	.000	-2.000	-2.000	.000

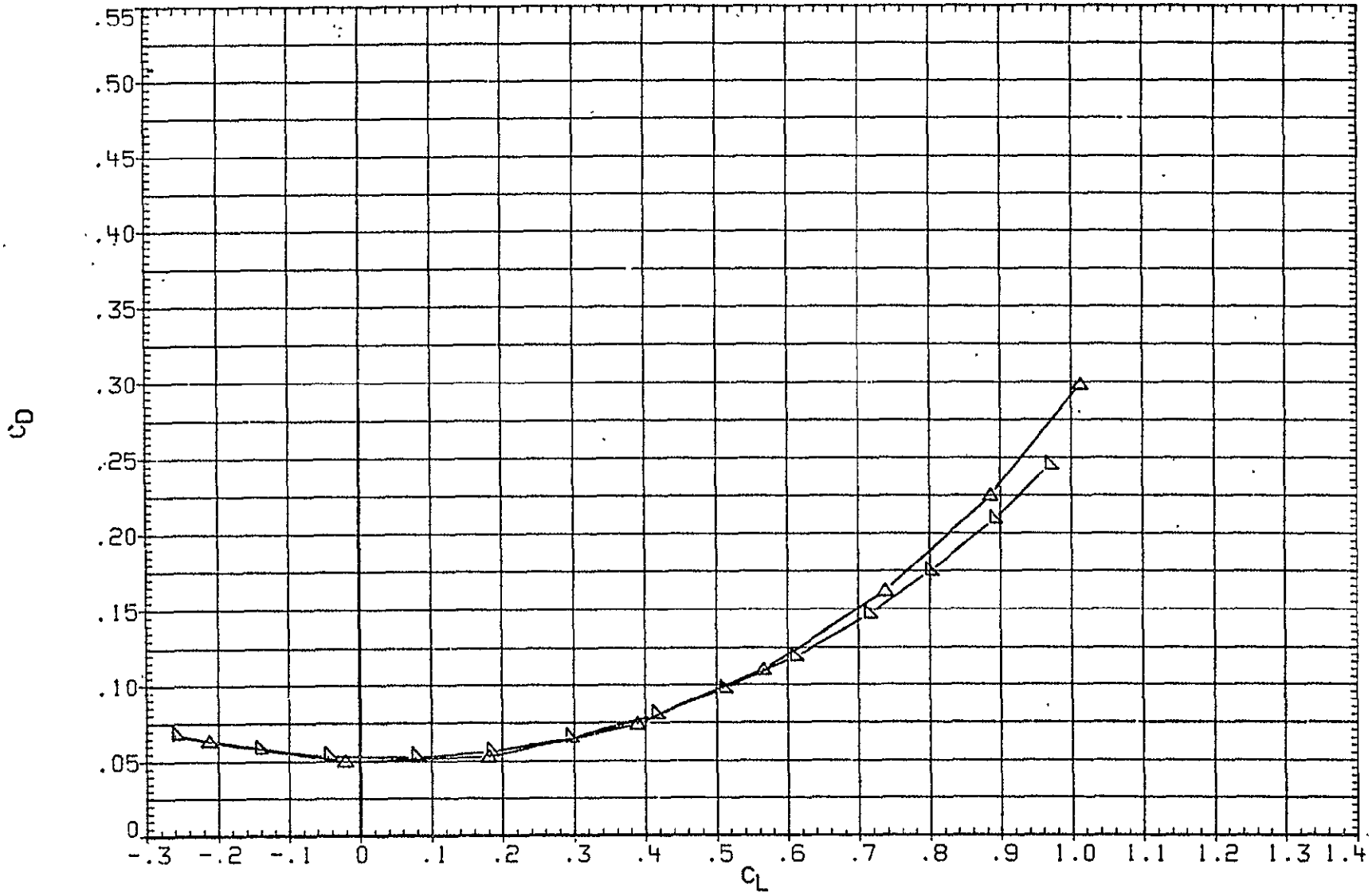

FIG. 12 EFFECT OF HORIZ. TAIL WITH SYMM. CONFORMAL FLAP DEFLECTIONS: DLE=0 OR 30

(C) MACH = 1.15

DATA SET	SYMBOL	CONFIGURATION DESCRIPTION	DH	DTEO	DTEI	DLE
(JFK024)	○	B V W3		10.000	10.000	30.000
(JFK022)	□	B V W3H	.000	10.000	10.000	30.000
(JFK023)	◇	B V W3H	-5.000	10.000	10.000	30.000
(JFK034)	△	B V W2		-2.000	-2.000	.000
(JFK035)	◁	B V W2H	.000	-2.000	-2.000	.000

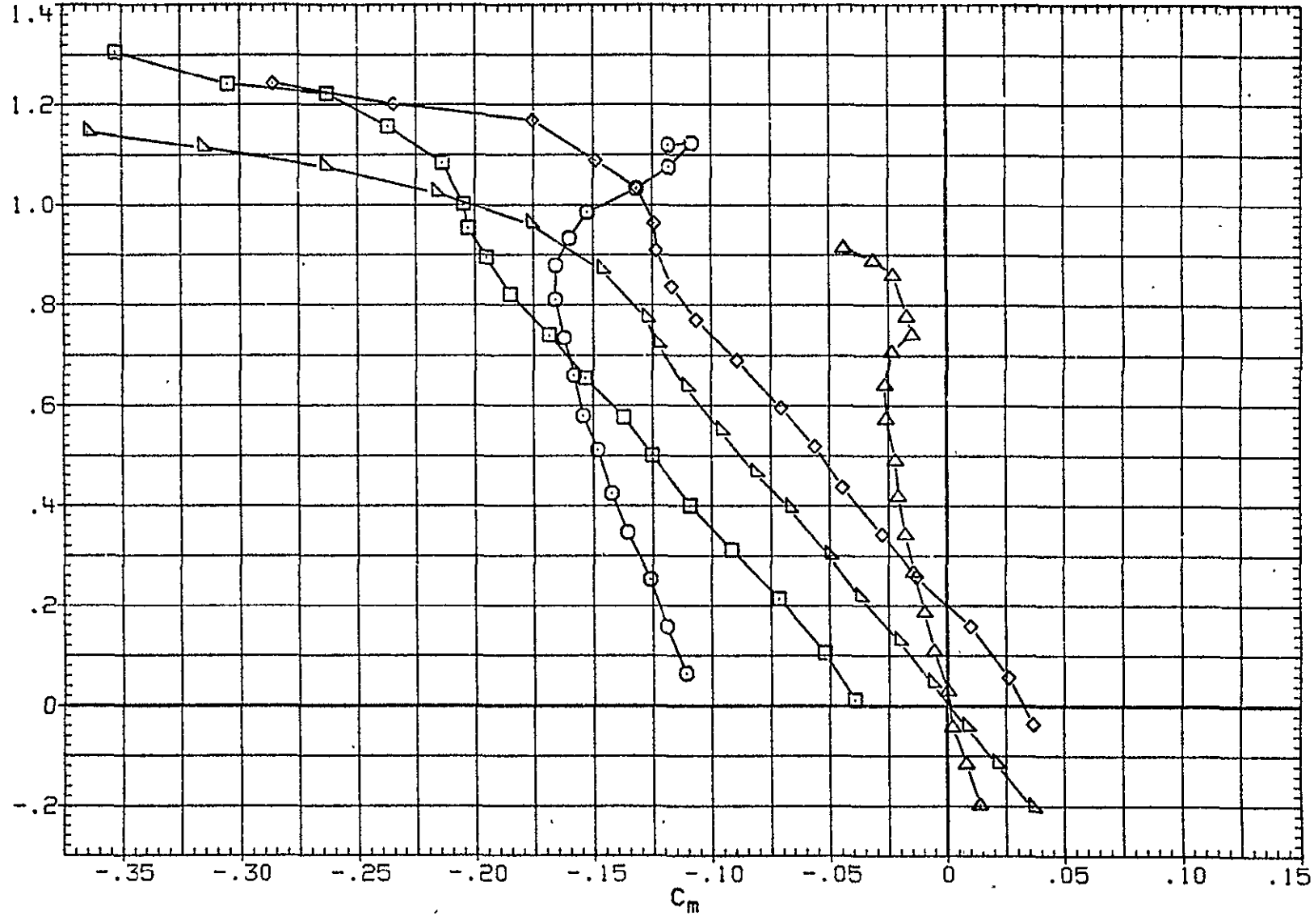

FIG. 12 EFFECT OF HORIZ. TAIL WITH SYMM. CONFORMAL FLAP DEFLECTIONS. DLE=0 OR 30

(A) MACH = .70

DATA SET	SYMBOL	CONFIGURATION DESCRIPTION	DH	DTEO	DTEI	DLE
(JFK024)	○	B V W3		10.000	10.000	30.000
(JFK022)	□	B V W3H	.000	10.000	10.000	30.000
(JFK023)	◇	B V W3H	-5.000	10.000	10.000	30.000
(JFK034)	△	B V W2		-2.000	-2.000	.000
(JFK035)	◺	B V W2H	.000	-2.000	-2.000	.000

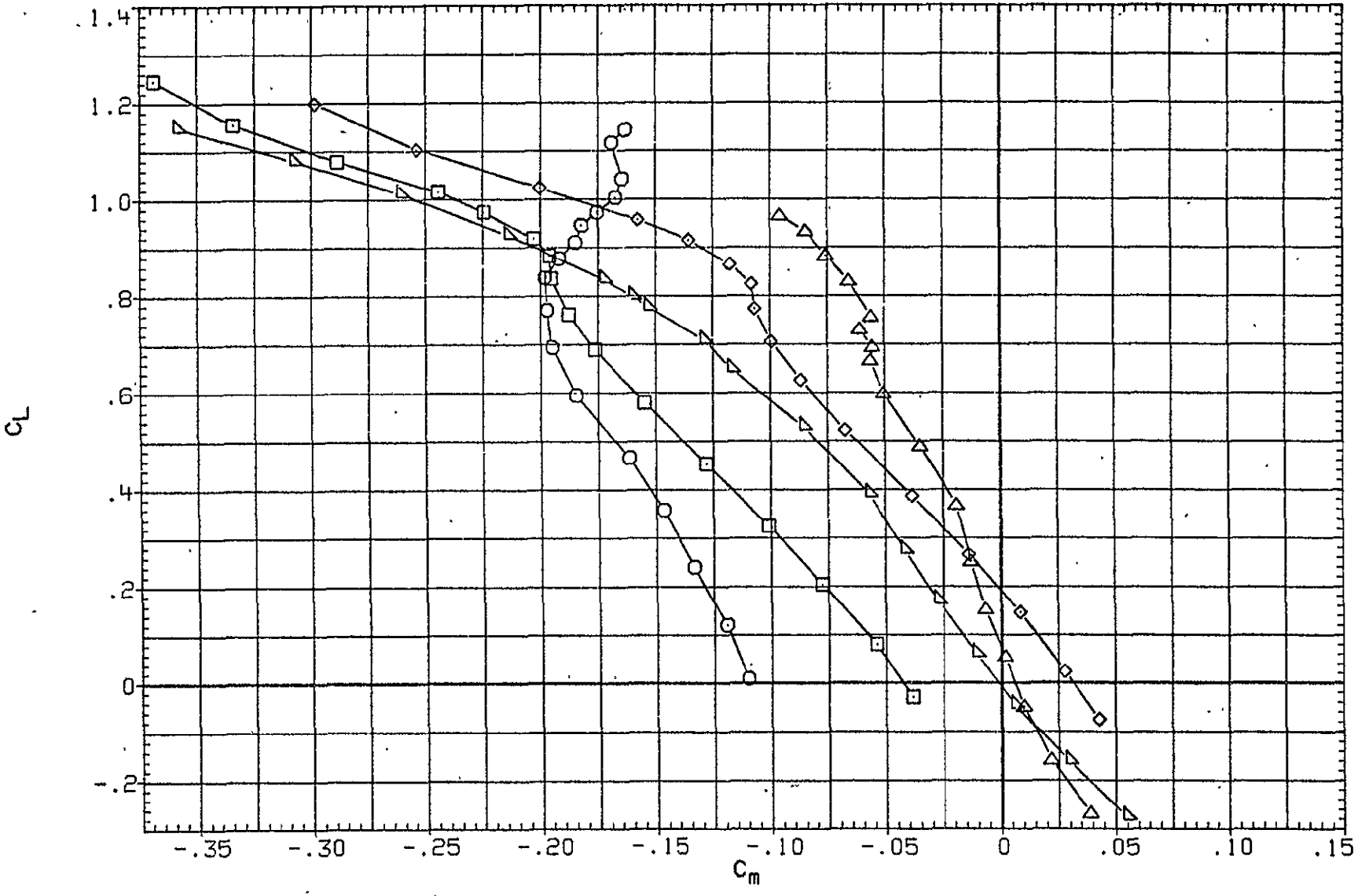

FIG. 12 EFFECT OF HORIZ. TAIL WITH SYMM.-CONFORMAL FLAP DEFLECTIONS. DLE=0 OR 30

(B) MACH = .90

DATA SET	SYMBOL	CONFIGURATION DESCRIPTION	DH	DTEO	DTEI	DLE
(JFK024)	○	DATA NOT AVAILABLE		10.000	10.000	30.000
(JFK022)	□	DATA NOT AVAILABLE	.000	10.000	10.000	30.000
(JFK023)	◇	DATA NOT AVAILABLE	-5.000	10.000	10.000	30.000
(JFK034)	△	B V W2		-2.000	-2.000	.000
(JFK035)	▷	B V W2H	.000	-2.000	-2.000	.000

FIG. 12 EFFECT OF HORIZ. TAIL WITH SYMM. CONFORMAL FLAP DEFLECTIONS. DLE=0 OR 30

(C)MACH = 1.15

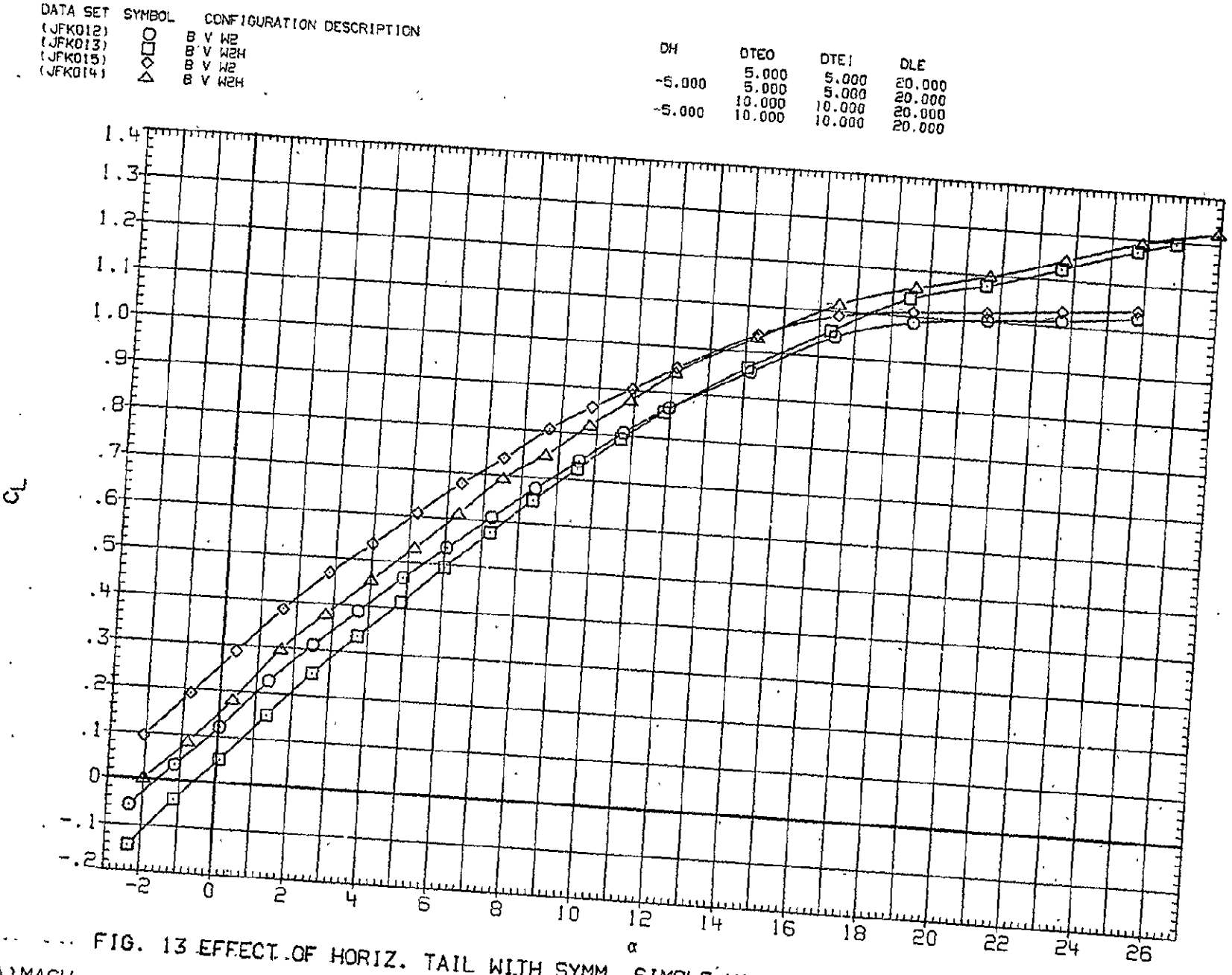

FIG. 13 EFFECT OF HORIZ. TAIL WITH SYMM. SIMPLE HINGE FLAP DEFLECTIONS. DLE=20.

(A)MACH = .70

DATA SET	SYMBOL	CONFIGURATION DESCRIPTION	DH	DTEO	DTEI	DLE
(JFK012)	○	B V W2		5.000	5.000	20.000
(JFK013)	□	B V W2H	-5.000	5.000	5.000	20.000
(JFK015)	◇	B V W2		10.000	10.000	20.000
(JFK014)	△	B V W2H	-5.000	10.000	10.000	20.000

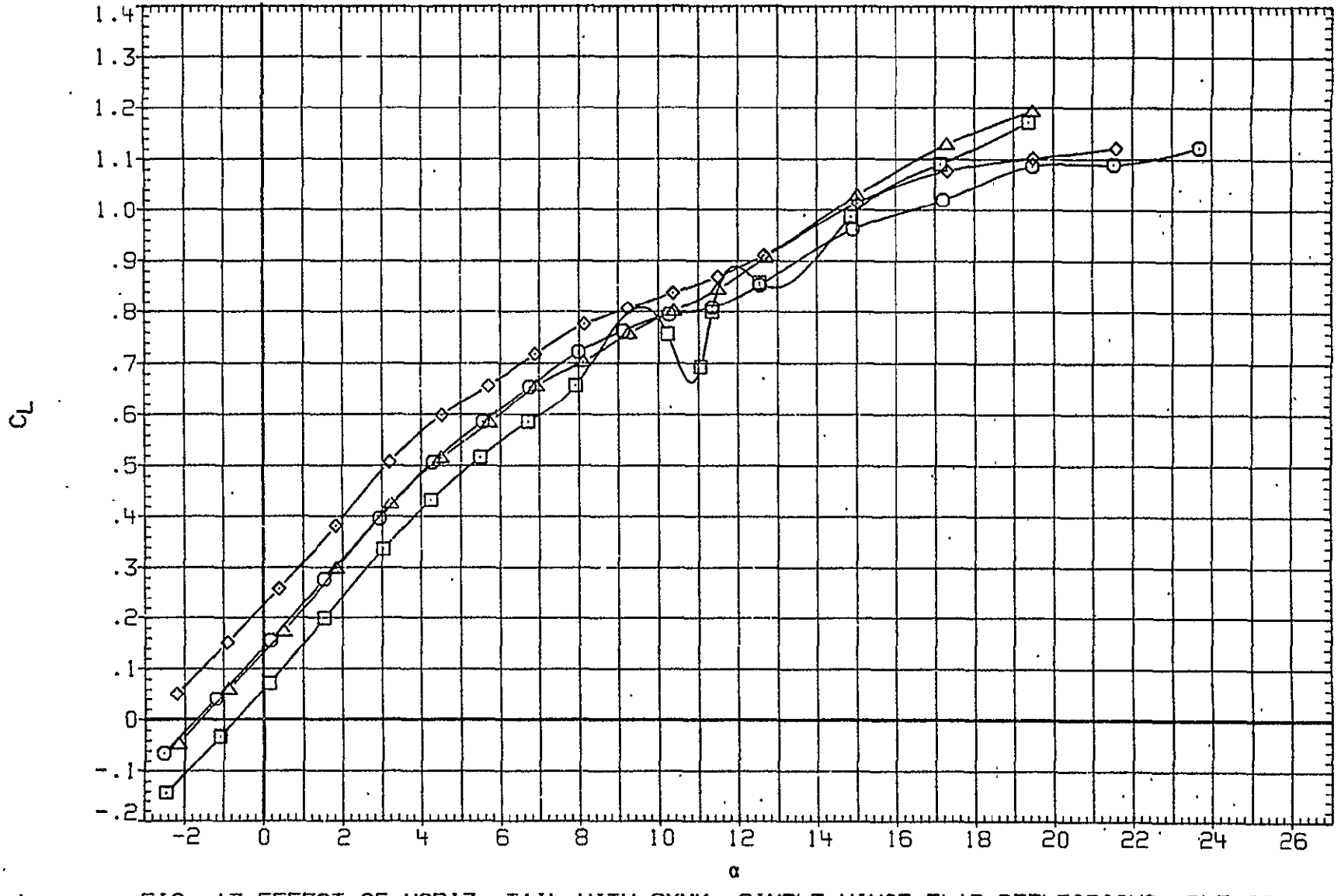

FIG. 13 EFFECT OF HORIZ. TAIL WITH SYMM. SIMPLE HINGE FLAP DEFLECTIONS. DLE=20.

(B)MACH = .90

ORIGINAL PAGE IS
OF POOR QUALITY

DATA SET	SYMBOL	CONFIGURATION DESCRIPTION	DH	DTEO	DTEI	DLE
(JFK012)	○	B V W2		5.000	5.000	20.000
(JFK013)	□	B V W2H	-5.000	5.000	5.000	20.000
(JFK015)	◇	B V W2		10.000	10.000	20.000
(JFK014)	△	B V W2H	-5.000	10.000	10.000	20.000

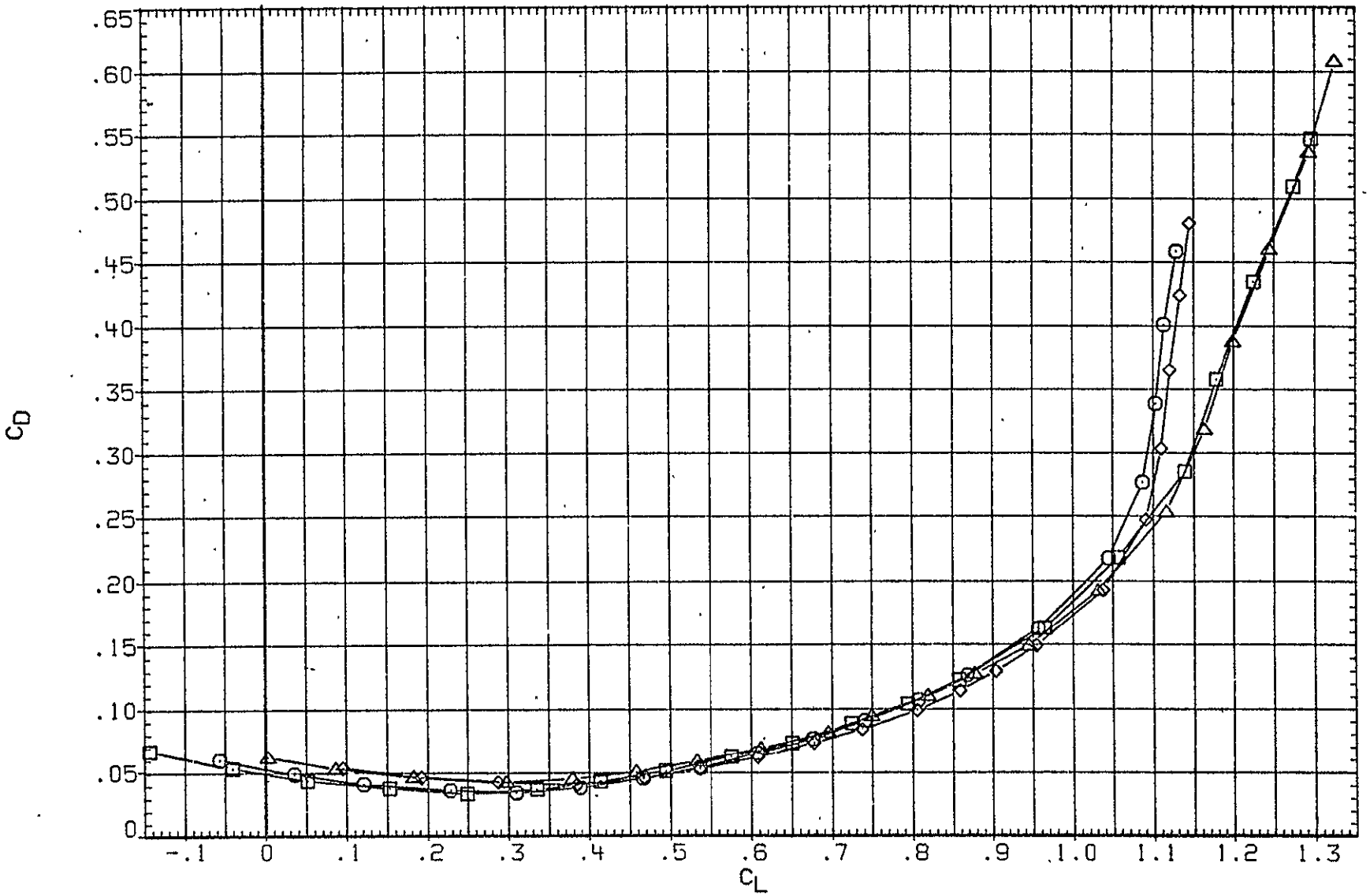

FIG. 13 EFFECT OF HORIZ. TAIL WITH SYMM. SIMPLE HINGE FLAP DEFLECTIONS. DLE=20.

(A)MACH = .70

DATA SET	SYMBOL	CONFIGURATION DESCRIPTION	DH	DTEO	DTEI	DLE
(JFK012)	○	B V W2		5.000	5.000	20.000
(JFK013)	□	B V W2H	-5.000	5.000	5.000	20.000
(JFK015)	◇	B V W2		10.000	10.000	20.000
(JFK014)	△	B V W2H	-5.000	10.000	10.000	20.000

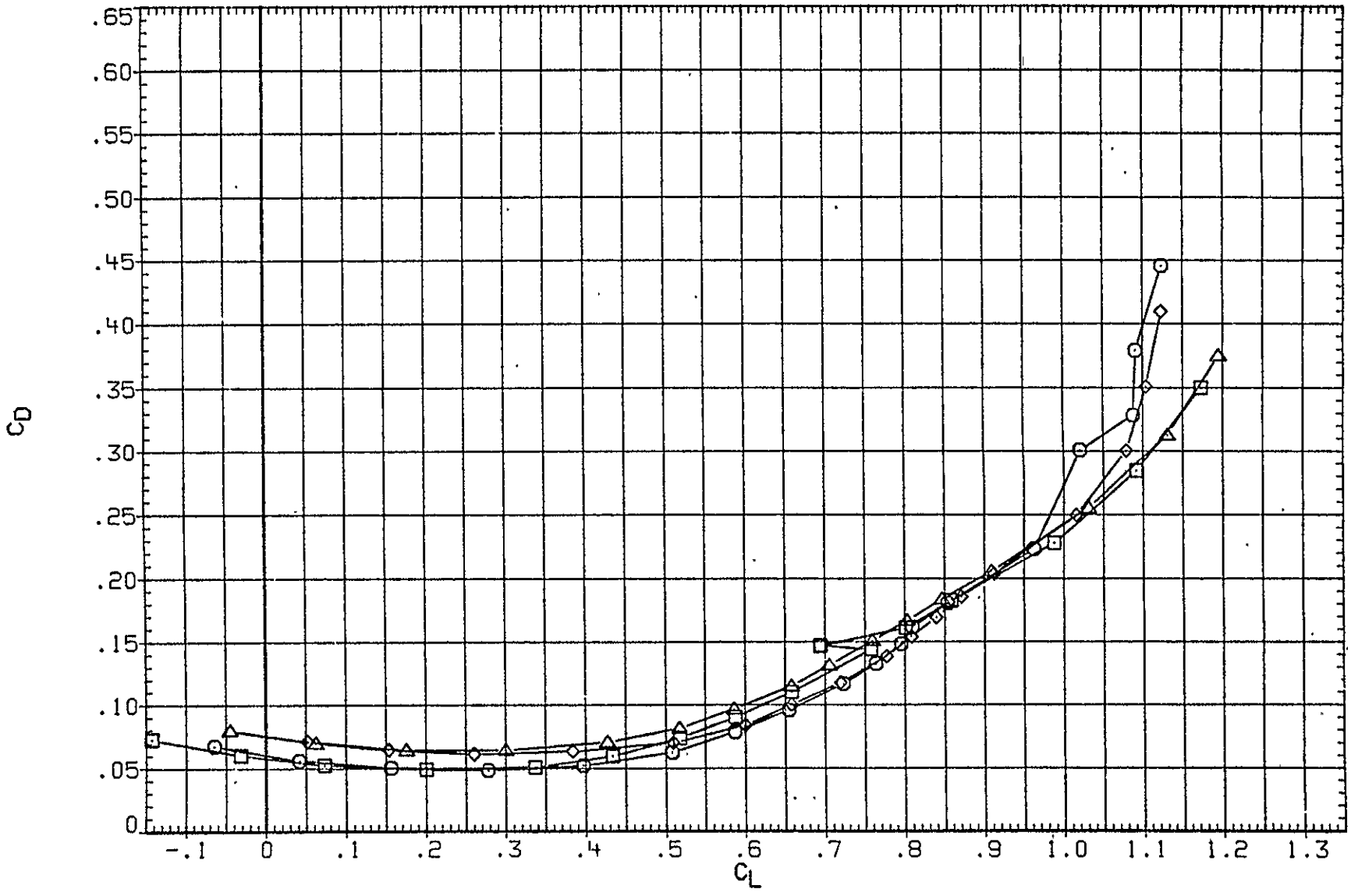

FIG. 13 EFFECT OF HORIZ. TAIL WITH SYMM. SIMPLE HINGE FLAP DEFLECTIONS. DLE=20.

(B)MACH = .90

DATA SET	SYMBOL	CONFIGURATION DESCRIPTION	DH	DTEO	DTEI	DLE
(JFK012)	○	B V W2		5.000	5.000	20.000
(JFK013)	□	B V W2H	-5.000	5.000	5.000	20.000
(JFK015)	◇	B V W2		10.000	10.000	20.000
(JFK014)	△	B V W2H	-5.000	10.000	10.000	20.000

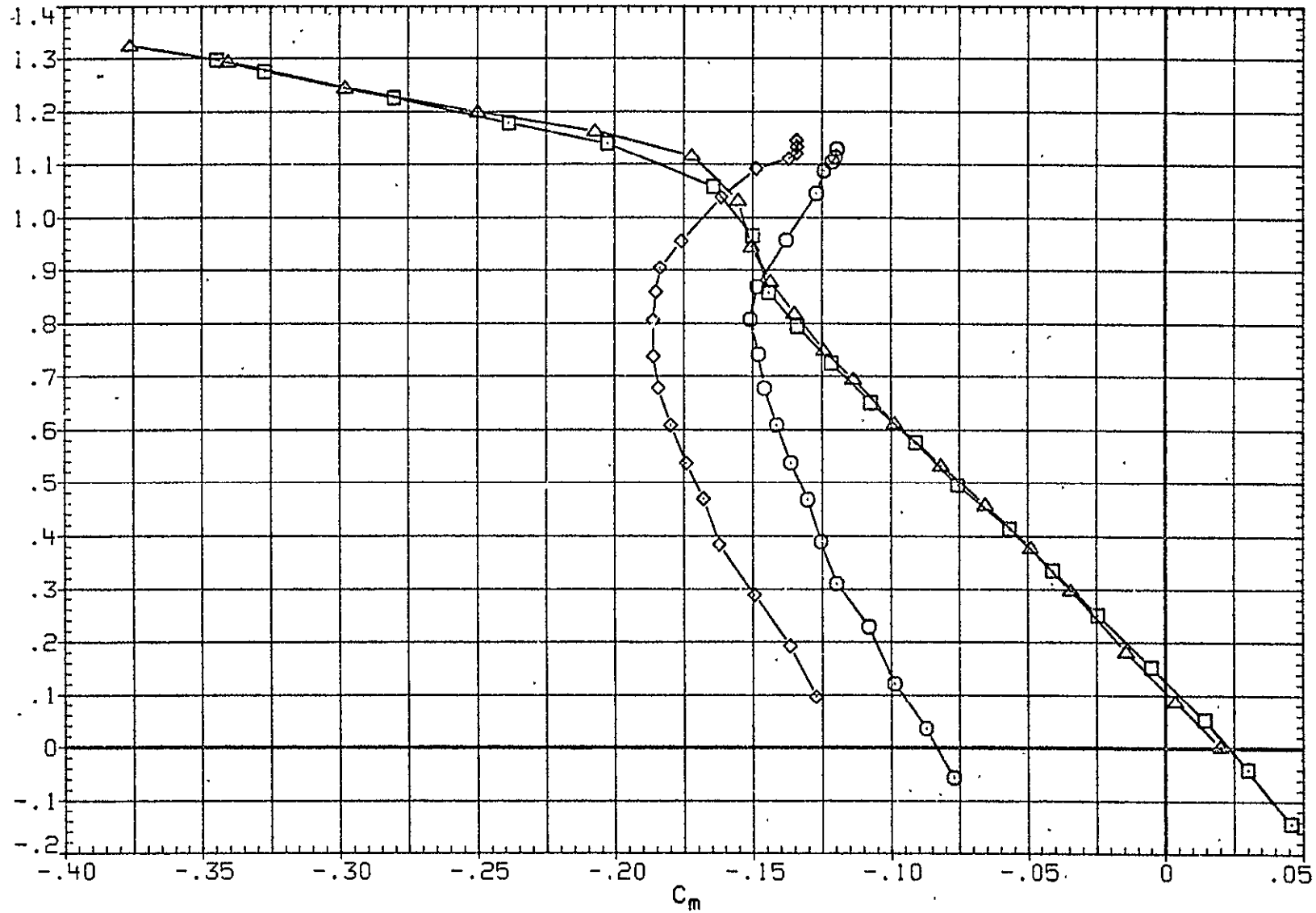

FIG. 13 EFFECT OF HORIZ. TAIL WITH SYMM. SIMPLE HINGE FLAP DEFLECTIONS. DLE=20.

(A)MACH = .70

DATA SET	SYMBOL	CONFIGURATION DESCRIPTION	DH	DTEO	DTEI	DLE
(JFK012)	○	B V W2		5.000	5.000	20.000
(JFK013)	□	B V W2H	-5.000	5.000	5.000	20.000
(JFK015)	◇	B V W2		10.000	10.000	20.000
(JFK014)	△	B V W2H	-5.000	10.000	10.000	20.000

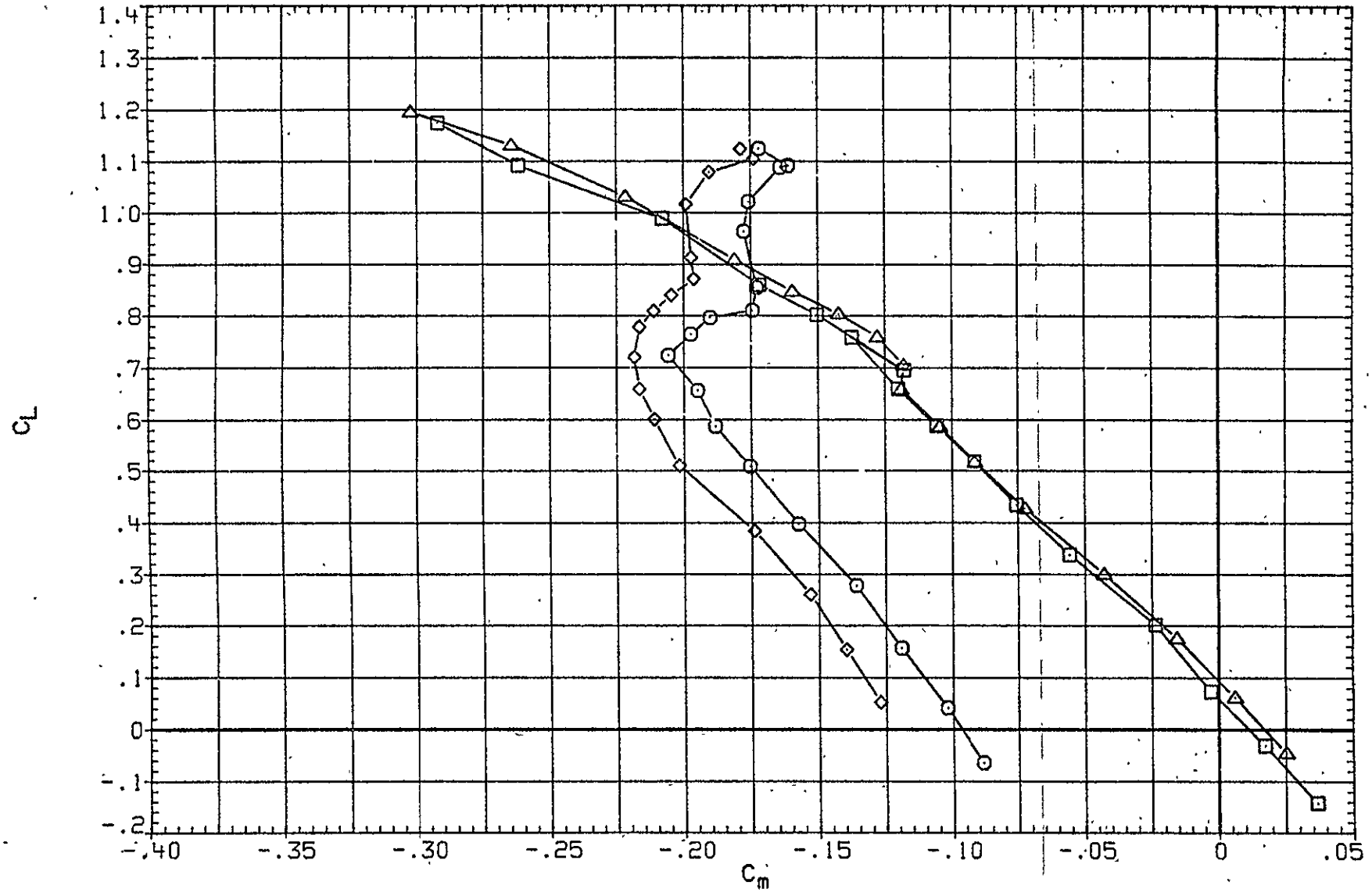

FIG. 13 EFFECT OF HORIZ. TAIL WITH SYMM. SIMPLE HINGE FLAP DEFLECTIONS. DLE=20.

(B) MACH = .90

DATA SET	SYMBOL	CONFIGURATION DESCRIPTION	BETA	DH
(JFK002)	○	B V WIH	.000	.000
(JFK003)	□	B V WIH	-5.000	.000
(JFK006)	◇	B V W2H	.000	.000
(JFK005)	△	B V W2H	-5.000	.000

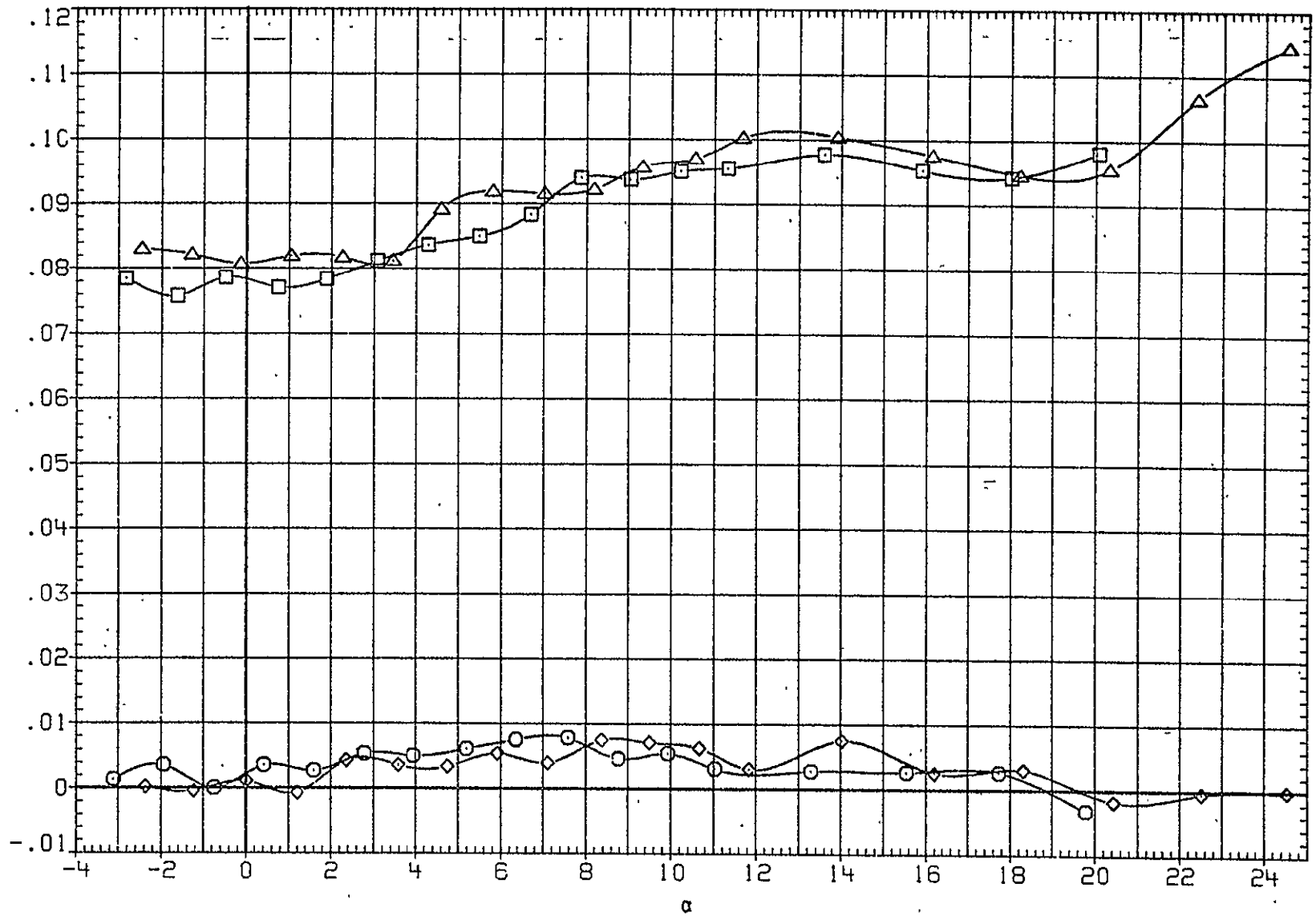

FIG. 14 EFFECT OF SIDESLIP ANGLE FOR BOTH WINGS. ALL CONT. SURF. ZERO. TAIL ON.

(A) MACH = .70

DATA SET	SYMBOL	CONFIGURATION DESCRIPTION	BETA	DH
(JFK002)	○	B V W1H	.000	.000
(JFK003)	□	B V W1H	-5.000	.000
(JFK006)	◇	B V W2H	.000	.000
(JFK005)	△	B V W2H	-5.000	.000

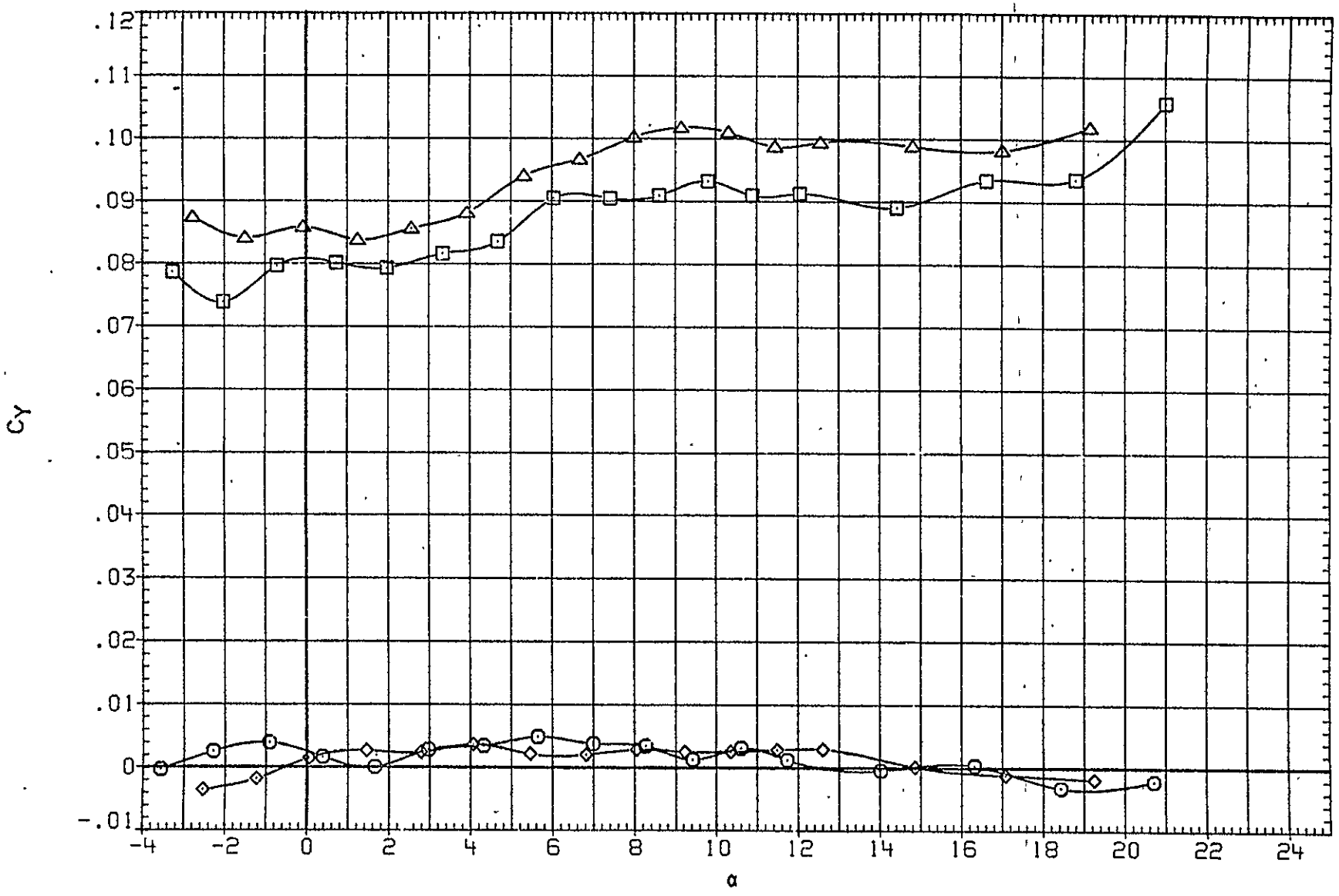

FIG. 14 EFFECT OF SIDESLIP ANGLE FOR BOTH WINGS. ALL CONT. SURF. ZERO. TAIL ON.

(B)MACH = .90

DATA SET	SYMBOL	CONFIGURATION DESCRIPTION	BETA	DH
(JFK002)	○	B V WIH	.000	.000
(JFK003)	□	B V WIH	-5.000	.000
(JFK006)	◇	B V W2H	.000	.000
(JFK005)	△	DATA NOT AVAILABLE	-5.000	.000

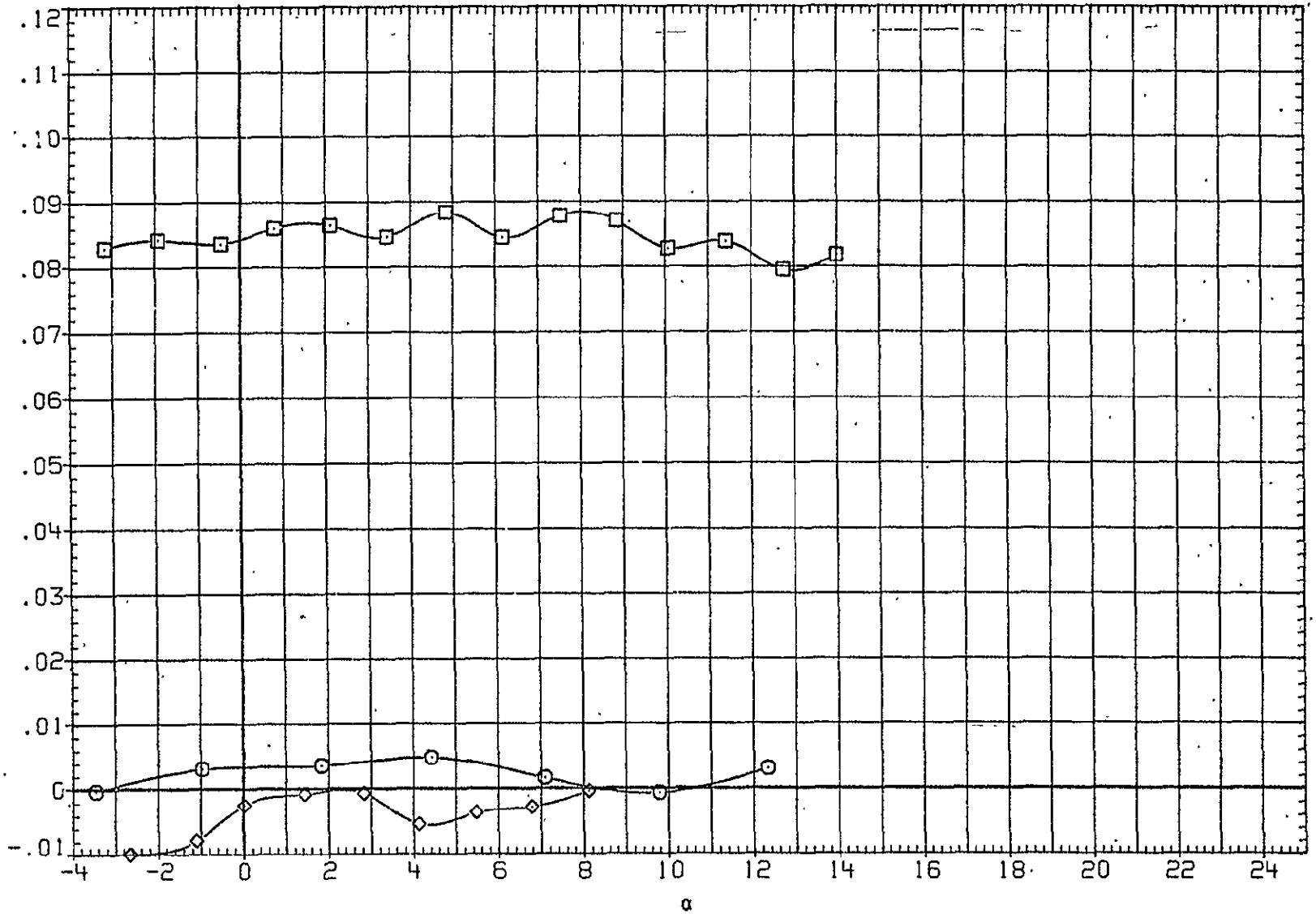

FIG. 14 EFFECT OF SIDESLIP ANGLE FOR BOTH WINGS. ALL CONT. SURF. ZERO. TAIL ON.

(C)MACH = 1.15

DATA SET	SYMBOL	CONFIGURATION DESCRIPTION	BETA	DH
(JFK002)	○	B V W1H	.000	.000
(JFK003)	□	B V W1H	-5.000	.000
(JFK006)	◇	B V W2H	.000	.000
(JFK005)	△	B V W2H	-5.000	.000

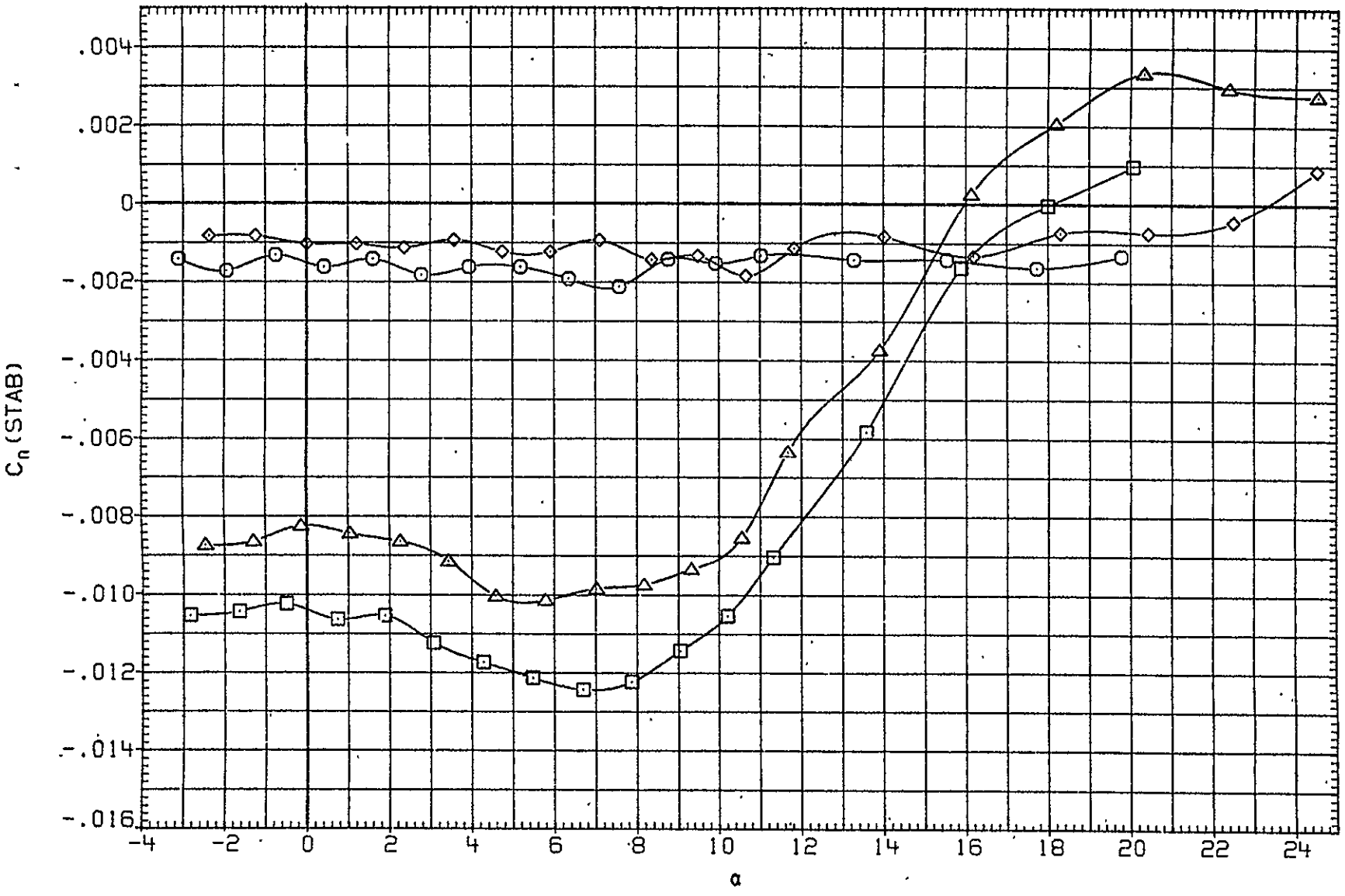

FIG. 14 EFFECT OF SIDESLIP ANGLE FOR BOTH WINGS. ALL CONT. SURF. ZERO. TAIL ON.

(A) MACH = .70

DATA SET	SYMBOL	CONFIGURATION DESCRIPTION	BETA	DH
(JFK002)	○	B V W1H	.000	.000
(JFK003)	□	B V W1H	-5.000	.000
(JFK006)	◇	B V W2H	.000	.000
(JFK005)	△	B V W2H	-5.000	.000

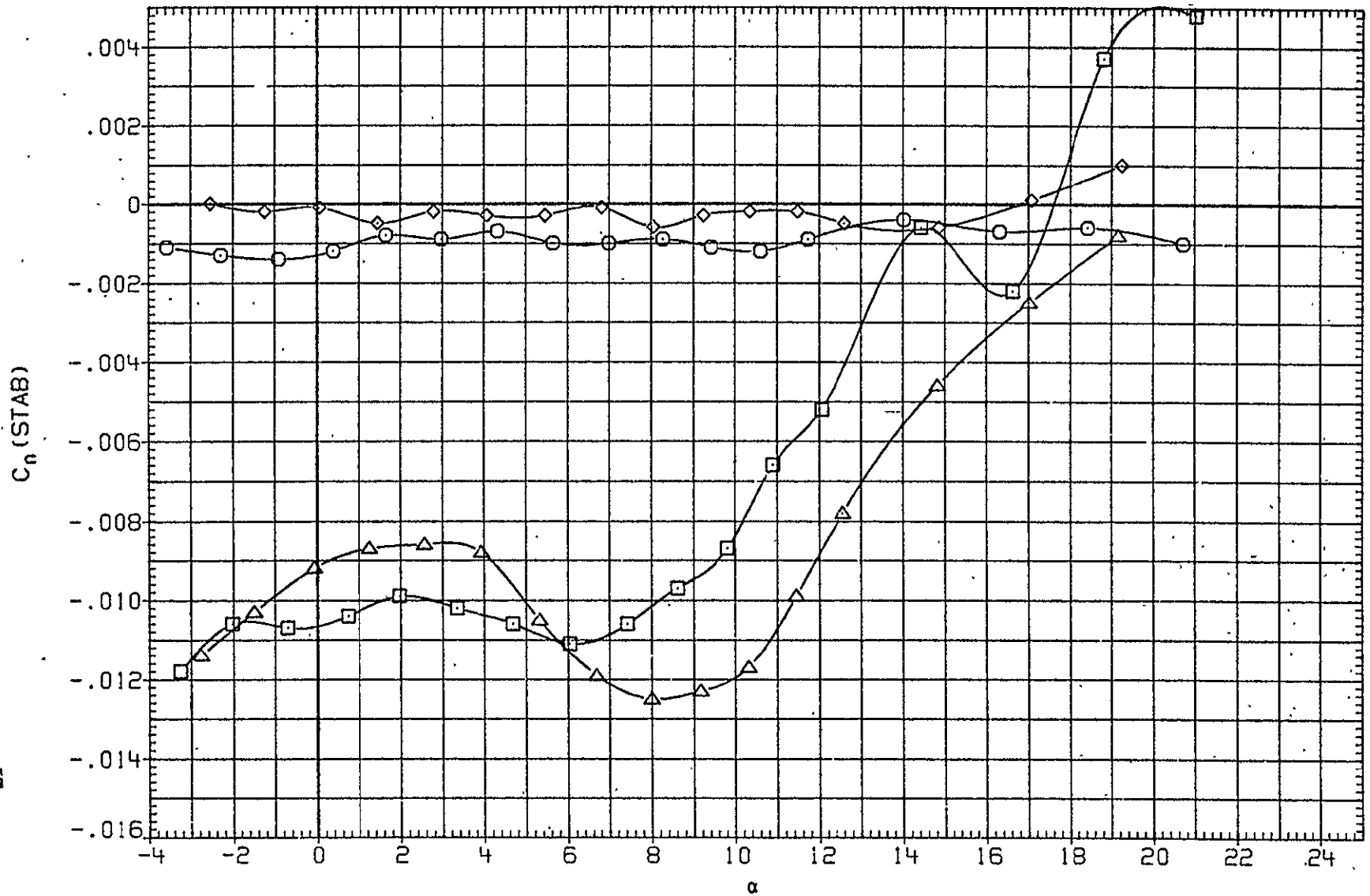

FIG. 14 EFFECT OF SIDESLIP ANGLE FOR BOTH WINGS: ALL CONT. SURF: ZERO. TAIL ON:

(B) MACH = .90

DATA SET	SYMBOL	CONFIGURATION DESCRIPTION	BETA	DH
(JFK002)	○	B V W1H	.000	.000
(JFK003)	□	B V W1H	-5.000	.000
(JFK006)	◇	B V W2H	.000	.000
(JFK005)	△	DATA NOT AVAILABLE	-5.000	.000

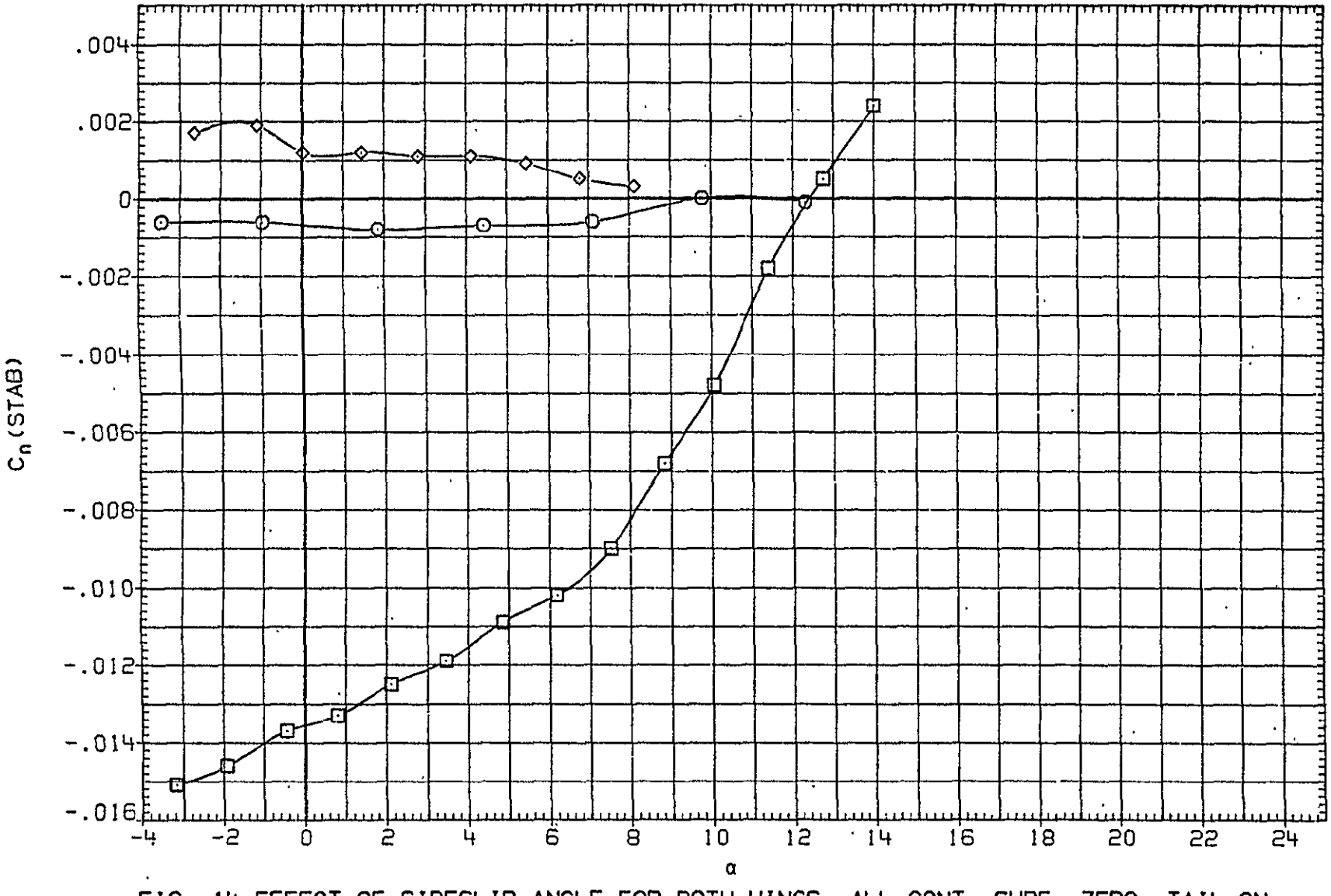

FIG. 14 EFFECT OF SIDESLIP ANGLE FOR BOTH WINGS. ALL CONT. SURF. ZERO. TAIL ON.

(C) MACH = 1.15

DATA SET	SYMBOL	CONFIGURATION DESCRIPTION	BETA	DH
(JFK002)	○	B V W1H	.000	.000
(JFK003)	□	B V W1H	-5.000	.000
(JFK006)	◇	B V W2H	.000	.000
(JFK005)	△	B V W2H	-5.000	.000

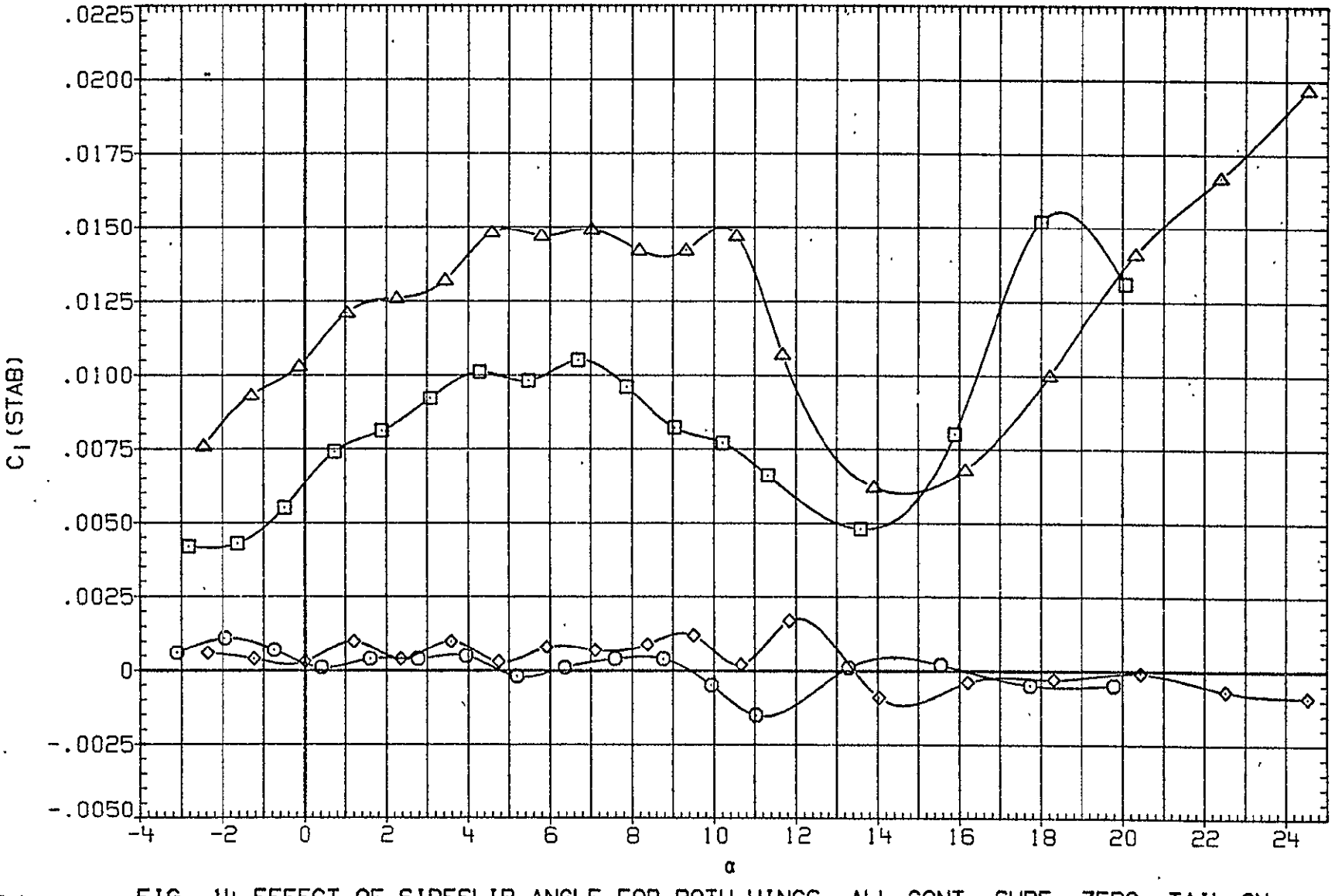

FIG. 14 EFFECT OF SIDESLIP ANGLE FOR BOTH WINGS. ALL CONT. SURF. ZERO. TAIL ON.

(A)MACH = .70

DATA SET	SYMBOL	CONFIGURATION DESCRIPTION	BETA	DH
(JFK002)	○	B V W1H	.000	.000
(JFK003)	□	B V W1H	-5.000	.000
(JFK006)	◇	B V W2H	.000	.000
(JFK005)	△	B V W2H	-5.000	.000

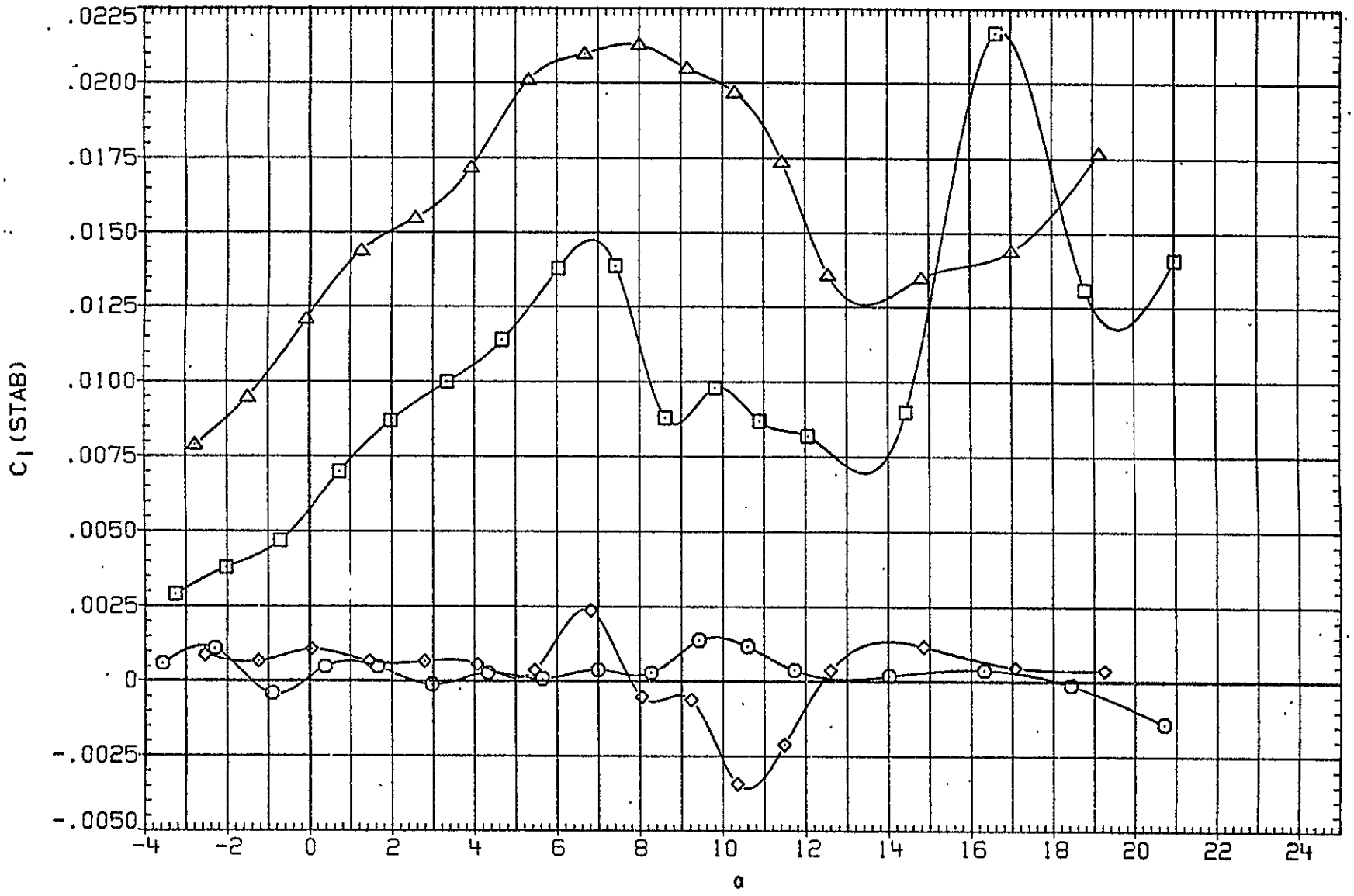

FIG. 14 EFFECT OF SIDESLIP ANGLE FOR BOTH WINGS. ALL CONT. SURF. ZERO. TAIL ON.

(B)MACH = .90

DATA SET	SYMBOL	CONFIGURATION DESCRIPTION	BETA	DH
(JFK002)	○	B V WIH	.000	.000
(JFK003)	□	B V WIH	-5.000	.000
(JFK006)	◇	B V W2H	.000	.000
(JFK005)	△	DATA NOT AVAILABLE	-5.000	.000

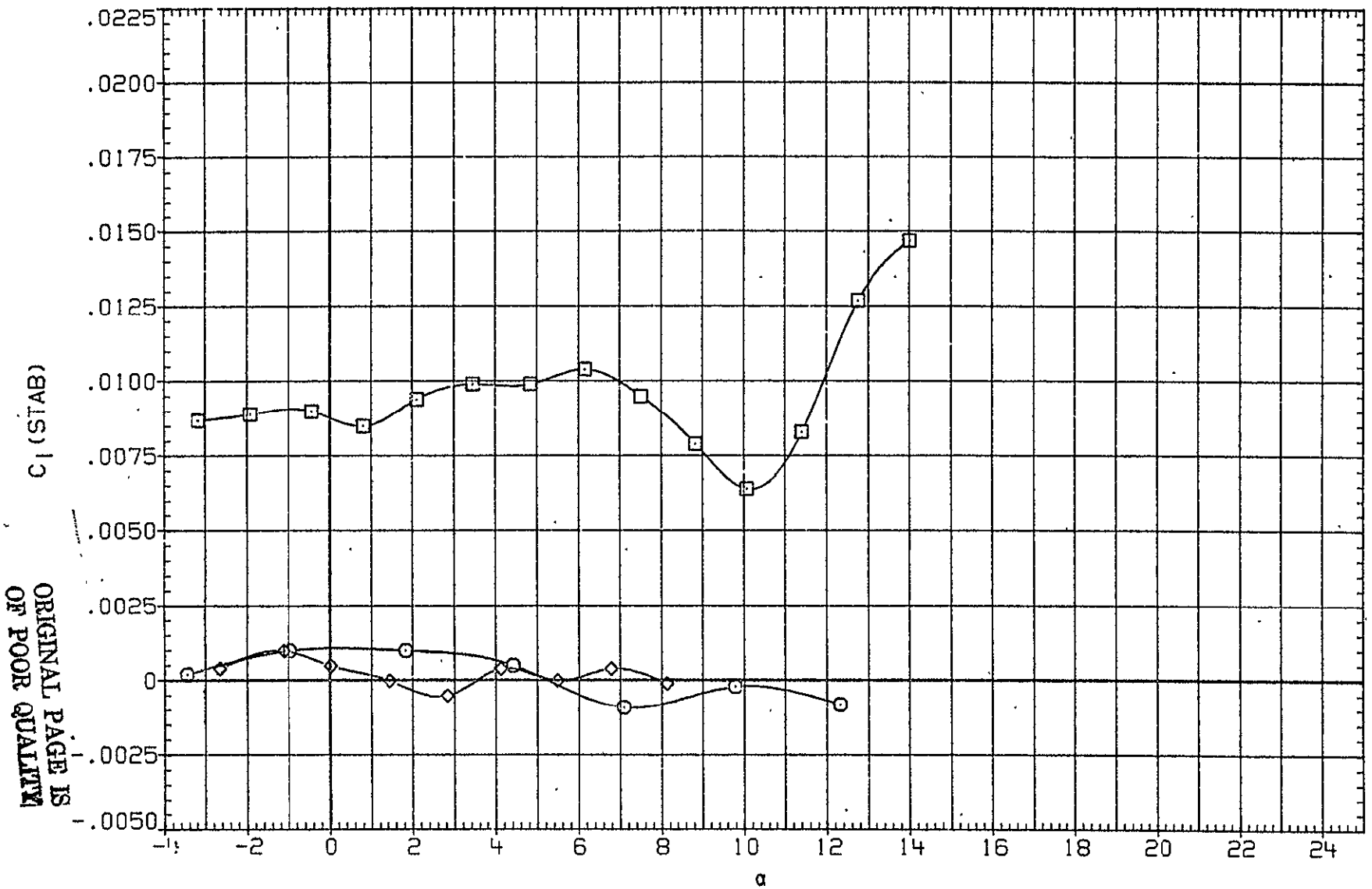

FIG. 14 EFFECT OF SIDESLIP ANGLE FOR BOTH WINGS. ALL CONT. SURF. ZERO. TAIL ON.

(C)MACH = 1.15

DATA SET	SYMBOL	CONFIGURATION DESCRIPTION	BETA	DH
(JFK002)	○	B V W1H	.000	.000
(JFK003)	□	B V W1H	-5.000	.000
(JFK006)	◇	B V W2H	.000	.000
(JFK005)	△	B V W2H	-5.000	.000

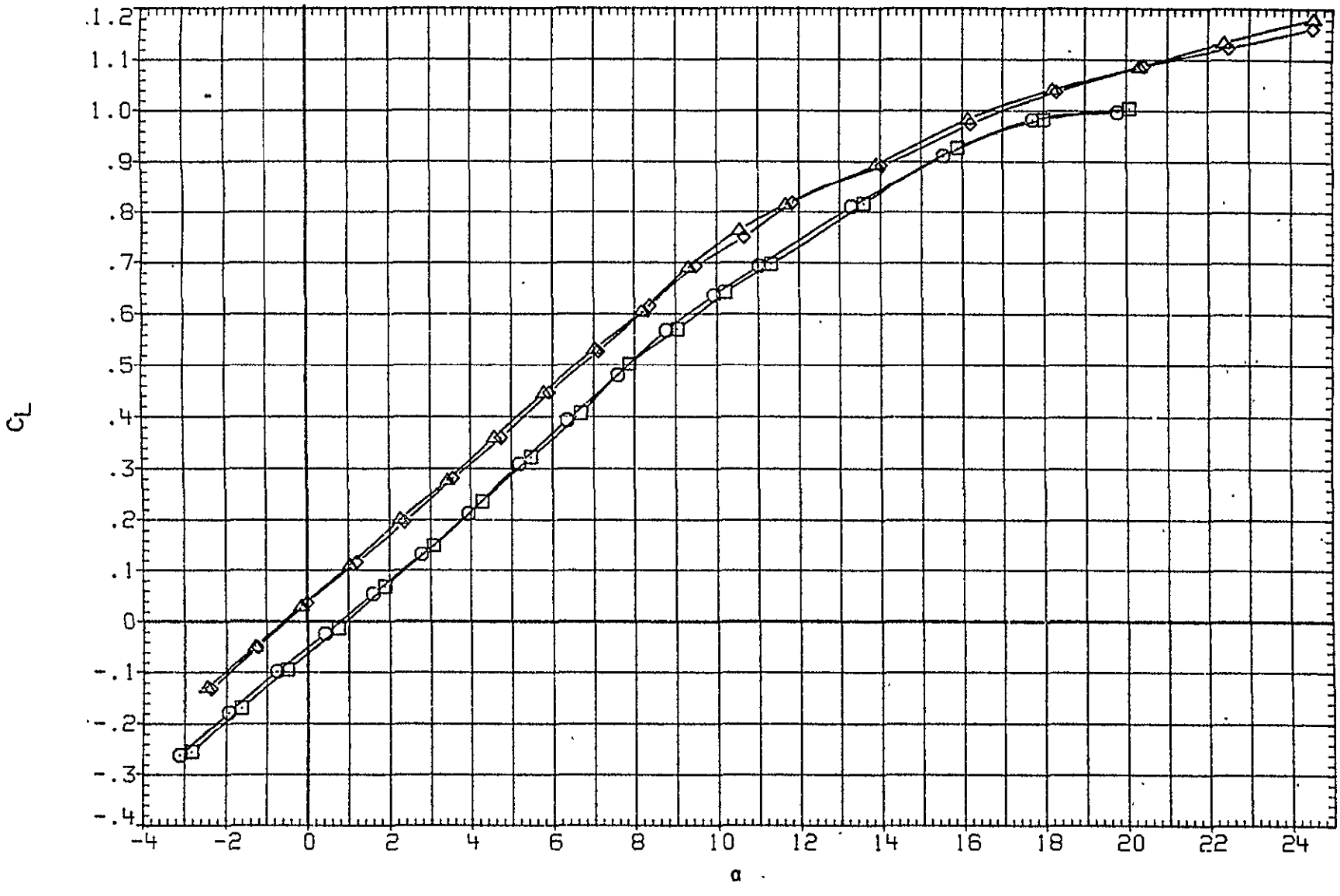

FIG. 14 EFFECT OF SIDESLIP ANGLE FOR BOTH WINGS. ALL CONT. SURF. ZERO. TAIL ON.

(A)MACH = .70

DATA SET	SYMBOL	CONFIGURATION DESCRIPTION	BETA	DH
(JFK002)	○	B V W1H	.000	.000
(JFK003)	□	B V W1H	-5.000	.000
(JFK006)	◇	B V W2H	.000	.000
(JFK005)	△	B V W2H	-5.000	.000

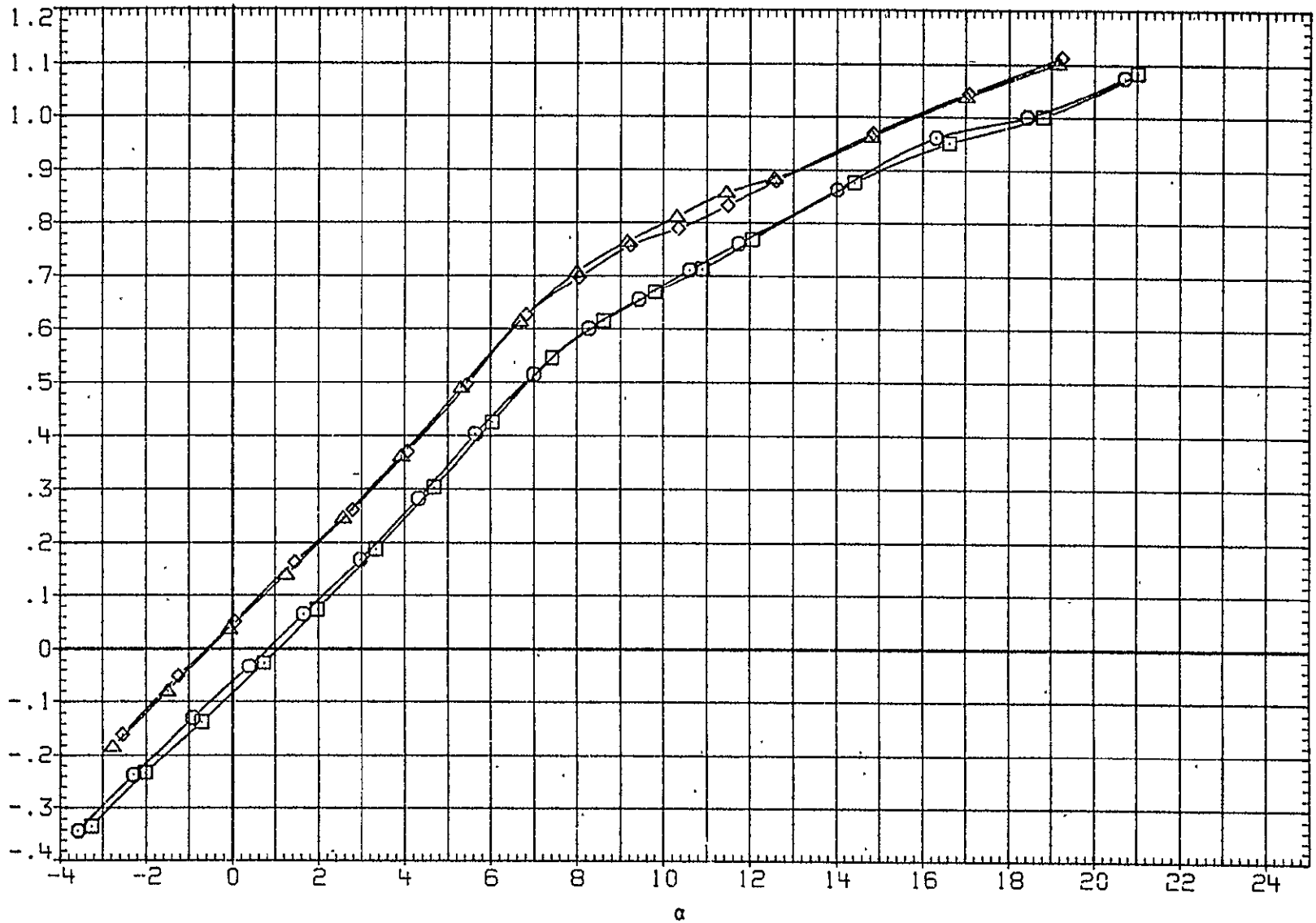

FIG. 14 EFFECT OF SIDESLIP ANGLE FOR BOTH WINGS. ALL CONT. SURF. ZERO. TAIL ON.

(B)MACH = .90

DATA SET	SYMBOL	CONFIGURATION DESCRIPTION	BETA	DH
(JFK002)	○	B V W1H	.000	.000
(JFK003)	□	B V W1H	-5.000	.000
(JFK006)	◇	B V W2H	.000	.000
(JFK005)	△	DATA NOT AVAILABLE	-5.000	.000

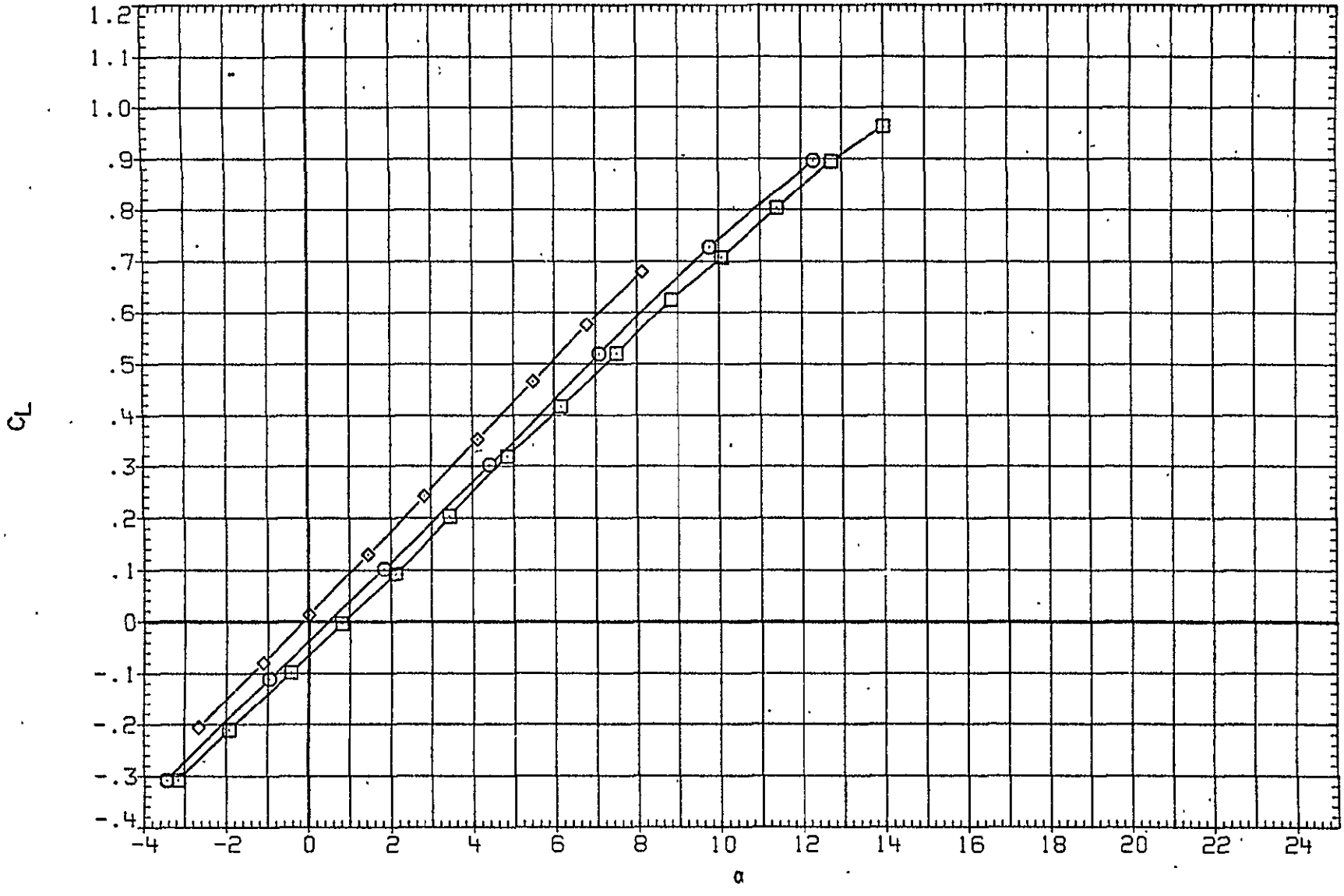

FIG. 14 EFFECT OF SIDESLIP ANGLE FOR BOTH WINGS. ALL CONT. SURF. ZERO. TAIL ON.

(C)MACH = 1.15

DATA SET	SYMBOL	CONFIGURATION DESCRIPTION	BETA	DH
(JFK002)	○	B V W1H	.000	.000
(JFK003)	□	B V W1H	-5.000	.000
(JFK006)	◇	B V W2H	.000	.000
(JFK005)	△	B V W2H	-5.000	.000

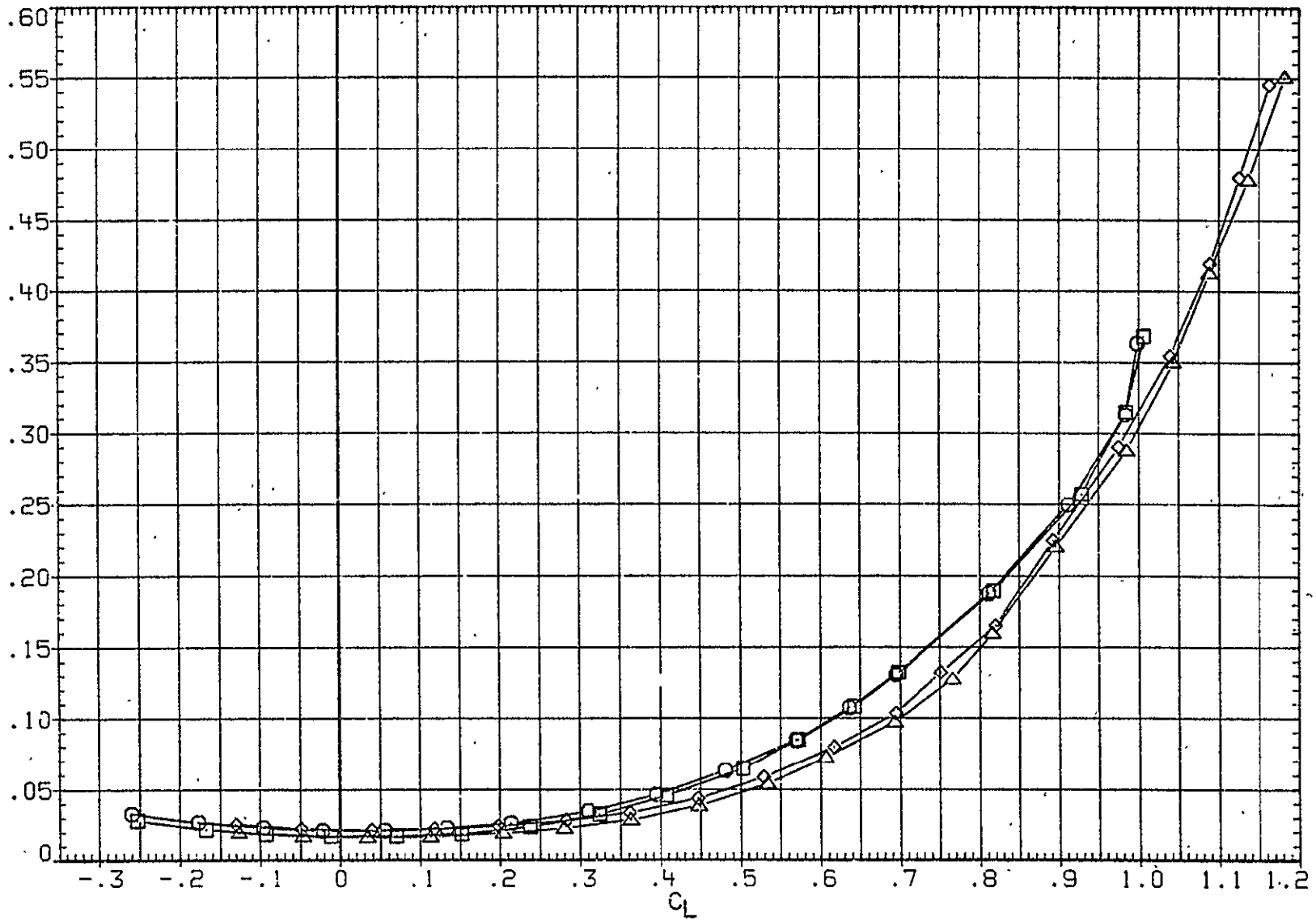

FIG. 14 EFFECT OF SIDESLIP ANGLE FOR BOTH WINGS. ALL CONT. SURF. ZERO. TAIL ON.

(A)MACH = .70

DATA SET	SYMBOL	CONFIGURATION DESCRIPTION	BETA	DH
(JFK002)	○	B V W1H	.000	.000
(JFK003)	□	B V W1H	-5.000	.000
(JFK006)	◇	B V W2H	.000	.000
(JFK005)	△	B V W2H	-5.000	.000

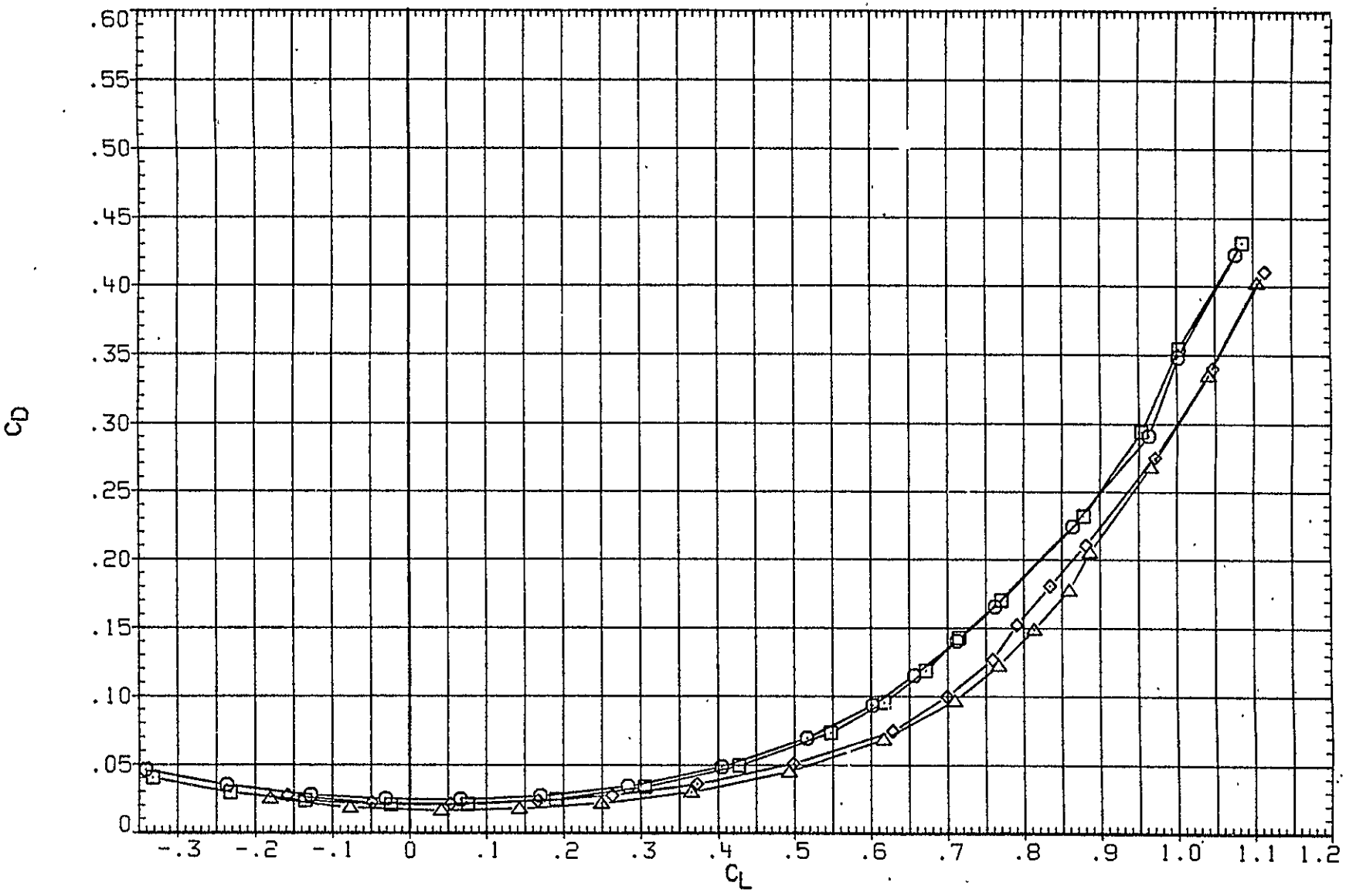

FIG. 14 EFFECT OF SIDESLIP ANGLE FOR BOTH WINGS. ALL CONT. SURF. ZERO. TAIL ON.

(B)MACH = .90

DATA SET	SYMBOL	CONFIGURATION DESCRIPTION	BETA	DH
(JFK002)	○	B V WIH	.000	.000
(JFK003)	□	B V WIH	-5.000	.000
(JFK006)	◇	B V W2H	.000	.000
(JFK005)	△	DATA NOT AVAILABLE	-5.000	.000

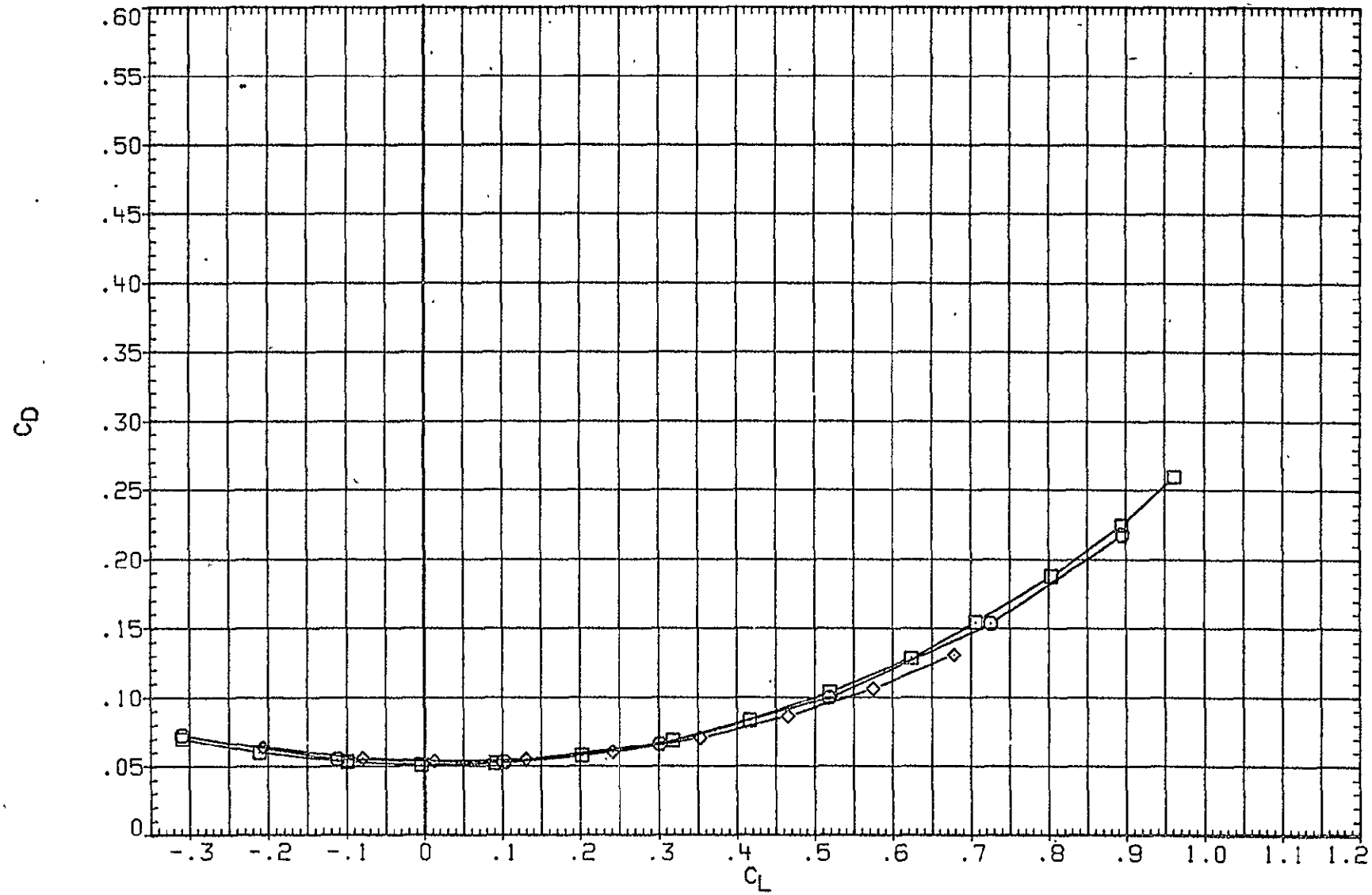

FIG. 14 EFFECT OF SIDESLIP ANGLE FOR BOTH WINGS. ALL CONT. SURF. ZERO. TAIL ON.

(C)MACH = 1.15

DATA SET	SYMBOL	CONFIGURATION DESCRIPTION	BETA	DH
(JFK002)	○	B V W1H	.000	.000
(JFK003)	□	B V W1H	-5.000	.000
(JFK006)	◇	B V W2H	.000	.000
(JFK005)	△	B V W2H	-5.000	.000

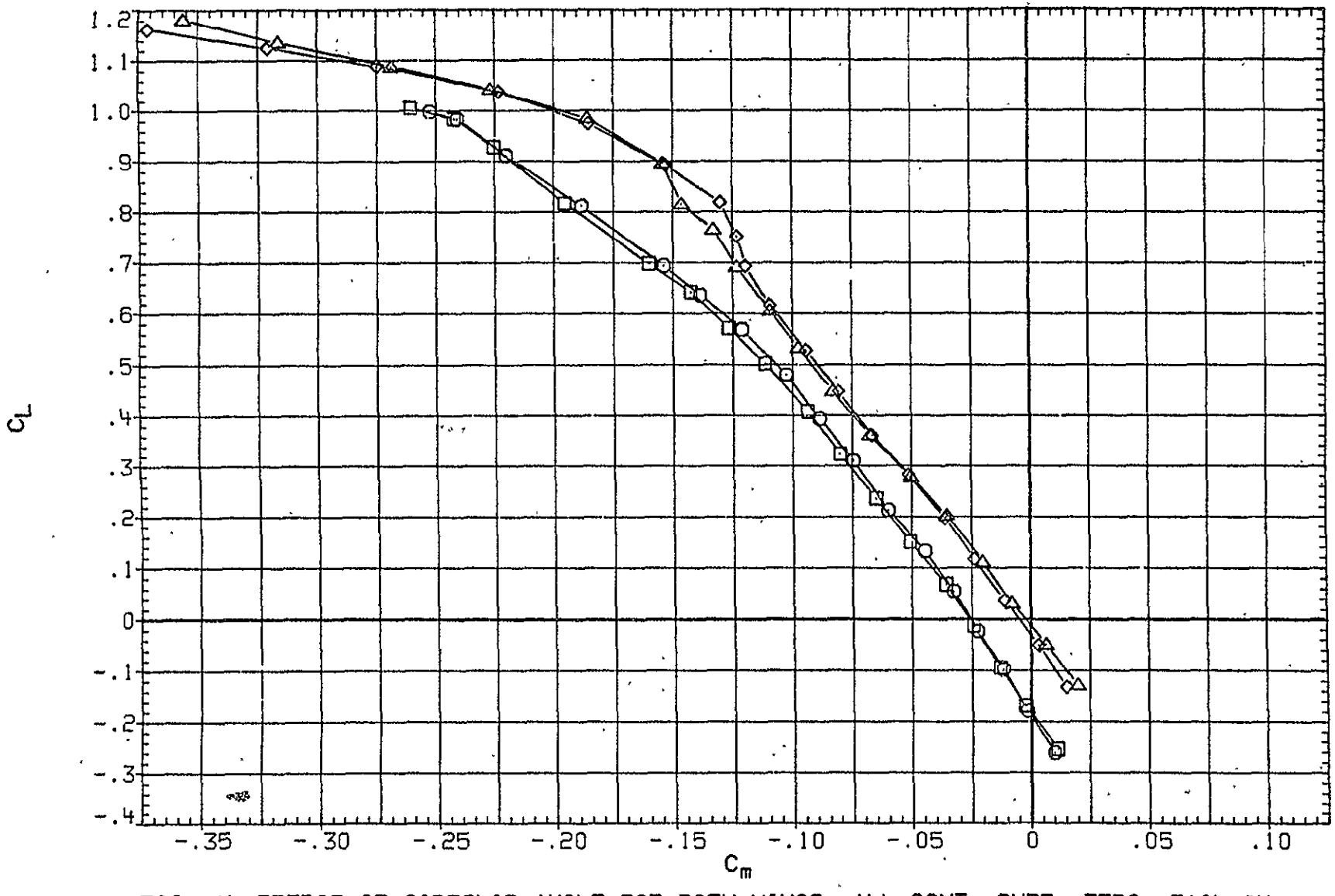

FIG. 14 EFFECT OF SIDESLIP ANGLE FOR BOTH WINGS. ALL CONT. SURF. ZERO. TAIL ON.

(A) MACH = .70

DATA SET	SYMBOL	CONFIGURATION DESCRIPTION	BETA	DH
(JFK002)	○	B V W1H	.000	.000
(JFK003)	□	B V W1H	-5.000	.000
(JFK006)	◇	B V W2H	.000	.000
(JFK005)	△	B V W2H	-5.000	.000

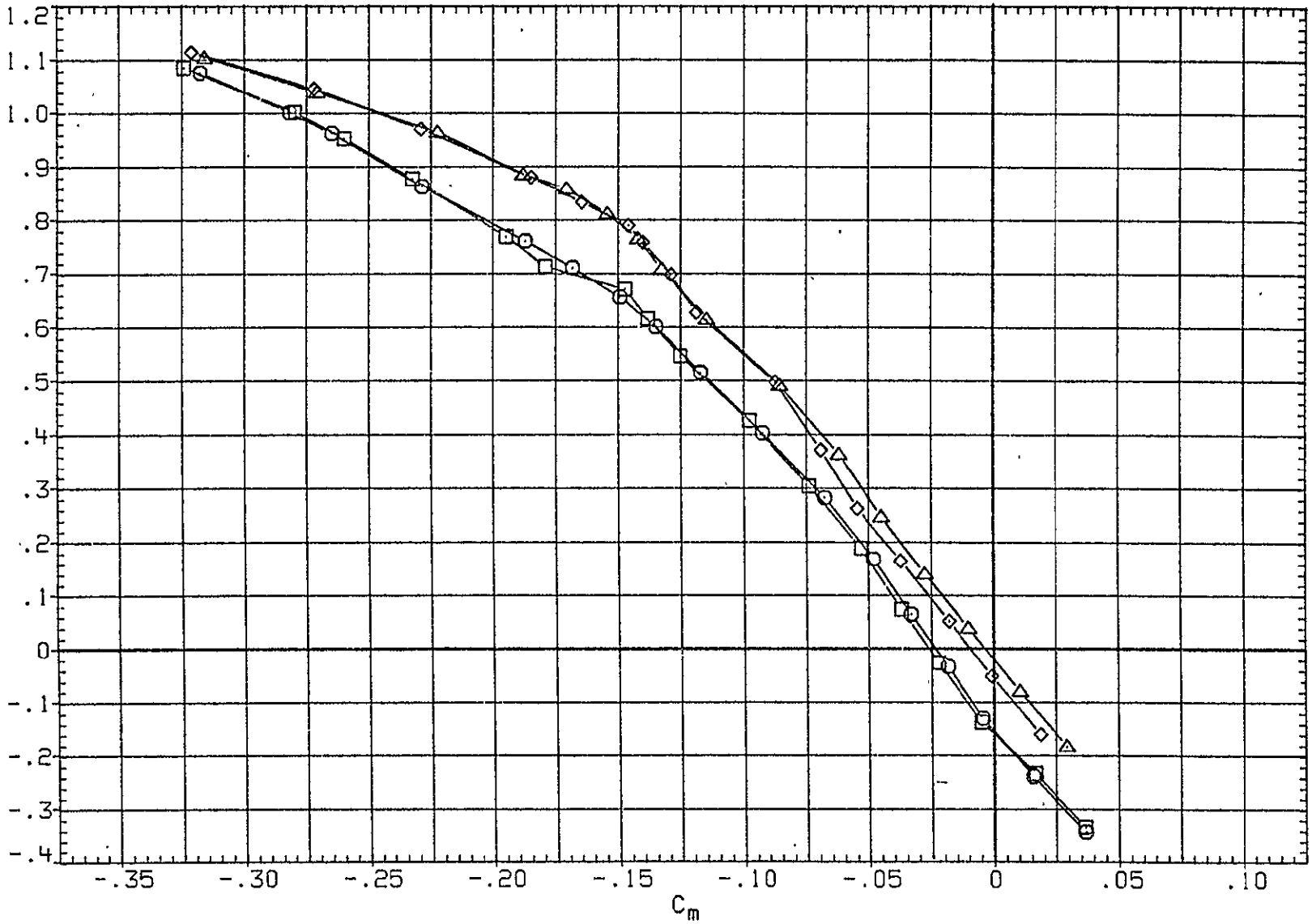

FIG. 14 EFFECT OF SIDESLIP ANGLE FOR BOTH WINGS. ALL CONT. SURF. ZERO. TAIL ON.

(B)MACH = .90

DATA SET	SYMBOL	CONFIGURATION DESCRIPTION	BETA	DH
(JFK002)	○	B V WIH	.000	.000
(JFK003)	□	B V WIH	-5.000	.000
(JFK006)	◇	B V W2H	.000	.000
(JFK005)	△	DATA NOT AVAILABLE	-5.000	.000

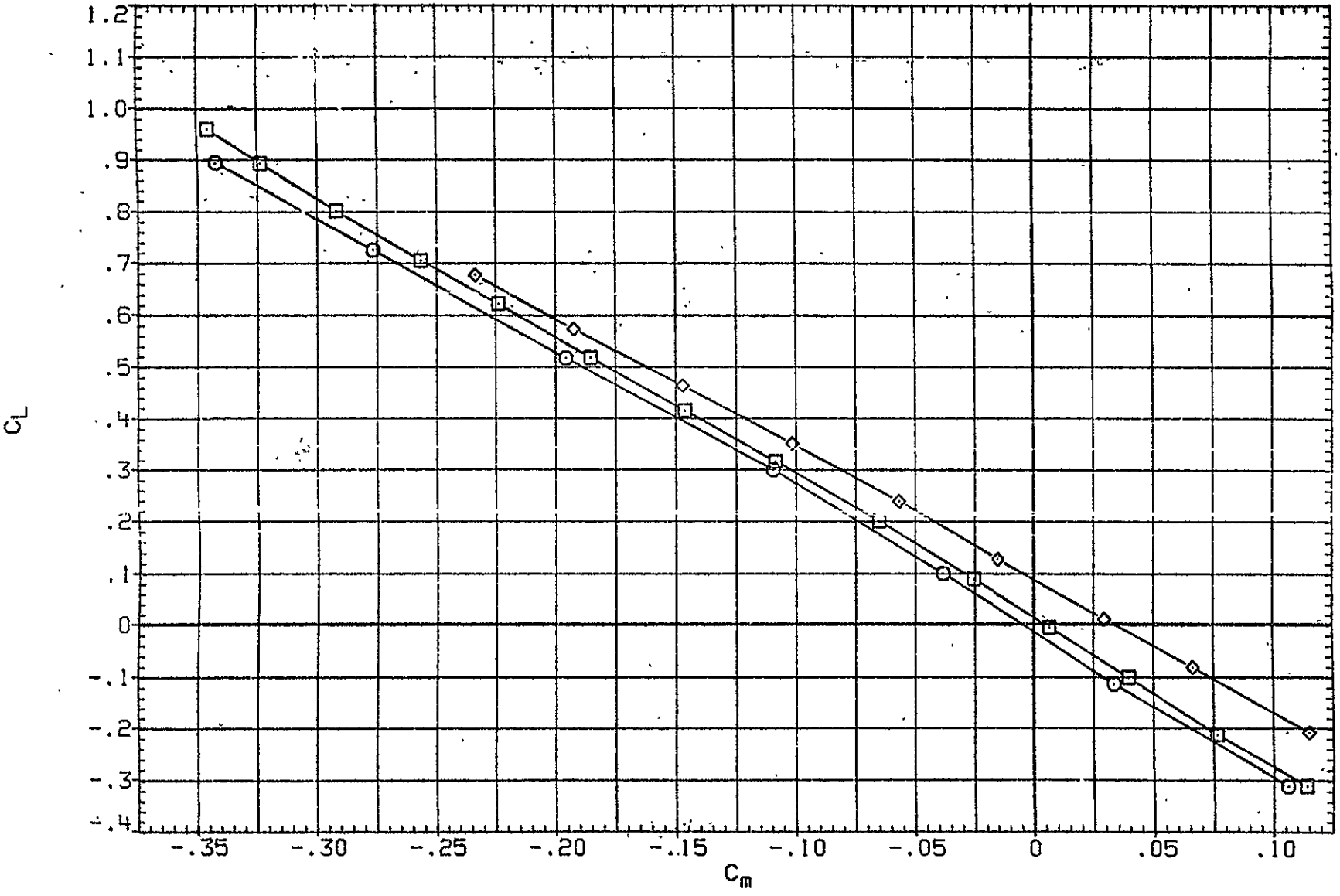

FIG. 14 EFFECT OF SIDESLIP ANGLE FOR BOTH WINGS. ALL CONT. SURF. ZERO. TAIL ON.

(C)MACH = 1.15